1999-06-08

Characterization, Mechanisms and Modulation of Calcium Signals in Glia: a Dissertation

Andreja Strahonja
University of Massachusetts Medical School

CHARACTERIZATION, MECHANISMS AND MODULATION OF CALCIUM SIGNALS IN GLIA

A Dissertation Presented

By

Andreja Strahonja

Submitted to the Faculty of the

University of Massachusetts Graduate School of Biomedical Sciences, Worcester

in partial fulfillment of the requirements for the degree of:

DOCTOR OF PHILOSOPHY

(May, 24th 1999)

(Physiology)

CHARACTERISATION, MECHANISMS AND MODULATION OF CALCIUM SIGNALS IN GLIA

A Dissertation Presented
By

ANDREJA STRAHONJA

Approved as to style and content by:

(Signature) _____
Dr. Daniel L. Kilpatrick, Chair of Committee

(Signature) _____
Dr. H. Maurice Goodman, Member of Committee

(Signature) _____
Dr. Ann R. Rittenhouse, Member of Committee

(Signature) _____
Dr. Zuoshang Xu, Member of Committee

(Signature) _____
Dr. David C. Spray, Member of Committee

(Signature) _____
Dr. Michael J. Sanderson, Dissertation Mentor
(Signature) _____
Dr. Thomas B. Miller, Dean of the Graduate School of Biomedical Sciences

Department of Physiology
Month, Day and Year _____

ABBREVIATIONS

acetylmethylcholine	AMCh
acetylcholine	ACh
cyclic adenosine monophosphate	cAMP
blood-brain barrier	BBB
calcium	Ca^{2+}
central nervous system	CNS
calcium induced calcium release	CICR
connexin	Cx
calmodulin	CaM
cyclic adenosine disphosphate ribose	cADPR
diacylglycerol	DAG
Dulbecco's modified Eagle medium	DMEM
endoplasmic reticulum	ER
glial fibrilary acidic protein	GFAP
galactosidase C	GalC
gamma amino butyric acid	GABA
Hanks' balanced salt solution	HBSS
Hanks' balanced salt solution supplemented with HEPES buffer	HBSS-HEPES
intracellular Ca^{2+} concentration	$[Ca^{2+}]_i$
intracellular Ca^{2+} store	ICS
IP_3 receptors	IP_3Rs
inositol trisphosphate	IP_3
intracellular IP_3 concentration	$[IP_3]_i$
gap junction	GJ
muscarinic agonist-induced	MR-induced
18 α-glycyrrhetinic acid	AGA
nitrophenyl-EGTA	NP-EGTA
phosphatidylinositol 4,5-bisphosphate	PIP_2
phosphatidyl-inositol	PI
phospholipase C	PLC
phosphate buffered saline	PBS
protein kinase A	PKA
protein kinase C	PKC

ryanodine receptors	RyRs	ultraviolet	UV
		vasoactive intestinal	
sarco/endoplasmic reticulum		polypeptide	VIP
Ca^{2+}-ATPase	SERCA		

ACKNOWLEDGEMENTS

I gratefully acknowledge the intellectual and personal support of my colleagues, without which this thesis would have been impossible. I wish to thank Dr. M.J. Sanderson for the excellent technical training as well as for his sharing of views and ideas and our frequent discussions during my graduate school years. I also wish to thank all the past and present members of the Sanderson lab for making my graduate school years a truly unique experience.

I have greatly appreciated the opportunity to collaborate with Drs. Luc Leybaert and Koen Paelmeire on the blood -brain barrier project. I would like to thank Dr. Leybaert for his stimulating discussions of this work, for which he always showed tremendous interest. My thanks to Dr. James Sneyd for lively e-mail discussions and successful collaboration on the Ca^{2+} waves and Ca^{2+} oscillations modeling project.

I am thankful to Dr. Ann Rittenhouse and the members of her lab for readily supplying me with neonatal rat brain tissue.

I thank the members of my thesis committee that guided me in the journey of biomedical research and gave me excellent suggestions on the work in progress.

I am indebted to Dr. Thomas B. Miller, Dean of the Graduate School, for his support.

DEDICATION

Mojim dragim roditeljima, mami Nevenki i tati Andriji, kao i baki Ziti.

Mojim prijateljima u domovini.

For Brian, my best friend, without whom I would not have persevered and accomplished anything, and who reminds me daily of the true values in life.

Experiment to me
Is every one I meet.
If it contain a kernel?
The figure of a nut

Presents upon a tree,
Equally plausibly;
But meat within is requisite,
To squirrels and to me.

Emily Dickinson

ABSTRACT

Glia are non-excitable cells found in nervous tissue, and have an important role in synaptic plasticity and the maintenance of neuronal environment, as well as the activity, development, degeneration, and repair of neurons. Glial cells are interconnected via gap junctions to form a multicellular syncytium and utilize intercellular and intracellular Ca^{2+} signals to regulate their functions.

Glial Ca^{2+} signals regulate important cell functions that include gene expression, cell proliferation, metabolism, ion transport systems, release of cell products, and cell death. Consequently, significant alterations of glial Ca^{2+} signals are associated with pathological processes such as epilepsy, Alzheimer's disease and stroke. Two major forms of Ca^{2+} signals, intercellular Ca^{2+} waves and intracellular Ca^{2+} oscillations occur within glia. Intercellular Ca^{2+} waves consist of the propagation of elevations in intracellular calcium concentration ($[Ca^{2+}]_i$) between neighboring cells, while intracellular Ca^{2+} oscillations consist of repetitive elevations in $[Ca^{2+}]_i$ that remain confined to single cells.

Ca^{2+} signals are initiated by either a localized chemical, mechanical and electrical stimuli. However, the exact mechanism of their initiation, propagation and modulation is not fully understood. Previous studies have led to the hypothesis that mechanically-induced intercellular Ca^{2+} waves in glia are mediated by the diffusion of second messenger inositol (1,4,5)-trisphosphate (IP_3) through the gap junctions (GJ). However, intracellular Ca^{2+} may also diffuse between cells during the spread of intercellular Ca^{2+} wave. Alternatively, Ca^{2+}

waves may be mediated by the release of extracellular messengers, e.g. ATP, that act via phospholipase C (PLC) -linked receptors, e.g. P_{2y} receptors. It is also unknown if the propagation of Ca^{2+} waves requires the regeneration of the signaling message by each cell.

An interesting consequence of the propagation of an intercellular Ca^{2+} wave in glia is that they induce intracellular Ca^{2+} oscillations in cells that participate in its propagation. These intracellular Ca^{2+} oscillations may serve to resolve information contained in the position and strength of a local stimulus that induces intercellular Ca^{2+} wave propagation. Although the mechanism by which Ca^{2+} waves initiate Ca^{2+} oscillations is unknown it would seem likely that the mechanism of wave propagation is linked to the mechanism of initiation of Ca^{2+} oscillations. Guided by previous findings, I hypothesized that **intercellular Ca^{2+} waves propagate by the diffusion of IP_3 via gap junctions between neighboring cells to establish an intercellular gradient of IP_3 concentration ($[IP_3]_i$) that within individual cells initiates distinct intracellular Ca^{2+} oscillations.** Two specific aims were investigated to test this hypothesis. **The First Specific Aim** was to determine if **intercellular Ca^{2+} waves in glia are initiated by the generation of IP_3 within a stimulated cell, and propagated by diffusion of IP_3 molecules between neighboring cells via gap junctions. The Second Specific Aim,** was to determine if **intercellular Ca^{2+} waves induce distinct intracellular Ca^{2+} oscillations by establishing a specific gradient of oscillation-promoting $[IP_3]_i$ within the glial syncytium.**

The initiation and propagation of intercellular Ca^{2+} waves and intracellular Ca^{2+} oscillations were examined in primary cultures of rat neonatal cortical glia, utilizing the techniques of a) the intracellular measurement of $[Ca^{2+}]_i$ by fluorescence videomicroscopy, b)

the photorelease of second messengers IP_3 and Ca^{2+} from their photolabile carriers, c) the loading of specific drugs by electroporation into defined zones of glial cultures, and d) identification of cell types by immunocytochemistry.

The results of the Specific Aim 1 demonstrated the following: Mechanically-induced intercellular Ca^{2+} waves required PLC activation, the subsequent production of IP_3 within the stimulated cell, and release of Ca^{2+} from intracellular calcium stores. Propagation of Ca^{2+} waves depended on the presence of gap junctions.

The release of Ca^{2+} via IP_3 receptor/channels (IP_3Rs) was necessary for Ca^{2+} wave propagation. In contrast, release of Ca^{2+} from ryanodine receptor/channels (RyRs) occurred in the mechanically-stimulated cell as well as in cells propagating a Ca^{2+} wave, but was not required for Ca^{2+} wave initiation and propagation. The propagation of Ca^{2+} waves through cells that contained heparin to block IP_3Rs, or additional $[Ca^{2+}]_i$ buffers, demonstrated that the regeneration of IP_3 in the non-stimulated cells was not necessary for the propagation of the Ca^{2+} wave. Ca^{2+} waves were not mediated by extracellular signals, since Ca^{2+} waves were not affected by the extracellular perfusion or the inhibition of G proteins. Ca^{2+} was found to be a poor propagating signal of Ca^{2+} waves, since intercellular Ca^{2+} diffusion was not detected during Ca^{2+} wave propagation. These results are consistent with the hypothesis that Ca^{2+} waves propagate by diffusion of IP_3 molecules between neighboring cells via GJs.

The $[Ca^{2+}]_i$ increase in the stimulated cell occurred due to a Ca^{2+} influx from extracellular environment, and a release of Ca^{2+} from intracellular Ca^{2+} stores, and appeared to contribute to the activation of PLC and the generation of IP_3. Ca^{2+} influx however, was not a necessary event in Ca^{2+} wave initiation or propagation, because Ca^{2+} waves occurred in the

absence of extracellular Ca^{2+}. By contrast, a $[Ca^{2+}]_i$ increase in the absence of $[IP_3]_i$ increase did not generate intercellular Ca^{2+} waves.

The results of the Specific Aim 2 demonstrated the following: An intercellular Ca^{2+} wave induced intracellular Ca^{2+} oscillations in a zone of cells at a specific distance from the stimulated cell. The initiation, frequency and duration of Ca^{2+} oscillations depended on the cells' distance from the Ca^{2+} wave origin, and not on the cell type or the magnitude of the Ca^{2+} wave. Modulation of the $[IP_3]_i$ achieved by acetylcholine (ACh), a neurotransmitter that initiates IP_3 production, or by intracellular photorelease of IP_3 altered the oscillatory activity of individual cells and shifted the zone of oscillating cells away from the stimulated cell. Ca^{2+} oscillations spread through individual cells as an intracellular Ca^{2+} wave that was initiated from a specific site within the cell, independent of the orientation of the initial intercellular Ca^{2+} wave. These results are consistent with the hypothesis that an intercellular Ca^{2+} wave initiates Ca^{2+} oscillations by establishing a specific gradient of oscillation-promoting $[IP_3]_i$ within the glial syncytium.

The findings of this study support the hypothesis that intercellular diffusion of IP_3 is the dominant mechanism of Ca^{2+} wave propagation and initiation of Ca^{2+} wave-induced Ca^{2+} oscillations. The significance of these results is that the glial syncytium may utilize specific intracellular Ca^{2+} oscillations to decode the position and strength of stimuli that induce intercellular Ca^{2+} waves, and thus integrate and coordinate multicellular functions of glia in the CNS.

TABLE OF CONTENTS

LIST OF FIGURES

LIST OF TABLES

CHAPTER I

BACKGROUND

I-1. Glial cells in the CNS: the predominant cell group

Different types of glial cells are found throughout the vertebrate central nervous system and constitute more than 60 % of its total cell volume. Astrocytes, oligodendrocytes and macroglial cells are of ectodermal origin, whereas microglia stem from the mesoderm (Franklin and Blakemore, 1995; Kastritsis and McCarthy, 1993; McKay, 1997; Ranscht et al., 1982). The two predominant glial cell types, astrocytes and oligodendrocytes are characterized by their different morphology and function within the CNS.

Classically, astrocytes have been divided into type 1 epitheloid (or protoplasmic) and type 2 stellate (or fibrous) astrocytes, the former found in the gray matter, the later in myelinated tracts. Developmental lineage studies show that oligodendrocytes and type 2 astrocytes derive from a common bipotential progenitor cell, whereas type 1 astrocytes develop from a different precursor. Functionally, type 1 astrocytes form the glial limiting membrane, and interact with endothelial cells at the blood-brain barrier (BBB). In contrast, most type 2 astrocytes have a stellate, process-bearing morphology and ensheath axonal cell membranes at the nodes of Ranvier (McKay, 1997). One of the important

characteristics of astrocytes is the expression of the intermediate filament proteins, glial fibrilary acidic protein (GFAP) and S100. In astrocytes, GFAP expression changes during development or in pathological conditions, and increases in response to injury in activated astrocytes that surround the injury site, called "reactive" astrocytes. Astrocytes in culture probably represent reactive astrocytes since their GFAP expression increases dramatically as they respond to the culturing environment. Type 1 and 2 astrocytes differ in cell membrane receptor expression, as well as in the accumulation, transport, and metabolism of a variety of neurotransmitters. For example, differences exist in the pharmacology and efficacy of GABA transport, glutamate uptake, and neurotransmitter degrading enzymes, as well as in responses to dopamine, vasoactive intestinal polypeptide (VIP) and the β-adrenergic agonists (Verkhratsky and Kettenmann, 1996). In addition to intertype differences, data from a number of laboratories shows that differences exist among astrocytes derived from anatomically distinct regions of the CNS. Of special importance to this study are the differences in receptors linked to phosphatidyl-inositol (PI) turnover and regional specificity in gap junctional coupling of astrocytes.

Brain oligodendrocytes are heavily branched cells (characterized by immunoreactivity against galactosidase C (GalC)) that produce myelin proteins such as myelin basic protein, proteolipid protein, and myelin-associated glycoprotein. They are predominantly found in white matter, where they enwrap axons and form the myelin sheaths. In addition to isolating neuronal processes with myelin sheaths, oligodendrocytes are also involved in axonal signaling processes. They express a great variety of voltage dependent ion channels, transporter systems that release and accumulate

neurotransmitters, and receptors for excitatory and inhibitory transmitters, such as glutamate and GABA (Barres et al., 1990; Deitmer et al., 1998; McCarthy and Salm, 1991; Verkhratsky and Kettenmann, 1996; Vornov, 1998).

Oligodendrocytes from different regions of the CNS also demonstrate regional specificity in the expression of voltage-gated Ca^{2+} channels, receptors and transporter systems (Barres et al., 1988; Barres et al., 1990, 1994; Barres and Raff, 1993; Verkhratsky and Kettenmann, 1996; von Blankenfeld and Kettenmann, 1991). Interestingly, in both astrocytes and oligodendrocytes, the expression of neuroligand receptors linked to Ca^{2+} signaling appears to be controlled by glia-neuronal contacts, since preventing these contacts reduces the number of cells sensitive to neuroligands such as ATP, acetylcholine and histamine (He et al., 1996).

I-2. Functions of glia in CNS

Although previously envisioned only as supportive cells, glia cells have recently emerged as important modulators in the processes of nervous system development and the neuronal environment maintenance (Silver, 1993; Smith, 1994). Glial cells have been recognized as important participants in the development of neural tissue by providing a scaffolding for neuronal migration, and by synthesis and secretion of a variety of growth factors and extracellular matrix components (Blakemore and Franklin, 1991; Shao and McCarthy, 1994; Vernadakis, 1996). In addition, glia aid in electrical differentiation of neurons by regulating developmental changes of potassium currents that influence

neuronal repolarization and repetitive activity (Barish, 1995).

I-2.i. Glia maintain neuronal environment.

The role glia play in maintaining an optimal ionic balance in the extracellular space, which allows neurons to fire repeated action potentials, is a well known function studied in some of the earliest reports on glial physiology (Gerschenfeld et al., 1959). It has been demonstrated that neurons transmit signals to glial cells by releasing K^+ into the intercellular space during neuronal activity, simultaneously depolarizing their membrane potential. Glial cells take up excess K^+ and thus protect neurons against perturbations in the extracellular potassium concentration (Franck et al., 1978). Cl^-, HCO_3^-, and I^- anions have also been shown to be transported into astrocytes in culture. Carbonic anhydrase, an enzyme within the CNS found exclusively in glial cells, provides the substrates for both HCO_3^-/Cl^- and Na^+/H^+ exchange and thus directly contributes to acid-base homeostasis in the CNS (Delaunoy et al., 1980; Schlue et al., 1991; Spicer et al., 1979).

Astrocytes contribute to glucose utilization during neuronal activity: they are the primary site for glucose uptake and production of lactate, the principle metabolic substrate for neurons (Tsacopoulos and Magistretti, 1996). Furthermore, glycogen stores in the CNS are localized almost exclusively in astrocytes in which glycogenolysis occurs under tight control of specific neurotransmitters that, during neuronal activity, activate a specific glial receptor-mediated signaling cascade (Magistretti et al., 1993). Another interesting feature of astrocytes is their maintenance of high intracellular levels of certain antioxidants, making them resistant to oxidative stress relative to oligodendrocytes and

neurons. In response to noxious stimuli, astrocytes increase expression of antioxidant enzymes, and take up oxidized vitamin C which gets reduced to ascorbate and released by astrocytes back to extracellular fluid.

I-2.ii. Glia-neuron interactions.

New advances in glial research demonstrate a variety of multifaceted glial-neuronal interactions: glia can produce a number of neurotrophic and neuroinhibitory factors (e.g., growth hormones and steroids). Although non-excitable (i.e., non-action potential producing), glial cells express a number of plasma membrane channels and neurotransmitter receptors (Porter and McCarthy, 1997). These membrane structures make glia responsive to neuronal release of neurotransmitters or to direct coupling to neurons (Dani et al., 1992; Murphy et al., 1993). On the other hand, glial cells modulate neuronal activity in both cell cultures and organotypic CNS tissue slices (Charles, 1994; Duffy and MacVicar, 1995; Nedergaard, 1994; Pfrieger and Barres, 1996; Pfrieger and Barres, 1997).

Glia surround synapses and are actively involved in the processes of synaptic plasticity associated with cyclic physiological changes, memory and aging (Vernadakis, 1996). For example, glia-specific metabolic blocker fluoroacetate inhibits spontaneous and induced synaptic transmission in the hippocampus (Keyser and Pellmar, 1994). Glia have also been noted to cyclically insert and retract their processes into synaptic clefts within nucleus arcuatus, one of the control centers for production and release of hormones in CNS, and thus either block or allow propagation of neuronal stimuli within the nucleus

(Garcia-Segura et al., 1994, 1995).

I-2.iii. Glia-endothelial cells interaction.

Different glial cell types interact not only with neurons, but also with other cell types, such as are endothelial cells. Close physical contacts and physiologic interactions between endothelial cells of brain capillaries and glia constitute the basis of the blood-brain barrier (Abbott et al., 1992; Leybaert et al., 1998). The transport of nutrients and therapeutic drugs through the BBB, as well as barrier breakdown due to infection and increased intracranial pressure, are only a few of the important physiological and pathophysiological reactions that occur due to intercellular signaling between glial and endothelial cells.

I-3. Non-synaptic glial signaling

A characteristic common to all glial interactions within CNS is that a variety of local stimuli can cause the activation of glial cells far from the initial point of stimulation via inter-glial signaling. Signaling between glial cells is non-synaptic: one mechanism involves the cytoplasmic exchange of ions and small molecules which is accomplished by glial coupling via intercellular channels, i.e., gap junctions.

I-3.i. Gap junctional connectivity.

Gap junctions are intercellular channels that consist of two hemi-channels, integral membrane protein assemblies called connexons, which span the plasma membranes of two adjacent cells and join together to form a narrow, extracellular "gap." Connexons are hexamers formed from connexins (Cx), a highly related multigene family of proteins consisting of 13 members cloned so far in mammals (Dermietzel and Spray, 1993, 1998; Evans, 1994; Giaume and Venance, 1995; White et al., 1995). Gap junction coupling is characteristic of astrocytes and oligodendrocytes both in vivo and in vitro. In addition to homologous coupling between cells of the same cell type, heterologous coupling has been observed between astrocytes and oligodendrocytes (Venance et al., 1995), endothelial cells (Abbott et al., 1992; Leybaert et al., 1998), ependymal cells (Miragall et al., 1997; Wouterlood et al., 1984), and neurons (Dermietzel, 1998; Dermietzel and Spray, 1993; Fulton, 1995; Wouterlood et al., 1984). In glia, astrocytes have been found to express Cx 43, Cx 45, Cx 40 and possibly Cx 30 and Cx 46 (Dermietzel et al., 1991; Hossain et al., 1994; Nagy et al., 1997; Scemes et al., 1998; Dermietzel and Spray 1998), while oligodendrocytes express Cx 32 and Cx 45 (Kunzelmann et al., 1997; Li et al., 1997; Nagy et al., 1997). Therefore, astrocyte-oligodendrocyte gap junctions demonstrated by coupling studies in vitro (Ochalski et al., 1997; Venance et al., 1995) may be formed by heteromeric hemi-channels made from different connexins, junctions homologously composed of single Cx type, or junctions composed of heterotypic hemi-channels (i.e., each hemi-channel composed of different types of connexins). Ependymal cells express both Cx 43 and Cx 26 and form homologous and/or heterologous gap junctions with

astrocytes (Miragall et al., 1997; Wouterlood et al., 1984). Finally, neurons express Cx 32 and Cx 26 in the developing and adult brain, and electrical coupling studies and Ca^{2+} imaging offer evidence of the existence of functional gap junctions between astrocytes and neurons (Connors et al., 1984; Murphy et al., 1993; Nedergaard, 1994; van den Pol et al., 1992).

Once considered to be fairly non-selective channels that participate in the bi-directional exchange of molecules of up to approximately 1 kd in size, gap junctions are now recognized as a diverse group of channels that vary in their permeability, voltage-sensitivities, and potential for modulation by intracellular factors (Blanc et al., 1998; Goodenough et al., 1996; Rorig and Sutor, 1996; Scemes and Spray, 1998; Wolburg and Rohlmann, 1995; Yeager and Nicholson, 1996). Therefore, the gap junction-mediated functions of glia are dependent on their Cx composition, and specific sensitivities to transjunctional voltage (Enkvist and McCarthy, 1994), intracellular pH (Anders, 1988; Connors et al., 1984; Negishi et al., 1985; Spray et al., 1985), PKC activation (Enkvist and McCarthy, 1992), $[Ca^{2+}]_i$ and phosphorylation state (Enkvist and McCarthy, 1994; Hossain et al., 1994; Kwak et al., 1995 a,b). The diversity of gap junctions and their susceptibility to regulation by neuromodulators and neurotransmitters (Hampson et al., 1992; Johnston, 1996; Rorig and Sutor, 1996; Spray et al., 1985) results in a potentially highly complex signaling system in the glial syncytium. One important consequence of gap junctions formed of different connexin types is chemical and electrical rectification that may allow selective passage of intracellular molecules only in one direction (Dermietzel and Spray, 1998).

I-3.ii. Extracellular diffusion of signals.

As a second mode of non-synaptic signaling, glia can synthesize, accumulate, and subsequently release and respond to a number of extracellularly diffusing signals. Astrocytes synthesize several eicosanoides, angiotensinogen, enkephalin peptides, thyroid, insulin-like and nerve growth factors, neuropeptide Y, somatostatin, steroids, taurine, adenine nucleotides, GABA and glutamate. The synthesis of these neuroactive substances occurs in response to variety of physiological agonists or drugs (for review, see Martin, 1992). Glia release synthesized neuroactive substances like glutamate (Chiu and Kriegler, 1994; Diamond et al., 1998; Parpura et al., 1994), ATP (Guthrie et al., 1999), GABA (New and Rabkin, 1998; Sacchettoni et al., 1998), and nitric oxide and nitric oxide precursors (Bakardjiev, 1998; Grima et al., 1997). Finally, glia also possess a range of neurotransmitters and neuropeptide receptors that make glia responsive to a wide variety of neuroactive compounds generated by neurons and other cell types present in the CNS (Porter and McCarthy, 1997).

I-3.iii. Non-synaptic signaling in glia mediates intercellular Ca^{2+} waves.

The mechanism by which glia encode local stimuli into stimuli-specific long-distance signals, that evoke specific actions in glial cells hundreds of micrometers away from the site of local stimuli, is presently uncertain. Interestingly, modulations in $[Ca^{2+}]_i$ are the signals that are involved in both global and local glial actions during the physiological and pathophysiological processes described in previous sections of this

review. One of the important functions of both modes of non-synaptic glial signaling is the generation and propagation of intercellular Ca^{2+} waves, which are signals that are hypothesized to provide temporal and spatial coordination of glial gene expression, ion channel activation, and release of neurotrophic factors (Charles, 1998). Modulations of glial $[Ca^{2+}]_i$ are the focus of this study and will be discussed in more detail.

I-4. Calcium signals in glial cells

I-4.i. Calcium homeostasis in glial cells.

The intracellular Ca^{2+} concentration in glial cells is tightly regulated. $[Ca^{2+}]_i$ is determined by the interaction of molecules that transport Ca^{2+} (e.g., Ca^{2+}-permeable channels), cytoplasmic calcium buffers, and intracellular organelles, such as endoplasmic reticulum (ER) and mitochondria, which are able to accumulate, store, and release Ca^{2+} and together form intracellular Ca^{2+} stores (ICSs) (Finkbeiner, 1993; Kostyuk and Verkhratsky, 1994) (**Fig. 1**).

Figure 1: Molecules involved in intracellular Ca^{2+} signaling in glia.

Ca^{2+}-BP = Ca^{2+} binding proteins, VGCC = voltage gated calcium channel, SOCC = stores operated calcium channel, IR = ionotropic receptor, MR = metabotropic receptor, PLC = phospholipase C, IP_3R = IP_3 receptor / channel, RyR = ryanodine receptor / channel, SERCA = sarco/endoplasmic reticulum Ca^{2+} ATP-ase pump, GJ = gap junction. Ca^{2+} enters glial cell via VGCC, SOCC, IR, MR, or Na^+/Ca^{2+} exchanger, and is buffered in cytoplasm by Ca^{2+}-BP, or alternatively, is stored in the ER due to SERCAs activity and in mitochondria due to an electrochemical gradient. Free Ca^{2+} ions may activate/inhibit RyRs and IP_3Rs and thus modulate Ca^{2+} release from ER.In micromolar concentrations Ca^{2+} activates PLC.

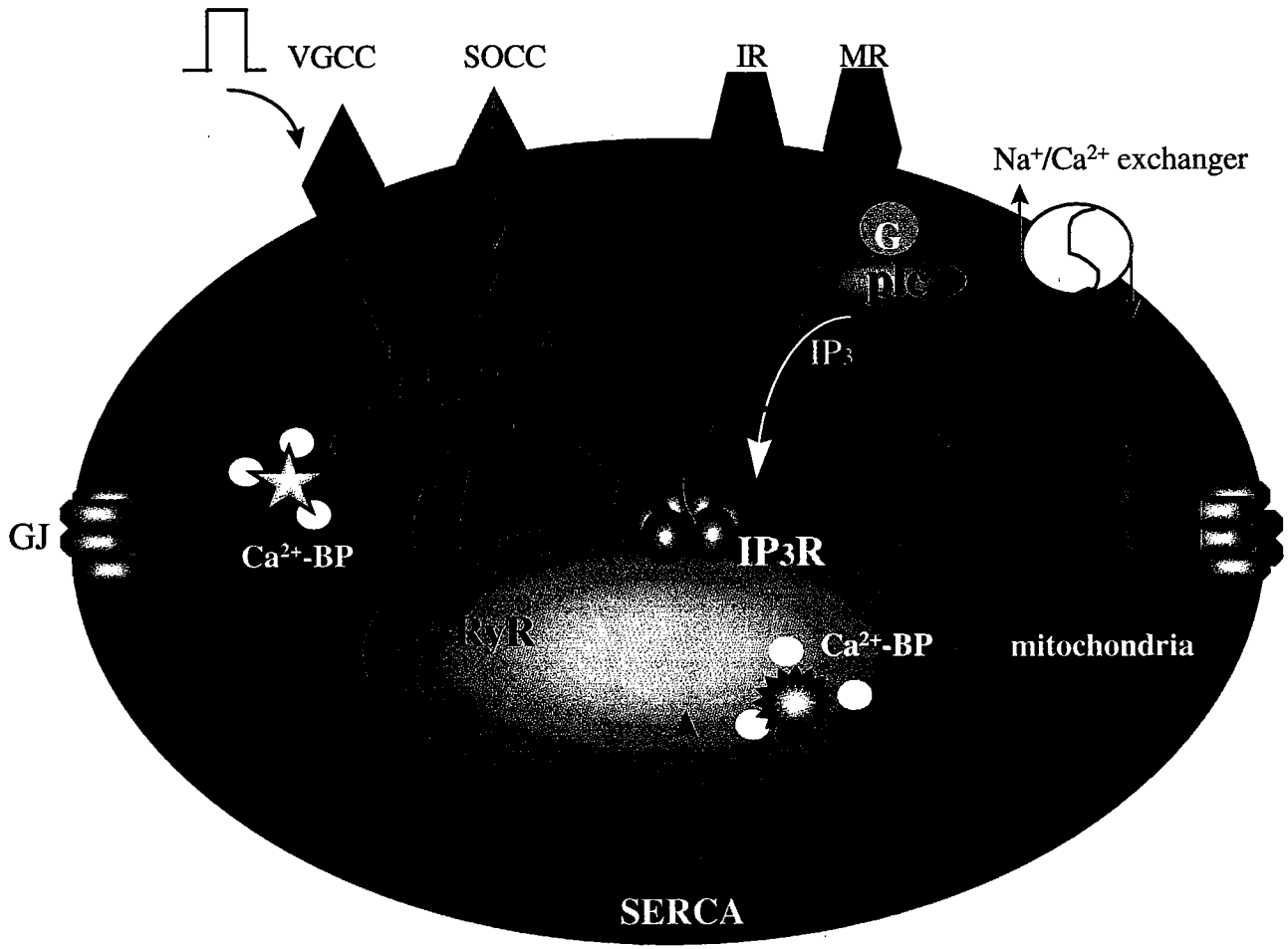
VGCC
SOCC
IR
MR
Na+/Ca2+ exchanger
G
IP3
GJ
Ca2+-BP
IP3R
RyR
Ca2+-BP
mitochondria
SERCA

Figure 1

In glia, the molecules that transport Ca^{2+} are represented by several superfamilies of transmembrane Ca^{2+} permeable channels, ATP-driven Ca^{2+} pumps, and electrochemically driven Ca^{2+} exchangers (Pozzan et al., 1994). The actions of these molecules result in Ca^{2+} fluxes that either deliver or remove Ca^{2+} from the cytoplasm. Most intracellular Ca^{2+} is associated with intracellular Ca^{2+} stores (ICSs) and only a minor part is in the form of free cytoplasmic Ca^{2+}. The rest of the Ca^{2+} in the cytoplasm is trapped by endogenous Ca^{2+} - binding proteins which are responsible for the Ca^{2+}-buffering capacity of the cytoplasm. Measurements of the resting $[Ca^{2+}]_i$ in glial cells vary from 30 to 200 nM (Finkbeiner, 1993). Different resting $[Ca^{2+}]_i$ have been reported not only among different glial subtypes, but also within the same population of cells. The variation of $[Ca^{2+}]_i$ probably reflects differences in the levels and functional states of intracellular proteins involved in maintenance of Ca^{2+} homeostasis that may exist within a population of glial cells, although method-induced artifacts may contribute to the variability of measurements (Finkbeiner, 1993).

I-4.ii. Ca^{2+}permeable channels.

There is a steep electrochemical gradient favoring Ca^{2+} entry into glial cells from the extracellular environment. Influx of Ca^{2+} occurs in glia via voltage-gated or ligand-gated Ca^{2+} channels. In freshly isolated and cultured glial cells, membrane depolarization achieved by elevating extracellular K^+ concentration may result in 3-5 fold increases in $[Ca^{2+}]_i$ (Sontheimer, 1994). Both astrocytes and oligodendrocytes have been shown to express a variety of voltage-gated Ca^{2+} channels that were previously believed to

be present only in electrically excitable cells. Studies utilizing electrophysiological techniques have demonstrated that the parameters of glial Ca^{2+} currents (Ica), and the types of Ca^{2+} channels expressed varies in cells of different origins: for example, hippocampal astrocytes coexpress T-, L- and N-type Ca^{2+} channels, while optic nerve astrocytes coexpress only T- and L-type Ca^{2+} channels (Akopian et al., 1996; Barres et al., 1988, 1990). Furthermore, cortical astrocytes, but not striatal astrocytes respond to depolarization with an increase in $[Ca^{2+}]_i$ (Bender et al., 1998; Duffy and MacVicar, 1994). Similarly, cortical oligodendrocytes express both T-type and L-type Ca^{2+} currents, while oligodendrocytes isolated from optic nerve did not reveal Ca^{2+} currents (Barres et al., 1988; Kirischuk et al., 1995).

The opening of voltage-gated Ca^{2+} channels requires depolarization (**Fig. 1**). This depolarization might normally result from local changes in K^+ concentration that accompany neuronal activity. Alternatively, depolarization of the glial cell membrane may be achieved by the binding of different neuropeptides to their receptors on glia: for example, GABA, neuropeptide Y, bradykinin and angiotensin II can cause cell depolarization and the subsequent entry of Ca^{2+} via voltage-gated channels (Verkhratsky and Kettenmann, 1996).

Ca^{2+} may also enter the glial cytoplasm by passing through ligand-gated cationic channels that are abundantly expressed in all glial cell subtypes (Araque et al., 1998; Belachew et al., 1998; Bender et al., 1998; Dani and Smith, 1995). For example, glutamate acts on AMPA/kainate ionotropic glutamate receptors present on glial cell membranes (Cornell-Bell et al., 1990; David et al., 1996) and raises $[Ca^{2+}]_i$ in cultured

cerebral, hippocampal, and cerebellar astrocytes (Finkbeiner, 1993).

I-4.iii. Inositol trisphosphate-induced $[Ca^{2+}]_i$ increase.

Another important mechanism of $[Ca^{2+}]_i$ increase in glia is activation of the second messenger IP_3 signaling cascade, which causes Ca^{2+} release from IP_3-sensitive ICSs. The production of IP_3 is achieved by the activation of phospholipase C (PLC), an enzyme coupled to a number of cell membrane receptors. For example, stimulation of metabotropic glutamate receptors, adrenergic $\alpha 1$ receptors, P_{2y}, P_{2u} receptors, serotonergic $5HT_{1A}$ receptors, muscarinic M_1 and M_3 receptors, H_1 histaminic receptors, and substance P receptors results in elevation of $[IP_3]_i$ in glia **(Fig. 1)** (Porter and McCarthy, 1997, 1996).

PLC binds to the lipid interface of cell membrane and forms multiple contacts with the substrate phosphatidylinositol 4,5-bisphosphate (PIP_2), which is then hydrolyzed into the second messenger molecules IP_3 and diacylglycerol (DAG). PLC is a family of enzymes consisting of three major classes: PLC β, PLC γ, and PLC δ. PLC β isoforms are activated in response to the binding of an agonist to a G-protein coupled receptor, while PLC γ isoforms are activated by receptors with tyrosine kinase activity. Interestingly, PLCs are Ca^{2+}-dependent enzymes, since Ca^{2+} stabilizes the enzyme-substrate complex during catalysis (James and Downes, 1997). Furthermore, conserved EF domains in PLCs are necessary for the catalytic activity of these enzymes. All PLC isoenzymes can be activated by micromolar levels of Ca^{2+} in vitro, and Ca^{2+} influx may cause PLC activation

in neuronal and other tissues (Baird and Nahorski, 1990; Chandler and Crews, 1990; Eberhard and Holz, 1988). On the other hand, lower concentrations of Ca^{2+} may influence agonist-induced PLC activity (James and Downes, 1997). Interestingly, the response pattern of PLC to $[Ca^{2+}]_i$ rise differs from that produced by an agonist (i.e., Ca^{2+}-activated phosphoinositide metabolism generates IP_2 more markedly than IP_3), and indicates that Ca^{2+}-dependent hydrolysis may involve different pools of lipids, PLC enzymes, or both (Baird and Nahorski, 1990). PLC δ isoenzymes are more sensitive to Ca^{2+} when compared to the other isoenzymes. Since neither the receptors nor transducers that are coupled to PLC δ isoform are known, activation of PLC δ might occur secondary to receptor-mediated activation of other PLC isozymes or Ca^{2+} channels (Mangoura et al., 1995). In cortical astrocytes, PLC can be activated by extracellular Ca^{2+} entering the cell (Balazs et al., 1998). It appears that for certain agonists, such as glutamate, Ca^{2+} influx is the primary trigger for PLC activation in oligodendrocytes, most probably through the involvement of PLC β (Liu et al., 1997).

I-4.iv. Endoplasmic reticulum as an intracellular Ca^{2+} store.

Intracellular calcium stores (ICSs) in glial cells are the crucial component of $[Ca^{2+}]_i$ modulation. Glia contain an elaborate endoplasmic reticulum (ER) that serves as the major ICS (Golovina et al., 1996; Golovina and Blaustein, 1997; Pozzan et al., 1994) and regulates cytosolic $[Ca^{2+}]_i$ by releasing Ca^{2+} that is sequestered within the lumen of ER through two types of intracellular Ca^{2+} channels, IP_3 receptor/channels (IP_3Rs) and

ryanodine receptor/channels (RyRs), and by the accumulation of Ca^{2+} within ER due to the activity of sarco/endoplasmic reticulum Ca^{2+}-ATPases (SERCAs) (**Fig. 1**). Ca^{2+} release from ER can occur via IP_3Rs, or RyRs, or both, depending on which channels are present in the ER. The current data indicates that glial cells contain both IP_3-sensitive and Ry-sensitive intracellular Ca^{2+} stores (Golovina et al., 1996; Golovina and Blaustein, 1997).

I-4.iv.a. IP_3 receptors.

The major glial mechanism for Ca^{2+} release from ICSs involves the activation of IP_3-gated IP_3Rs located on the ER's surface (Charles et al., 1993; Finkbeiner, 1992; Giaume and Venance, 1998) that occurs in response to a number of neurotransmitters and neurohormones (Finkbeiner, 1993). The direct activation of IP_3Rs by photorelease of IP_3 from a caged compound was shown in cultured astrocytes (Khodakhah and Ogden, 1993; Leybaert et al., 1998), with a measured $[IP_3]_i$ threshold for IP_3R activation of 0.2-0.5 μM (Khodakhah and Ogden, 1993).

To date, at least three IP_3R isoforms have been distinguished: IP_3R1, IP_3R2 and IP_3R3. Functional IP_3R channels are tetrameric complexes consisting of either homologous or heterologous isoforms (Berridge, 1993; Pozzan et al., 1994). Differential distribution of the specific IP_3R isoforms in different glial cells has not yet been clearly demonstrated. Western blotting and immunocytochemistry of cultured cortical astrocytes demonstrated high levels of the IP_3R2 isoform (Sheppard et al., 1997). In other studies of rat cortical astrocytes and cerebellar Bergmann glial cells, only IP_3R3 and not IP_3R1 and

IP_3R2 were immunolocalized to astrocytes (Yamamoto-Hino et al., 1995). In contrast, cerebellar astrocytes were reported to express IP_3R1 and IP_3R2 (Oberdorf et al., 1997). Finally, Western blot experiments that I carried out on the cultures of perinatal cortical astrocytes detected the presence of IP_3R1 in these cells. Oligodendrocytes transiently express IP_3R1 receptors during the onset of myelination, but continuously express IP_3R2 at much higher levels than IP_3R1 (Dent et al., 1996).

The structure of IP_3R reveals channel properties important for its function. The amino terminus is conserved among all members of the IP_3R family and possesses IP_3 binding activity (Mikoshiba et al., 1993). Studies on IP_3R kinetics have determined that the binding of at least three molecules of IP_3 to the IP_3R tetramer is necessary for opening of the channel (Marchant and Taylor, 1997; Marchant and Taylor, 1998). An interesting property of IP_3Rs is that cytosolic Ca^{2+} acts as a coagonist of IP_3Rs at low $[Ca^{2+}]_i$, but inactivates IP_3R at high $[Ca^{2+}]_i$ (Bezprozvanny et al., 1991; Finch et al., 1991). This property of Ca^{2+}-mediated activation of IP_3Rs, termed calcium induced calcium release (CICR), followed by Ca^{2+}-mediated inhibition of Ca^{2+} release via IP_3Rs frequently results in repetitive increases and decreases in $[Ca^{2+}]_i$ called Ca^{2+} oscillations (Hajnoczky and Thomas, 1997). In single channel studies, the Ca^{2+} dependence of cerebellar IP_3Rs activity, monitored at 2 μM IP_3, is described by a bell-shaped curve that peaks at 0.25 μM Ca^{2+} (Bezprozvanny et al., 1991). Interestingly, for lower concentrations of IP_3, the peak of the Ca^{2+}-dependence curve shifts to lower Ca^{2+} concentrations (Kaftan et al., 1997). IP_3Rs have both high affinity (Michikawa et al., 1996; Mikoshiba, 1997) as well as low affinity Ca^{2+} binding sites, which accounts for the shift in the Ca^{2+} dependence curve at low IP_3

levels and the maintained channel activity at high Ca^{2+} and IP_3 levels. This differential Ca^{2+} dependence found in IP_3Rs allows the cell to abbreviate the rise of intracellular $[Ca^{2+}]_i$ in the presence of low levels of IP_3, but also provides means of maintaining high intracellular $[Ca^{2+}]_i$ during periods of prolonged stimulation (Kaftan et al., 1997). On the other hand, prolonged exposures to constant $[IP_3]$ without alterations in $[Ca^{2+}]_i$ lead to inactivation of IP_3R (Mak and Foskett, 1997). The activation of IP_3Rs by sequential binding of IP_3 and Ca^{2+} results in a narrow temporal window during which each receptor subunit must bind both of its agonists if the channel is to open rather than inactivate (Marchant and Taylor, 1997; Marchant and Taylor, 1998).

The interactions of the IP_3R with other intracellular proteins are multifaceted: ATP increases both frequency and duration of IP_3R channel opening (Bezprozvanny and Ehrlich, 1993), PKA increases sensitivity to IP_3 (Hajnoczky et al., 1993), and calmodulin, ankyrin, and phosphatidylinositol 4,5-bisphosphate (PIP_2) inhibit IP_3R channel opening (Bourguignon et al., 1993; Cardy and Taylor, 1998; Lupu et al., 1998).

Resolving the properties of IP_3R isoforms is currently in progress. Interesting reports have demonstrated that IP_3R1 and IP_3R3 are differentially modulated by cytosolic Ca^{2+}: an increase in $[Ca^{2+}]$ inhibits IP_3 binding to IP_3R1 by decreasing the number of IP_3-binding sites (Bmax) without affecting their affinity for IP_3. Conversely, increasing $[Ca^{2+}]$ first stimulates IP_3 binding to IP_3R3 by increasing Bmax, and then inhibits it, by causing a decrease in the affinity of the receptor for IP_3 (Cardy et al., 1997).

I-4.iv.b. Ryanodine receptors.

The expression in glia of another type of intracellular Ca^{2+} release channel, the ryanodine receptor (RyR), is still a matter of some debate (Ehrlich, 1995; Furuichi et al., 1994; Striggow and Ehrlich, 1996). RyRs were originally found in the sarcoplasmic reticulum of skeletal muscle and thought to be a component of excitation-contraction coupling, but have later been found in other tissues, and particularly in the CNS (Furuichi et al., 1994). In astrocytes, the release of calcium from RyRs is controversial. For example, the RyR agonist caffeine was shown to trigger a Ca^{2+} increase in cultured embryonic cortical astrocytes (Golovina and Blaustein, 1997), but several observations in cultured and freshly isolated astrocytes failed to detect an obvious caffeine-triggered effect (Charles et al., 1993; Duffy and MacVicar, 1994). On the other hand, ryanodine and dantrolene were shown to modulate Ca^{2+} responses in cortical astrocytes and trigger Ca^{2+} elevation in Bergman glial cells (Charles et al., 1993; Kirischuk et al., 1995; Langley and Pearce, 1994). In oligodendrocytes, attempts to pharmacologically activate RyRs by caffeine and ryanodine did not result in $[Ca^{2+}]_i$ elevations (Kirischuk et al., 1995). Finally, immunocytochemical studies have identified RyRs in cultured astrocytes and oligodendrocytes (Simpson et al., 1998). In this study, caffeine-elicited increases in $[Ca^{2+}]_i$ were specifically inhibited by ryanodine pretreatment, while ionotropic glutamate receptor activation was found to fill the caffeine-sensitive stores in these cells (Simpson et al., 1998). To date, three isoforms of RyR have been described. The CNS RyR family is composed of all three isoforms, RyR 2 being predominant type in the brain. Unfortunately, differential distribution of the three isoforms among glia is presently unknown (Furuichi et

al., 1994).

One of the major regulators of RyRs is Ca^{2+} itself, which can both potentiate and inhibit Ca^{2+} release. This phenomenon of calcium induced calcium release (CICR) was first described in cardiac muscle RyRs and seems to be a general property of the RyR family. It has been proposed that Ca^{2+} released from IP_3Rs may cause Ca^{2+} release from RyRs, and thus augment $[Ca^{2+}]_i$ increase (Pozzan et al., 1994). RyRs, just as IP_3Rs, display a bell-shaped activation curve: increasing cytosolic $[Ca^{2+}]_i$ in the low micromolar range stimulates channel opening, while further elevation of cytosolic $[Ca^{2+}]_i$ is inhibitory. RyR channel activity can also be affected by various modulators and compounds, including Mg^{2+}, ATP, calmodulin (CaM), ruthenium red, procaine, and spermidine (Ehrlich, 1995; Pozzan et al., 1994).

RyRs in glia are predominantly activated by Ca^{2+} derived from either external or internal sources. Ca^{2+} release via RyR may also be modulated or triggered directly by means of the putative second messenger cyclic adenosine disphosphate ribose (cADPR). By analogy to IP_3, an external stimulus would promote an increase in the level of cADPR, which would then act on the RyRs to initiate the release of Ca^{2+}. Like IP_3Rs, which are sensitive to IP_3 and Ca^{2+}, RyRs might be under dual agonist control, since cADPR was found to sensitize the process of CICR in sea urchin homogenates (Lee, 1993). To fully establish a second messenger role for cADPR more evidence is needed to show that external stimuli act to increase the level of this messenger. In glial physiology, the role of cADPR is presently unclear. Recent studies have demonstrated high activity of enzymes that are involved in production of cADPR in glial cultures, but not in neuronal cultures

(Pawlikowska et al., 1996).

I-4.iv.c. Ca^{2+} storage and capacitative Ca^{2+} entry.

Calcium ions in ICSs cannot all remain free in the lumina, and require efficient mechanisms of storage. Calreticulins, proteins segregated in the lumen of ER, are Ca^{2+} storing proteins, and have high capacity and low affinity to Ca^{2+}. Calreticulins do not include molecularly recognizable Ca^{2+}-binding sites; instead, Ca^{2+} interacts with clusters of acidic amino acids localized in the COOH-terminal domain of the protein (Pozzan et al., 1994). The amount of Ca^{2+} stored in ICSs may regulate a distinct type of plasmalemmal Ca^{2+} permeability: it is widely recognized that the depletion of Ca^{2+} stores activates a capacitative Ca^{2+} influx via an unknown messenger (Hofer et al., 1998; Peuchen et al., 1996). This influx is associated with the activation of specific, putative ICS-operated plasmalemmal Ca^{2+} channels (SOCC, **Fig. 1**) (Clementi and Meldolesi, 1996). The existence of these channels in glial cells has not been clearly shown, although there are number of indications that they may play an important role in Ca^{2+} homeostasis in gliomas (Hildebrandt and Hildebrandt, 1997; Reetz and Reiser, 1996), and astrocytes (Prothero et al., 1998; Tuschick et al., 1997).

I-4.iv.d. Ca^{2+} transporters.

There are two basic subgroups of calcium transporters in glial cells: sarco/endoplasmic reticulum ATP-ase pumps (SERCAs), plasmalemmal Ca^{2+} pumps and Na^{+}/Ca^{2+} exchangers (Finkbeiner, 1993; Pozzan et al., 1994). Transmembrane fluxes of

Ca^{2+} mediated by Na^{+}/Ca^{2+} exchangers are controlled by extracellular Na^{+} concentration (Kiedrowski et al., 1994; Kim et al., 1994) which when lowered, increases $[Ca^{2+}]_i$, reduces the efflux of Ca^{2+}, and affects the kinetics of stimulus evoked $[Ca^{2+}]_i$ (Benninger et al., 1980; Cornell-Bell and Finkbeiner, 1991).

Calcium ATP-ase pumps are essential for removing cytosolic Ca^{2+} into ICSs. Three different genes encode three isoforms of Ca^{2+} ATP-ase pumps, SERCA 1 SERCA 2, and SERCA 3. SERCA 2 and SERCA 3 are expressed in the CNS, and it appears that, due to their different biochemical properties, the relative expression of different isoforms is of great importance to the fine modulation of ICSs activity. For example, SERCA 3 has a significantly lower Ca^{2+} affinity than other isoforms, while SERCA 2 exhibits a reduced turnover rate (Pozzan et al., 1994). There are two major regulators of SERCAs: dephosphorylated phospholamban inhibits SERCAs, while calmodulin lowers the Km of SERCAs for Ca^{2+}. SERCAs are also regulated by phosphorylation via cyclic nucleotide-dependent protein kinases.

I-4.v. Mitochondria as intracellular Ca^{2+} stores.

Mitochondria can also act as intracellular Ca^{2+} stores. The driving force for Ca^{2+} uptake into mitochondria is provided by the mitochondrial membrane potential established by the activity of the respiratory chain. The role of mitochondria in Ca^{2+} homeostasis in glial cells is poorly understood. The dissipation of the mithochondrial electrochemical gradient by protonophores triggers Ca^{2+} release in oligodendrocytes but does not influence the kinetics of depolarization-induced $[Ca^{2+}]_i$ changes (Kirischuk et al.,

1995). On the other hand, in cultured astrocytes, histamine induced Ca^{2+} oscillations are accompanied by oscillations in intramitochondrial free Ca^{2+}, and norepinephrine-induced $[Ca^{2+}]_i$ increases result in simultaneous mitochondrial $[Ca^{2+}]$ increases (Jou et al., 1996). Therefore, mitochondria may contribute to glial calcium signaling under physiological conditions by acting predominantly as a sink for Ca^{2+} ions released from ER.

I-4.vi. Spatio-temporal organization of calcium signals.

I-4.vi.a. Intercellular Ca^{2+} waves.

One form of long-distance signaling in glia are intercellular Ca^{2+} waves, which consist of sequential elevations of $[Ca^{2+}]_i$ that propagate between cells. Mechanical or electrical stimulation and exposure to a variety of chemical signals initiate intercellular Ca^{2+} waves (Charles et al., 1991; Cornell-Bell and Finkbeiner, 1991; Cornell-Bell et al., 1990; Sanderson, 1995; Hassinger et al., 1996; Sanderson, 1996). Intercellular Ca^{2+} waves can be propagated by signals that spread either through the intracellular space (Charles et al., 1992; Finkbeiner, 1992; Nedergaard et al., 1995; Newman and Zahs, 1997; Sanderson et al., 1994; Venance et al., 1997), or through the extracellular space (Guthrie et al., 1999; Hassinger et al., 1996), or both. In rat glial cells, a large number of studies suggest that the mechanical stimulation and focal application of several neurotransmitters induces intercellular Ca^{2+} waves predominantly via the diffusion of the second messenger IP_3 from the cell acting as the Ca^{2+} wave origin, through the gap junctions, to adjacent cells (Charles et al., 1992; Finkbeiner, 1992; Nedergaard et al., 1995; Newman and Zahs, 1997; Sanderson et al., 1994; Venance et al., 1997) (**Fig. 2**).

The hypothesis that IP_3 diffusion is the mechanism of intercellular Ca^{2+} wave propagation is supported by the findings that PLC activation (Hansen et al., 1993; Venance et al., 1997), IP_3-sensitive intracellular Ca^{2+} stores (Boitano et al., 1992; Charles et al., 1991, 1993; Cornell-Bell et al., 1990; Finkbeiner, 1993; Nadal et al., 1997; Venance et al., 1997) and functional gap junctions (Charles et al., 1992; Finkbeiner, 1992; Venance et al., 1995) are required for propagation of intercellular Ca^{2+} waves initiated by Ca^{2+} influx, mechanical stimulation, exposure to glutamate, albumin, endothelin and electrical stimuli in rat glial cell cultures.

An alternative mechanism for Ca^{2+} wave propagation involving an extracellular messenger released by a stimulated cell has been demonstrated in some other cell types, as well as in mouse cortical astrocytes (**Fig 2.**) (Guthrie et al., 1999; Hansen et al., 1993; Hassinger et al., 1996; Zanotti and Charles, 1997). After electrical or mechanical stimulation of a single mouse glial cell, the induced Ca^{2+} waves cross cell-free zones within the culture, and can be inhibited by extracellular flow.

The mechanism that propagates intercellular Ca^{2+} waves seems to be species-specific: while studies carried out in rat glia suggest that propagation of intercellular Ca^{2+} waves occur by diffusion of a signal through intracellular spaces of gap junction-connected glial cells, studies carried out in mouse glial cultures suggest that intercellular Ca^{2+} waves propagate via diffusion of an extracellular messenger (**Table 1**). The search for possible exogenous factors in rat glia have yielded no results, since both ATP-

Figure 2: Propagation of the intercellular Ca^{2+} wave. Propagation occurs by diffusion of IP_3, or IP_3 and Ca^{2+} molecules between neighboring cells via gap junctions. Alternatively, propagation occurs by diffusion of a messenger (e.g., ATP) through the extracellular space.

PLC = phospholipase C,

ICS = intracellular calcium store,

GJ = gap junctions,

IP_3R = IP_3 receptor.

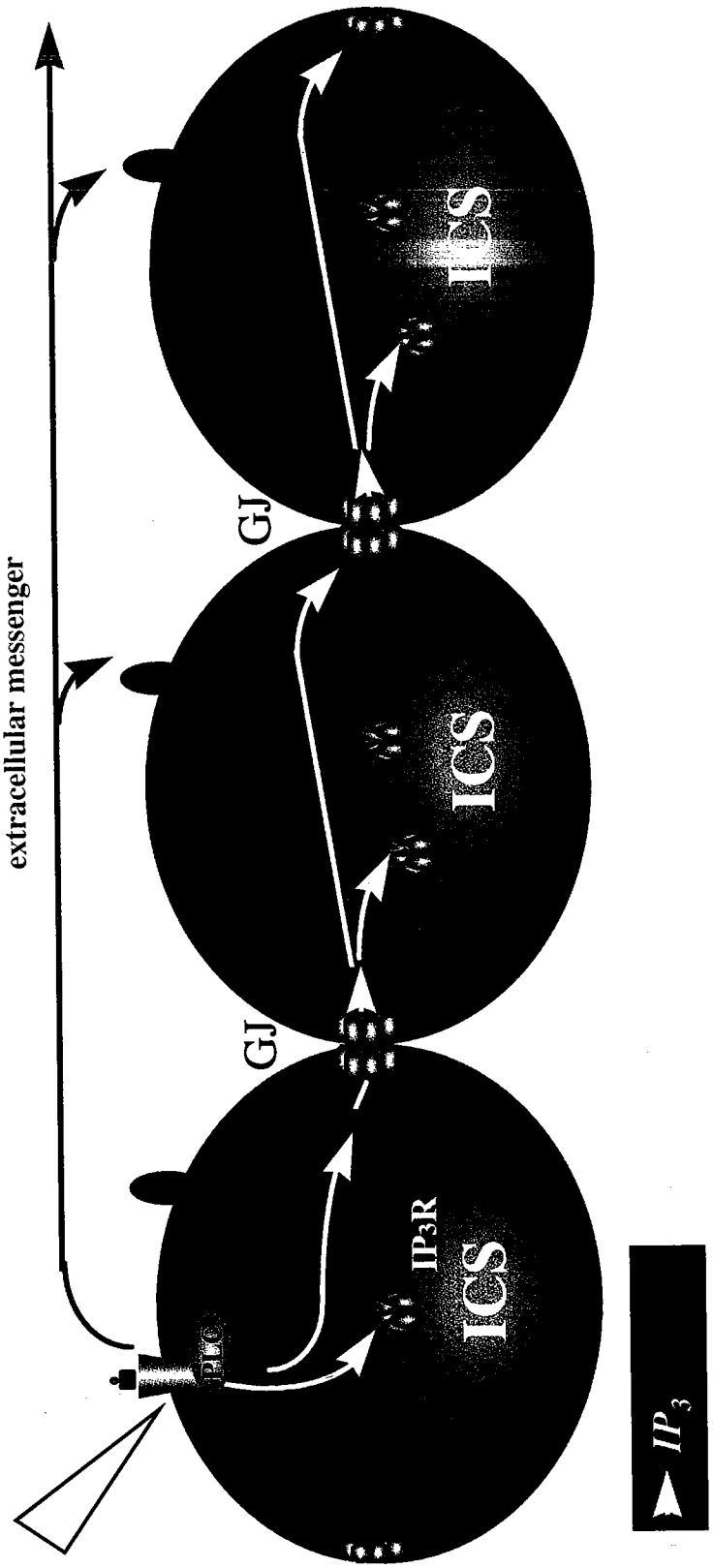

Figure 2

degrading enzyme (Venance et al., 1997) and glutamate receptors antagonists (Fatatis and Russell, 1992; Venance et al., 1997) show no significant effect on Ca^{2+} waves. In contrast, recent study by Guthrie et al., (1999) suggested that, in mouse astrocytes, Ca^{2+} waves propagate by extracellular diffusion of ATP.

The existence of these two Ca^{2+} wave-propagating mechanisms, intracellular and extracellular, implies that these mechanisms may work in concert. Furthermore, Ca^{2+} waves may regulate different glial functions by utilizing different modes of wave initiation and propagation (Lee et al., 1994; Venance et al., 1998). Since glial cells have been found to exhibit regional specificity in gap junction coupling as well as in sensitivity to different neurotransmitters, it can be expected that in different regions of the CNS glial Ca^{2+} waves may be quantitatively and qualitatively different. In support of this idea is the finding that only subpopulations of astrocytes express specific purinergic receptor subtypes (Ho et al., 1995). Furthermore, Ca^{2+} waves are blocked by anandamide in rat striatal astrocytes (Venance et al., 1995), but not in cortical astrocytes, showing regional specificity of gap junction conductivity and mechanisms of Ca^{2+} wave propagation in the CNS (Guan et al., 1997).

Table 1: Mechanism of propagation of Ca^{2+} waves depends on the species (modified from Giaume and Venance, 1998)

References	species	mechanism of Ca^{2+} wave propagation (ways tested)
	RAT	
Glaum et al.,1990 **Fatatis and Russel, 1992** **Newman and Zahs, 1997**	hippocampus, cerebellum, cortex rat isolated retina	GJ MEDIATED (no effect of flow)
Enkvist and McCarthy, 1992 **Finkbeiner, 1992**	cortex hippocampus	GJ MEDIATED (2-mt-ATP, PMA, octanol, halothane)
Venance et al., 1995 **Madden et al., 1996** **Nadal et al., 1997** **Venance et al., 1997**	striatum hippocampus cortex striatum	GJ MEDIATED (anandamide, octanol halothane, AGA)
Charles et al, 1992	C6 glioma cell line	GJ MEDIATED (no propagation unless GJ expression)
	MOUSE	
Naus et al., 1996	striatum, whole brain	EXTRACELLULAR (not blocked by AGA)
Hassinger et al., 1996 **Zanotti and Charles, 1997**	cortex forebrain	EXTRACELLULAR (blocked by perfusion)
Guthrie et al., 1999	cortex	EXTRACELLULAR ATP (blocked by perfusion)
Yamasaki et al, 1994	203 glioma cell line	EXTRACELLULAR (propagate waves w/out GJ)
Naus et al., 1997 **Scemes et al., 1998**	Cx 43 knockout MOUSE	EXTRACELLULAR (ATP) + GJ MEDIATED (residual Cx 40, Cx 45, Cx 46) (suramin, AGA, heptanol)

Different mechanisms of intercellular Ca^{2+} wave propagation can influence one another. For example, depolarizing ligands, such as is glutamate secreted by glia, enhance gap junction communication between cells, thus maintaining increased communication between cells in the face of elevated $[Ca^{2+}]_i$ during Ca^{2+} wave propagation (Enkvist and McCarthy, 1994). On the other hand, expression of gap junctions in gap junction-deficient cell lines enables Ca^{2+} wave propagation by enhancement of ATP release (Cotrina et al., 1998; Cotrina et al., 1998). Therefore, one mechanism of wave propagation does not exclude the other, on the contrary, it is easy to envision that the combination of gap junctional communication and release of an extracellular messenger may be involved in intercellular Ca^{2+} wave propagation in vivo.

To date, the source of the signal that propagates Ca^{2+} waves has not been clearly demonstrated. A number of studies favor passive diffusion of a messenger generated at the Ca^{2+} wave origin (Sanderson, 1995; Sanderson et al., 1994; Sneyd et al., 1995a; Sneyd et al., 1998), while others point to diffusion of a messenger generated not only by the stimulated cell but also, in a sequential manner, regenerated along the path of the Ca^{2+} wave (Giaume and Venance, 1998; Guthrie et al., 1999; Hassinger et al., 1996; Venance et al., 1997).

Although a number of in vitro studies, that will be discussed later in detail, suggest an important role of Ca^{2+} waves in a range of physiological and pathological processes within brain, it is unclear whether intercellular Ca^{2+} waves occur in intact nervous tissue. Intercellular Ca^{2+} waves in brain tissue have only recently been demonstrated in organotypic hippocampal slice cultures after stimulation of mossy fibers (Dani et al.,

1992). The intercellular Ca^{2+} waves in this study however, propagated for shorter distances than observed in dissociated cell cultures, which might be due to a higher degree of coupling of glial cells in dissociated cell cultures. Propagating Ca^{2+} waves generated by intracellular Ca^{2+} release and mediated by gap junctions were also recorded in glial cells from acutely isolated rat retina after stimulation by ATP, carbachol, and phenylephrine (Newman and Zahs, 1997). Neurophysiological studies have identified changes in blood flow, electrical activity and CNS metabolism that are propagated with spatio-temporal properties that are similar to those of glial Ca^{2+} waves observed in culture (Lauritzen and Fabricius, 1995; Woods et al., 1994), suggesting that glial Ca^{2+} waves are likely to participate in intercellular signaling in the brain in vivo. A study conducted in freely moving rats suggests that intercellular Ca^{2+} waves participate in responses to physiological stimuli eliciting a specific animal grooming behavior by inducing the release of glutamate from glia (Miele et al., 1996) .

I-4.vi.b. Intracellular Ca^{2+} oscillations.

A second common form of glial Ca^{2+} signaling are $[Ca^{2+}]_i$ modulations that stay confined within single cells. The time course of a cell's $[Ca^{2+}]_i$ increase may be a single spike, an initial peak followed by a plateau, or intracellular Ca^{2+} oscillations (Cornell-Bell et al., 1990; Finkbeiner, 1993). Ca^{2+} oscillations consist of repetitive elevations in $[Ca^{2+}]_i$ within a single cell that can be induced in glia by glutamate, noradrenaline, serotonin, ATP, acetylcholine, and endothelin (Goldman et al., 1991; Kim et al., 1994; Nilsson et al., 1991; Yagodin et al., 1994). In general, Ca^{2+} oscillations are driven by CICR through IP_3R

sensitized with IP_3 (Bezprozvanny et al., 1991; Finch et al., 1991; Iino and Endo, 1992). The frequency at which Ca^{2+} oscillations occur and the appearance of an alternative single spike and plateau response seems to depend on agonist concentration and therefore, ultimately on $[IP_3]_i$ (Berridge, 1993; Berridge and Dupont, 1994). In glia, this agonist concentration/$[Ca^{2+}]_i$ response dependence was demonstrated for glutamate, norepinephrine, histamine and endothelin (Cohen and Almazan, 1993; Cornell-Bell et al., 1990; Dave et al., 1991; Duffy and MacVicar, 1995; Fukui et al., 1991; Goldman et al., 1991; Wood et al., 1993). Interestingly, in contrast to intercellular Ca^{2+} waves, Ca^{2+} oscillations usually occur asynchronously in populations of cells and do not propagate to neighboring cells. Therefore, it is particularly interesting to find that intercellular Ca^{2+} waves can initiate Ca^{2+} oscillations in the same cells through which they pass (Charles et al., 1991).

In addition to a complex temporal pattern, glial Ca^{2+} signaling exhibits intracellular spatial heterogeneity. Ca^{2+} responses of astrocytes to neurotransmitters reveal two distinct intracellular oscillatory behaviors. Norepinephrine-induced intracellular Ca^{2+} oscillations originate from a single intracellular site (Yagodin et al., 1994) whereas histamine-induced oscillations arise from multiple intracellular sites (Inagaki and Wada, 1994). Similarly, in ATP- and KCl-stimulated oligodendrocytes, $[Ca^{2+}]_i$ rises first in the cell processes and then spreads toward the soma (Kirischuk et al., 1995; Kirischuk et al., 1995). One explanation for these observations is that each cell is unique in its distribution of intracellular calcium stores and store-forming proteins that, although part of highly motile endoplasmic reticulum, occupy distinct intracellular positions due to extensive interactions

with the cytoskeleton (Bourguignon et al., 1993; Pozzan et al., 1994).

I-5. Role of Ca^{2+} waves and Ca^{2+} oscillations in glial physiology

Changes in glial Ca^{2+} have been implicated in gene regulation and cytoskeletal changes (Finkbeiner, 1993). In order to modulate these important processes, Ca^{2+} binds to a number of proteins that trigger various intracellular signal transduction pathways. For example, the cytoplasmic Ca^{2+} sensor calmodulin (CaM) regulates the activity of three classes of enzymes: CaM-dependent protein kinases, protein phosphatases and adenylate cyclases. These enzymes interact with other cytoplasmic proteins, or transfer the signal further down to the nucleus, initiating pathways responsible for gene expression (De Koninck and Schulman, 1998; Inagaki et al., 1997). Alternatively, Ca^{2+} activates Ras proteins that in turn trigger a cascade of phosphorylation events that lead to the modulation of gene expression (Finkbeiner and Greenberg, 1996). For example, Ca^{2+} and agents that mimic or elevate cAMP play a role in regulation of astrocyte and Schwann cell GFAP genes (Reeves et al., 1994; Thomson et al., 1993). Although not yet demonstrated in glial cells, cytoplasmic Ca^{2+} signals have been found to propagate to the nucleus and directly stimulate the synthesis of immediate early genes and structural genes products (Finkbeiner and Greenberg, 1997, 1998).

Temporal and spatial characteristics of Ca^{2+} waves and Ca^{2+} oscillations may be utilized by glia in the regulation of diverse intracellular and multicellular processes. The specificity of reactions to different signals which lead to changes in $[Ca^{2+}]_i$ within the

single cell seems to be achieved by different spatio-temporal patterns of Ca^{2+} changes. Glial cells are able to differentiate between ATP, norepinephrine and endothelin stimuli by responding with different $[Ca^{2+}]_i$ patterns in different cellular regions (Finkbeiner, 1993; Kirischuk et al., 1996). Thus, increases in glial Ca^{2+} achieved specifically by exposure to norepinephrine regulate the uptake of GABA and glutamate into astrocytes. Ca^{2+} oscillations may also achieve their signaling specificity by oscillatory frequency modulation, as seen in the control of the rate of fluid secretion by salivary glands, glycogen metabolism by liver cells, and neuronal differentiation (Berridge, 1997). Alternatively, differential gene transcription can be achieved through amplitude modulation as is the case in B lymphocytes (Dolmetsch et al., 1997). Glial Ca^{2+} oscillations may also play a role in the higher functions of the CNS such as memory. Recent studies in astrocytes have described long-term changes in the response elicited by glutamate in the form of long-lasting modifications in the $[Ca^{2+}]_i$ oscillatory response, demonstrating that in the CNS cellular memory is not a feature unique to neurons (Pasti et al., 1995, 1997).

A number of studies indicate that a change in glial $[Ca^{2+}]_i$ affects glial K^+ channels and thus modulates glial K^+ buffering function (Cooper, 1995). Ca^{2+} waves might play a mediating role in glia as a regulator of ionic balance in the extracellular environment by providing "spatial buffering" of K^+. Increases in Ca^{2+} induce glycogen breakdown and trigger release of neuroactive substances; an intercellular Ca^{2+} wave could be involved in coordinating these processes. Glia respond to the lowering of external $[Ca^{2+}]_i$ with intercellular Ca^{2+} waves that involve release of Ca^{2+} from the intracellular stores

potentially in order to replenish extracellular Ca^{2+} levels (Zanotti and Charles, 1997). Intercellular Ca^{2+} waves in glial cells may be involved in the physiology of sleep, since anandamide, a sleep inducing compound, inhibits intercellular coupling and intercellular Ca^{2+} waves in glia (Venance et al., 1995). Glial Ca^{2+} waves may also participate in the processes of growth and development in the CNS. The extent to which connexin molecules act as supressors of growth is unclear. In a study by Charles et al. (1992) the extent of propagation of intercellular Ca^{2+} waves in C6 glioma cell lines transfected with Cx43 correlated with the reduced rate of culture proliferation. On the other hand, astrocytes cultured from Cx 43 knockout mice display a retarded growth rate when compared to astrocytes cultured from wild type mice (Naus et al., 1997).

I-5.i. Glial Ca^{2+} waves and oscillations and neuron-glial interactions.

The coordination of neuronal and glial activity requires that signals pass from one cell type to another. As discussed before, neurons release a variety of substances, neurotransmitters, peptides, amines and hormones which diffuse through extracellular space and may thus influence neurons and glia alike. Both peripheral and central glial cells are found to sense neuronal activity and neuron-released substances, and initiate, in response, a specific pattern of glial Ca^{2+} signals (Chiu and Kriegler, 1994; Duffy and MacVicar, 1995; Jahromi et al., 1992; Parpura et al., 1994; Parpura et al., 1995). For example, in neuronal-glial co-cultures, selective stimulation of neurons with NMDA triggered $[Ca^{2+}]_i$ spikes and oscillations in the neighboring astrocytes (Dani and Smith, 1995). Electrical stimulation of presynaptic afferents in hippocampal slices triggered glial

Ca^{2+} oscillations that changed their frequency in proportion to the change of stimulus frequency (Pasti et al., 1997).

Conversely, glial Ca^{2+} signals may trigger Ca^{2+} signals in neurons. This phenomena was first observed in glial-neuronal co-cultures, and appears to be mediated by signal propagation through gap junctions (Nedergaard, 1994). Newer studies have demonstrated that glial Ca^{2+} waves induced by mechanical, electrical, or agonist stimulation, result in Ca^{2+} signals in neurons in cultures from visual cortex, hippocampus and forebrain (Charles, 1994; Hassinger et al., 1995; Parpura et al., 1994). In these experiments, glial-to-neuronal Ca^{2+} signaling was sensitive to a glutamate receptor antagonist, suggesting a primary role of glial release of glutamate. Neurotransmitter-induced alterations in levels of $[Ca^{2+}]_i$ in glia may be a mechanism for regulating gene expression in perisynaptic glial cells thus triggering changes that can stabilize the synapse or enhance synaptic activity (Jahromi et al., 1992).

I-5.ii. Glial Ca^{2+} waves and Ca^{2+} oscillations in neuropathology.

Modulations of glial Ca^{2+} signals have been implicated in a number of pathophysiological processes such as reactive injury gliosis, epileptic seizure activity, migraine and Alzheimer's disease (Compston, 1995; Flint and Kriegstein, 1997; McMillian and Hong, 1994; McMillian et al., 1994; Mollace and Nistico, 1995). Within hours after CNS injury, the phenotype of glial cells significantly changes in areas immediately adjacent to the injury, as well as in areas hundreds of micrometers away. These phenotypically changed "reactive" glial cells multiply and migrate towards the injury site, initially

promoting recovery of injured neurons and neuronal tracts, but ultimately causing the generation of glial scarring tissue. The initial stimuli causing these long term changes are not well understood: there is some evidence that intercellular Ca^{2+} waves are triggering factors in glial responses to brain insults (Compston, 1995; Matsuda et al., 1998; McMillian et al., 1994; Qi and Dawson, 1993; Rzigalinski et al., 1998; Vornov, 1998). In vivo and in vitro studies of ischemic damage revealed that exposure of astrocytes to hypoxic/hypoglycemic conditions triggers an increase in $[Ca^{2+}]_i$ as a result of activation of voltage gated Ca^{2+} channels and Ca^{2+} release from ICSs (Duffy and MacVicar, 1996; Haun et al., 1992). This ischemia-induced increases in $[Ca^{2+}]_i$ in astrocytes are predominantly caused by agents released from damaged neurons, such as are neurotransmitters and elevated K^+ concentration (Duffy and MacVicar, 1996).

The mechanism of Ca^{2+} waves initiation and propagation is probably altered by the processes of neurodegeneration. In trisomy 16 mice, an animal model of Down's syndrome and Alzheimer's disease, a dysfunction in calcium homeostasis leading to increased $[Ca^{2+}]_i$ and ICS's Ca^{2+} capacity has been reported (Bambrick et al., 1997) suggesting abnormal properties of both glial Ca^{2+} oscillations and Ca^{2+} waves in these diseases.

The propagation of seizure activity from a single locus of abnormal neuronal firing to surrounding areas occurs in part due to the spreading of intercellular Ca^{2+} waves through populations of glial cells that surround the firing neurons. Interestingly, glial cells within foci of seizure activity display increased interconnectivity, which is demonstrated as an increase in levels of Cx proteins (Delgado-Escueta et al., 1986; Flint and Kriegstein,

1997; Lee et al., 1995; Manning and Sontheimer, 1997). Furthermore, an increase in spontaneous oscillatory activity has been observed in astrocytes from patients with epilepsy (Manning and Sontheimer, 1997). In the pathophysiology of headache and migraine, the seizure-like propagation of Ca^{2+} waves through populations of glia is one of the hypothesized mechanisms (Leibowitz, 1992).

Astrocytes play an important role in glutamine-induced neurotoxicity and neurodegeneration. In contrast to neurons, astrocytes appear to tolerate very high glutamate concentrations (Kanai et al., 1993). Glutamate is taken up from the extracellular space and subsequently metabolized to glutamine by astrocytes, but not by neurons (Yu et al., 1982). This process is carried out by the astrocyte-exclusive enzyme glutamine synthetase (Derouiche and Frotscher, 1991). One factor contributing to an increase in extracellular glutamate is the failure of high affinity glutamate uptake by astrocytes. The reversal of Na^{2+}-dependent uptake is a major route of excitatory amino acid efflux from astrocyte cultures under conditions of energy failure that occur during cerebral ischemia (Longuemare and Swanson, 1995). This change in extracellular glutamate during ischemia initiates a series of neurotoxic events, possibly involving the generation of intercellular Ca^{2+} waves and an increase in glial oscillatory activity.

There is a growing amount of evidence which suggests the participation of glial Ca^{2+} signals in infectious and immune disorders. Pathological Ca^{2+} signals in glial cells are triggered by the HIV-1 virus envelope protein gp120. This protein induces Ca^{2+} increases in both astrocytes and oligodendrocytes, but not in neurons (Benos et al., 1994; Lipton, 1994; Lipton, 1994). Glial $[Ca^{2+}]_i$ increases have also been demonstrated after exposure of

glial cells to a fragment of the infectious prion (Florio et al., 1996). Oligodendrocytes react to complement exposure by initiation of Ca^{2+} oscillations (Wood et al., 1993). Prostaglandins formed by glia in response to pro-inflammatory agents have been found to induce astrocytes to release glutamate in Ca^{2+} wave-inducing concentrations, suggesting the participation of Ca^{2+} waves in a number of prostaglandin-mediated infectious and immune diseases (Bezzi et al., 1998).

I-6. Thesis objectives

Within past years, contradicting studies have been reported explaining the mechanism of initiation and propagation of Ca^{2+} signals in glia. This study focuses on the characterization and mechanisms of glial intercellular Ca^{2+} waves and intracellular Ca^{2+} oscillations. I was particularly interested in determining how intercellular Ca^{2+} waves, which propagate for long distances, induce spatially and temporally characteristic local intracellular Ca^{2+} oscillations. Since this process induces specific responses in glial cells far from the site of initial stimulus, Ca^{2+} wave-induced Ca^{2+} oscillations might represent one of the mechanisms that glial cells utilize in the interpretation of local stimuli that induce propagating Ca^{2+} wave signals. By utilizing mechanical initiation of intercellular Ca^{2+} waves in the cultures of rat cortical glia, and selective inhibition or activation of proteins involved in glial Ca^{2+} signals, the necessary processes involved in two major aspects of intercellular Ca^{2+} waves, initiation and propagation, were determined. Furthermore, the necessary requirements for the induction of Ca^{2+} oscillations were also investigated. The

dependency of both the propagation of intercellular Ca^{2+} waves and initiation of Ca^{2+} oscillations on $[IP_3]_i$ may provide a common factor (i.e., intercellular messenger) that couples the propagation of the long-distance Ca^{2+} signals to the initiation of specific, local intracellular Ca^{2+} signals.

Since cells in a glial culture express robust intercellular Ca^{2+} waves as well as intracellular Ca^{2+} oscillations, glial cultures are an excellent model to study the processes and mechanisms of Ca^{2+} signaling in multicellular systems. The results obtained in this study will therefore bring a further understanding of Ca^{2+} signaling in other types of multicellular, syncytium-forming systems, such as are smooth muscle and epithelial cells. More importantly, a better understanding of the fundamental processes that underlie many physiological and pathophysiological actions of glia reviewed above offer more clues in the understanding of complex, glia-dependent processes within the CNS.

CHAPTER II

MATERIALS AND METHODS

II-1. Cell culture

Primary cultures of mixed glial cells were prepared from the brains of 2-3 day old rat pups (Cole and de Vellis, 1989). After removal of the meninges, forebrains were chopped into 1 mm pieces and triturated with a Pasteur pipette. A cell suspension was obtained by filtering the tissue sequentially through 1) a Nitex mesh (210 × 210 μm openings, Teteco, New York, NY), 2) a #60 mesh and 3) #100 mesh in a Cellector sieve (E-C Apparatus Corp, St Petersburg, FL). Isolation medium consisted of a 1:1 mixture of Dulbecco's modified Eagle medium and F-12 medium (DMEM/F12), supplemented with L-glutamine, 15 mM HEPES and 1.2 g/l sodium bicarbonate (Gibco, Gaithersburg, MD). Dissociated cells were plated at 2×10^5 cells/cm^2 on poly-L-lysine-coated round glass coverslips (incubated 1 hr in 10 μg/ml poly-L-lysine, 15 mm diameter, Carolina Biological) and cultured at 37 °C in 5 % CO_2 for 15 - 20 days in DMEM/F12, 10 % fetal calf serum (FCS) and penicillin (100U/ml), streptomycin (100 μg/ml) and amphotericin B (0.25μg/ml) (Gibco). Culture medium was changed every 4 - 5 days.

II-2. Identification of cell types

Immunofluorescence staining for cell specific markers was performed to quantify the different cell types in the culture. Astrocytes, oligodendrocytes, and neurons in cultures were identified by staining for glial fibrilary acidic protein (GFAP), galactosidase C (GalC), and neurofilaments (NF), respectively. Cultures were fixed with cold acetone for 15 min, washed in phosphate buffered saline without Ca^{2+} or Mg^{2+} (PBS, Gibco), and incubated with polyclonal rabbit antibodies to GFAP (1:100 dilution, Chemicon, Temecula, CA; AB1980), GalC IgG (1:60 dilution, Sigma G9152), or NF IgG (1:200 dilution, Chemicon; AB1981) for 30 min at room temperature. Cells were washed in PBS and incubated with goat anti-rabbit IgG, conjugated with FITC (1:100 dilution, # F0511, Sigma, St Louis, MO) for 30 min. To preserve cells after staining, coverslips were washed in PBS, covered with mounting medium (Sigma), and sealed with nail polish.

To correlate cell identity with changes in $[Ca^{2+}]_i$, cells were double-stained with antibodies to GFAP and GalC on the microscope stage immediately after the $[Ca^{2+}]_i$ measurements were made, without moving the cover-slip. After fixation (15 min, acetone, 4 °C), coverslips were incubated with Cy3-conjugated monoclonal mouse anti-GFAP antibodies (30 min, 1:400 dilution, C-9205, Sigma) and washed with PBS. Images of Cy3 fluorescent cells were digitally collected with a silicon intensified target camera (Cohu, San Diego, CA) and averaged to reduce noise. The excitation wavelength was 535 nm (bandwidth 35 nm), the emission wavelength was 570 nm (bandwidth 30 nm). To reduce

non-specific binding of antibodies, coverslips were incubated in a blocking solution of 10% goat serum for 10 min. Cells were then incubated with rabbit anti-GalC antibody (1:50 dilution, 30 min, Sigma G9152), washed again with PBS, and incubated with FITC-conjugated goat anti-rabbit antibody (1:100 dilution, 30 min, Sigma F0511). To control for cross reactivity of the FITC-conjugated secondary antibody, cells stained with anti-GFAP Cy3-conjugated antibodies were incubated with the FITC secondary antibody only. After washing, digitally averaged images of FITC fluorescent cells were obtained from the same place on the coverslip (excitation wavelength 485 nm, bandwidth 22 nm, emission wavelength 535 nm, bandwidth 35 nm). To further identify and verify the presence of the cells within the observed area, a phase-contrast image of the same area was acquired after obtaining images of FITC and Cy3 fluorescence. Cells which only bound anti-GFAP were identified as astrocytes, while cells which bound anti-GalC were identified as oligodendrocytes. Cells which bound both anti-GFAP and anti-GalC were identified as cells of mixed phenotype or precursor cells (Raff et al., 1983; Ranscht et al., 1982; Skoft and Knapp, 1995; Trotter and Schachner, 1989). For clarity, images of antibody staining were presented with pseudocolor. The color scale represented a linear intensity of a single color.

II-3. Mechanical stimulation

Mechanical stimulation of a single cell was performed by distorting the cell surface

with a micropipette attached to piezoelectric element (Sanderson et al., 1990). After aligning the micropipette over a single cell, a single square-wave voltage pulse of 3.0-3.6 V was applied to the pipette to displace the cell membrane 2-3 μm downward for 150 ms.

II-4. Measurements of $[Ca^{2+}]_i$ with fura-2

The measurement of $[Ca^{2+}]_i$ was performed as previously described (Charles et al., 1991; Leybaert et al., 1998). Cultured cells were loaded with the Ca^{2+}-specific reporter dye fura-2 by incubating in 2.5 μM fura-2-AM (Calbiochem, La Jolla, CA) in Hanks' balanced salt solution (without phenol red) supplemented with HEPES buffer (25 mM, Sigma; HBSS-HEPES) for 45 min at 37°C. The cells were then washed with, and placed in HBSS-HEPES for at least 30 min at room temperature to allow for the de-esterification of the fura-2. Excitation wavelengths of 336 and 380 nm (bandwidth 15 nm) were produced by filtration of a 100 W Hg arc lamp. A 405 nm dichroic mirror was used to separate excitation from emitted light. Emitted fluorescence was observed through a 510 nm filter (bandwidth 40 nm). Cellular fluorescence was observed with a Nikon Diaphot microscope (Nikon, Garden City, NY) fitted with a x 40 Fluor, 1.3 NA lens. Images of fura-2 fluorescence were recorded with a silicon intensified target camera (Cohu, San Diego CA) and stored on an optical memory disc recorder (Panasonic, TQ-3031F). The recorded field of view was either 283 x 213 μm or 336 x 253 μm. Absolute $[Ca^{2+}]_i$ values were calculated by substituting the 336/380 intensity ratio (R) of double wavelength measurements into the equation Kd(Sf/Sb)(R-Rmin)/(Rmax-R) (Grynkiewicz et al., 1985)

where Kd (224 nM) is the dissociation constant of fura-2, Rmin is the ratio of 336/380 intensity at 0 [Ca^{2+}] and Rmax is the ratio at 1 mM [Ca^{2+}]. Values of Rmin, Rmax, and Sf/Sb were calculated from the calibration measurements of fluorescence of 50 μM fura-2 pentasodium salt diluted in 0 and 1 mM [Ca^{2+}] solutions (Charles et al., 1991).

Experiments were recorded in two distinct modes: 1) single wavelength real-time video imaging in which images of fluorescence were recorded at 30 images per second, and 2) single wavelength time-lapse video imaging in which images of fluorescence were recorded every 0.5 or 1 seconds. In real-time experiments, conventional 336 and 380 nm image pairs were obtained at the beginning of the recording, while in time-lapse experiments, these image pairs were obtained every 30 sec. The $[Ca^{2+}]_i$ calculated from these image pairs served as reference points for the single wavelength measurements (Leybaert et al., 1998) and were subsequently used to construct image maps of $[Ca^{2+}]_i$ (Charles et al., 1991). To determine $[Ca^{2+}]_i$ changes with respect to time, small areas of 6x6 pixels (3.3 x 2.6 μm) were selected for each cell (average cell diameter 25 μm) in the field of view and averaged fluorescence values were obtained from sequential images and converted to $[Ca^{2+}]_i$. The boundaries of wave propagation were easily determined when the wave was initiated in a corner of the field of view. All fluorescent images were subjected to background subtraction, shading correction, and linearization prior to calculating ratios.

II-5. Measurements of $[Ca^{2+}]_i$ changes with fluo-3

In experiments that required the uncaging of photolabile molecules, $[Ca^{2+}]_i$ imaging

was performed with fluo-3. Cultured cells were loaded with the Ca^{2+} specific reporter dye fluo-3 by incubation in 10 μM fluo-3-AM and HBSS-HEPES. An excitation light wavelength of 485 nm was produced by filtration of a 100W mercury arc. Emitted fluorescence was observed through a 535 nm filter. Changes in $[Ca^{2+}]_i$ during experiments were calculated by substituting intensity of fluo-3 fluorescence at a time t (Ft) into equation $(Ft-F_0)/F_0$ where F_0 was the intensity of fluo-3 fluorescence at time zero. Experiments were recorded by time-lapse video imaging, in which images of fluo-3 fluorescence were recorded every 0.5 or 1 seconds.

II-6. Experimental solutions

Mechanical stimulations were performed in HBSS-HEPES. Acetylcholine (ACh), acetylmethylcholine (AMCh), ATP, thapsigargin, and caffeine were added by exchanging the extracellular solution with a similar solution containing the desired concentration of a drug. The high potassium (50 mM K^+) and calcium-free (0 Ca^{2+} and 2 mM EGTA) HBSS solutions were applied to the cells by exchanging the volume of extracellular solution bathing the cells. As a control for specific experiments, the extracellular solution was exchanged with control (HBSS only) solution.

Gap junction blocker 18 α glycyrrhetinic acid (AGA, Sigma G-8503) was first dissolved in DMSO and later diluted with HBSS to a working concentration of 10 μM. Saturated gap junction blocker halothane solution in HBSS was made by adding 10 ml of

halothane (Sigma, B-4388) to 30 ml of HBSS. After 2 days, HBSS saturated with halothane was used for experimentation. Similar saturated solutions of halothane have been measured by chromatography to contain 16-17 mM halothane (Burt and Spray, 1989). Experimental solutions were made by diluting saturated stock solution with HBSS.

In experiments examining the dependence of wave-induced Ca^{2+} oscillations on $[IP_3]_i$, ACh application was performed by adding 10 µl of 20 mM ACh in HBSS-HEPES to 490 µl of bath solution (HBSS-HEPES) to achieve a final concentration of 400 µM. This concentration was experimentally determined to be the concentration which altered the Ca^{2+} signaling in 90% of the cells that propagated a Ca^{2+} wave. Acetylcholine applications were performed 100-120 s after initiation of an intercellular Ca^{2+} wave.

II-7. Extracellular perfusion

The propagation of Ca^{2+} waves via an extracellular messenger was tested by extracellular perfusion. Perfusion of the cell cultures with extracellular medium was carried out by placing a coverslip with cell culture on the bottom of the custom-made perfusion chamber (approx. measures 30 x 15 x 5 mm) that was connected to a reservoir of extracellular solution on one end, and to a vacuum suction on the opposite end of the chamber. Rate of perfusion was 4 ml/min.

Alternatively, the perfusion of the cell cultures grown on electroconductive coverslips was achieved by attaching the coverslip to wax ridges so that they form a channel, and placing glass pipettes, one connected to a reservoir of the extracellular

solution and other to a vacuum suction, at each end of the channel.

II-8. Flash photolysis of 'caged' compounds

The photolabile compound o-nitrophenyl EGTA (NP-EGTA, N-6803, Molecular Probes) was loaded into cells loaded with fluo-3 by incubating in 2.5 μM NP-EGTA-AM in HBSS-HEPES for 10 min at room temperature (Leybaert et al., 1998). When required, the photorelease of Ca^{2+} from NP-EGTA was achieved by exposing the cells to a focused point source of the ultraviolet (UV) light (**Fig. 3a**). The UV flash was delivered by a HG-arc lamp coupled to the epifluorescence input via a dichroic mirror with a cut-off at 400 nm and focused to the field diaphragm with a biconvex lens (focal distance 250 mm) (**Fig. 3b**). The exposure time was controlled by a mechanical shutter (uniblitz, Vincent Associates, Rochester, NY). The UV spot had a diameter of 7.1 mm, as determined by flashing a dried layer of caged fluorescein dextran (MW 3000, Molecular Probes). $[Ca^{2+}]_i$ was continuously monitored during exposure to the UV light.

To ensure that the Ca^{2+} buffering properties of NP-EGTA do not significantly alter the cells' physiological responses, cells were tested for their ability to propagate intercellular Ca^{2+} waves in response to mechanical stimulation before and after NP-EGTA loading. Longer incubations and/or higher concentrations however, had significant Ca^{2+} buffering effects.

In order to monitor changes in $[Ca^{2+}]_i$ induced by uncaging of the photolabile carrier of IP_3 D-myo-inositol 1,4,5-trisphosphate, P4(5)-(1-(2-nitrophenyl)ethyl) ester trisodium salt

(i.e., "caged IP_3", Molecular Probes, I-13801) simultaneously within all the cells in culture, cells were loaded with Ca^{2+} reporter dye fluo-3. When required, recording of fluo-3 fluorescence was quickly interrupted and the photorelease of IP_3 from its photolabile carrier was achieved by exposing the culture to UV light for 3 seconds. After the flash, the recording of changes of fluo-3 fluorescence was resumed. The optimal duration of the UV flash was determined by a series of experiments in which flashes of different lengths were used to uncage dextran-caged flourescein (100 μM, 3000 MW, Molecular Probes). The ratio of florescence intensity before and after the flash was used to determine the shortest flash that will uncage the maximum number of flourescein molecules.

Figure 3: Flash photolysis of 'caged Ca^{2+}'. a) Exposure to UV light releases the caged molecule (i.e., NP-EGTA, represented as a green sphere) from its carrier (brown). b) Diagram of the imaging system used in flash photolysis experiments: the first lamp generates UV light required for photolysis, while the second lamp generates the excitation wavelengths for fluo-3 fluorescence.

a

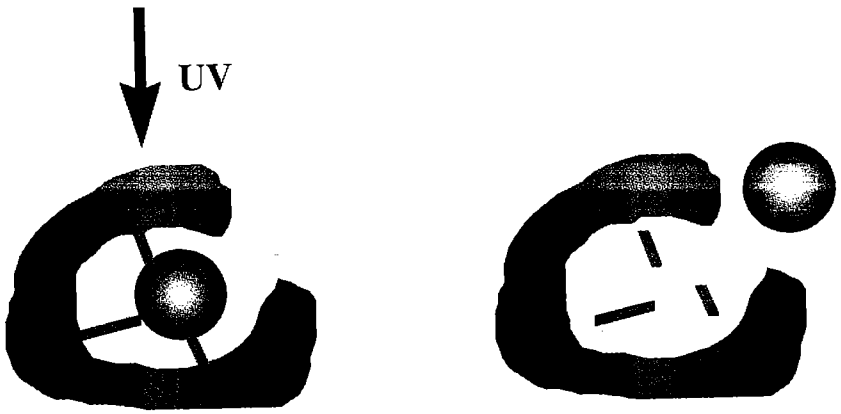

NP-EGTA "caged calcium"

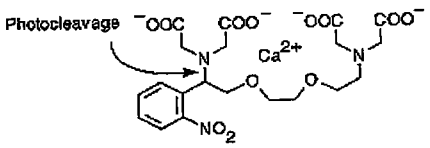

b

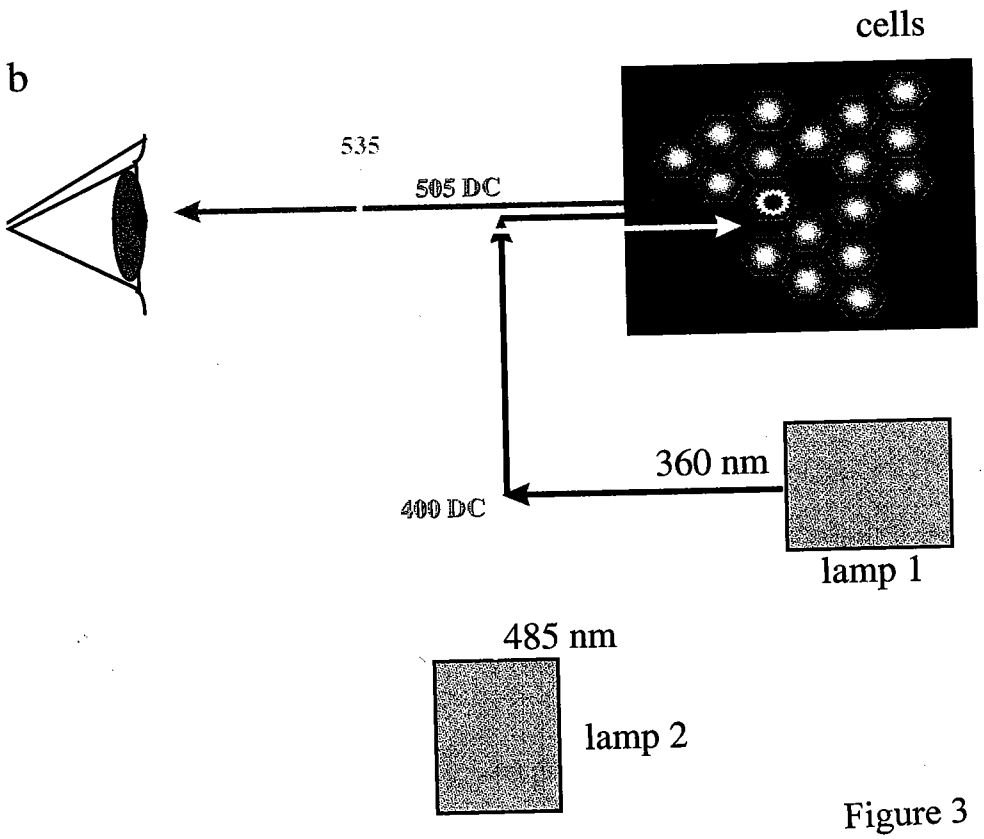

Figure 3

II-9. Electroporation

Cell membrane-impermeant molecules were loaded into glial cells via electroporation using the technique described previously by Raptis et al., 1994, Raptis et al., 1995, and Boitano et al., 1992. Primary cultures of glial cells were grown on glass coverslips coated with electrically conductive, optically transparent indium-tin oxide (**Fig. 4 a,b**) . To achieve good adhesion of glial cells to the coverslips, coverslips were additionally coated with poly-d-ornithine and laminin. First, coverslips were coated with poly-d-ornithine solution (0.5 mg/ml, 2 hours incubation, Sigma). After removing ornithine solution and drying the coverslips (30 min), mouse laminin solution was applied (2 μg/ml, 1 hour incubation, Sigma). After coating, coverslips were dried, and kept at 4°C until the use. No difference was noted between the responses of glial cells grown on ornithine/laminin coating and cells grown on poly-l-lysine coated coverslips.

Cells were plated on pretreated conductive glass coverslips, within a window formed with a piece of electrically insulating adhesive tape attached to the slide. A small piece of a No1 coverslip was placed on the each side of the adhesive tape window to support the electrode above the cells (**Fig. 4 c**). The electrode face was slightly larger than the cell growth area. To produce a zone of non-loaded cells as a control, the conductive coating was removed from half the area within the insulating window by etching with a solution of 4 M HCl added over the coat of zinc powder (**Fig. 4 a**) (Raptis et al., 1995). This resulted in the loading of the drug selectively into glial cells on the coated part of the coverslip (**Fig. 4 b**).

The circuit of the electroporator set-up was formed by placing the positive stainless steel electrode over the window of cells and negative electrode outside the window area of the coverslip. During a current pulse (50 kHz, field strength 500-600 V/cm) current flowed from the computer-controlled pulsed radio-frequency power supply through the negative electrode, along the conductive coating of the coverslip, through the cells and the electroporation media bathing the cells, to the positive electrode and back to the power supply (**Fig. 4 a,c**).

Compounds to be electroporated were diluted to the desired concentration in an electroporation buffer containing 300 mM sorbitol, 2 mM HEPES, 4.2 mM KH_2PO_4, 10.8 mM K_2HPO_4 and 1 mM $MgCl_2$. In order to visualize electroporated, i.e. loaded cells, the inert conjugate Texas Red -dextran (10,000 MW, D-1828, Molecular Probes) was added to the electroporation buffer. The electroporation buffer containing Texas Red dextran and the compound to be electroporated was applied to the window of cells enclosed by the insulating tape. After electrical pulsing, the electrodes were removed and the coverslip placed in HBSS-HEPES solution prior to microscopic observation.

The electroporation protocol was adjusted depending on: a) the MW of the molecules, and b) whether an entire cell window (i.e. unetched coverslip) or a half of the window (i.e. etched coverslip) was being electroporated. The electroporation of BAPTA dextran (Calcium Sponge 10,000 MW, Molecular Probes, C-3040) and heparin (H-9133,

Figure 4: High frequency electroporation. a) Diagram represents cells grown on the indium tin oxide-coated coverslip and the current path through the electroporator setup. b) The electroporation of the coverslip shown in a) loads a drug (red) only into the cells on the coated area of the coverslip. c) Side view of the system: cells are grown within a window formed with adhesive tape. Positive electrode lies above the cells, while negative electrode lies on the electroconductive surface of the coverslip.

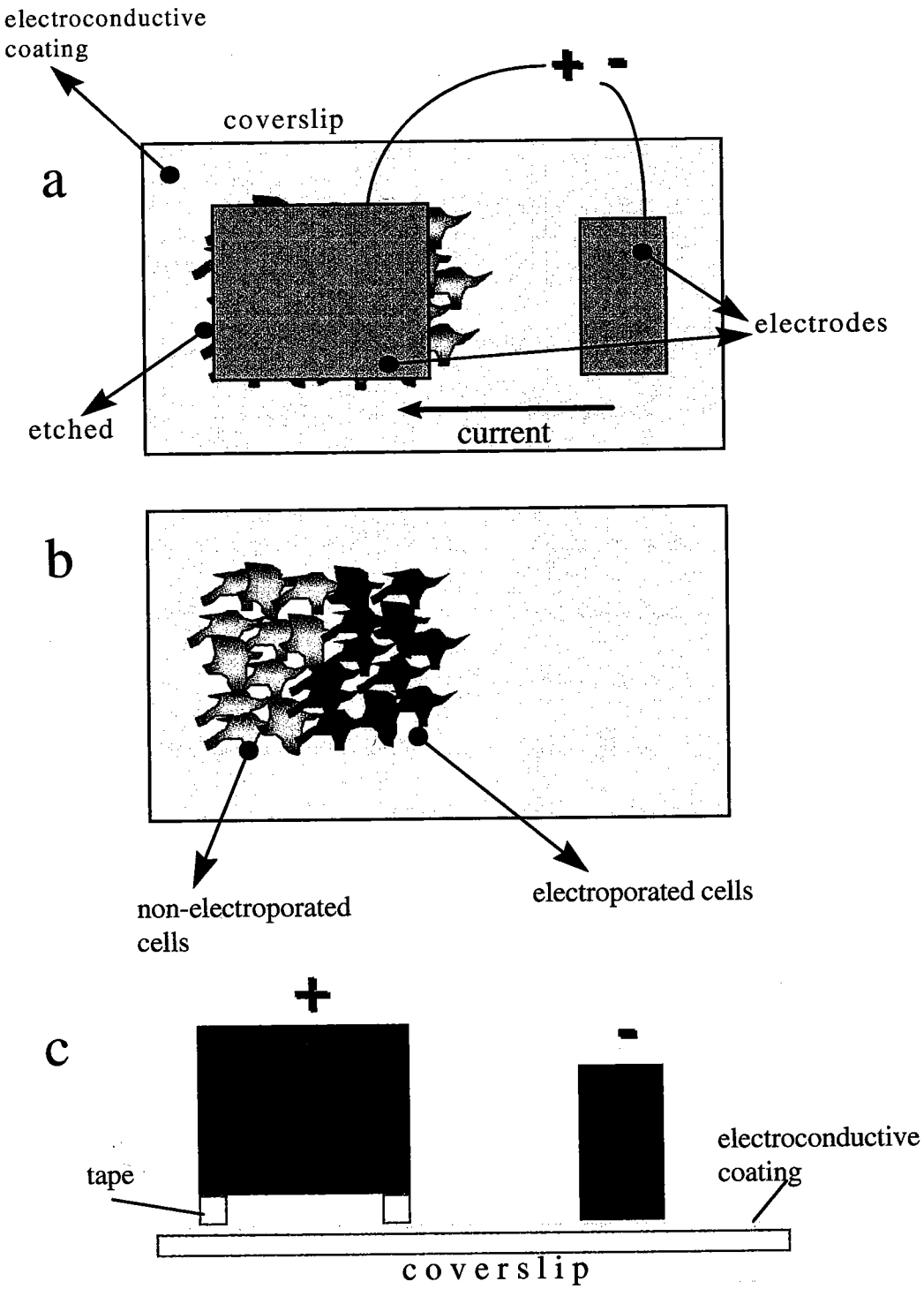
electroconductive
coating
coverslip
a
+ -
electrodes
etched
current
b
non-electroporated
cells
electroporated cells
c
+
-
tape
electroconductive
coating
coverslip

Figure 4

Sigma) was carried out using the following parameters: pulse width 1ms, time between pulses 100 ms, number of pulses 5, time between bursts 10 s, number of bursts 5, pulse period 20 μs, field 600 V/cm. After electroporation, coverslips were placed back into the cell culturing media, and were allowed to recover for at least two hours on 37°C before experimentation.

The electroporation of GDPβS and ruthenium red (Sigma) into cells growing on unetched coverslips was carried out using an electroporation protocol similar to the protocol described above, except that the number of pulses was 4, the number of bursts was 6, and the field strength was 500 V/cm. The electroporation of 'caged IP_3' into the cells growing on the unetched coverslips was carried out using electroporation protocol that differed from the GDPβS poration protocol in number of bursts (7). After electroporation with 'caged IP_3', GDPβS, and ruthenium red, cultures were allowed to recover in culturing media for at least 30 min at 37°C before experimentation.

Following different electroporation protocols and recovery period, cells were loaded with calcium reporter dye fura-2 or calcium reporter dye fluo-3 according to the loading protocols described earlier.

To determine the effects of electroporation on cell cultures a control electroporation solution containing only the Texas Red-dextran conjugate was electroporated into cells. After electroporation, recovery, and loading with the calcium reporter dye, Texas Red-dextran-loaded cultures were exposed to different compounds

that act on cells' membrane receptors, channels and intracellular Ca^{2+} pumps. The ability of cultures to propagate Ca^{2+} waves was also tested.

CHAPTER III

SPECIFIC AIM 1

Specific Aim 1 investigates the mechanisms of initiation and propagation of intercellular Ca^{2+} waves in rat cortical glia. Specifically, experiments of Specific Aim 1 are designed to test whether intercellular Ca^{2+} waves are initiated via generation of IP_3 within a stimulated cell, and propagate by diffusion of IP_3 molecules between neighboring cells. The dependence of Ca^{2+} wave generation on functional gap junctions, intracellular calcium stores, $[IP_3]_i$ and $[Ca^{2+}]_i$ elevations are tested and the sequence of events necessary for propagation of intercellular Ca^{2+} waves is determined.

III-1. Characteristics of primary rat glial cultures

Confluent primary cell cultures of rat neonatal cortical glia were used in this study. Immunofluorescence staining for cell specific markers of astrocytes (GFAP), oligodendrocytes (GalC), and neurons (NF) confirmed that cultures predominantly contained glial cells. From double-staining experiments with GFAP and GalC antibodies, three major groups of cells were identified in cultures: 23 ± 8% of the cells were only GFAP+ and were identified as astrocytes, 39 ± 14 % of the cells were only GalC+ and

identified as oligodendrocytes, while 38 ± 9 % were both GFAP+ and GalC+ and were identified as mixed phenotype or precursor cells. This identification scheme follows that described by Ranscht et al., (1982), Raff et al., (1983) and Frotter and Schachner, (1989). The cell density was 1216 ± 224 cells/mm^2.

III-2. Characteristics of mechanically-induced intercellular Ca^{2+} waves in primary rat glial cultures

Mechanical stimulation of a single cell in a primary rat glial culture initially induced an increase in $[Ca^{2+}]_i$, in the stimulated cell and subsequently in neighboring cells resulting in generation of an intercellular Ca^{2+} wave (**Fig. 5 a**) that spread radially in all directions for 307 ± 29 μm (n = 8) from the origin of the Ca^{2+} wave. Stimulations of different cells in culture resulted in multiple intercellular Ca^{2+} waves (**Fig. 5 a,b**). Mechanically-induced waves initially propagated with the average velocity of 15 μm/s, 75 μm from the stimulated cell, but slowed down to 6.5 μm/s, 250 μm from the stimulated cell. While passing through the cells, the intercellular Ca^{2+} waves increased the $[Ca^{2+}]_i$ by 342 ± 167 nM (mean ± SD, range 50-1020 nM, 29 experiments, 350 cells). These measurements of wave propagation parameters were comparable to the earlier measurements reported by our, and other groups (Wang et al., 1997). Following the passage of an intercellular Ca^{2+} wave, oscillations in $[Ca^{2+}]_i$ (i.e., Ca^{2+} oscillations) were initiated in 34% of the cells that propagated the Ca^{2+} wave (**Fig. 5 c,d**). These Ca^{2+}

Figure 5: The $[Ca^{2+}]_i$ changes associated with the propagation of intercellular Ca^{2+} waves induced by mechanical stimulation of a single glial cell and subsequent Ca^{2+} oscillations. a) An increase in $[Ca^{2+}]_i$ spreads from the stimulated cell (white arrow) to adjacent cells as an intercellular Ca^{2+} wave. Gray arrow shows the orientation of the Ca^{2+} wave propagation. b) A second mechanical stimulation, 5 minutes later, of another cell 89 μm away (white arrow) in the same culture also initiated an intercellular Ca^{2+} wave. Gray arrow shows the orientation of the Ca^{2+} wave propagation. The origin of the first Ca^{2+} wave is marked with the gray dot. Note intercellular Ca^{2+} waves in cells between the two stimulation points propagate in the opposite directions. c and d) Cells showing asynchronous Ca^{2+} oscillations (small white arrows) c) induced by the Ca^{2+} wave shown in a), and d) induced by the Ca^{2+} wave shown in b). The changes in $[Ca^{2+}]_i$ associated with each Ca^{2+} oscillation do not propagate to neighboring cells. The acquisition times are indicated below each image. Color calibration bar indicates changes in $[Ca^{2+}]_i$. Average diameter of a cell is 25 μm.

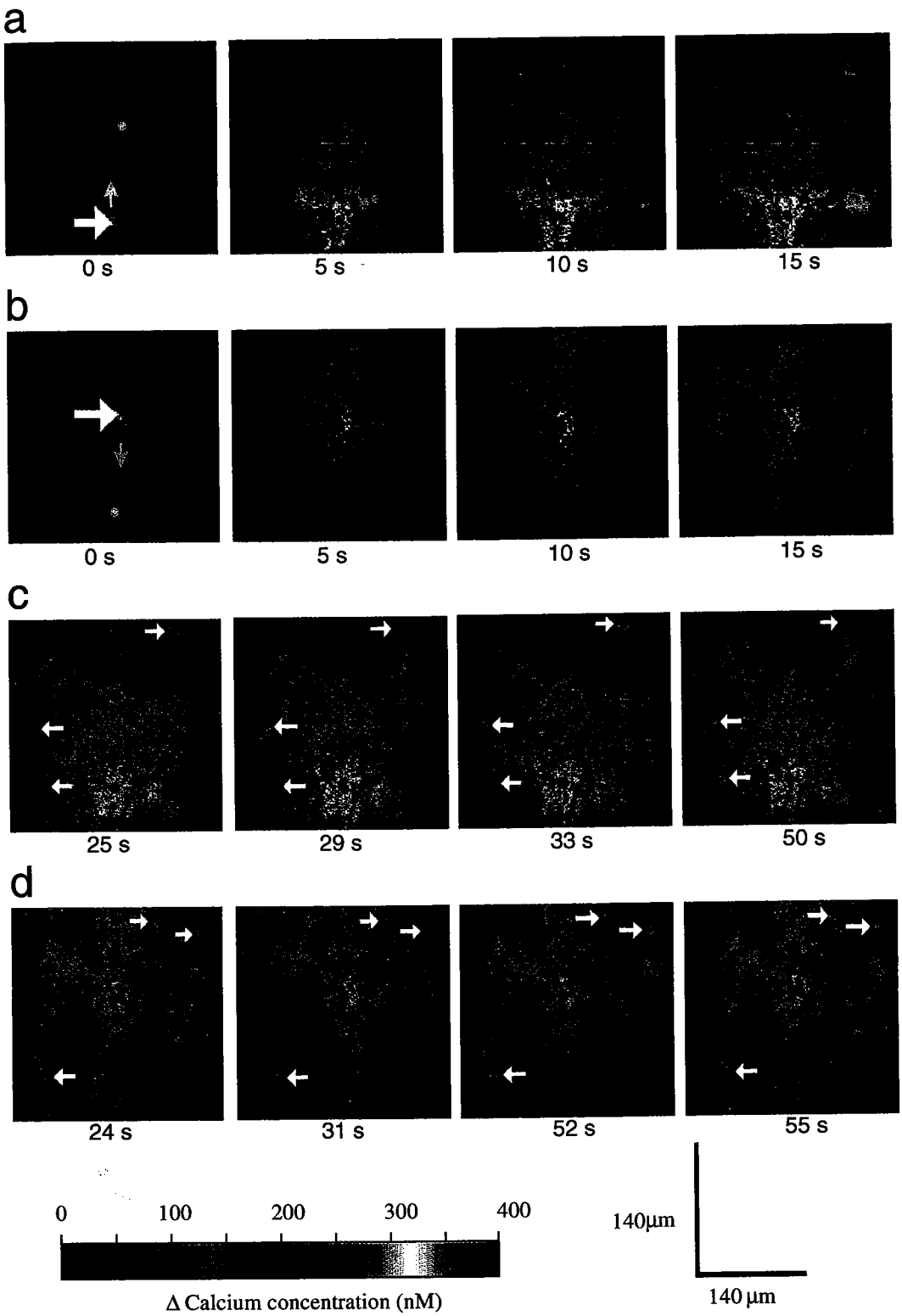
a
0 s
5 s
10 s
15 s
b
0 s
5 s
10 s
15 s
c
25 s
29 s
33 s
50 s
d
24 s
31 s
52 s
55 s
0
100
200
300
400
Δ Calcium concentration (nM)
140μm
140 μm

Figure 5

oscillations occurred asynchronously, that is, independently of the changes in $[Ca^{2+}]_i$ of adjacent cells and did not initiate additional intercellular Ca^{2+} waves.

III-3. Functional gap junctions are required for Ca^{2+} wave propagation in glia

Depending on the inducing stimulus, cell type, and species, Ca^{2+} waves may propagate either through the *intra*cellular space of gap junction-coupled cells, or through the *extra*cellular space. A considerable number of previous studies investigating Ca^{2+} wave propagation have found that gap junctions are required for wave propagation in rat glia. By contrast, an extracellular component, identified as ATP, seems to be the dominant mechanism for Ca^{2+} wave propagation in mouse glia. The role of gap junction-mediated communication in Ca^{2+} wave propagation was investigated by examining the effect of gap junction blockers halothane and 18 α-glycyrrhetinic acid (AGA) (Davidson et al., 1986; Sanderson et al., 1990; Venance et al., 1997) on the Ca^{2+} waves. Both halothane (4-5 mM, n = 10) and AGA (10 μM, n = 5, **Fig. 6 a, b**) significantly reduced the number of cells participating in the propagation of Ca^{2+} waves through glial cell cultures to 11% and 8% of the control values, respectively (**Fig. 6 c**). Side effects of the uncoupling agents include a reduction in $[Ca^{2+}]_i$ increase in the stimulated cell (Deutsch et al., 1995). The inhibition of Ca^{2+} wave propagation however, could not be attributed to this side effect, since the analysis of the $[Ca^{2+}]_i$ in

Figure 6: The effect of gap junction blockers on Ca^{2+} waves. a) Ca^{2+} wave in control conditions, b) Ca^{2+} wave in cells exposed to gap junction blocker AGA (10 μM, n = 5), c) comparison of halothane (n = 10) and AGA (n = 5) effects on Ca^{2+} waves. The scale bar represents 88 μm. The acquisition times for a) and b) are indicated below each image. Color calibration bar indicates changes in $[Ca^{2+}]_i$.

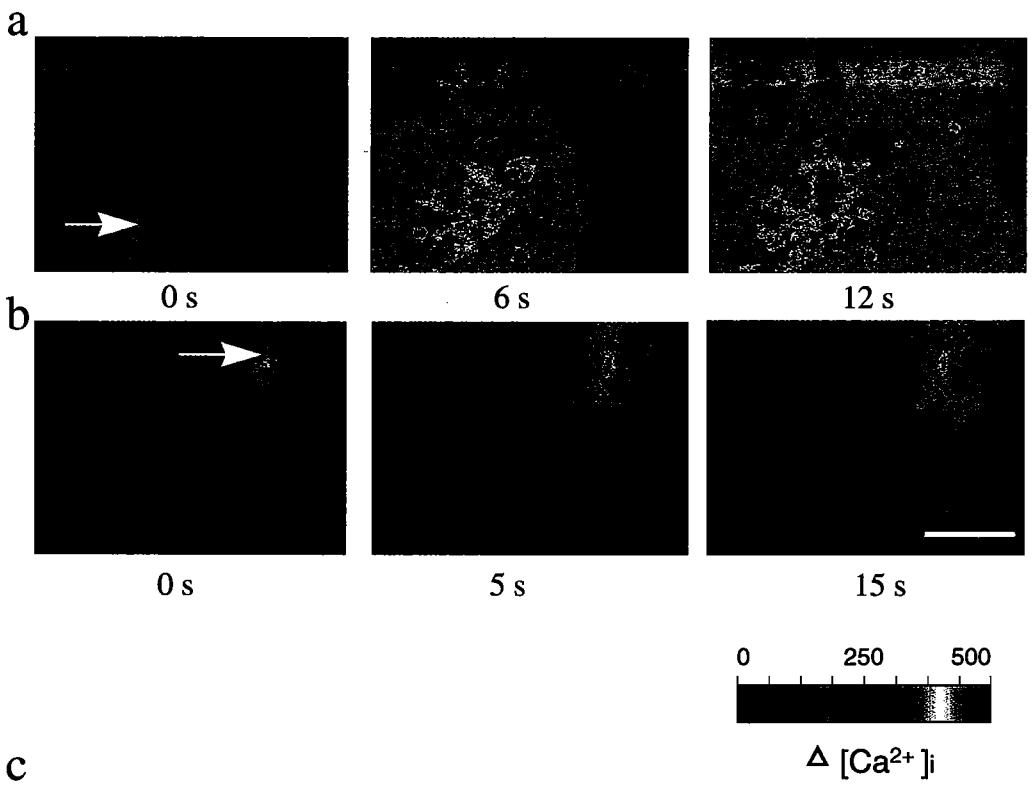
a
0 s
6 s
12 s
b
0 s
5 s
15 s
0
250
500
Δ [Ca2+]i
c
100
50
0
cells/ wave (%)
control
halothane
AGA

Figure 6

stimulated cells indicated that the amplitudes of calcium signals were comparable in both control and uncoupling conditions. In addition, the effect of gap junction blockers on Ca^{2+} wave propagation was not due to the potential side effects of these compounds on the responsiveness of glia to neurotransmitters, since cells in cultures treated with halothane and AGA responded to both AMCh (200 μM, n = 11) and ATP (10 μM, n = 5) by $[Ca^{2+}]_i$ elevations that were comparable to the responses of cells in untreated cultures.

The possibility that Ca^{2+} waves propagate extracellularly was investigated by experiments utilizing a constant perfusion of extracellular solution. The perfusion constantly replaces the solution bathing the cells, thus removing substances that may be released in the process of the Ca^{2+} wave propagation. If Ca^{2+} waves propagate by diffusion of an excitatory substance through the extracellular space, Ca^{2+} waves would not be able to propagate against the orientation of the extracellular flow. A directional flow of extracellular solution (4 ml/min) did not block Ca^{2+} wave propagation (n = 8, mean propagated distance 288 ± 22 μm, **Fig. 7**) suggesting that extracellular communication is not a necessary mechanism of Ca^{2+} wave propagation.

The experiments described in this section are in agreement with earlier studies that demonstrated that the functional gap junctions are necessary for the propagation of intercellular Ca^{2+} waves in rat glia (Charles et al., 1992; Finkbeiner, 1992; Nadal et al., 1997; Venance et al., 1995; Venance et al., 1998).

Figure 7: Propagation of Ca^{2+} wave against the flow of extracellular medium. A Ca^{2+} wave was mechanically-induced (white arrow), and continued to propagate against the orientation of the flow of perfusion (gray arrows). The scale bar in 0 s represents 86 μm. The acquisition times are indicated below each image. Color calibration bar indicates changes in $[Ca^{2+}]_i$.

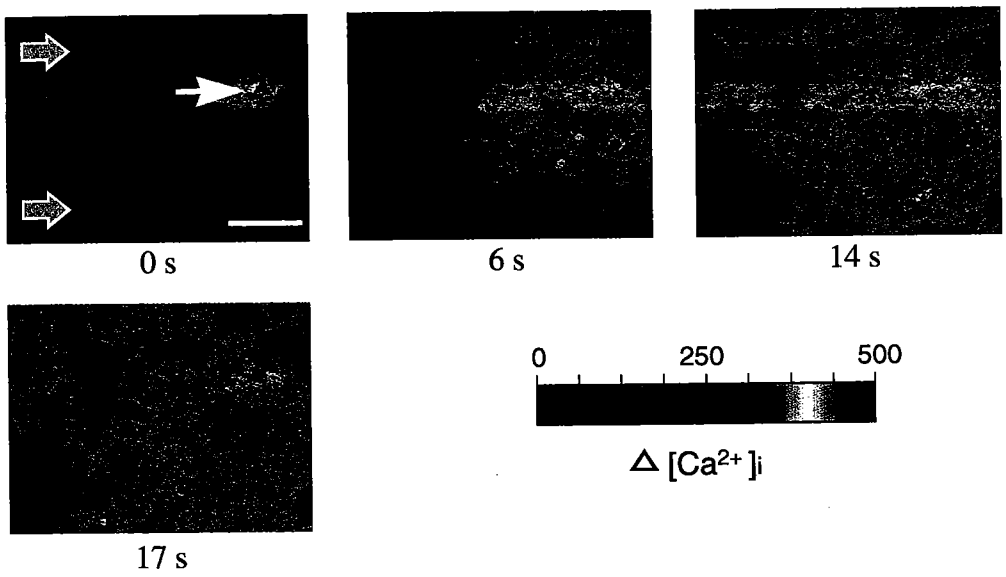

Figure 7

III-4. Ca^{2+} waves depend on Ca^{2+} release from intracellular Ca^{2+} stores

In order to determine whether $[Ca^{2+}]_i$ increases associated with Ca^{2+} waves are caused by release of Ca^{2+} from internal Ca^{2+} stores, or by the influx of extracellular Ca^{2+} into the cells, mechanical stimulations were carried out either in the presence of the intracellular Ca^{2+} pump blocker thapsigargin, or in Ca^{2+}-free extracellular solution. In the first set of experiments, exposure to thapsigargin (1 μM) resulted in an increase in $[Ca^{2+}]_i$ ranging from 150 to 400 nM within the observed cells. Mechanical stimulation of a single cell after 3 min exposure to thapsigargin did not induce an intercellular Ca^{2+} wave, suggesting that Ca^{2+} release from intracellular Ca^{2+} stores is necessary for generation of Ca^{2+} waves (n = 5). In the second set of experiments, mechanical stimulations successfully initiated intercellular Ca^{2+} waves in Ca^{2+}-free conditions (HBSS containing 0 Ca^{2+} and 2 mM EGTA, n = 5, propagation distance 217 ± 38 μm), suggesting that the Ca^{2+} influx is not necessary for the Ca^{2+} wave generation. These observations are in agreement with previous reports that show that intercellular Ca^{2+} waves can be initiated and propagated in Ca^{2+}- free extracellular medium (Charles et al., 1991; Newman and Zahs, 1997; Zanotti and Charles, 1997), but are inhibited by depletion of the intracellular Ca^{2+} stores by thapsigargin (Charles et al., 1993; Newman and Zahs, 1997; Venance et al., 1997)}. These findings suggest that Ca^{2+} waves occur as a result of the release of Ca^{2+} from intracellular Ca^{2+} stores.

III-5. IP_3 generation is necessary for the initiation and propagation of Ca^{2+} waves

The release of Ca^{2+} from intracellular Ca^{2+} stores can occur due to the activation of intracellular IP_3Rs by IP_3 molecules. The role that IP_3 plays in the generation of Ca^{2+} waves was investigated by evaluating the effects of compounds that blocked the production of IP_3. Cell cultures were exposed to either PLC inhibitor U-73122, its inactive structural analogue U-73343 (Smith et al., 1990), LiCl, an inhibitor of the hydrolysis of intermediate inositol phosphates and supressor of inositol recycling (Berridge et al., 1989), or PLC inhibitor neomycin sulfate (Prentki et al., 1986; Seregi et al., 1992).

The number of cells participating in the Ca^{2+} wave propagation was significantly decreased by U-73122 treatment (1 min, 5 μM, n= 7) to 7 % of the control value (**Fig. 8a**), and $[Ca^{2+}]_i$ increases were usually restricted only to the stimulated cell (4 out of 7 experiments). On the other hand, Ca^{2+} waves were unaffected by treatment with the inactive U-73343 compound (1 min, 5 μM, **Fig. 8a**, n = 4). Of the cells still responding, U-73122 caused a reduction in the $[Ca^{2+}]_i$ increase in the stimulated cell as well as in cells in the 2nd and 3rd row from the wave origin. This result suggests a reduced release of Ca^{2+} from IP_3-sensitive calcium stores (**Fig. 8b**). The implications of the difference in the extent of reduction between the stimulated cell and neighboring cells will be discussed later in the study.

Figure 8: Effect of PLC blocker U-73122 on the Ca^{2+} wave propagation. U-73122 (1 min, 5 μM incubation) reduces the number of cells participating in the wave (checked bar, n = 7 experiments), while inactive U-73343 has no effect (striped bar, n = 4 experiments). The number of the cells propagating Ca^{2+} waves in U-73122-treated cells is normalized to the number of cells propagating Ca^{2+} waves in control conditions. b) Effect of U-73122 and U-73343 on $[Ca^{2+}]_i$ increases during Ca^{2+} wave propagation in the first three cell rows. $[Ca^{2+}]_i$ increase in the stimulated cell is smaller after U-73122 treatment. Bars and graph symbols represent mean values and vertical lines represent standard deviations.

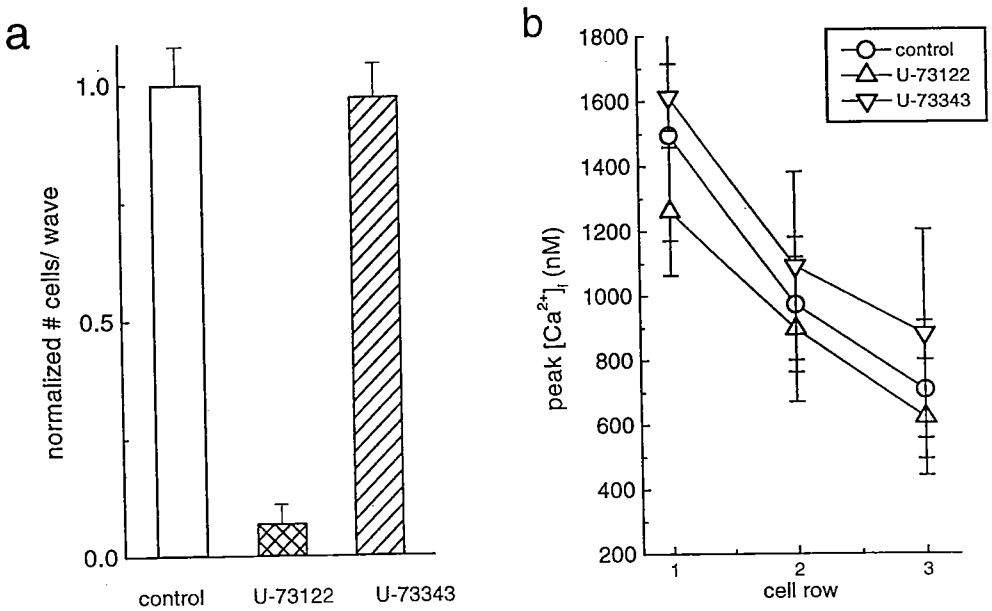
a
normalized # cells/ wave
1.0
0.5
0.0
control
U-73122
U-73343
b
peak [Ca2+]i (nM)
1800
1600
1400
1200
1000
800
600
400
200
1
2
3
cell row
control
U-73122
U-73343

Figure 8

Similarly, preincubation with LiCl (10 mM, 45 min) decreased the number of cells participating in Ca^{2+} wave propagation to 38 % of the control (**Fig. 9**, n=5). Finally, the exposure of glial cultures to neomycin sulfate for either 30 or 45 min (200 μM) caused a decrease in the total number of cells participating in the propagation of Ca^{2+} waves to 48 % and 17 % of the control value, respectively (**Fig. 10a**, n= 6, 30 min incubation, n = 6, 45 min incubation). The effect of neomycin sulfate was reversed after a 30 min recovery period in neomycin-free extracellular solution. In neomycin sulfate solution, $[Ca^{2+}]_i$ increases in the stimulated cells and cells in subsequent cell rows were reduced, suggesting reduced Ca^{2+} release from IP_3-sensitive calcium stores (**Fig. 10b**). Neomycin sulfate however, may act as an inhibitor of voltage-gated membrane Ca^{2+} channels (Canzoniero et al., 1993; Guan et al., 1988) and the resulting inhibition of Ca^{2+} waves might have been a result of the combination of both effects. The implications of this result will be discussed in more detail later in this study.

Neomycin sulfate, LiCl, and U-73122 experiments, together with the successful initiation of Ca^{2+} waves by photorelease of IP_3 from its photolabile carrier within single glial cells reported by our group (Leybaert et al., 1998), have demonstrated that the activation of PLC and subsequent production of IP_3 is a necessary step in generation of intercellular Ca^{2+} waves.

III-6. Physiologic elevations in $[Ca^{2+}]_i$ do not initiate intercellular Ca^{2+} waves

Release of Ca^{2+} from intracellular Ca^{2+} stores can also occur due to the activation

of intracellular RyRs by Ca^{2+}. In other cell types, Ca^{2+} waves have been hypothesized to occur via increases in $[Ca^{2+}]_i$ that propagate via diffusion of Ca^{2+} through the gap junctions of the neighboring cells. To determine whether Ca^{2+} ions can directly initiate generation of intercellular Ca^{2+} waves, Ca^{2+} ions were photoreleased from photolabile Ca^{2+} carrier molecules (NP-EGTA) within individual cells. Subsequent changes in $[Ca^{2+}]_i$ were monitored by non-ratiometric calcium dye fluo-3, because the excitation wavelength of fluo-3 does not overlap with the UV wavelengths that are capable of releasing caged molecules (**Fig. 3**). Since NP-EGTA molecules can bind free Ca^{2+}, it was important to test whether the loading of NP-EGTA into the cell cultures might inhibit the propagation of Ca^{2+} waves by buffering $[Ca^{2+}]_i$ increases. Mechanical stimulation of a cell in NP-EGTA-loaded culture resulted in Ca^{2+} waves that were comparable to the Ca^{2+} waves in control cultures, demonstrating that under the loading conditions used, NP-EGTA did not act as a significant Ca^{2+} buffer (**Fig. 11a,** n = 6). When the same cell was exposed to a UV flash of up to 2 s duration, photorelease of Ca^{2+} from NP-EGTA resulted in an increase of $[Ca^{2+}]_i$. This increase in $[Ca^{2+}]_i$ within the single cell did not initiate propagating Ca^{2+} waves (**Fig. 11b,** n = 6).

Figure 9: Effect of LiCl on Ca^{2+} wave propagation. LiCl (45 min incubation, 10 mM) decreased the number of cells participating in Ca^{2+} wave propagation (n=5 experiments). The number of cells propagating Ca^{2+} waves in LiCl-treated cultures is normalized to the number of cells propagating Ca^{2+} waves in control conditions. Bars represent mean values and lines represent standard deviations.

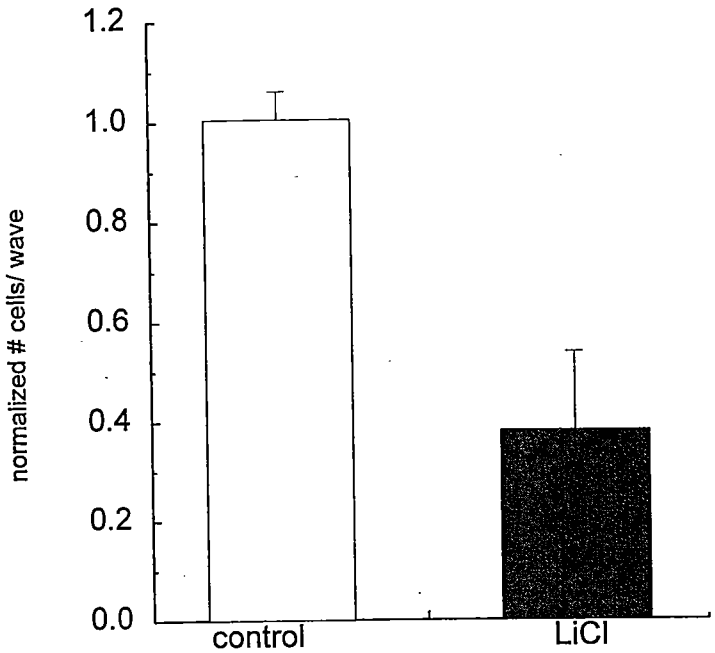

Figure 9

Figure 10: Effects of neomycin sulfate on the Ca^{2+} wave propagation. a) Incubation in neomycin sulfate (200 μM, 30 min) decreases the number of cells participating in Ca^{2+} wave propagation (checked bar, n = 6 experiments); longer incubation (45min) is more effective (striped bar, n = 6 experiments). The number of cells propagating Ca^{2+} waves in neomycin-treated cells is normalized to the number of cells propagating Ca^{2+} waves in control conditions. b) Effect of neomycin sulfate on $[Ca^{2+}]_i$ increases during Ca^{2+} wave propagation in the first 5 cell rows. $[Ca^{2+}]_i$ increase in stimulated cell is substantially smaller after neomycin sulfate treatment. Bars and graph symbols represent mean values and vertical lines represent standard deviations.

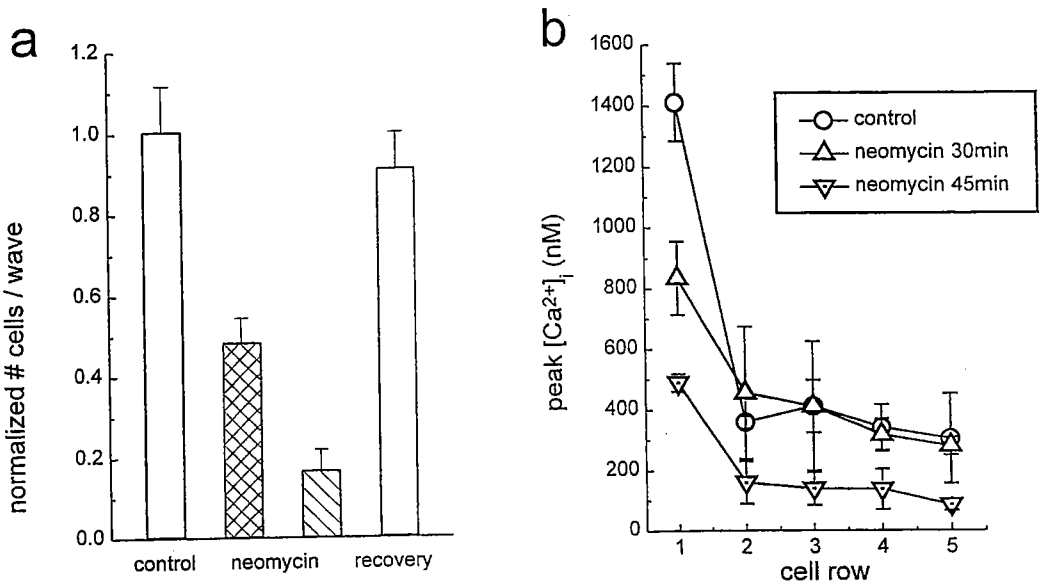
a
normalized # cells / wave
1.2
1.0
0.8
0.6
0.4
0.2
0.0
control
neomycin
recovery
b
peak [Ca2+]i (nM)
1600
1400
1200
1000
800
600
400
200
0
1
2
3
4
5
cell row
control
neomycin 30min
neomycin 45min

Figure 10

Figure 11: An increase in $[Ca^{2+}]_i$ does not induce Ca^{2+} wave propagation. a) Ca^{2+} wave propagation occurs following mechanical stimulation of a single cell (arrow). b) An increase in $[Ca^{2+}]_i$ in the same cell (arrow) achieved by photolysis of NP-EGTA does not initiate the propagation of an intercellular Ca^{2+} wave. c) An increase in $[Ca^{2+}]_i$ in another cell achieved by photolysis of NP-EGTA does not initiate the propagation of an intercellular Ca^{2+} wave, but d) mechanical stimulation of the cell shown in c) induces intercellular Ca^{2+} wave. Color calibration bar indicates the percentage changes in $[Ca^{2+}]_i$ calculated relative to the $[Ca^{2+}]_i$ observed at 0 s. The acquisition times are indicated below each image.

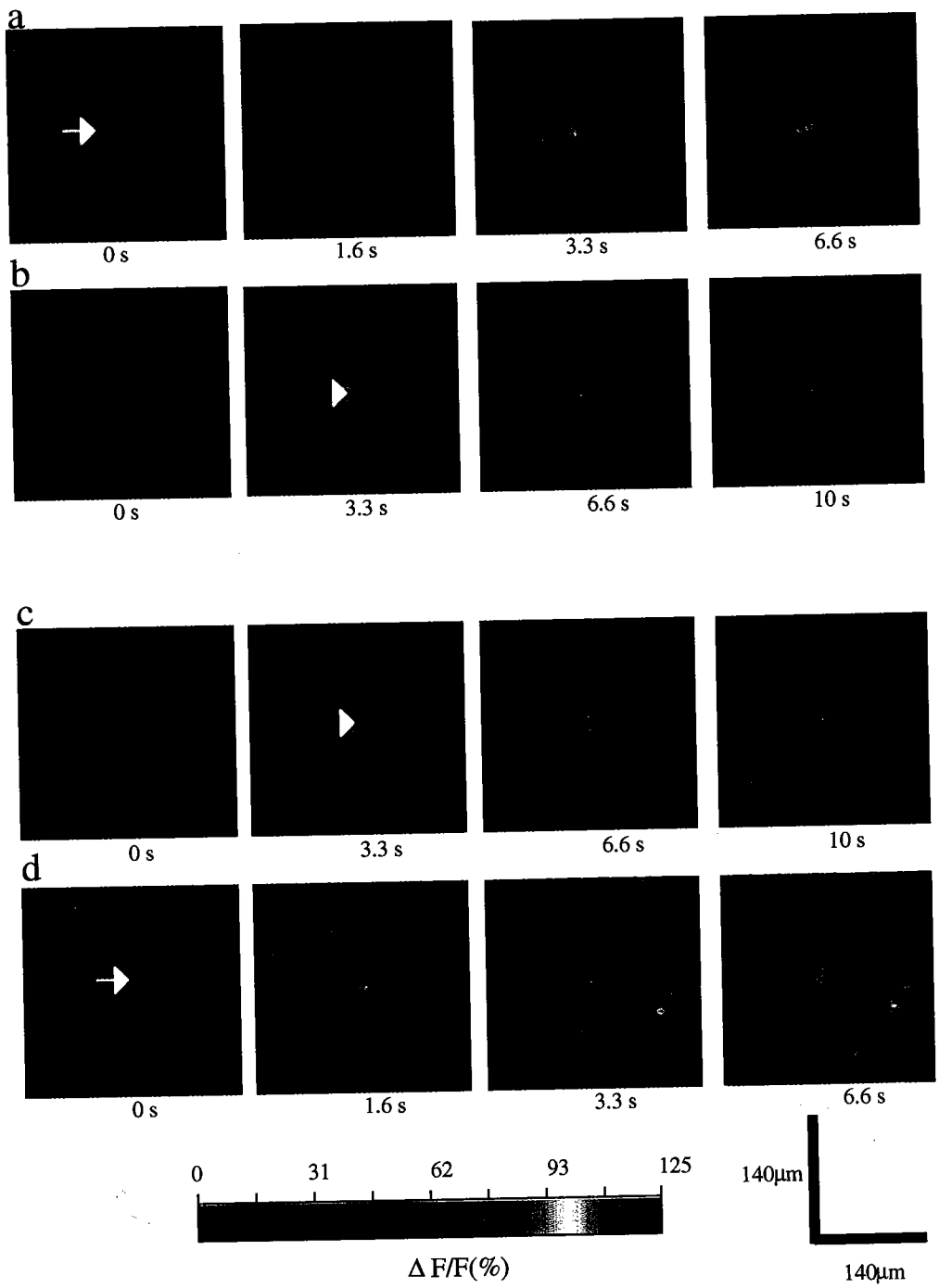
a
0 s
1.6 s
3.3 s
6.6 s
b
0 s
3.3 s
6.6 s
10 s
c
0 s
3.3 s
6.6 s
10 s
d
0 s
1.6 s
3.3 s
6.6 s
0
31
62
93
125
ΔF/F(%)
140μm
140μm

Figure 11

The possibility that the mechanical stimulations rendered stimulated cells unresponsive to the subsequent $[Ca^{2+}]_i$ increase was also investigated. In these experiments, the exposure to a UV flash, up to 2 s duration, for an individual cell caused an increase of $[Ca^{2+}]_i$ but did not initiate a propagating intercellular Ca^{2+} wave (**Fig. 11c,** n = 8). When the same cell was mechanically stimulated however, an intercellular Ca^{2+} wave was successfully initiated (**Fig. 11d, n** = 8). Although measurements of the change in fluorescence of non-ratiometric Ca^{2+} dye fluo-3 cannot be reliably expressed as $[Ca^{2+}]_i$, comparison of fluo-3 measurements of $[Ca^{2+}]_i$ changes during propagating Ca^{2+} wave suggested that the magnitude and duration of $[Ca^{2+}]_i$ increase induced by the NP-EGTA photolysis was comparable to the magnitude and duration of $[Ca^{2+}]_i$ increase induced by mechanical stimulation. Therefore, the increase in $[Ca^{2+}]_i$ achieved by the photorelease of Ca^{2+} within a cell does not seem to induce the release of Ca^{2+} from intracellular Ca^{2+} stores in an amount that would be sufficient for the initiation of Ca^{2+} wave propagation. Ca^{2+} oscillations that occurred in response to Ca^{2+} wave propagation **(Fig. 5 c,d)** did not propagate to neighboring cells in the form of Ca^{2+} waves, again suggesting that physiological increases in $[Ca^{2+}]_i$ alone cannot initiate Ca^{2+} waves. This property of Ca^{2+} oscillations was previously described by our group (Charles et al., 1991).

In summary, the studies suggest that the increase of $[Ca^{2+}]_i$ in the stimulated cell is not sufficient for the generation of intercellular Ca^{2+} waves in rat cortical glia. Also, Ca^{2+} seems to be a poor mediator of Ca^{2+} waves in rat cortical glia, because the diffusion of Ca^{2+} between the cells was not detected by the imaging system. These findings reinforce the findings reported by this and other groups indicating that Ca^{2+} is not the main signal

that propagates a Ca^{2+} wave in glia (for reviews see Charles, 1998; Finkbeiner, 1993; Sanderson, 1995; Verkhratsky and Kettenmann, 1996).

III-7. High frequency electroporation as a method for the study of initiation and propagation of intercellular Ca^{2+} waves

In order to experimentally address the questions of initiation and propagation of intercellular Ca^{2+} waves, it is important that the experimental technique of choice allows the selective introduction of activators and/or blockers of a hypothesized signaling pathway into spatially confined areas of cell syncytium. Only by introducing the drugs of interest into either the zone of cells from which Ca^{2+} waves are initiated, or the zone of cells through which Ca^{2+} waves are propagated, would one be able to answer which signaling molecules (and their receptors) are necessary and sufficient for initiation and propagation of intercellular Ca^{2+} waves. Therefore, the technique of high frequency electroporation (Boitano et al., 1992) was used to introduce various compounds of interest into cells grown on coverslips coated with the electroconductive indium tin oxide, described by Raptis and colleagues (Raptis et al., 1994; Raptis et al., 1995). The introduction of drugs into the cells depends on whether the cells are growing on the electroconductive zone of the coverslip, or on the etched, non-electroconductive zone of the coverslip (**Fig. 4**).

In order to analyze and interpret electroporation experiments, it was crucial to show that the effects of the electroporation protocol alone on the relevant physiology of

glial cells was minimal. After testing the responses of glial cells to a number of stimuli following different electroporation protocols characterized by different voltage, frequency and time variables, electroporation protocols were chosen that had minimal effects on relevant glial physiology, (i.e., initiation and propagation of Ca^{2+} waves, responses to depolarizing stimuli, integrity of intracellular Ca^{2+} stores, and responsiveness to neurotransmitters that cause IP_3 generation). In control experiments, Texas Red-dextran conjugate was electroporated into cells. Texas Red-dextran is an inert molecule that, due to the Texas Red fluorochrome, indicated which cells were successfully electroporated, and, because of the different emission wavelength of Texas Red, it did not interfere with imaging of the calcium dye fluorescence. The size of the dextran (10,000 MW) ensured that Texas Red-dextran molecules do not diffuse through the gap junctions into neighboring cells, and therefore indicated only the electroporated cells.

Cultures electroporated with the control, Texas Red-dextran solution, propagated Ca^{2+} waves that were similar, with respect to intracellular and intercellular wave velocity, maximum distance traveled, and dynamic changes in $[Ca^{2+}]_i$ to the Ca^{2+} waves that propagated through the non-electroporated glia. Furthermore, after control electroporation of Texas Red-dextran into glia growing on half etched coverslips, Ca^{2+} waves initiated in the electroporated zone of the culture propagated into the zone of cells growing on the non-electroporated side (**Fig. 12**, n = 10). Similarly, Ca^{2+} waves initiated from the non-electroporated, i.e., non-loaded half of the glial cultures propagated into the zone of Texas Red-dextran-loaded cells, without alteration in Ca^{2+} wave kinetics at the border of the two zones (**Fig. 13**, n = 9).

To test whether the electroporation procedure effects glial responses to depolarizing stimuli, increases in $[Ca^{2+}]_i$ induced by exposure to an extracellular solution containing 50 mM K^+ were compared for both Texas Red-dextran-loaded and non-loaded cells (**Fig. 14**). Furthermore, the effects of electroporation on glial intracellular Ca^{2+} stores were tested by analysis of glial responses to exposure to the intracellular Ca^{2+} pump blocker thapsigargin (1 μM, **Fig. 15**) (Boitano et al., 1992; Charles et al., 1993). The same percentage of both Texas Red-dextran-loaded and non-loaded glial cells responded to K^+-induced depolarization (**Fig. 16 a,** n = 3). Additionally, increases in $[Ca^{2+}]_i$ were comparable in average magnitude (**Fig. 16 b**, n = 3). The same percentage of both Texas Red-dextran-loaded and non-loaded cells responded to thapsigargin, and induced increases in $[Ca^{2+}]_i$ that were of a comparable magnitude in both loaded and non-loaded cells (**Fig. 16 c,d**, n = 4).

Figure 12: Ca^{2+} wave initiated (arrow) from the zone of cells loaded with Texas Red-dextran propagates through the non-loaded zone of glial cells. Texas Red image demonstrates the shape and extent of the loaded zone of cells. The first frame is a pseudocolored image of Texas Red fluorescence, and the second frame is a gray scale image of fura-2 fluorescence. Note the comparable loading with fura-2 of cells in both the loaded and the non-loaded zones. The dotted line marks the boundary between loaded and the non-loaded zone. The acquisition times are indicated below each image. Color calibration bar indicates changes in $[Ca^{2+}]_i$. The scale bar in 0 s image represents 85 μm.

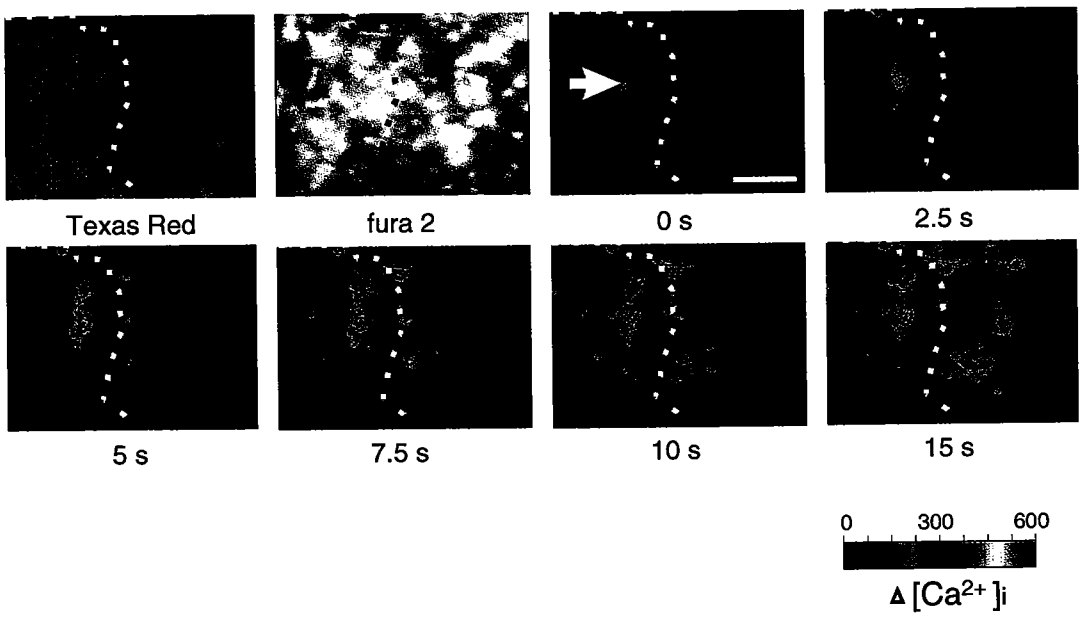

Figure 12

Figure 13: A Ca^{2+} wave initiated from the non-loaded zone (arrow) propagates through the Texas Red-dextran-loaded zone of glial cells. The first frame is a pseudocolored image of Texas Red fluorescence of glial cells monitored during the Ca^{2+} imaging experiment. Dotted line marks the boundary between loaded and non-loaded zone. The acquisition times are indicated below each image. Color calibration bar indicates changes in $[Ca^{2+}]_i$. The scale bar in 0s image represents 92 μm.

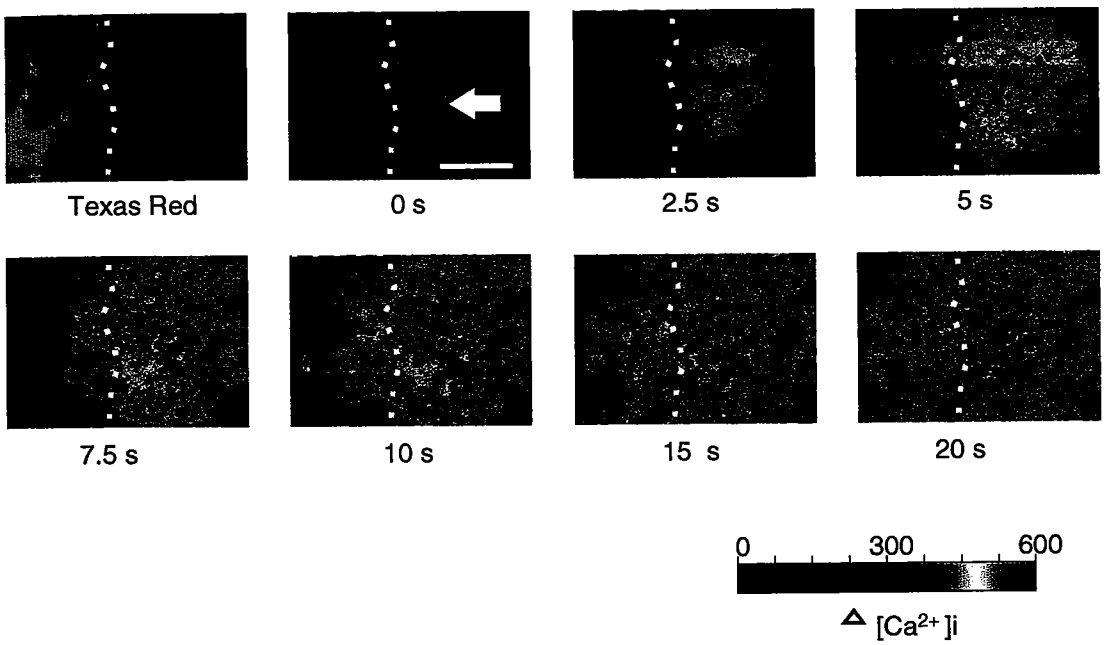

Figure 13

Figure 14: Effect of high K^+ solution on glial $[Ca^{2+}]_i$. Each graph represents the variation in $[Ca^{2+}]_i$ with respect to time of a different cell in the a) Texas Red dextran-loaded, and b) non-loaded area of 17-day old cell culture. Extracellular solution containing 50 mM K^+ was applied via bath to glial culture. Black bar on the top of $[Ca^{2+}]_i$ traces indicates the presence of high K^+ solution.

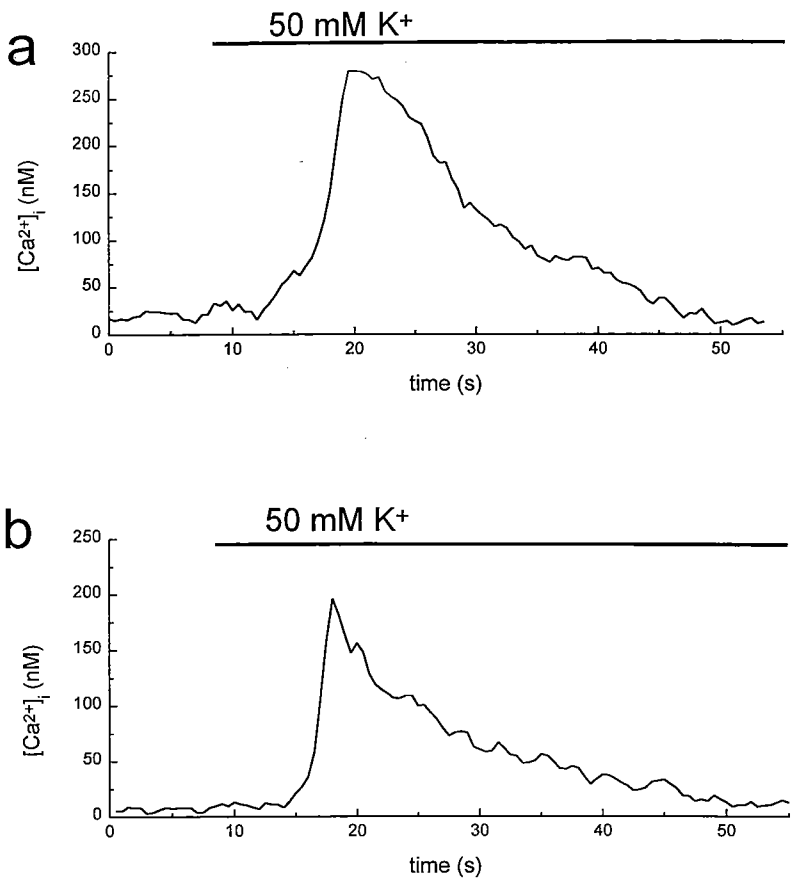
a
50 mM K+
300
250
200
150
100
50
0
[Ca2+]i (nM)
0
10
20
30
40
50
time (s)
b
50 mM K+
250
200
150
100
50
0
[Ca2+]i (nM)
0
10
20
30
40
50
time (s)

Figure 14

Figure 15: Effect of Ca^{2+} ATP-ase pump blocker thapsigargin on $[Ca^{2+}]_i$. Each graph represents the variation in $[Ca^{2+}]_i$ with respect to time of a different cell in: a) Texas Red-dextran loaded and b) non-loaded area of 17-day old cell culture. Black bar on the top of $[Ca^{2+}]_i$ traces indicates the addition of thapsigargin solution (1 μM).

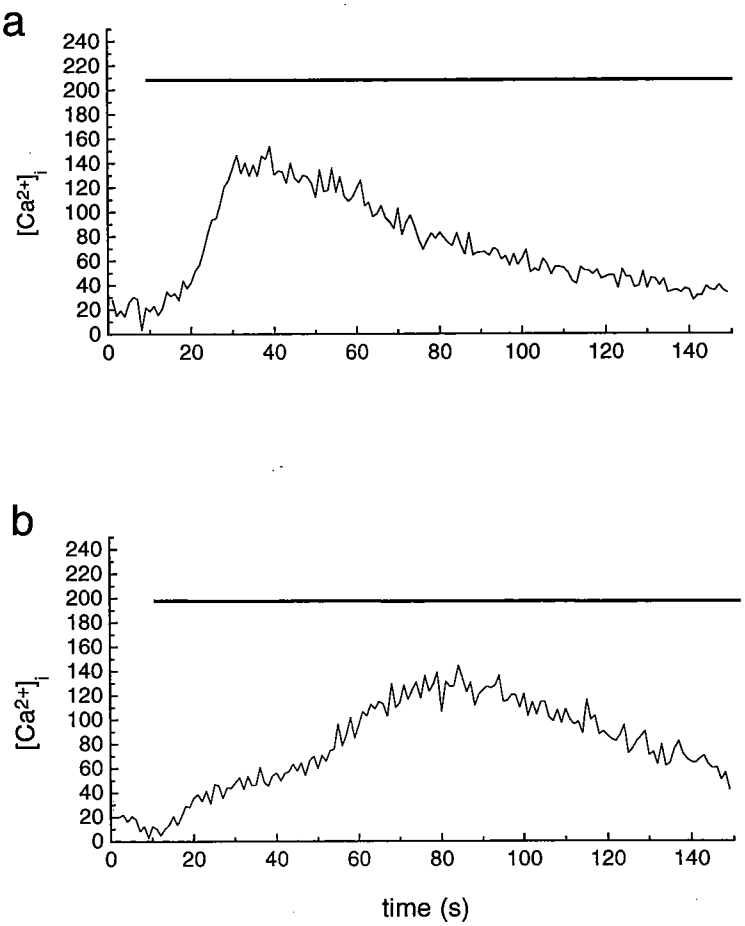
a
b
[Ca2+]i
240
220
200
180
160
140
120
100
80
60
40
20
0
0
20
40
60
80
100
120
140
time (s)

Figure 15

Figure 16: Analysis of the effects of electroporation on the depolarization-induced and Ca^{2+} pump blocker-induced $[Ca^{2+}]_i$ changes in glial cells. Cultures grown on half-etched coverslips were first loaded with the control solution containing Texas Red-dextran molecules and then exposed to test stimuli. Responses of cells on the non-loaded side were compared to the responses of cells on the Texas Red-dextran-loaded side. Electroporation induced no change in responses of glial cells to high K^+ depolarizing stimulus in: a) the percentage of cells responding to depolarization, and b) the level of $[Ca^{2+}]_i$ increases in response to depolarization (n = 3). Electroporation did not influence intracellular calcium stores as c) number of the cells responding, and d) $[Ca^{2+}]_i$ elevations in response to thapsigargin were identical on loaded and non-loaded side of the coverslip (n = 4).

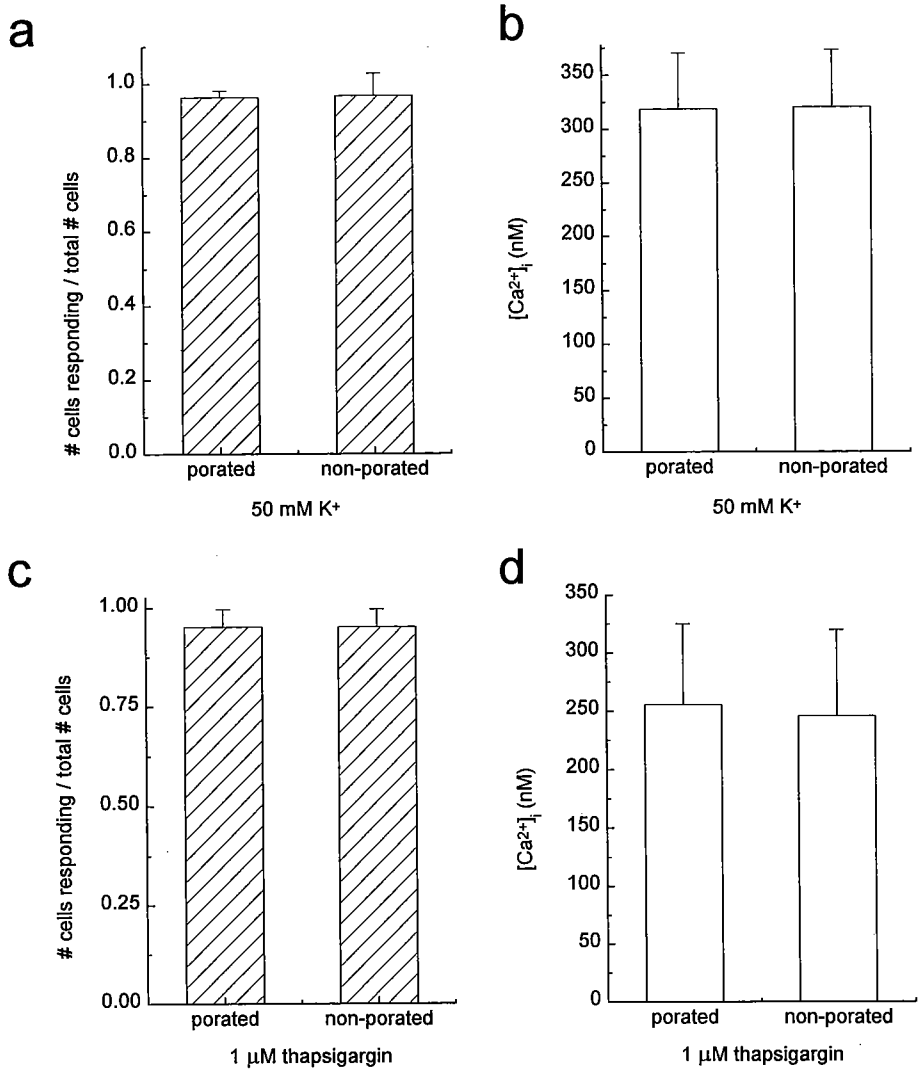
a
cells responding / total # cells
1.0
0.8
0.6
0.4
0.2
0.0
porated
non-porated
50 mM K+
b
[Ca2+]i (nM)
350
300
250
200
150
100
50
0
porated
non-porated
50 mM K+
c
cells responding / total # cells
1.00
0.75
0.50
0.25
0.00
porated
non-porated
1 μM thapsigargin
d
[Ca2+]i (nM)
350
300
250
200
150
100
50
0
porated
non-porated
1 μM thapsigargin

Figure 16

The possible side-effects of electroporation on glial responsiveness to neurotransmitters linked to IP_3 production were also investigated, because studies described in section III-5 demonstrated that the activation of PLC and generation of IP_3 are necessary for the generation of intercellular Ca^{2+} waves. Because the response of a cell to a neurotransmitter challenge involves a complex activation cascade of neurotransmitter receptors, receptor coupling proteins, secondary messengers, and secondary messenger receptors, these experiments were the most rigorous tests of the effects of electroporation on the cells.

The effects of electroporation on glial responses to muscarinic stimuli was tested by exposure to a range of concentrations of acetylmethilcholine (AMCh, 25, 50, 100, and 200 μM). Responses to AMCh were comparable between Texas Red-dextran-loaded and non-loaded glial cells for all AMCh concentrations used. Analysis showed that the same percentage of cells responded to AMCh stimuli with comparable rises in $[Ca^{2+}]_i$ (**Fig. 17 a,b,** 100 μM AMCh, n = 4). Glial responses to purinergic stimuli were also investigated due to recent reports of the potential involvement of ATP in propagation of intercellular Ca^{2+} waves in mouse glial cells (Guthrie et al., 1999; Hassinger et al., 1996; Yamasaki et al., 1994). The effect of electroporation on glial responses to purinergic stimuli was tested by exposure of cells to ATP (1, 10 μM). In these experiments, ATP induced comparable $[Ca^{2+}]_i$ elevations in the same percentage of cells on both the Texas Red-dextran loaded and non-loaded side of the coverslip (**Fig. 17 c,d,** n = 4, 10 μM ATP).

These control experiments demonstrated that electroporation does not affect

initiation and propagation of Ca^{2+} waves, responses to depolarizing stimuli, integrity of intracellular Ca^{2+} stores, and responsiveness to neurotransmitters that cause IP_3 generation.

III-8. Efficacy of electroporation

After determining the optimal electroporation protocol, electroporation efficacy was determined. All drugs used in the electroporation experiments were diluted in an electroporation buffer that contained a fixed concentration of Texas Red-dextran conjugates, thus enabling visualization of loaded cells, as well as calculation of the efficacy of the electroporation. In order to calculate the efficacy of the electroporation, images of a) a thin layer of the solution that was electroporated into cells, b) zones of cells on the electroporated side of coverslips, and c) zones of cells on the non-electroporated sides of the coverslip were acquired. Intensity of the Texas Red fluorescence was then measured from multiple points on these images and averaged. The efficacy of electroporation was calculated as $(I_p-I_n)/I_{max}$, where I_p is averaged intensity of the fluorescence in Texas Red-dextran-loaded zones, I_n is the averaged intensity of the fluorescence in non-loaded zones, and I_{max} is the averaged intensity of the fluorescence of the electroporation solution. The calculated efficacy of electroporation was 40%.

Figure 17: Analysis of the effects of electroporation on neurotransmitter-induced $[Ca^{2+}]_i$ changes in glial cells. Cultures grown on half-etched coverslips were electroporated with Texas Red-dextran molecules, and then exposed to test stimuli. Responses of cells on the non-loaded side of coverslip were compared to responses of cells on the loaded side of the coverslip. Electroporation induced no change in responses of glial cells to AMCh (100 μM), in both a) the percentage of cells responding and b) $[Ca^{2+}]_i$ increases induced (n = 4). No difference was observed between cells on loaded and non-loaded side of coverslip in terms of c) percentage of cells responding to ATP (10 μM), and d) $[Ca^{2+}]_i$ increases induced by ATP (10 μM, n = 4).

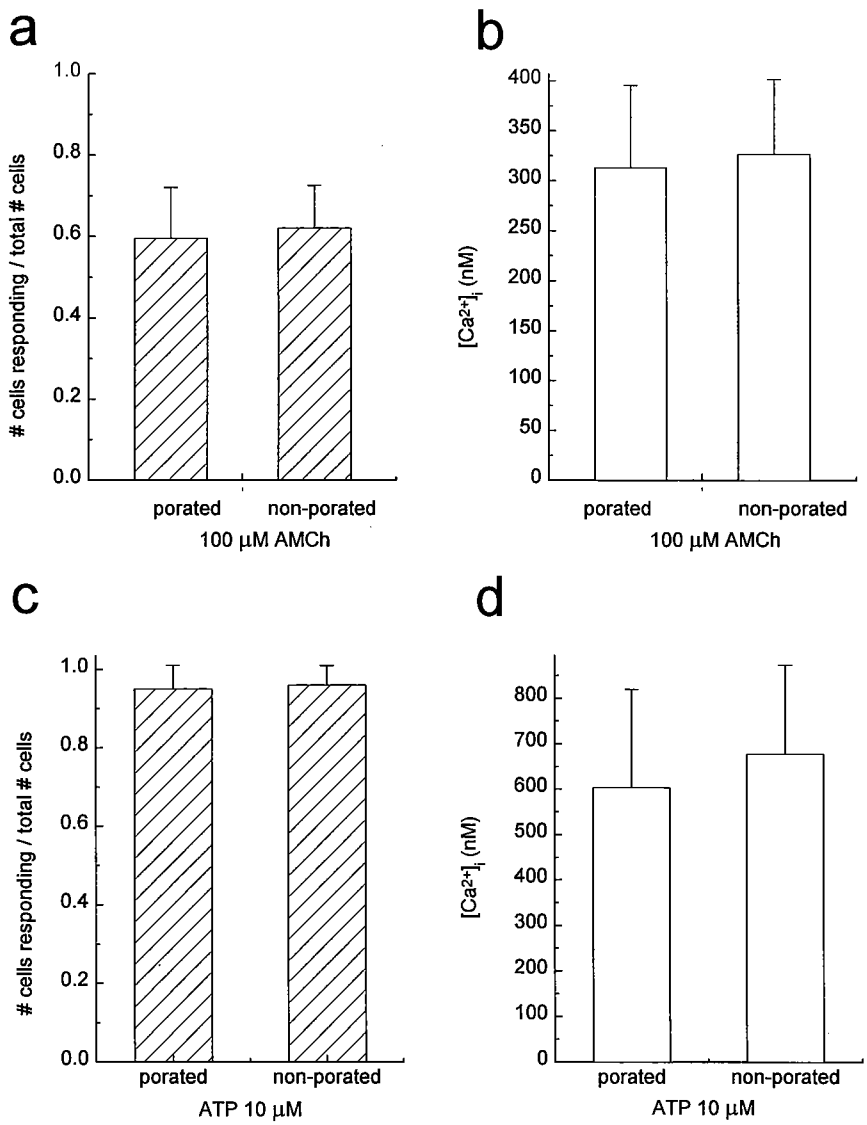
a
cells responding / total # cells
1.0
0.8
0.6
0.4
0.2
0.0
porated
non-porated
100 µM AMCh
b
[Ca2+]i (nM)
400
350
300
250
200
150
100
50
0
porated
non-porated
100 µM AMCh
c
cells responding / total # cells
1.0
0.8
0.6
0.4
0.2
0.0
porated
non-porated
ATP 10 µM
d
[Ca2+]i (nM)
800
700
600
500
400
300
200
100
0
porated
non-porated
ATP 10 µM

Figure 17

III-9. The role of an extracellular mediator in propagation of intercellular Ca^{2+} waves

In the experiments presented in the section III-3, mechanically-induced Ca^{2+} waves were not blocked by extracellular perfusion, but were significantly reduced by gap junction uncouplers. These results suggest that the propagation of intracellular mediator(s) is the dominant mechanism underlying Ca^{2+} wave propagation within rat cortical glia. Due to the ongoing debate among investigators regarding intracellular vs. extracellular Ca^{2+} wave propagation (for reviews, see Charles, 1998; Giaume and Venance, 1998), the possibility of Ca^{2+} wave propagation via an extracellular communication system was addressed by two additional groups of experiments. First, the propagation of Ca^{2+} waves initiated from the zone of cells loaded with the BAPTA-10kd dextran conjugate, a Ca^{2+} buffer that prevents elevations in $[Ca^{2+}]_i$ and does not diffuse through gap junctions ('Calcium Sponge', Molecular Probes), into the control, non-loaded zone of cells during simultaneous extracellular perfusion was investigated. Buffering of $[Ca^{2+}]_i$ increases was carried out to impair the Ca^{2+}-mediated release of excitatory substances, such as is glutamate, that might be released from glia during propagation of Ca^{2+} waves (Bezzi et al., 1998; Hassinger et al., 1995; Jeftinija and Jeftinija, 1998; Newman and Zahs, 1998). The orientation of the perfusion flow was opposite to the expected direction of Ca^{2+} wave propagation, i.e., the extracellular medium was flowing from the control zone of cells

towards the BAPTA-dextran-loaded zone. Under these conditions Ca^{2+} waves successfully propagated from the zone of buffered $[Ca^{2+}]_i$ to the control zone, against the orientation of the extracellular flow (**Fig. 18,** n = 5). This experiment was consistent with the hypothesis that the propagation of mechanically-induced intercellular Ca^{2+} waves in rat glia does not require release and diffusion of an extracellular substance.

The second set of experiments tested whether the activation of receptors coupled via G-proteins to PLC is necessary for the generation of intercellular Ca^{2+} waves. For this, a G-protein inhibitor, nonhydrolyzable GDP analog guanosine-5'-O-(2-thiodiphosphate), GDPβS (20 mM) was electroporated into the cell cultures. It was hypothesized that the inhibition of G proteins would uncouple membrane receptors from PLC enzymes, and thus prevent extracellular activators from evoking IP_3 generation and Ca^{2+} release from ICSs. Since GDPβS is sufficiently small to pass through gap junctions, electroporation of the half-etched coverslips was not carried out, as the time needed for loading of calcium reporter dye would allow GDPβS to start diffusing from loaded into non-loaded zone. This diffusion of GDPβS would make the assessment of propagation between control zone and loaded zone difficult. Instead, GDPβS was electroporated into the entire glial cultures.

Following electroporation of GDPβS, effectiveness of the uncoupling of membrane receptors from PLC enzymes was tested. GDPβS-loaded cells did not respond to stimulations with ATP (1 μM, n = 2, and 10 μM, n = 4, **Fig. 19 b**) and AMCh (50 μM,

Figure 18: Ca^{2+} wave propagation through the zone of cells with buffered $[Ca^{2+}]_i$, against the flow of extracellular medium. The first image represents the zone of cells that were monitored for $[Ca^{2+}]_i$ changes; pseudocolored image of Texas Red fluorescence indicates cells loaded with BAPTA-dextran. A Ca^{2+} wave was mechanically-initiated (white arrow) from a single cell in the culture. Thick gray arrows show orientation of the extracellular medium flow. Elevations in $[Ca^{2+}]_i$ are successfully buffered by BAPTA. After a time interval, the Ca^{2+} wave appears at the border of non-loaded zone of cells, and continues to propagate against the orientation of the extracellular medium flow. The acquisition times are indicated below each image. Color calibration bar indicates changes in $[Ca^{2+}]_i$. The scale bar in the 0s image represents 80 μm.

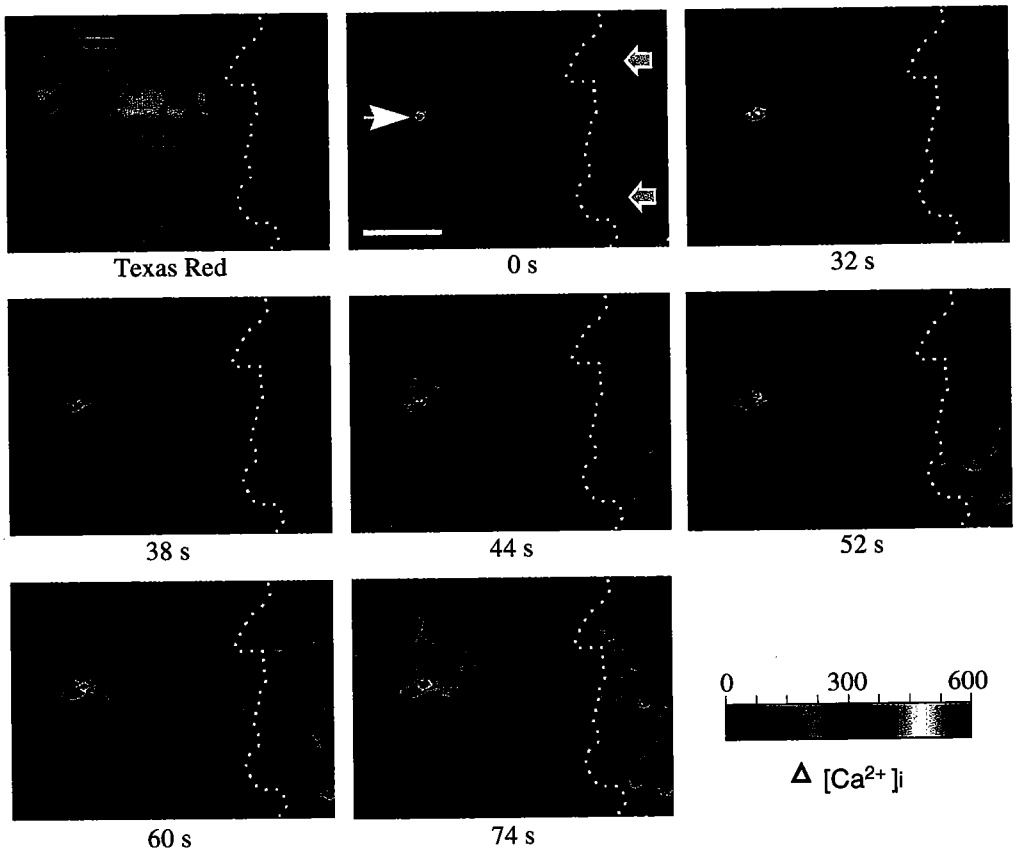

Figure 18

Figure 19: Ca^{2+} wave propagation through the zone of cells loaded with GDPβS. a) The first image represents the pseudocolored image of Texas Red fluorescence in the zone of cells that were monitored for $[Ca^{2+}]_i$ changes. The entire cell culture was loaded with GDPβS as demonstrated by Texas Red fluorescence. A Ca^{2+} wave was mechanically-initiated (white arrow) and propagated to neighboring cells in the culture. The acquisition times are indicated below each image. Color calibration bar indicates changes in $[Ca^{2+}]_i$. The scale bar in the 0s image represents 89 μm.

b) The effect of GDPβS on ATP-induced $[Ca^{2+}]_i$ elevations in glia. Bars represent maximum $[Ca^{2+}]_i$ in control-loaded cells prior to exposure to ATP (bar labeled "control"), after exposure to ATP (bar labeled "ATP"), and after exposure to ATP in cells loaded with GDPβS (bar labeled "ATP + GDPbetaS", n = 4 experiments, 120 cells). ATP (10 μM) was applied via bath. Bars represent mean values, lines represent standard deviations.

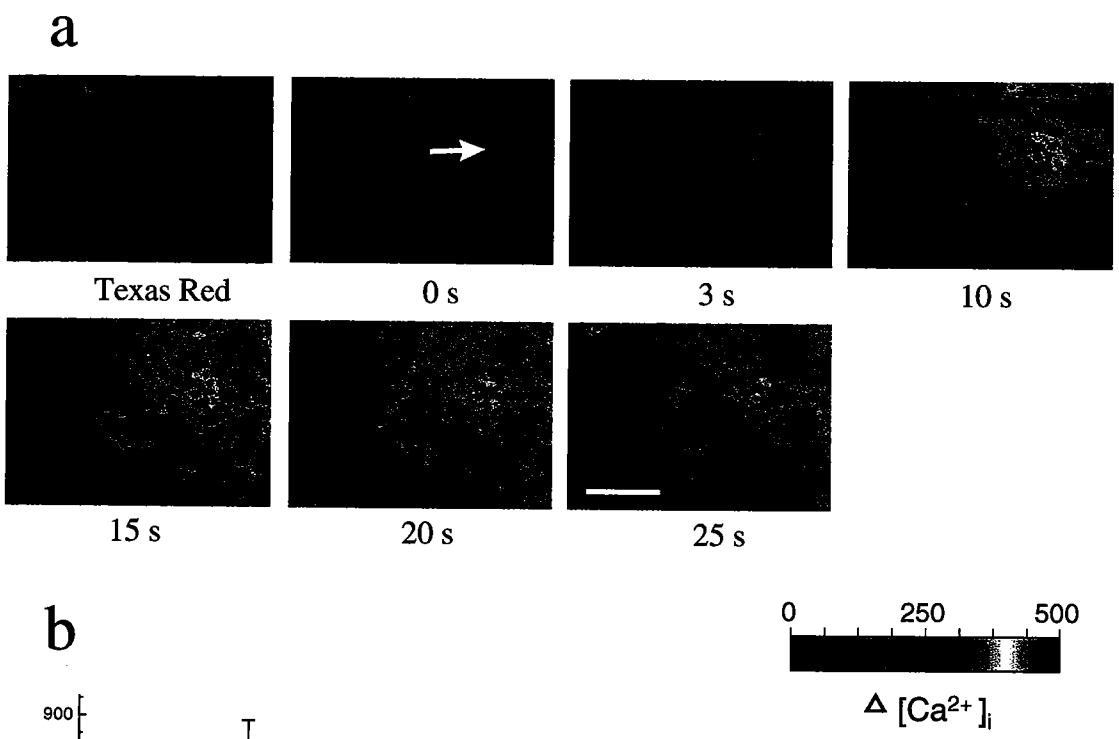
a
Texas Red
0 s
3 s
10 s
15 s
20 s
25 s
b
0
250
500
Δ [Ca2+]i
900
800
700
600
500
400
300
200
100
0
[Ca2+]i
control
ATP
ATP+GDPbetaS

Figure 19

n = 2, and 100 μM, n = 3), which demonstrated that GDPβS effectively blocked G protein-mediated glial responses. Ca^{2+} waves however, were successfully initiated and propagated through the GDPβS-loaded cells (n = 12, **Fig. 19 a**). Although electroporation with GDPβS did not block Ca^{2+} wave propagation, GDPβS may have an effect on the kinetics of Ca^{2+} wave propagation, that would suggest activation of G proteins during propagation of Ca^{2+} waves. Therefore, to calculate the velocity of Ca^{2+} waves in GDPβS- and control-loaded cells, the onset time of $[Ca^{2+}]_i$ rise during Ca^{2+} wave propagation was measured in cells at different distances from the Ca^{2+} wave origin. In order to compare wave propagation through the GDPβS-loaded cells to propagation through the control-loaded cells, the results for individual cells were plotted as time verses distance graphs and fitted to a curve that gave the smallest χ^2 value (**Fig. 20 a**, n = 4 GDPβS experiments, 120 cells; n = 3 control experiments, 85 cells). A hyperbolic nonlinear curve proved to be the best fit curve for data collected from both control- and GDPβS-loaded cultures (χ^2 = 544 and 571, respectively). Comparison of the curve fits revealed that the velocity of Ca^{2+} waves propagating through the GDPβS-loaded cells was comparable to the velocity of Ca^{2+} waves propagating through the Texas Red-dextran-loaded cells, i.e., control-loaded cells (**Fig. 20 a**). Analysis of the normalized number of cells that participated in Ca^{2+} waves and calculation of propagation distances of Ca^{2+} waves, showed only a small difference between Ca^{2+} waves propagating through the control-loaded cells and Ca^{2+} waves propagating through the GDPβS-loaded cells. Ca^{2+} waves propagating through GDPβS-loaded cells propagated through 84 % of the control number of cells for distances

Figure 20: Effects of GDPβS on initiation and propagation of Ca^{2+} waves. a) Analysis of the velocity of Ca^{2+} wave through the cells loaded with GDPβS. The position and the time of $[Ca^{2+}]_i$ change of individual cells participating in Ca^{2+} wave propagation are plotted (time, distance). Both control (Texas Red dextran) and GDPβS-influenced propagation are fitted with nonlinear hyperbolic curve fit (χ^2= 544 and 571 respectively). Control curve: n = 3 experiments, 85 cells; GDPβS curve: n = 4 experiments, 120 cells. b) GDPβS decreases the size of Ca^{2+} waves to 84% of the size of Ca^{2+} waves in control conditions ($p < 0.01$). The normalized number of cells propagating Ca^{2+} wave was calculated as the percentage of the total number of cells present in the field of view. Mean value of the number of cells propagating Ca^{2+} wave in control conditions is regarded as the maximum response (n = 16), and the value obtained for the waves in GDPβS is represented as a percentage of the control value (n = 12).

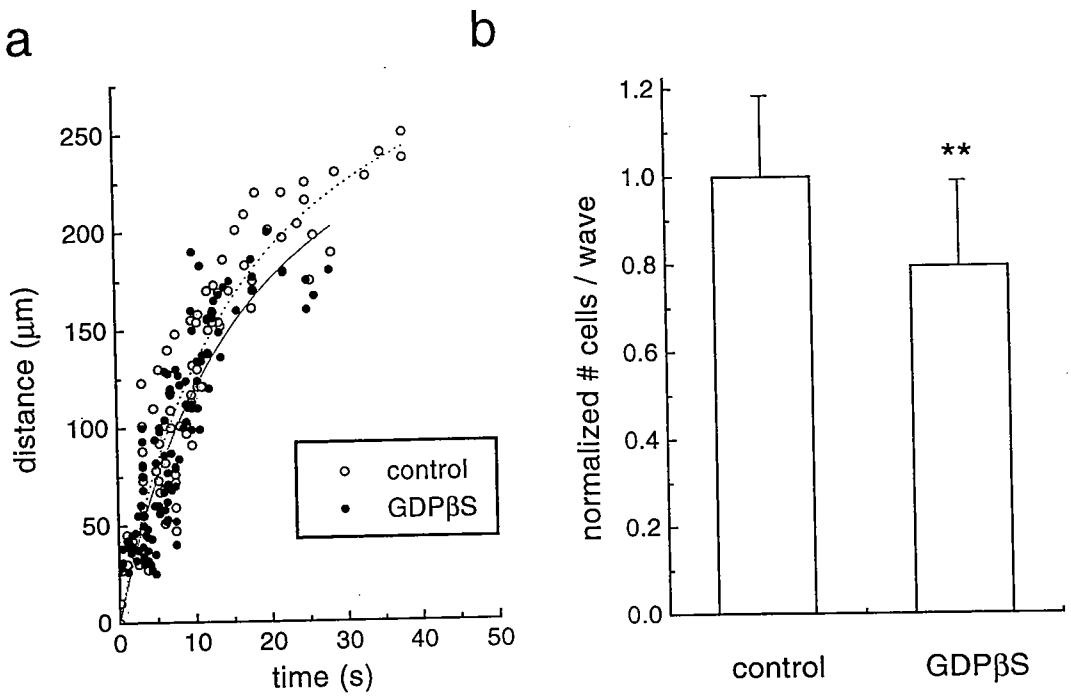
a
b
distance (μm)
time (s)
control
GDPβS
normalized # cells / wave
**
control
GDPβS

Figure 20

that were approximately only two cell diameters in size shorter than propagation distances of control waves (**Fig. 20 b**, n = 28). Thus, Ca^{2+} waves in GDPβS loaded cultures propagated only marginally smaller distances when compared to waves in control cultures. These results further support the hypothesis that the excitatory substances released from glia are not a necessary component of Ca^{2+} initiation and propagation. In addition, these results suggest that PLC is directly activated by mechanical stimulation, since G protein inhibition by GDPβS did not inhibit Ca^{2+} wave initiation.

III-10. Signal(s) that propagate Ca^{2+} waves

The results of experiments described within sections III-3 and III-4 were consistent with the hypothesis that the release of Ca^{2+} from ICSs and functional gap junctions are necessary for generation of Ca^{2+} waves. Experiments that investigated PLC activity during Ca^{2+} wave generation also suggested that IP_3 molecules may be the signal that propagates between cells during Ca^{2+} wave propagation. Nevertheless, both Ca^{2+} and IP_3 molecules are small enough to pass through gap junctions during Ca^{2+} wave propagation and may activate the release of Ca^{2+} from ICSs. In the past few years more evidence has emerged that glial cells contain, in addition to an abundance of IP_3Rs, a second type of intracellular Ca^{2+} receptor/channels, ryanodine receptor/channels (RyRs) (Golovina et al., 1996; Golovina and Blaustein, 1997; Langley and Pearce, 1994; Simpson et al., 1998; Simpson et al., 1998) that release Ca^{2+} via CICR mechanism. The following experiments were designed to investigate which activators of intracellular Ca^{2+} release,

IP_3, Ca^{2+}, or both IP_3 and Ca^{2+}, diffuse through the gap junctions of neighboring cells during Ca^{2+} wave propagation. Since $[IP_3]_i$ cannot be visualized by currently available imaging techniques, experiments were conducted by monitoring $[Ca^{2+}]_i$ changes in cells induced to propagate Ca^{2+} waves. To determine the involvement of Ca^{2+} and IP_3 in Ca^{2+} wave propagation, experiments were conducted on cell cultures that were loaded with heparin (a compound that prevents binding of IP_3 to IP_3Rs (Berridge, 1993; Boitano et al., 1992)), and BAPTA-dextran. The involvement of glial RyRs in the propagation of intercellular Ca^{2+} waves was tested by experiments on glial cell cultures loaded with ruthenium red (ruthenium oxychloride), a well known inhibitor of Ca^{2+} release through RyRs (Chamberlain et al., 1984; Kannan et al., 1997).

III-10.i. The role of IP_3 in the propagation of intercellular Ca^{2+} waves.

The propagation of Ca^{2+} waves into and from the zone of cells loaded with the IP_3Rs blocker heparin was investigated. Since heparin is a large molecule (6,000 MW) that does not pass through gap junctions, introduction of heparin into cells was performed by electroporation of heparin solution (660 μM) into defined areas of glial culture grown on the half-etched coverslips. Cells growing on the etched (non-conductive) half of the coverslip were not loaded, and served as a control field of cells. If intercellular Ca^{2+} waves are solely IP_3-mediated, i.e., if the increase in $[Ca^{2+}]_i$ during the wave propagation is due to Ca^{2+} release from IP_3-sensitive Ca^{2+} stores, the Ca^{2+} wave initiated from the control zone of cells should have 'disappeared' when it reached the cells with blocked IP_3 receptors. If Ca^{2+} ions however, propagate between the cells during Ca^{2+} wave

propagation, the propagation of Ca^{2+} wave should continue through the heparin-loaded zone.

Intercellular Ca^{2+} waves initiated within the non-loaded area of the coverslip propagated to, but did not cross the border into the region of heparin-loaded cells (**Fig. 21,** n = 13) suggesting that binding of IP_3 to its receptors is a necessary step for the increase in $[Ca^{2+}]_i$ which occurs during Ca^{2+} wave propagation. Furthermore, this result supported the hypothesis that Ca^{2+} ions cannot act as independent messengers of the Ca^{2+} wave propagation, since that mechanism would be expected to result in $[Ca^{2+}]_i$ elevations in the area of heparin-loaded cells that have inactive IP_3Rs. Following the stimulation of a cell within the heparin-loaded area, a small $[Ca^{2+}]_i$ increase was detected in the mechanically-stimulated cell, but a Ca^{2+} wave was not visualized in the surrounding heparin-loaded cells. After a time delay proportional to the distance of the border of the non-loaded zone of cells from the Ca^{2+} wave origin, a Ca^{2+} wave front emerged at the border of the non-loaded zone of cells, and continued to propagate through these cells (**Fig. 22,** n = 6). This observation suggested that Ca^{2+} is a poor mediator of Ca^{2+} waves and that $[Ca^{2+}]_i$ elevations in the cells that are on the path of Ca^{2+} wave are not necessary for the propagation of Ca^{2+} wave.

Figure 21: A Ca^{2+} wave does not propagate in the zone of cells loaded with IP_3 receptor blocker heparin. Ca^{2+} wave initiated in non-loaded zone of the culture (white arrow) propagates to, but does not cross the border with the heparin-loaded cells. Texas Red image indicates the cells loaded with heparin. Dotted line marks the boundary between heparin-loaded and non-loaded zone. The acquisition times are indicated below each image. Color calibration bar indicates changes in $[Ca^{2+}]_i$, and the scale bar indicates 65 μm.

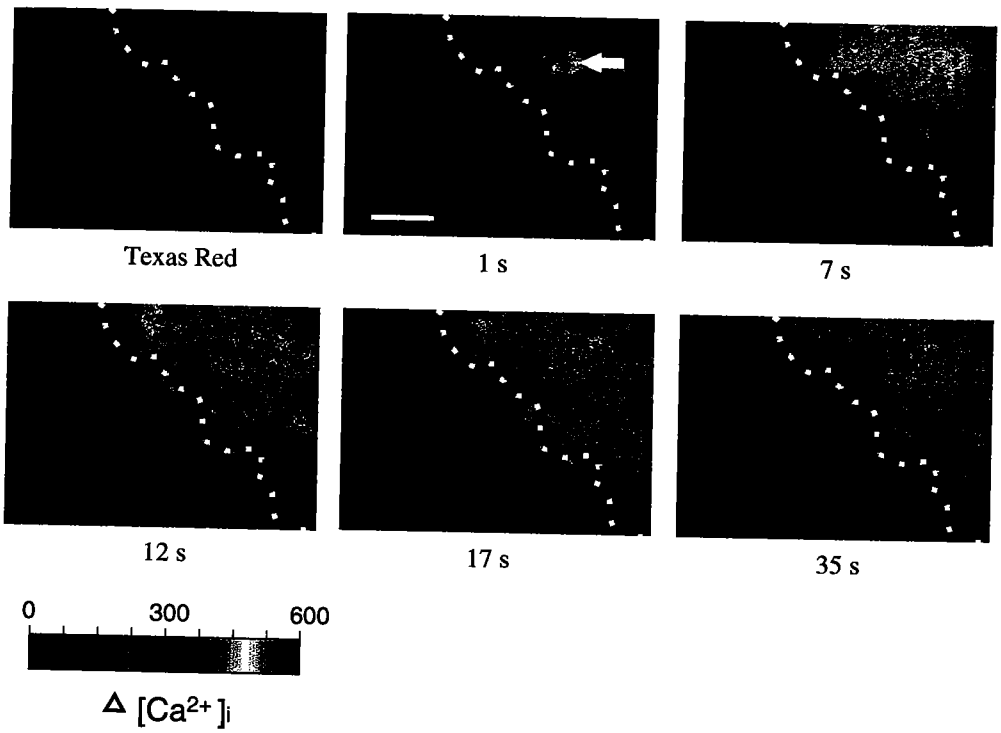

Figure 21

Figure 22: A Ca^{2+} wave propagates through the zone of heparin-loaded cells. Upon single cell stimulation (arrow) no Ca^{2+} wave propagation is visualized through the heparin-loaded zone. After a time interval, a Ca^{2+} wave appears at the border of the non-loaded cell zone and continues to propagate through that zone. First frame is a pseudocolored image of Texas Red fluorescence that indicates cells loaded with heparin. Dotted line marks the boundary between heparin-loaded and non-loaded zone. The scale bar in 0 s image represents 78 μm. The acquisition times are indicated below each image. Color calibration bar indicates changes in $[Ca^{2+}]_i$.

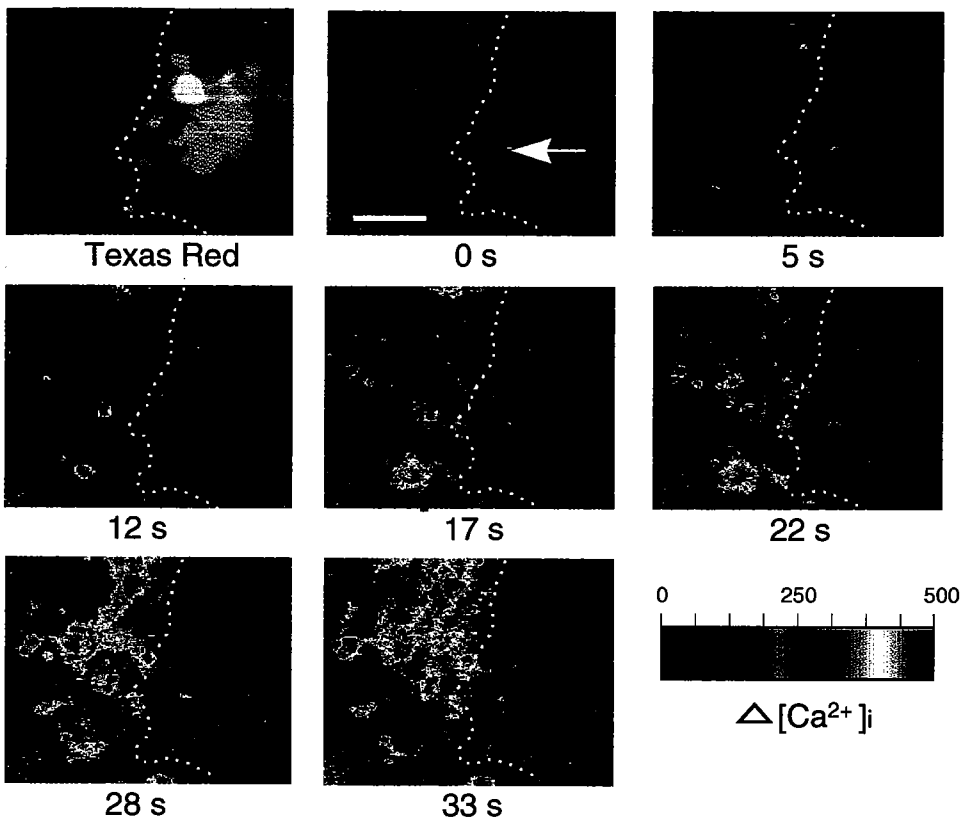

Figure 22

In the second group of experiments, the propagation of Ca^{2+} waves into and from a zone of cells loaded with BAPTA-dextran (6 mM) was investigated. Since BAPTA is a molecule small enough to diffuse through the gap junctions, BAPTA-dextran (i.e., Calcium Sponge) was used to assure that the Ca^{2+} buffer stayed confined within the loaded cells.

In order to perform Ca^{2+} wave propagation experiments while effectively buffering $[Ca^{2+}]_i$, several working concentrations of Calcium Sponge were tested. Muscarinic agonist AMCh and purinergic agonist ATP which induce Ca^{2+} oscillations in glial cells, were used to titrate the concentration of BAPTA-dextran required to completely buffer increases in $[Ca^{2+}]_i$ in glial cells. The results for different concentrations of BAPTA-dextran ranged from minimal buffering of a Ca^{2+} wave and AMCh- and ATP-induced Ca^{2+} oscillations, to moderate levels of $[Ca^{2+}]_i$ buffering, to the complete buffering of Ca^{2+} waves as well as AMCh- and ATP-induced responses. For example, electroporation with a 2 mM solution of BAPTA-dextran decreased peak $[Ca^{2+}]_i$ changes occurring in response to 100 μM AMCh by approximately 50% in loaded cells (**Fig. 23,** n = 3). The concentration of BAPTA-dextran (6 mM) used did not reduce the basal levels of $[Ca^{2+}]_i$, but was effective in inhibiting Ca^{2+} wave- and agonist- induced increases of $[Ca^{2+}]_i$.

These experiments showed that intercellular Ca^{2+} waves initiated within the non-loaded zone of the culture propagated to, but did not cross the border with BAPTA-dextran-loaded cells (**Fig. 24,** n = 15), showing that BAPTA-dextran successfully buffered $[Ca^{2+}]_i$ elevations associated with Ca^{2+} waves. On the other hand, when a single

Figure 23: Effects of $[Ca^{2+}]_i$ buffering on AMCh-induced Ca^{2+} oscillations. BAPTA-dextran (2mM) decreases the amplitude of $[Ca^{2+}]_i$ changes in response to 100 μM AMCh. White arrows indicate the position of the cells that oscillate on the non-loaded side of the coverslip. Large gray arrows indicate cells that oscillate on the loaded side of the coverslip. Note higher $[Ca^{2+}]_i$ elevations in the cells on the non-loaded side. The first frame is a pseudocolored image of Texas Red fluorescence that shows cells loaded with BAPTA dextran. Dotted line marks the boundary between loaded and non-loaded zone. The acquisition times are indicated below each image. Color calibration bar indicates changes in $[Ca^{2+}]_i$. The scale bar in the 0 s image represents 85 μm.

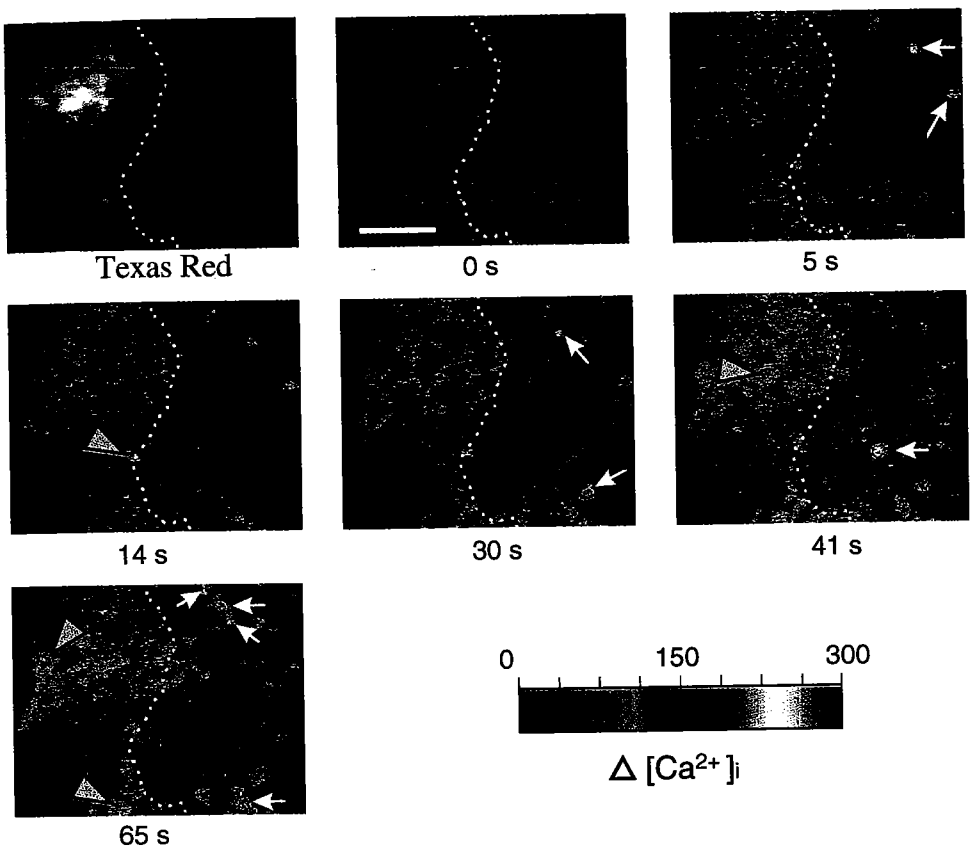

Figure 23

Figure 24: Ca^{2+} wave does not propagate into the zone of cells with buffered $[Ca^{2+}]_i$. A Ca^{2+} wave is initiated (arrow) within non-loaded zone of the culture and propagates to, but does not cross the border with the zone of cells loaded with BAPTA-dextran. Texas Red fluorescence indicates cells loaded with BAPTA-dextran. The last frame is a phase contrast image of the monitored field of cells. Dotted line marks the boundary between loaded and non-loaded zone. The acquisition times are indicated below each image. Color calibration bar indicates changes in $[Ca^{2+}]_i$. The scale bar in the 0 s image represents 87 μm.

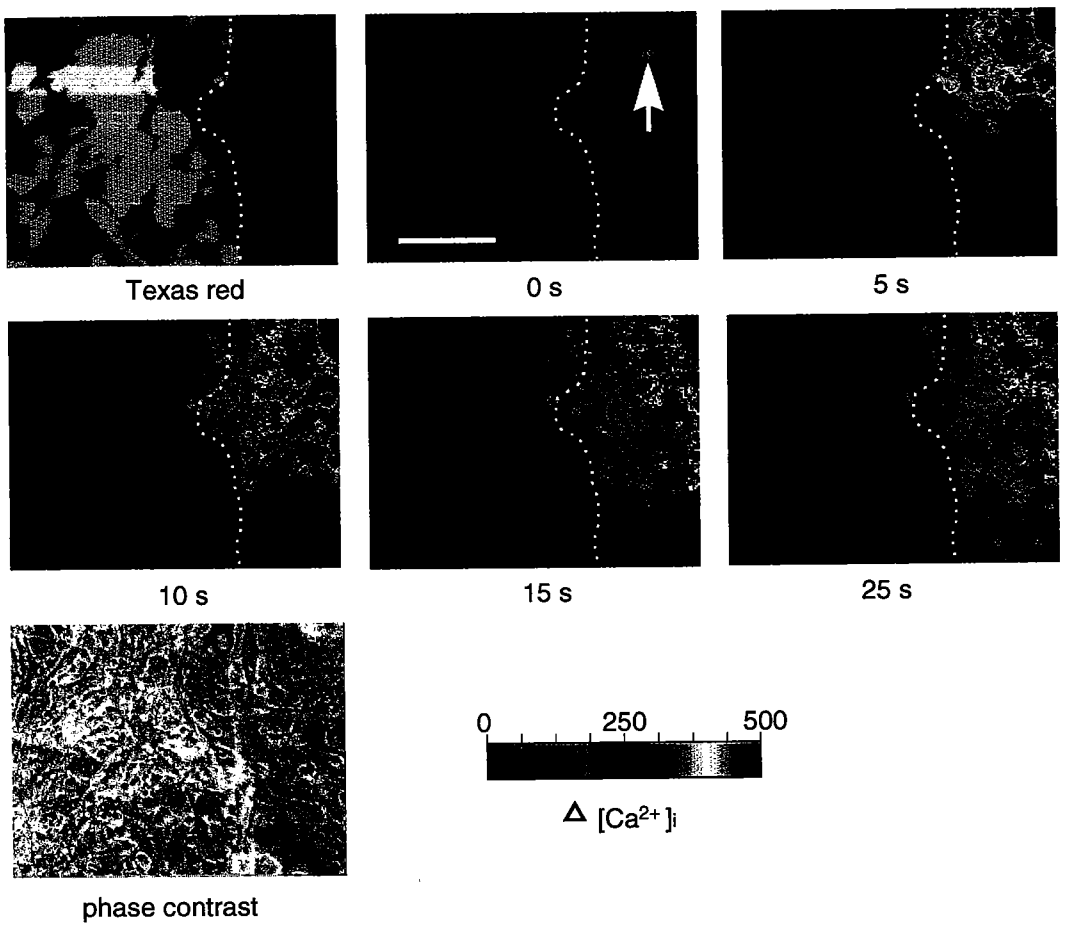

Figure 24

cell within the BAPTA-dextran-loaded zone was mechanically stimulated, an increase in $[Ca^{2+}]_i$ was observed in the simulated cell that was smaller than the increase of $[Ca^{2+}]_i$ observed in the presence of heparin. Analysis of the effects of loaded compounds on the $[Ca^{2+}]_i$ increase in stimulated cell will be addressed later in the study. BAPTA-dextran effectively blocked $[Ca^{2+}]_i$ increases in the loaded cells surrounding the stimulated cell. Interestingly, after a time interval that was proportional to the distance of the non-loaded zone from the Ca^{2+} wave origin , an increase in $[Ca^{2+}]_i$ was observed in the non-loaded cells at the border with the loaded area and propagated through the non-loaded zone in a form of a Ca^{2+} wave (**Fig. 25**, n = 5). The velocity of the Ca^{2+} wave through the non-loaded area was similar to the velocity of Ca^{2+} wave under control conditions. Therefore, the buffering of $[Ca^{2+}]_i$ did not block the propagation of intercellular Ca^{2+} waves.

III-10.ii. The role of Ca^{2+} release via ryanodine receptors in Ca^{2+} wave propagation.

The role of RyRs in generation of intercellular Ca^{2+} waves was assessed utilizing ruthenium red. Ruthenium red was loaded into glial cultures adopting the protocol used for electroporation of GDPβS, since both compounds are molecules small enough to diffuse through gap junctions.

Ruthenium red (80 μM) successfully inhibited $[Ca^{2+}]_i$ release by the RyR agonist caffeine (10 mM, n = 3). Mechanical stimulation of a single cell in ruthenium red-loaded culture induced Ca^{2+} wave propagation (**Fig. 26**, n = 8). These experiments demonstrated

Figure 25: Ca^{2+} wave propagates through the zone of cells with buffered $[Ca^{2+}]_i$. Ca^{2+} wave is initiated (arrow) within BAPTA-dextran-loaded zone. No increases in $[Ca^{2+}]_i$ are visualized surrounding the stimulated cell. An increase in $[Ca^{2+}]_i$ however, is observed at the border with the non-loaded zone of cells, and is followed by propagation of Ca^{2+} wave through that zone. The first frame is a gray scale image of fura-2 fluorescence, and indicates the extent of loading and the position of cells in the culture. The second frame is a pseudocolored image of Texas Red fluorescence of glial cells loaded with BAPTA-dextran. Dotted line marks the boundary between loaded and non-loaded zone. The acquisition times are indicated below each image. Color calibration bar indicates changes in $[Ca^{2+}]_i$. The scale bar in the 0 s image represents 82 μm.

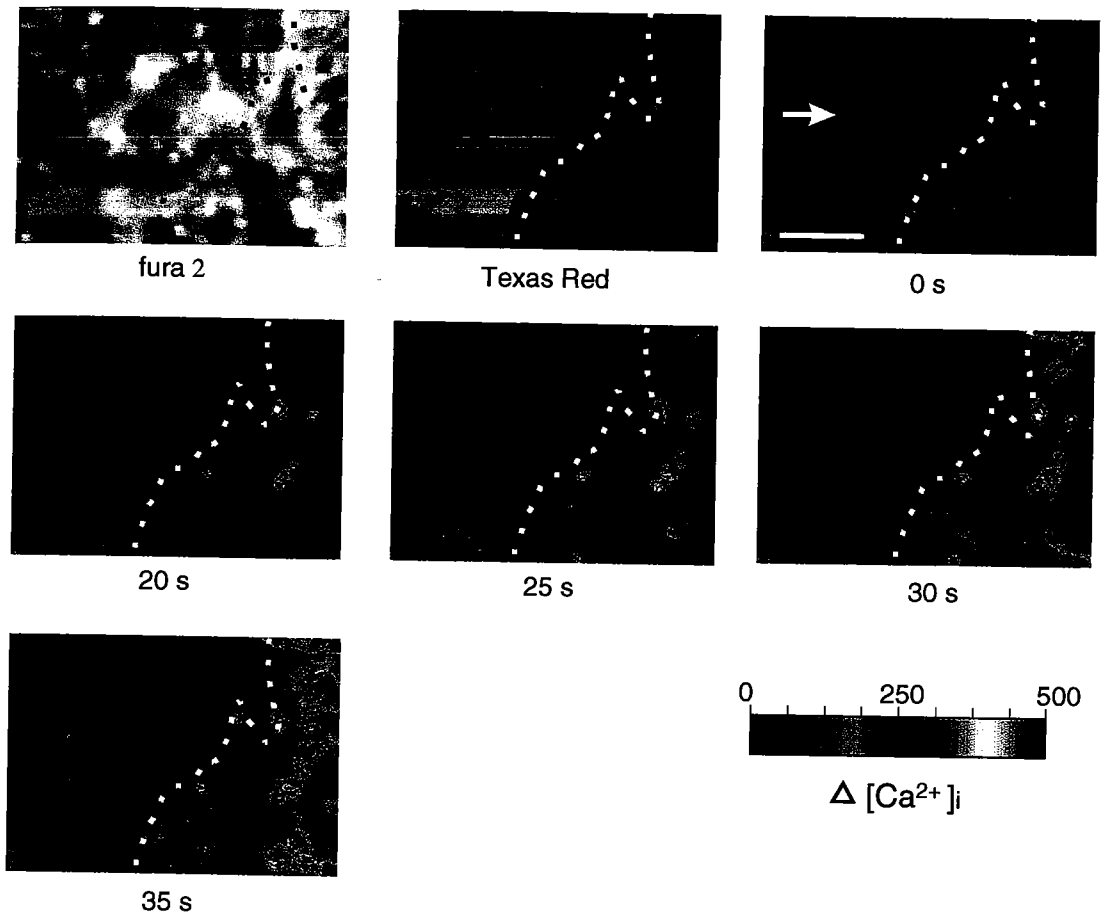

Figure 25

Figure 26: Ca^{2+} wave propagates through the zone of RyR block. Ca^{2+} wave is initiated (arrow) in ruthenium red-loaded culture (80 μM). First frame is a pseudocolored image of Texas Red fluorescence of glial cells loaded with ruthenium red. The acquisition times are indicated below each image. Color calibration bar indicates changes in $[Ca^{2+}]_i$. The scale bar in 0 s image represents 86 μm.

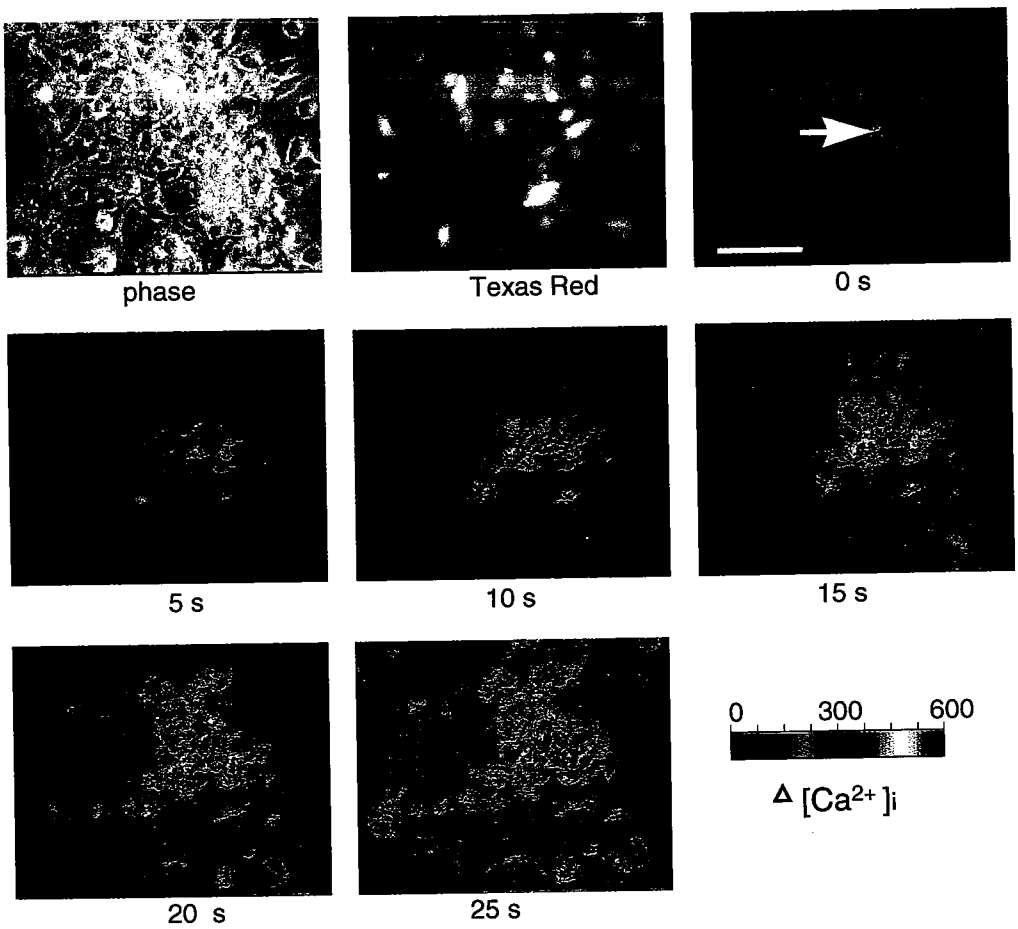

Figure 26

that intercellular Ca^{2+} waves can be initiated and propagated through the zone of cells with blocked RyRs, thus suggesting that CICR from the RyRs is not a necessary component of Ca^{2+} wave initiation and propagation. The release of Ca^{2+} via RyRs however, did contribute to $[Ca^{2+}]_i$ rises in cells that propagated Ca^{2+} waves, since mean values of $[Ca^{2+}]_i$ elevations decreased from 290 ± 90 nM in the control-loaded cells to 230 ± 70 nM in the ruthenium red-loaded cells ($t=3.99$, $p < 0.01$, $n = 101$ cells). This analysis suggested that during Ca^{2+} wave propagation IP_3-sensitive Ca^{2+} stores release Ca^{2+} that via CICR induces release of Ca^{2+} from Ry-sensitive stores. Still, since pharmacological tools for studying intracellular Ca^{2+} signaling lack specificity, the ruthenium red effect may be due to a combination of both effect on RyRs as well as a non-specific effect on ICSs' proteins (Taylor and Broad, 1998).

III-10.iii. Ca^{2+} does not contribute to propagation of Ca^{2+} waves through the cells with sensitized IP_3Rs.

Although electroporation experiments suggested that Ca^{2+} alone does not serve as the major mediator of intercellular Ca^{2+} waves in glia, Ca^{2+} could contribute to propagation of intercellular Ca^{2+} waves if IP_3Rs, sensitized by binding of IP_3, respond by the CICR mechanism to small and otherwise quickly buffered quantities of Ca^{2+} ions that may diffuse through the gap junctions. To test this hypothesis two types of experiments were conducted. In the first set of experiments, $[IP_3]_i$ was raised by propagation of a Ca^{2+} wave in order to sensitize glial IP_3Rs. Following the Ca^{2+} wave, a further increase of $[Ca^{2+}]_i$ within a single cell that had participated in the propagation of the Ca^{2+} wave was

achieved by photorelease of Ca^{2+} from NP-EGTA. The photorelease of Ca^{2+} within single cells (flash duration ≤ 2 s) that were at different distances from the origin of intercellular Ca^{2+} wave were performed 5 - 45 seconds after wave propagation, therefore testing responses to $[Ca^{2+}]_i$ increase in cells with different $[IP_3]_i$. In all experiments, the increase of $[Ca^{2+}]_i$ within a single cell did not generate a new intercellular Ca^{2+} wave originating from the flashed cell (**Fig. 27,** n = 10). The inability to initiate Ca^{2+} waves could not be explained by the first Ca^{2+} wave rendering Ca^{2+} stores empty or refractory to the $[Ca^{2+}]_i$ rise, since mechanical stimulus of a cell that propagated Ca^{2+} wave induced a new Ca^{2+} wave in the same time interval used for the photorelease (**Fig. 28**).

In the second set of experiments, $[IP_3]_i$ was raised within glial cells by bath application of neurotransmitter AMCh before increasing $[Ca^{2+}]_i$ by flash photolysis of a single cell in an attempt to initiate an intercellular Ca^{2+} wave. Although AMCh successfully increased $[IP_3]_i$, as indicated by the initiation of the Ca^{2+} oscillations in culture, the photorelease of Ca^{2+} within single cells (flash duration = 1 and 2 s) in cultures that were exposed to AMCh (50, 100, 200 μM, n = 14) for 30-60 seconds duration did not initiate a Ca^{2+} wave (**Fig. 29**).

Figure 27: Increase of $[Ca^{2+}]_i$ in a cell that propagated mechanically-induced intercellular Ca^{2+} wave does not initiate propagation of a second intercellular Ca^{2+} wave. Culture was loaded with NP-EGTA, i.e., 'caged Ca^{2+}' and changes in $[Ca^{2+}]_i$ were monitored withfluo-3. The first row: Single cell (thin arrow) was mechanically stimulated in order to induce intercellular Ca^{2+} wave. The second row: A cell that participated in the propagation of Ca^{2+} wave (thick arrow) was exposed to UV light, which caused release of Ca^{2+} from its photolabile carrier NP-EGTA. The first image in the second row represents the whole field of view, the second image represents the area of the culture delineated in the first image that is zoomed-in in order to closely observe the area surrounding the flashed cell. The third and the fourth row: Uncaging of NP-EGTA increases $[Ca^{2+}]_i$ in the cell, but does not induce an intercellular Ca^{2+} wave. Fluo-3 fluorescence recorded 1 second before UV flash served as the basal fluorescence (Fo) in calculations of change in fluorescence during and after the flash (Δ F/Fo). Color calibration bar indicates the percentage changes in $[Ca^{2+}]_i$. The acquisition times are indicated below each image.

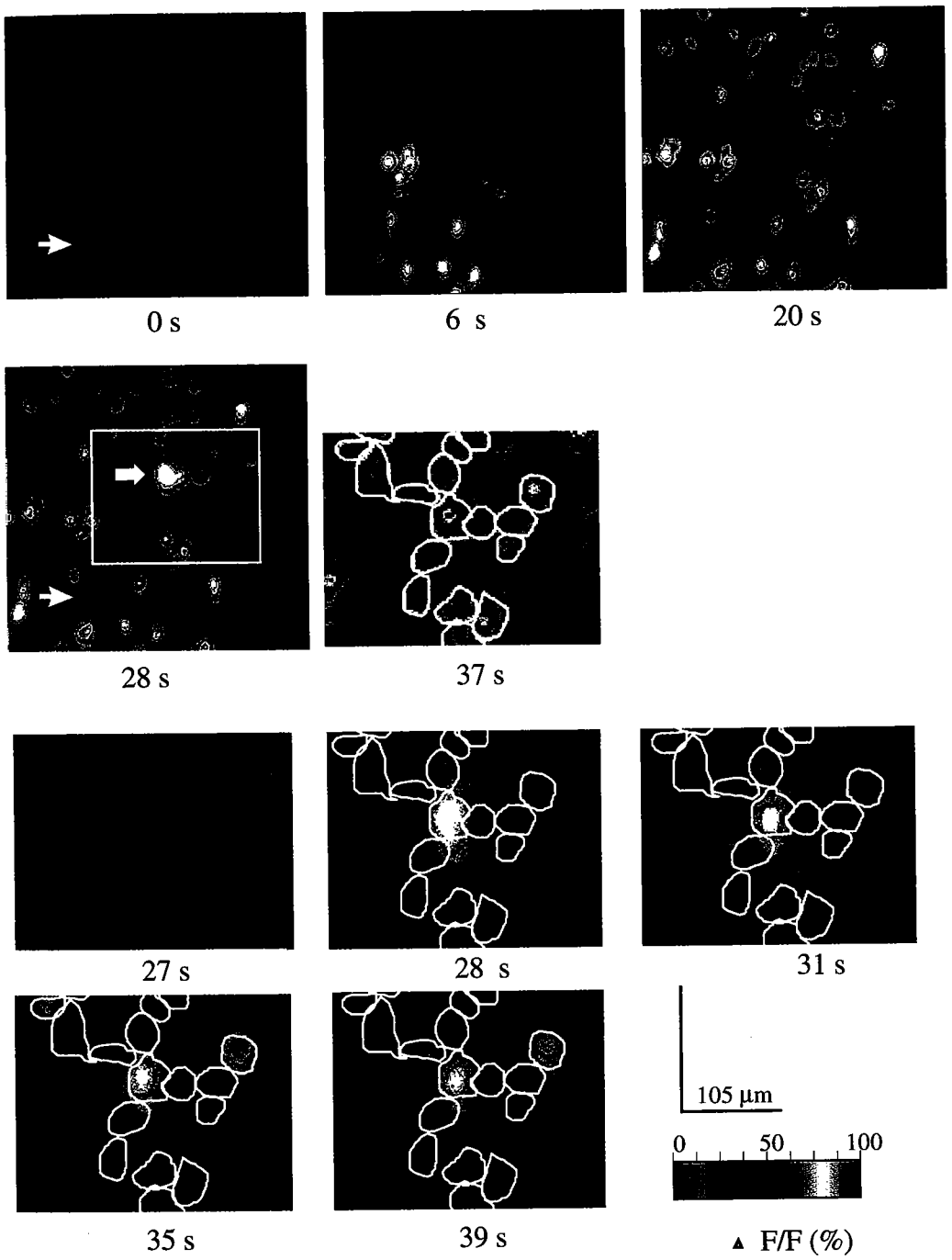

Figure 27

Figure 28: Propagation of two Ca^{2+} waves through the same zone of cells. Ca^{2+} waves were mechanically induced (white arrows). The second wave was initiated from the cell that propagated the first wave, 31 s after the initiation of the first wave. The third row of images represents changes in $[Ca^{2+}]_i$ occurring during the second wave in relation to $[Ca^{2+}]_i$ before the second stimulus. The second mechanical stimulation successfully induced propagation of intercellular Ca^{2+} wave. The scale bar in 0 s image represents 75 μm. The acquisition times are indicated below each image. Color calibration bar indicates changes in $[Ca^{2+}]_i$.

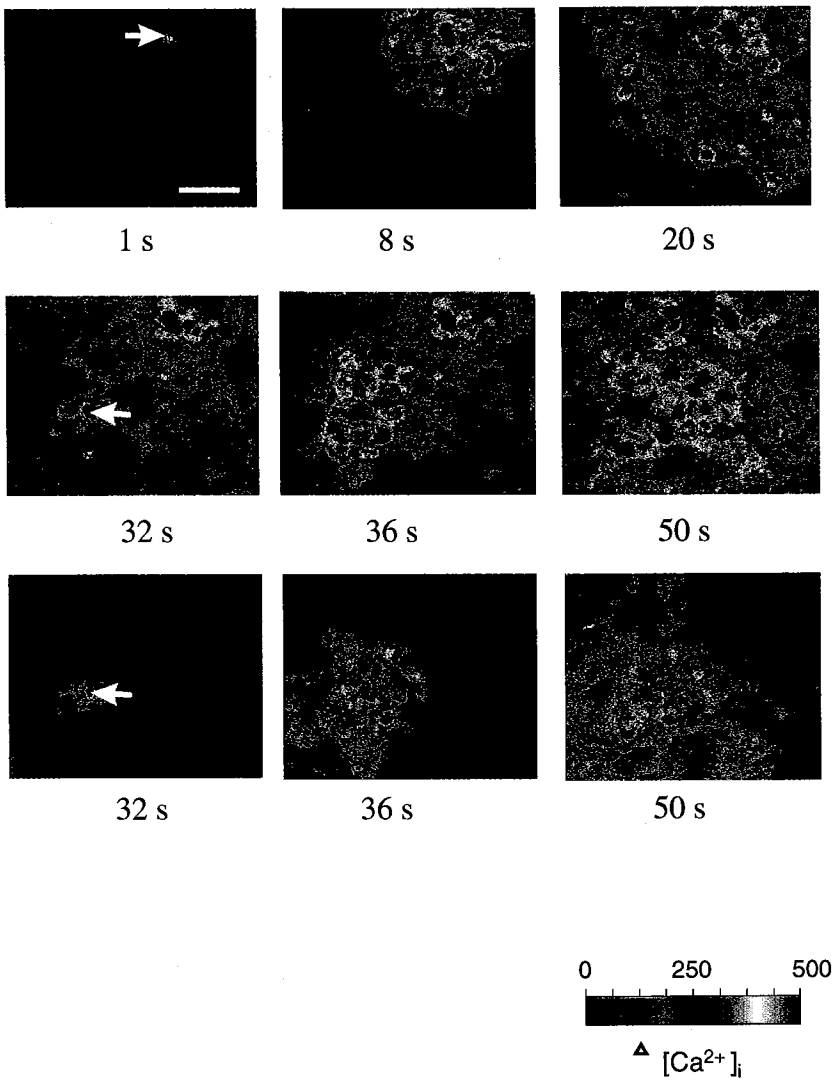

Figure 28

Figure 29: Photorelease of Ca^{2+} within a cell exposed to AMCh. The addition of 200 μm AMCh to the culture induced Ca^{2+} oscillations that occur within the observed zone of cells as $[Ca^{2+}]_i$ increases and decreases. A single cell (arrow) was exposed to UV light 40 s after AMCh application, which caused release of Ca^{2+} from its photolabile carrier and an increase in $[Ca^{2+}]_i$ within the flashed cell. No Ca^{2+} waves were observed. The scale bar indicates 87 μm. Color calibration bar indicates changes in $[Ca^{2+}]_i$.

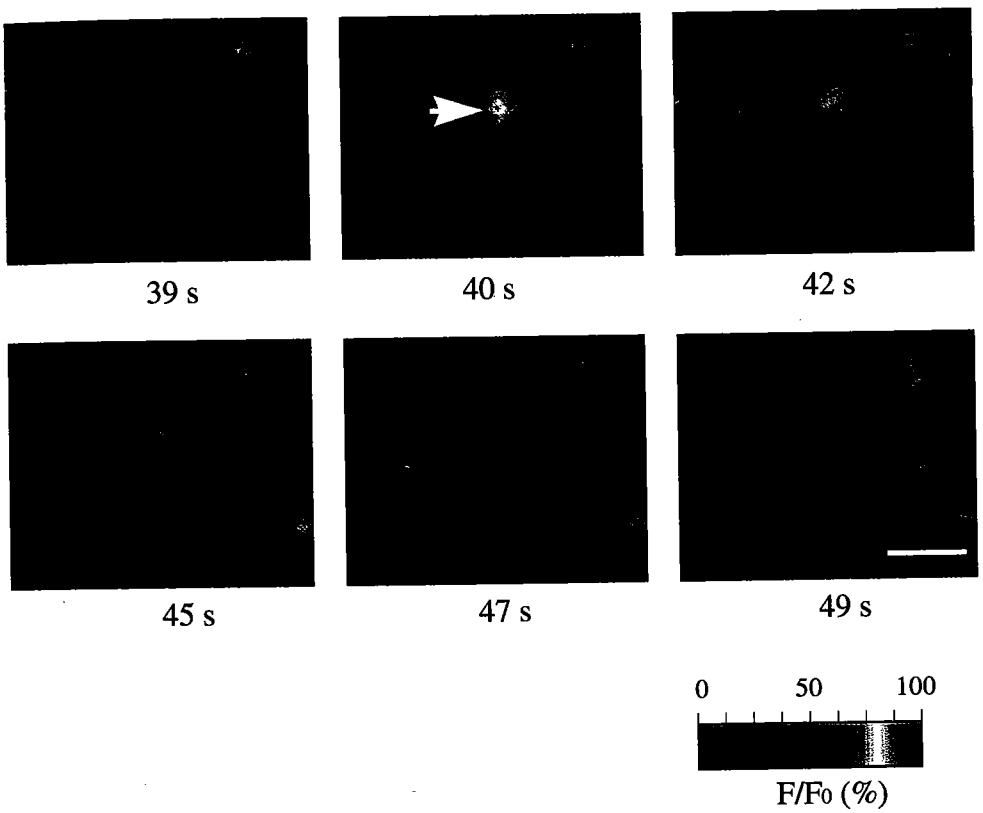

Figure 29

The results of these experiments are consistent with the hypothesis that the diffusion of IP_3 between cells, and IP_3 binding to its intracellular receptors, is necessary for the propagation of Ca^{2+} waves through glial syncytium. Furthermore, experiments in heparin-loaded cells suggest that Ca^{2+} does not co-diffuse with IP_3 molecules between the cells during the Ca^{2+} wave propagation. An increase in $[Ca^{2+}]_i$ in cells that propagate Ca^{2+} waves does not seem to be necessary for Ca^{2+} wave propagation. These experiments are consistent with the hypothesis that in glial cells Ca^{2+} diffusion does not contribute to the propagation of Ca^{2+} waves, regardless of the activation state of intracellular IP_3Rs.

III-11. Ca^{2+} wave propagation: diffusion vs. regeneration of the propagating signaling molecules

The passive diffusion model of Ca^{2+} wave propagation requires that all the molecules of IP_3 that mediate the Ca^{2+} wave are made in one cell (Sanderson, 1995; Sneyd et al., 1994; Sneyd et al., 1995a). On the other hand, if the Ca^{2+} waves propagate by regeneration, IP_3 molecules are made in the stimulated cell (i.e., the cell of the Ca^{2+} wave origin) as well as in cells that propagate a Ca^{2+} wave. One possibility is that regeneration of IP_3 in cells that propagate Ca^{2+} wave occurs due to the Ca^{2+} induced activation of PLC (Giaume and Venance, 1998; Venance et al., 1995; Venance et al., 1997). To determine whether Ca^{2+} waves propagate by diffusion or regeneration mechanisms, analysis of Ca^{2+} wave propagation through the zones of cells that could not participate in Ca^{2+}-dependent IP_3 regeneration was carried out. Ca^{2+}-dependent IP_3 regeneration was prevented by either

inhibiting the Ca^{2+} release via IP_3Rs by heparin, or by buffering of $[Ca^{2+}]_i$ elevations by BAPTA-dextran. If Ca^{2+} waves propagate by regeneration of IP_3, Ca^{2+} waves should either slow down or cease to propagate through the zones of inhibited IP_3 regeneration. On the other hand, if Ca^{2+} waves propagate by diffusion of IP_3 molecules that are generated within a single cell, propagation distance and velocity of a Ca^{2+} wave should predominantly depend on the quantity of IP_3 produced in the stimulated cell. Therefore, in the following experiments the relationship between $[Ca^{2+}]_i$ in the cells on the path of Ca^{2+} waves and the kinetics of intercellular Ca^{2+} waves was analyzed.

III-11.i. Effect of heparin on the Ca^{2+} wave propagation.

The velocity of a Ca^{2+} wave propagating through the cells with heparin-blocked IP_3Rs was quantified by measuring the time that was required for the Ca^{2+} wave to reach the non-loaded cells located at the border with heparin-loaded zone (**Fig. 30**). Similar measurements were carried out for waves propagating through cells loaded only with the control (i.e., Texas Red-dextran) solution. Nonlinear hyperbolic curves were fitted to the data since they gave the lowest χ^2 error values for both propagation in control and heparin-loaded cells (χ^2 = 562 and 1060, respectively, n = 10). A comparison of curves revealed that Ca^{2+} waves propagating through the heparin-loaded cells were slower and smaller when compared to control waves (**Fig. 31**). The longest wave propagation distance through the zone of heparin-loaded cells was 200 μm, while the propagation distance of Ca^{2+} waves through the Texas Red dextran-loaded zone was greater than 275

μm.

The effect of heparin on the propagation of Ca^{2+} waves may have occurred due to either the effect of heparin in the mechanically-stimulated cell, or the effect of heparin in cells that propagated a Ca^{2+} wave. In the stimulated cell, heparin could have caused less IP_3 production by preventing Ca^{2+} release from IP_3Rs, thus reducing Ca^{2+}-mediated activation of PLC. On the other hand, in cells that propagated Ca^{2+} waves, heparin may also have influenced the regeneration or the degradation rate of IP_3, or the permeability of gap junctions.

Figure 30: Method of measuring Ca^{2+} wave propagation. The distance and the time required for the Ca^{2+} wave to reach non-loaded cells at the border with the loaded cells were measured. Note that Ca^{2+} waves propagate radially through the glial cell cultures.

Ca2+ wave propagation measurements
electroporated
control
wave
(distance, time)
(distance, time)
(distance, time)
(distance, time)

Figure 30

Figure 31: Comparison of the velocity of Ca^{2+} wave propagation through the cell zone of IP_3 receptor block and control. Both control- and heparin-influenced propagation velocity graphs were fitted with a nonlinear hyperbolic curve fit (χ^2= 562 and 860 respectively). Control propagation curve n = 4 experiments, 60 cells; heparin propagation curve n = 6 experiments, 75 cells.

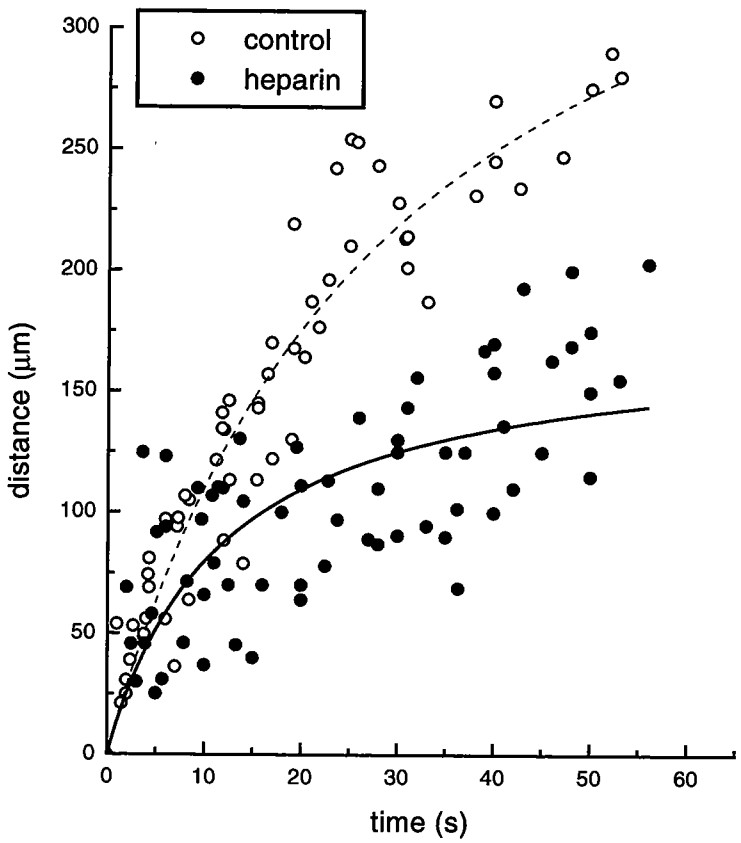
control
heparin
distance (µm)
time (s)
0
50
100
150
200
250
300
0
10
20
30
40
50
60

Figure 31

To distinguish whether the initiation or propagation of Ca^{2+} waves was influenced by heparin, Ca^{2+} waves that propagated *through* the zone of heparin-loaded cells were compared with Ca^{2+} waves that propagated through the non-loaded zone of cells but were initiated *from* a single heparin-loaded cell located at the edge of the loaded zone (**Fig. 32**). Ca^{2+} waves initiated from a single heparin-loaded cell propagated through the control zone of cells for significantly shorter distances (155 ± 25 μm, n = 5) when compared to waves that were initiated in, and propagated through the control zone of cells, but propagated similar distances to Ca^{2+} waves that propagated through the heparin-loaded zone (161 ± 26 μm, n = 6).

A comparable propagation distance of Ca^{2+} waves that were only initiated *from*, or were initiated *from and propagated through* heparin-loaded cells, suggested that the effect of heparin on the Ca^{2+} wave occurred in the stimulated cell. Therefore, the altered velocity of Ca^{2+} waves in heparin-loaded cells is a result of the effect of heparin in the cell of Ca^{2+} wave origin. Since heparin effects predominantly occurred in the cell of Ca^{2+} wave origin and not in the cells through which Ca^{2+} wave propagated, these results suggest that alterations of gap junctional permeability and IP_3 degradation rate in the zone of cells that propagate Ca^{2+} waves are not the major effects of heparin. In addition, since heparin successfully blocked $[Ca^{2+}]_i$ elevations and presumably prevented Ca^{2+}-induced PLC activation, the results of these experiments suggest that IP_3 regeneration is not necessary for the Ca^{2+} wave propagation.

III-11.ii. Effect of $[Ca^{2+}]_i$ buffering on the Ca^{2+} wave propagation.

The propagation of Ca^{2+} waves through cells loaded with BAPTA-dextran was quantified by measuring the time that was required for the Ca^{2+} wave to reach the border of non-loaded cells. Again, hyperbolic curves were fitted to the data as they gave the lowest χ^2 error values for propagation measurements through both control and BAPTA-dextran-loaded zone (χ^2 = 562 and 755, respectively, n = 9). A comparison of the fitted curves revealed that Ca^{2+} waves propagating through the zone of $[Ca^{2+}]_i$ buffering were slower and smaller when compared to control (**Fig. 33**). The farthest distance traveled through the zone of $[Ca^{2+}]_i$ buffering was 180 μm. Interestingly, the velocity of Ca^{2+} wave propagation through the zone of $[Ca^{2+}]_i$ buffering was comparable to the velocity of wave propagation through the zone of IP_3 receptor block.

The mean propagation distance traveled by the waves initiated at the edge of $[Ca^{2+}]_i$ buffered zone (i.e., *from* a single BAPTA-dextran-loaded cell) was 149 ± 20μm (n = 8), and was comparable to the mean propagation distance of Ca^{2+} waves that traveled *through* the BAPTA-dextran-loaded zone (140 ± 30 μm, n = 6) (**Fig. 32**). Therefore, the slowed Ca^{2+} wave propagation through the cells loaded with BAPTA-dextran (**Fig. 33**) was caused predominantly by the effect of BAPTA-dextran in the cell of the Ca^{2+} wave origin.

Analyses of Ca^{2+} wave velocity through the zones of the IP_3R-block and $[Ca^{2+}]_i$ buffering indicated that $[Ca^{2+}]_i$ elevations in the cells through which Ca^{2+} wave propagates do not modulate propagation of intercellular Ca^{2+} waves. Therefore, these results suggest

that the regeneration of IP_3 molecules within the cells that propagate Ca^{2+} waves is not necessary for the propagation of Ca^{2+} waves. These, results are consistent with the hypothesis that Ca^{2+} waves propagate via diffusion of IP_3 molecules generated within a stimulated cell.

III-11.iii. Effect of ruthenium red on Ca^{2+} wave propagation.

As described previously, the inhibition of RyRs did not prevent induction and propagation of intercellular Ca^{2+} waves, suggesting that RyRs are not obligatory participants in Ca^{2+} wave induction and propagation. The results of heparin and BAPTA-dextran experiments suggested that Ca^{2+} released in cells that propagate Ca^{2+} waves is not necessary for Ca^{2+} wave propagation and does not contribute to regeneration of IP_3. Therefore, this suggests that, if RyRs participate during Ca^{2+} wave propagation, the role of RyRs is predominantly linked to the effect of RyRs in the stimulated cell. Analysis of the velocity of Ca^{2+} waves initiated in ruthenium red loaded-cultures revealed moderately smaller and slower Ca^{2+} waves when compared to waves in control-loaded cultures (**Fig. 34 a,** hyperbolic curve fits, χ^2= 364 and 374, n= 8). Interestingly, RyR block-induced decrease in Ca^{2+} wave velocity and size was significantly less prominent than the

Figure 32: Comparison between Ca^{2+} waves propagating *through* an electroporated area and Ca^{2+} waves initiated *from* a loaded cell. The distance traveled by Ca^{2+} waves is one parameter that can indicate whether an electroporated drug influences initiation or propagation of a Ca^{2+} wave.

Effect on initiation vs. propagation of Ca^{2+} wave
electroporated
control
wave
wave

Figure 32

Figure 33: Comparison of the velocity of Ca^{2+} wave propagation through the zone of $[Ca^{2+}]_i$ buffering achieved with BAPTA-dextran (i.e., Calcium Sponge) and control. Velocity of Ca^{2+} wave propagation through the Texas Red-dextran-loaded zone of cells, and propagation through the BAPTA-dextran-loaded zone of cells were fitted with nonlinear hyperbolic curve fit (χ^2= 562 and 755 respectively). Control propagation curve n = 4 experiments, 60 cells; Calcium Sponge propagation curve n = 5 experiments 78 cells.

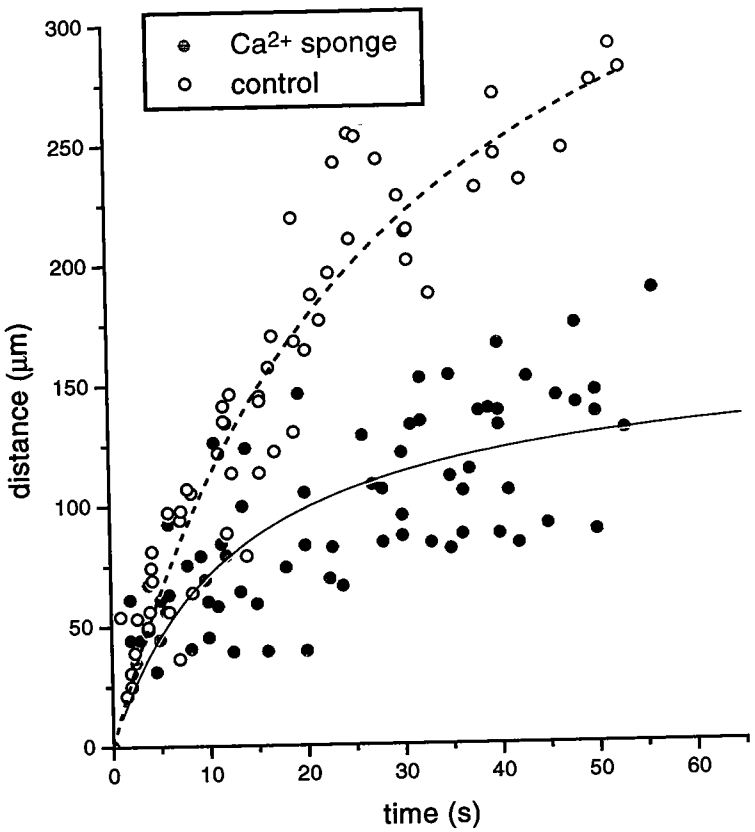
Ca2+ sponge
control
distance (µm)
time (s)
0
50
100
150
200
250
300
0
10
20
30
40
50
60

Figure 33

Figure 34 : Effect of ruthenium red on Ca^{2+} waves. a) Comparison of the velocity of Ca^{2+} wave propagation through the ruthenium red-loaded cells and Texas Red-dextran-loaded (i.e., control-loaded) cells. The position and the time of $[Ca^{2+}]_i$ change of individual cells participating in Ca^{2+} wave propagation are plotted on a time verses distance graph. Data is fitted with nonlinear hyperbolic curves (χ^2= 364 and 374 respectively). Control curve: n = 3 experiments, 74 cells; Ruthenium red curve n = 5 experiments, 119 cells. b) Comparison of the size of Ca^{2+} waves in ruthenium red-loaded cells vs. control-loaded cells. Ruthenium red decreased the size of Ca^{2+} waves to 65% of the size of Ca^{2+} waves in control conditions ($p<0.05$, n = 8). The mean number of cells propagating a Ca^{2+} wave through ruthenium red-loaded cells (striped bar labeled 'ruthenium red') was normalized to the mean number of Texas Red-dextran-loaded cells propagating a Ca^{2+} wave (white bar labeled 'control' n = 5). Bars represent mean values and lines represent standard deviations.

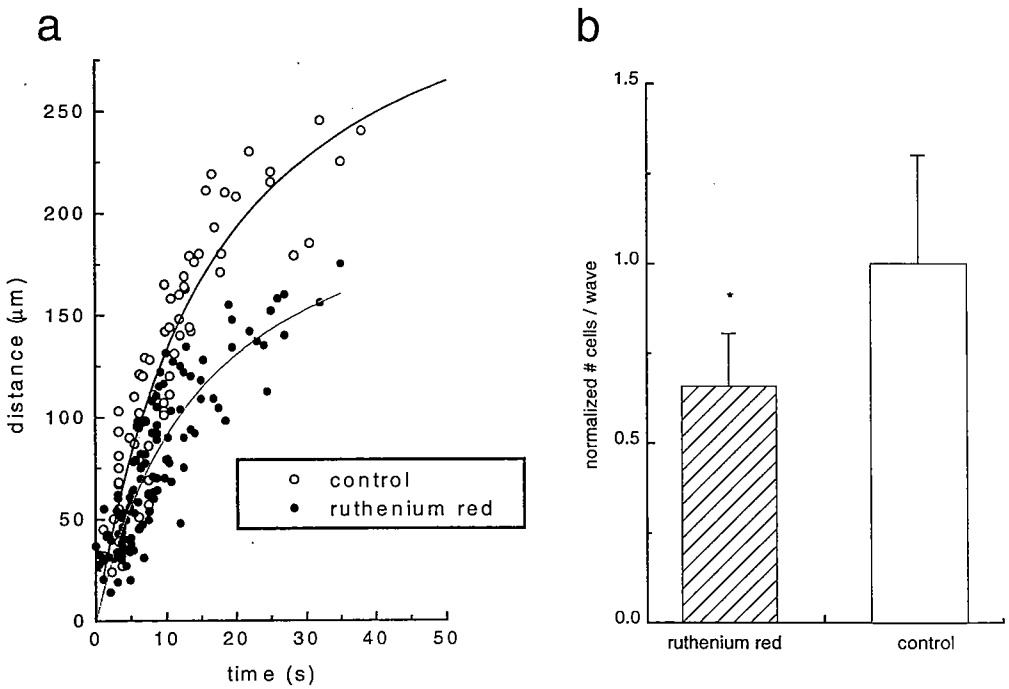
a
b
distance (μm)
time (s)
control
ruthenium red
normalized # cells / wave
ruthenium red
control

Figure 34

decrease due to IP_3R block and $[Ca^{2+}]i$ buffering. The number of cells that participated in the propagation of an intercellular Ca^{2+} wave was decreased in ruthenium red-loaded cultures when compared to control-loaded cultures (**Fig. 34 b**, $t = 2.733$, $p<0.05$, unpaired t test, $n = 13$).

These results, and the results of the experiments which indicated that Ca^{2+} released in cells that propagate Ca^{2+} waves is not necessary for Ca^{2+} wave propagation, suggest that CICR from RyRs within a stimulated cell may contribute to the generation of an intercellular Ca^{2+} wave.

III-12. Initiation of Ca^{2+} wave is influenced by $[Ca^{2+}]_i$ increase in the stimulated cell

Results of the previous experiments suggested that the major mechanism of Ca^{2+} wave propagation in rat glia is the diffusion of IP_3 molecules from a single cell. The propagation distance and velocity of Ca^{2+} waves that propagate via diffusion through cells with uniform gap-junctional communication should depend on the quantity of IP_3 generated in the stimulated cell. Analyses of Ca^{2+} wave kinetics indicated that heparin, BAPTA-dextran and ruthenium red influenced the propagation of Ca^{2+} waves by acting predominantly within the stimulated cell, which suggests that these experimental compounds affect the production of IP_3 in the stimulated cell.

Micromolar $[Ca^{2+}]_i$ increases have been found to activate PLC in situ and in vitro (Balazs et al., 1998; Chandler and Crews, 1990; Eberhard and Holz, 1988; Gardner, 1989;

Mouillac et al., 1990; Rebecchi and Rosen, 1987; Ryu et al., 1987; Wahl et al., 1992). Since all the compounds tested modulate $[Ca^{2+}]_i$ handling within glial cells, the reduction of Ca^{2+}-induced PLC catalytic activity may have caused decreased IP_3 production. Therefore, it was investigated whether different compounds used in experiments effected $[Ca^{2+}]_i$ rise in the stimulated cell.

Although the strength of the wave-inducing stimuli was kept constant, mechanically-stimulated cells, loaded with heparin, displayed substantially smaller increases in $[Ca^{2+}]_i$ compared to cells loaded with only Texas Red-dextran (**Table 2**). Similarly, the mechanical stimulation of cells loaded with BAPTA-dextran or ruthenium red or cells stimulated in the absence of extracellular Ca^{2+} also displayed significantly reduced $[Ca^{2+}]_i$ increases (**Table 2**). In addition, Ca^{2+} waves induced in the absence of extracellular Ca^{2+} were also moderately smaller (mean propagated distance 217 ± 38 μm).

Table 2: Effect of compounds on $[Ca^{2+}]_i$ in stimulated cell

compound tested	$[Ca^{2+}]_i$ **in stimulated cell** **(% of control, 673 ± 191 nM)**
HEPARIN **no release through IP_3Rs**	57 ± 13%, n =11
CALCIUM SPONGE **(BAPTA-dextran)** **buffering of $[Ca^{2+}]_i$**	22 ± 11%, n = 14
RUTHENIUM RED **no release through RyRs**	75 ± 12%, n = 7
Ca^{2+}-FREE extracell. Sol. **no Ca^{2+} influx**	69 ± 9%, n = 5

This data suggests that the rise in $[Ca^{2+}]_i$ in stimulated cells occurs as a result of several processes: these include the influx of extracellular Ca^{2+}, the release of Ca^{2+} from IP_3-sensitive Ca^{2+} stores, and release of Ca^{2+} from Ry-sensitive Ca^{2+} stores. Furthermore, the data is consistent with the hypothesis that $[Ca^{2+}]_i$ rise in stimulated cell potentiates PLC catalytic activity and IP_3 production. In control conditions, the averaged $[Ca^{2+}]_i$ increase in the stimulated cell (673 ± 191 nM, n = 25) is higher than in cells propagating a Ca^{2+} wave (265 ± 122 nM, n = 50). Because regeneration of IP_3 does not appear to be required for Ca^{2+} wave propagation, this result indicates that a specific $[Ca^{2+}]_i$ increase might be involved in PLC activation in glial cells.

Similarly, the analysis of $[Ca^{2+}]_i$ increases during wave propagation in the presence of neomycin supports the idea that $[Ca^{2+}]_i$ increases are involved in PLC activation, because increases in $[Ca^{2+}]_i$ in mechanically stimulated neomycin-treated cells were smaller when compared to control conditions (**Fig. 10b**). Since neomycin acts as both a PLC inhibitor as well as an inhibitor of voltage-gated membrane Ca^{2+} channels (Canzoniero et al., 1993; Guan et al., 1988) the resulting inhibition of Ca^{2+} waves might have been a result of the combination of both effects. Interestingly, $[Ca^{2+}]_i$ increases in mechanically stimulated cells within U-73122-treated cultures were smaller than the increases in stimulated cells in control conditions (**Fig. 8b**) and this effect could have been the result of both PLC inhibition and the direct inhibition of Ca^{2+} release from IP_3-sensitive Ca^{2+} stores by U-73122 (Willems et al., 1994). Therefore, Ca^{2+} waves could have been inhibited by neomycin and U73122 not only by direct inhibition of IP_3 production, but also by partial inhibition of $[Ca^{2+}]_i$ increases in the stimulated cells, and subsequently, by inhibition of

Ca^{2+}-mediated activation of PLC.

It is important to point out that the Ca^{2+} activation of PLC in the cell of Ca^{2+} wave origin does not seem to be a necessary step in the initiation of an intercellular Ca^{2+} wave since a robust mechanical stimulation in a Ca^{2+}-free environment can cause a decrease in $[Ca^{2+}]_i$ in the stimulated cell, probably by efflux of Ca^{2+} through the damaged cell membrane, and still successfully initiate a Ca^{2+} wave (Sanderson et al., 1990). Therefore, the Ca^{2+}-mediated activation of PLC is most likely a potentiating factor, and is not necessary for initiation of intercellular Ca^{2+} wave.

III-13. Discussion of the Specific Aim 1

The objective of this aim was to identify the intra- and intercellular events involved in initiation and propagation of intercellular Ca^{2+} waves in cultured cortical rat glia. The results of this study indicate two main phases of intercellular Ca^{2+} waves: the initiation of a Ca^{2+} wave in a stimulated cell resulting from the generation of a second messenger IP_3 and the propagation of Ca^{2+} wave through the adjacent cells by gap junction-mediated diffusion of IP_3.

III-13.i. The roles of ICSs and PLC in generation of Ca^{2+} waves.

Ca^{2+} waves were not inhibited by the absence of extracellular Ca^{2+} but were abolished by emptying the Ca^{2+} stores with thapsigargin, indicating that the propagation of

intercellular Ca^{2+} waves requires the release of Ca^{2+} from intracellular Ca^{2+} stores. This data supports earlier studies of glial intercellular Ca^{2+} waves (Charles et al., 1993; Cornell-Bell and Finkbeiner, 1991; Cornell-Bell et al., 1990; Nadal et al., 1997; Newman and Zahs, 1997; Venance et al., 1995; Venance et al., 1997).

Treatment of glia with inhibitors of the IP_3 production e.g., neomycin sulfate, and U73122 demonstrated that PLC activation and subsequent IP_3 production are required for intercellular Ca^{2+} wave initiation. This finding reinforces earlier results that PLC activation and IP_3 production are necessary for generation of intercellular Ca^{2+} waves (Boitano et al., 1992; Cornell-Bell and Finkbeiner, 1991; Finkbeiner, 1992; Leybaert et al., 1998; Newman and Zahs, 1997; Venance et al., 1997). Furthermore, sufficient quantities of membrane-bound IP_3 precursors are necessary for Ca^{2+} wave initiation, since LiCl, an inhibitor of inositol recycling, successfully inhibited initiation of Ca^{2+} waves. The generation of IP_3 as a necessary step in the initiation of Ca^{2+} waves in rat glia was also supported by the ability of photoreleased IP_3 within a single cell to initiate a Ca^{2+} wave (Leybaert et al., 1998).

PLC activation leading to Ca^{2+} wave propagation can be evoked in glia by number of neurotransmitters (Cornell-Bell et al., 1990; Hansen et al., 1993; Kim et al., 1994; Newman and Zahs, 1997; Finkbeiner, 1993; Simpson et al., 1998; van den Pol et al., 1992; Yagodin et al., 1995). In addition, stretching the cell membrane of glia and other cell types by a mechanical stimuli induces activation of PLC and production of IP_3 (McDonald et al., 1996; Churchill and Louis, 1998; Felix et al., 1996; Lamb et al., 1997; Okada et al., 1998). The results of this study indicate that mechanical stimulation activates PLC directly,

without mediation of G proteins, since the G protein inhibitor, GDPβS, did not inhibit the generation of Ca^{2+} waves. Thus, in glial cells, mechanical stimulation may induce a conformational change of the enzyme or may activate PLC by making membrane phospholipids available for metabolism. Interestingly, G protein-mediated activation of PLC has been suggested for stretch stimuli in endothelial cells and osteoblasts (Brophy et al., 1993; Ishida et al., 1997; McDonald et al., 1996). The reason for this difference is unclear and may be dependent on the cell type.

III-13.ii. The route of intercellular Ca^{2+} wave propagation.

The requirement of gap junctional communication for the propagation of intercellular Ca^{2+} waves was demonstrated in experiments using halothane and AGA, two compounds that uncouple gap junctions. Both halothane and AGA significantly reduced the number of cells that participated in a Ca^{2+} wave. Although gap junction uncouplers may effect $[Ca^{2+}]_i$ (Deutsch et al., 1995), the effect of these compounds on Ca^{2+} waves was not due to a reduced $[Ca^{2+}]_i$ in stimulated cells, because the amplitude of the $[Ca^{2+}]_i$ responses in stimulated cells was not affected. The incomplete block of Ca^{2+} wave propagation by gap junction inhibitors left open the possibility that there is an extracellular component of Ca^{2+} wave propagation. Further analysis however, showed that this possibility was unlikely. In the concentrations used, halothane and AGA were found to have no effect on the ability of glial cells to respond to extracellular stimuli, such as AMCh and ATP that may serve as extracellular signals of Ca^{2+} waves. Ca^{2+} waves were also not affected by extracellular perfusion. Furthermore, inhibition of G-proteins by GDPβS

resulting in a complete block of glial responses to ATP and AMCh did not block initiation and propagation of intercellular Ca^{2+} waves. G-protein block not only addressed the role of glial G-protein coupled purinergic receptors present in astrocytes (Centemeri et al., 1997; Chen and Chen, 1996; Chen et al., 1995; Ho et al., 1995; King et al., 1996; Salter and Hicks, 1995), but also demonstrates that other agonists of G-protein coupled receptors are not involved in the propagation of intercellular Ca^{2+} waves. Ca^{2+} waves also crossed the zone of $[Ca^{2+}]_i$ buffering and propagated against the orientation of perfusion, without a change in Ca^{2+} wave kinetics, again suggesting that the participation of an extracellular mediator of Ca^{2+} waves is minimal.

These findings were consistent with earlier results that found that uncoupling conditions generated by gap junction blockers lead to a significant reduction in the extent of intercellular Ca^{2+} waves in rat astrocytes, by either restricting the Ca^{2+} increase to only the stimulated cell (Finkbeiner, 1992), or to a narrow zone of cells surrounding the stimulated cell (Enkvist and McCarthy, 1992; Venance et al., 1997). In addition, the transfection of Cx43 into weakly coupled rat C6 glioma cells enabled these cultures to propagate Ca^{2+} waves (Charles et al., 1992), and an extracellular flow was reported to have no effect on propagation of Ca^{2+} waves in rat astrocytes (Fatatis and Russell, 1992; Finkbeiner, 1992; Newman and Zahs, 1997). Enzymatic degradation of ATP, the use of glutamate receptor antagonists, or voltage-dependent Ca^{2+} channel blockers showed no effect on the speed and extent of intercellular Ca^{2+} waves and did not abolish Ca^{2+} waves reduced by application of gap junction blockers (Venance et al., 1997).

Therefore, the incomplete inhibition of Ca^{2+} wave propagation by halothane and AGA can be contributed to the partial effectiveness of these compounds on gap junctions, rather than to an extracellular component of Ca^{2+} wave propagation. Collectively, these data strongly suggest that an extracellular messenger does not play a major role in the propagation of the mechanically-induced Ca^{2+} waves in rat cortical glia and that Ca^{2+} wave propagation is mediated by diffusion through the intracellular space.

III-13.iii. The mechanism of Ca^{2+} wave propagation is species- and anatomically- specific.

In contrast to the results of these studies, Ca^{2+} waves in mouse astrocytes seem to be propagated by diffusion of an extracellular mediator (Hassinger et al., 1996), and in comparison to rat glioma C6 cells, poorly coupled mouse 203-glioma cells propagate intercellular Ca^{2+} waves (Yamasaki et al., 1994). The two neurotransmitters, ATP and glutamate, were thought to be the extracellular mediators of Ca^{2+} waves in mouse glia since astrocytes are known to release these two compounds (Bruner and Murphy, 1993; Bruner and Murphy, 1993; Hassinger et al., 1995; Parpura et al., 1994). A recent study however indicated that ATP is the primary extracellular mediator in Ca^{2+} waves of mouse glia (Guthrie et al., 1999).

The exact reason for this difference in Ca^{2+} wave propagation between mouse and rat glia is not clear, but appears to be species-specific. In young, non-confluent cultures of mouse cortical astrocytes stimulation of a Ca^{2+} wave from one physically isolated island of cells leads to elevated Ca^{2+} levels in neighboring islands although no direct cell contact

with the first cell island exists (Guthrie et al., 1999; Hassinger et al., 1996). In contrast, rat glial cultures used for experimentation in this study were always at least 15 days old, since initial observations showed that younger, non-confluent cultures only poorly propagated Ca^{2+} waves. This was not due to the lack of neurotransmitter receptors in younger cultures, since both ATP and AMCh stimuli successfully induced $[Ca^{2+}]_i$ elevations. The differences between mouse and rat astrocytes do not seem to be the result of different culturing conditions, since differences in Ca^{2+} waves were observed when cells were cultured under identical conditions (Giaume and Venance, 1998). In addition, these differences are not linked to variations in the amplitude of the initial $[Ca^{2+}]_i$ increase in the stimulated cell, and are also not due to a difference in connexin proteins or the extent of coupling in the two species, since Cx43 is the major connexin in both preparations and junctional conductances for both species have similar values (Dermietzel et al., 1991; Giaume and Venance, 1998; Venance et al., 1995). Therefore, the difference between rat and mouse astrocytes probably lies in the efficiency of extracellular mediation of Ca^{2+} waves, since ATP release or the number of purinergic receptors may be different for the two species. Still, identical culturing methods may, from an otherwise heterogenic cell population, preferentially select for subtypes of cells that in mouse and rat differ in their responsiveness to neurotransmitters or the extent of cell coupling (Venance et al., 1998). In support of this premise is the finding that subpopulations of astrocytes express specific purinergic receptor subtypes (Ho et al., 1995) that may, for example, be readily expressed in mouse cultures but depleted in rat cultures in response to the same culturing technique. Also, Ca^{2+} waves are blocked by anandamide in rat striatal astrocytes (Venance et al.,

1995), but not in cortical astrocytes (Guan et al., 1997), thus reflecting previously observed regional differences in gap junctional coupling among glia (Lee et al., 1994). In light of the findings that astrocytes in the CNS exhibit regional specificity in gap junction coupling as well as in sensitivity to different neurotransmitters, it can be inferred that glia associated with different neuroanatomical structures, just as neurons, are specialized to conduct and regulate specific actions by different modes of initiation and propagation of intercellular Ca^{2+} waves.

The intriguing possibility, that intracellular and extracellular mechanisms of Ca^{2+} wave propagation interact and co-exist to differing extents in specific areas of the CNS, is reinforced by recent studies that indicate that the components involved in one of the two mechanisms of wave propagation can actively modulate components of the other. For example, depolarizing ligands secreted by glia, such as glutamate, enhance gap junction communication between cells, thus maintaining increased communication between cells in the face of elevated Ca^{2+} levels during Ca^{2+} wave propagation (Enkvist and McCarthy, 1994). On the other hand, the expression of gap junctions in gap junction-deficient cell lines contributes to Ca^{2+} wave propagation by enhancement of the ATP release that can serve as the extracellular mediator of Ca^{2+} waves (Cotrina et al., 1998; Cotrina et al., 1998). Therefore, one mechanism of wave propagation does not necessarily exclude the other. It is possible that, depending on a specific inducing stimulus, the combination of both mechanisms, gap junctional communication, and the release of extracellular messenger(s) may be involved in intercellular Ca^{2+} wave propagation in vivo. In fact, the specifics of wave inducing stimuli might be distinguished in glia by employing, to a

differing extents, one or a combination of both mechanisms. This interplay of intracellular and extracellular propagation of Ca^{2+} waves has also been suggested in other cell types (Dandrea et al., 1998; Frame and de Feijter, 1997).

III-13.iv. IP_3 is a candidate intercellular messenger.

Previous studies of mechanically-induced Ca^{2+} waves in variety of cell types have narrowed the search for the signaling molecule that passes from one cell to another to two molecules: IP_3 and Ca^{2+}. The findings presented in this study are consistent with the hypothesis that IP_3 is the major molecule that diffuses between neighboring cells and, via binding to IP_3Rs, generates sequential $[Ca^{2+}]_i$ increases within the glial syncytium. The mechanical stimulation of a heparin-loaded cell resulted in the reappearance of the Ca^{2+} wave at the edge of the non-loaded zone of cells. Loading of heparin into cells grown on one half of the coverslip eliminated the possibility of a Ca^{2+} wave propagation route which bypassed loaded cells. In parallel experiments, the mechanical stimulation of a cell within BAPTA-dextran-loaded zone of cells caused no increases in $[Ca^{2+}]_i$ within the zone of $[Ca^{2+}]_i$ buffered cells, with the Ca^{2+} wave front emerging at the border of non-loaded cells. On the other hand, Ca^{2+} waves propagated through the cells that had ruthenium red-blocked RyRs. These experiments suggest that: 1) IP_3 binding to IP_3R is necessary for achieving the sequential $[Ca^{2+}]_i$ elevations in Ca^{2+} waves, and 2) IP_3 may diffuse through the cells for the distances of over 175 μm. These findings are supported by previous studies in glia and other cell types. Astrocytic and endothelial gap junctions, both composed of Cx43, have been reported to be permeable to IP_3 molecules (Carter et al.,

1996; Leybaert et al., 1998). In retinal glia and endothelium increases in $[Ca^{2+}]_i$ during Ca^{2+} waves were reduced or inhibited in cells in which IP_3 receptors were blocked by heparin (Newman and Zahs, 1997; Boitano et al., 1992) suggesting that IP_3 is one of the mediators of Ca^{2+} wave propagation in these cells.

Recent measurements in Xenopus oocytes, whose IP_3Rs are nearly identical to type 1 IP_3Rs in mammalian cells, show that physiologic concentrations of IP_3 ranges from tens of nanomolar to a few micromolar (Luzzi et al., 1998). Furthermore, the range of action of IP_3 was estimated to ~ 300 μm, suggesting that IP_3 acts as a long-ranged messenger in the oocyte. Interestingly, measurements of the range of action of IP_3 in other cell types vary from 5 μm in olfactory neurons, 25 μm in smooth muscle, to 130 μm in skeletal muscle (Breer et al., 1990; Walker et al., 1987) suggesting that the concentration of IP_3-degrading enzymes in cells may depend both on the cell size and the extent of coupling of different cell types, thus reflecting the requirement for IP_3 to act as the long distance signal either intracellularly or intercellularly. It would be of interest to measure the half life for IP_3 in the glial syncytium.

III-13.v. Ca^{2+} is a non-essential intercellular messenger in glia.

Although direct exchange of Ca^{2+} between adjacent cells has been proposed as the propagation mechanism of Ca^{2+} signals in other cell types (Domenighetti et al., 1998; Lamont et al., 1998; Tordjmann et al., 1997; Zimmermann and Walz, 1997), earlier observations in glial cells, as well as experiments conducted in this study, make Ca^{2+} an unlikely intercellular messenger in glia. $[Ca^{2+}]_i$ increases due to the photolysis of 'caged

Ca^{2+}, as well as $[Ca^{2+}]_i$ increases that occur during Ca^{2+} oscillations did not initiate intercellular Ca^{2+} waves. A range of increasing $[Ca^{2+}]_i$ elevations achieved by increasing flash durations did not generate Ca^{2+} waves. This result was consistent with earlier findings (Charles et al., 1991; Leybaert et al., 1998). This inability of Ca^{2+} to initiate Ca^{2+} waves was not due to the possible inhibitory effect of $[Ca^{2+}]_i$ increases on gap junctions (Enkvist and McCarthy, 1994), since both oscillating cells and flashed cells propagated mechanically-induced intercellular Ca^{2+} waves. Earlier reports suggest that very high levels of $[Ca^{2+}]_i$ (5 -10 mM) or very long exposures to Ca^{2+} increases (5-20 min) are required to close junctional channels composed of Cx43 (Lazraak And Peracchia 1993, Crow et al. 1994). Neither the magnitude nor the duration of $[Ca^{2+}]_i$ elevation achieved by flash photolysis met these requirements.

$[Ca^{2+}]_i$ elevations were not detected during Ca^{2+} wave propagation across the zones of cells with excess $[Ca^{2+}]_i$ buffered by BAPTA-dextran or with IP_3Rs-blocked by heparin. This demonstrates that Ca^{2+} is not a necessary propagating molecule of Ca^{2+} waves. Since the blocking of IP_3Rs prevents $[Ca^{2+}]_i$ increases due to release of Ca^{2+} from ICS, but does not prevent $[Ca^{2+}]_i$ increases due to potential diffusion of Ca^{2+} from the stimulated cell, the result suggests that Ca^{2+} diffusion in glia appears to be below the levels that can be detected by the video imaging technique and that Ca^{2+} does not diffuse together with IP_3 molecules during Ca^{2+} wave propagation.

Another hypothesis tested was that Ca^{2+} may serve as a propagating signal for intercellular Ca^{2+} waves if IP_3- sensitized intracellular Ca^{2+} stores respond, via the CICR mechanism, to a small quantity (i.e., undetectable by imaging) of Ca^{2+} ions that may

diffuse through the gap junctions. This mechanism has been suggested as the major propagating mechanism of Ca^{2+} waves in a number of other cell types (Robb-Gaspers et al., 1998; Robb-Gaspers and Thomas, 1995; Tordjmann et al., 1997; Yule et al., 1996). Increases in $[Ca^{2+}]_i$ within glial cells which contained IP_3Rs that were sensitized by neurotransmitter AMCh, or by the propagation of a Ca^{2+} wave, did not however induce the propagation of a new Ca^{2+} wave. These results suggest that in rat cortical glia Ca^{2+} is a poor mediator of Ca^{2+} waves between cells that contain sensitized IP_3Rs.

There are a few possible reasons why this mechanism of CICR that occurs in pacreatic acini cells and hepatocytes, does not play a major role in the propagation of Ca^{2+} waves in rat glia. First, the quantity of Ca^{2+} that passes through the gap junctions in glia might be too small to activate sensitized IP_3R. This might be due to the size and conductivity of gap junctions. Both hepatocytes and pancreatic acini cells are characterized by large gap junctions and the coupling of these cell types is far more extensive than the coupling of glia (Kuraoka et al., 1993; Meda, 1996; Rahman et al., 1993; Stutenkemper et al., 1992). Second, Ca^{2+} is a short range messenger that gets quickly buffered in the cytoplasm of the cells, and endogenous buffering in glia might be more potent than endogenous buffering in the pancreatic cells or hepatocytes (Wang et al., 1997). In order to be reached by free cytoplasmic Ca^{2+}, IP_3Rs have to be strategically placed in close proximity of gap junctions, due to the short range of Ca^{2+} diffusion (Allbritton et al., 1992). IP_3Rs which are not adjacent to gap junctions would however still be able to bind IP_3 molecules, whose range of diffusion is much longer than that of Ca^{2+} (Allbritton et al., 1992; Luzzi et al., 1998; Sims and Allbritton, 1998).

III-13.vi. Pharmacological analysis of calcium waves.

The investigation of intracellular Ca^{2+} signaling is hampered by the lack of selective pharmacological tools (Ehrlich et al., 1994; Taylor and Broad, 1998), and care was taken to address the non-selective effects of the compounds used. Although heparin is widely used as a competitive antagonist of IP_3Rs it may have additional intracellular effects that need to be considered. The reduced velocity and propagation distance of Ca^{2+} waves in heparin-loaded cells might be due to the decreased intercellular diffusion coefficient of IP_3, if heparin decreases the permeability of gap junctions. Although the effect of heparin on gap junctions was not tested directly, mathematical models of Ca^{2+} wave propagation predict that Ca^{2+} waves should propagate slower through a glial syncytium with decreased gap junction permeability, although the maximal propagation distance should be comparable to the wave propagation through cells with normal gap junction permeability (Sneyd et al., 1995 a,b; Sneyd et al., 1998). In contrast, Ca^{2+} waves in hepatin-loaded cells were *both* slower and smaller suggesting that there is no major effect on gap junction permeability. This prediction is in agreement with reports that show that heparin has either no direct effect on gap junction permeability (Newman and Zahs, 1997), or can in fact suppress the uncoupling effect of some neurotransmitters (Li and Hatton, 1996; Rorig and Sutor, 1996; Sandberg et al., 1992). Since heparin is a negatively charged molecule, the results of this study might have been due to the effects of an increase in negative charges within cells. A decrease in intracellular pH however, has been described as a potent inhibitor of gap junctional connectivity in glia and other cells (Connors et al., 1984;

Dermietzel, 1998; Dermietzel and Spray, 1998; Dunina-Barkovskaya, 1998; Ek-Vitorin et al., 1996; Morley et al., 1997; Pappas et al., 1996; Spray et al., 1985). Heparin and BAPTA-dextran molecules, which do not share any common properties other than similar size, have comparable effects on the kinetics of Ca^{2+} waves. This observation makes a link between the charge of heparin molecules and any effect on Ca^{2+} wave propagation unlikely.

Heparin has also been reported to activate RyRs (Ehrlich et al., 1994). Experiments conducted in this study showed no evidence of heparin activation of RyRs, since, with the exception of the stimulated cell, $[Ca^{2+}]_i$ levels in the heparin-loaded cells did not change, and were comparable to the basal $[Ca^{2+}]_i$ levels.

Xestospongins, which are membrane-permeant antagonist of IP_3Rs that have recently been isolated from a marine sponge (Gafni et al., 1997), have yet to prove themselves as an alternative to heparin: their potency seems to be highly variable between different extracts (Berridge, personal communication), and they seem to inhibit RyRs at only slightly higher concentrations than those required for inhibition of IP_3Rs (Taylor and Broad, 1998). Furthermore, due to their membrane-permeability, the use of xestospongins would not allow the selective IP_3Rs block within a zone of glial cells. Electroporation of antibodies against IP_3Rs would probably be the most direct approach to block different isoforms of IP_3Rs, but unfortunately, although temporarily commercially available, IP_3R antibodies were taken off the market due to cross-reactivity problems.

Ca^{2+} wave retardation in BAPTA-dextran-loaded cells may be caused by a reduction in gap junction permeability, or an increase in IP_3 degradation. Dextran does not

alter the Ca^{2+} wave kinetics, since experiments conducted with Texas Red-dextran showed that this compound had no effect on Ca^{2+} wave propagation. Furthermore, BAPTA-dextran-induced decrease in the permeability of gap junctions seems unlikely since this effect would have slowed down the wave propagation, but the maximal distance traveled by the wave would have stayed comparable to control. Ca^{2+} waves propagating through BAPTA-dextran loaded cells were however both *slower* and *smaller*. It is unlikely that BAPTA-dextran affected gap junctional permeability due to its buffering of $[Ca^{2+}]_i$, since basal levels of $[Ca^{2+}]_i$ were unaffected by BAPTA-dextran, and only agonist- and Ca^{2+} wave-induced $[Ca^{2+}]_i$ elevations were buffered. Since BAPTA buffers $[Ca^{2+}]_i$ increases, its effect on gap junctions is also unlikely due to previously discussed reports showed that $[Ca^{2+}]_i$ increases, and not decreases, have been described to decrease gap junction permeability (Enkvist and McCarthy, 1994) and the study by Wang et al. (1998) that found that the effects of Ca^{2+} buffers on glial Ca^{2+} signaling could not be ascribed to an effect on gap junctions. Finally, the effect of BAPTA-dextran and heparin on IP_3 metabolism and gap junction permeability in the zone of cells that propagated Ca^{2+} waves was unlikely, since comparable effects on Ca^{2+} waves were achieved in experiments in which BAPTA-dextran and heparin were present only within the stimulated cells.

Ruthenium red may act as an inhibitor of mitochondrial Ca^{2+} uptake and SERCA activity and may therefore cause $[Ca^{2+}]_i$ increases (Taylor and Broad, 1998). In rat glia however, ruthenium red reduced the $[Ca^{2+}]_i$ increases in cells propagating a Ca^{2+} wave, suggesting that the effect of this compound was the inhibition of Ca^{2+} release via RyRs.

III-13.vii. Passive diffusion vs. regeneration of IP_3.

Two mechanisms, passive diffusion (Sanderson, 1995; Sanderson et al., 1994; Sneyd et al., 1995b; Sneyd et al., 1998), and the regeneration of a second messenger along the path of a Ca^{2+} wave (Giaume and Venance, 1998; Guthrie et al., 1999; Hassinger et al., 1996; Venance et al., 1997; Amundson and Clapham, 1993; Charles, 1998) have been proposed to account for Ca^{2+} wave propagation. Experiments conducted in this study support the hypothesis that the regeneration of IP_3 molecules in the cells that propagate Ca^{2+} wave is not necessary for Ca^{2+} wave propagation, and that the diffusion of IP_3 from the stimulated cell is the dominant mechanism of Ca^{2+} wave propagation in rat glia.

If each cell participated in a regenerative production of a messenger, an indefinitely propagating Ca^{2+} wave with a constant velocity would be expected. Intercellular Ca^{2+} wave propagation in rat glia however, showed a gradual decrease in wave velocity and termination after distances of approximately 300 μm, a result which was consistent with the diffusion of IP_3 molecules from the stimulated cell. A mathematical model for the diffusion of IP_3 from the origin of the Ca^{2+} wave correctly predicted the velocity and propagating distance of an experimental intercellular Ca^{2+} wave (Sneyd et al., 1995 a,b; Sneyd et al., 1998).

The propagation of a Ca^{2+} wave can be influenced by processes occurring in cells that propagate a Ca^{2+} wave (e.g., generation and degradation of IP_3, gap junction permeability) and/or by processes occurring in the stimulated cell (i.e., IP_3 generation). Therefore, the restriction and slowing of the Ca^{2+} waves that propagated through BAPTA-

dextran- or heparin-loaded cells could be explained in four ways: 1) regeneration of the Ca^{2+} wave was blocked due to the inhibition of the activation of PLC by Ca^{2+}, 2) degradation of IP_3 molecules was accelerated, 3) gap junction permeability was decreased due to side effects of the drugs loaded, and 4) less IP_3 was being generated in the stimulated cell. To distinguish whether processes in the stimulated cell or in cells propagating the Ca^{2+} wave were affected, Ca^{2+} waves in which initiation and propagation were influenced by loaded compounds were compared to Ca^{2+} waves in which only initiation was influenced by loaded compounds. Because Ca^{2+} waves that propagated *through* the heparin- or BAPTA-dextran-loaded cells were comparable with Ca^{2+} waves that were initiated *from* a heparin- or BAPTA-dextran-loaded cell but propagated through non-loaded cells, Ca^{2+} waves depend predominantly on the processes in the stimulated cell. Furthermore, these results demonstrated that an increase in $[Ca^{2+}]_i$ and release of Ca^{2+} from ICSs are not required for Ca^{2+} wave propagation and suggest that Ca^{2+} itself does not seem to participate in the regeneration of IP_3 molecules, and that the regeneration of IP_3 is not required for Ca^{2+} wave propagation. These findings are consistent with results of our previous study which showes that increasing the quantity of photoreleased IP_3 within a single cell resulted in the propagation of Ca^{2+} waves for longer distances (Leybaert et al, 1998).

On the other hand, if the change in Ca^{2+} wave properties can be attributed to the effect of loaded compounds on the processes in the stimulated cell, and is consistent with the idea of less IP_3 being made in stimulated cell, these changes are most likely due to decreased $[Ca^{2+}]_i$ elevations that induce PLC catalytic activity. The results supporting this

idea will be discussed in detail in the following paragraph.

III-13.viii. $[Ca^{2+}]_i$ increase in the stimulated cell.

Although not directly examined in this study, Ca^{2+} may activate PLC during mechanical stimulation of glial cells. Micromolar increases in $[Ca^{2+}]_i$ have been shown to activate different PLC isoforms (Baird and Nahorski, 1990; Balazs et al., 1998; Eberhard and Holz, 1988; Exton, 1996; James and Downes, 1997; James et al., 1997; Rhee and Bae, 1997). Because a mechanical stimulation induces an $[Ca^{2+}]_i$ increase in the stimulated cell, it is possible that $[Ca^{2+}]_i$ increases in single glial cells contribute to Ca^{2+} wave initiation by PLC activation. The hypothesis that the $[Ca^{2+}]_i$ rise in the stimulated cell is involved in the generation of Ca^{2+} wave is supported by the fact that mechanical stimulation, in the absence of extracellular Ca^{2+}, or in the presence of neomycin and U73122, heparin, BAPTA-dextran, or ruthenium red resulted in smaller $[Ca^{2+}]_i$ increases in stimulated cells and smaller Ca^{2+} waves. This effect was not due to differences in mechanical stimuli, since a consistent mechanical stimuli was used. Thus, the reduction of propagation distance and velocity of the Ca^{2+} waves due to the effect of these compounds may be explained by the fact that PLC activation was reduced in the stimulated cell.

There are four possible explanations why the photorelease of Ca^{2+} did not initiate intercellular Ca^{2+} waves. The first possibility, that Ca^{2+} inhibited Ca^{2+} wave generation, is unlikely, since mechanical stimulus preceding or following the photorelease of Ca^{2+} induced Ca^{2+} wave propagation. The second possibility, that CICR via RyR is not required for Ca^{2+} wave generation is supported by the finding that Ca^{2+} waves propagate through

ruthenium red-loaded cells. The third possibility, that photorelease-generated $[Ca^{2+}]_i$ elevations were not sufficient to induce PLC activation, is supported by the fact that PLC activation requires micromolar $[Ca^{2+}]_i$ (Eberhard and Holz, 1988). Furthermore, in rat striatal glia, a Ca^{2+} wave can be initiated by exposure to the Ca^{2+} ionophore ionomycin which generates a larger increase in $[Ca^{2+}]_i$ than is generated by the photorelease of Ca^{2+} (Venance et al., 1997). The fourth possibility is that $[Ca^{2+}]_i$ elevations can contribute to PLC activation that occurs due to another, independent stimulus, e.g., bending of the membrane. This idea is supported by the finding thet ionomycin-induced waves propagated through fewer cells than mechanically-induced waves suggesting that a $[Ca^{2+}]_i$ rise alone is not as efficient as mechanical stimulation in the induction of IP_3 production (Venance et al., 1997).

Unlike Ca^{2+} waves examined in this study, Ca^{2+} waves in striatal astrocytes were completely blocked by the absence of extracellular Ca^{2+}, suggesting that intracellular processes involved in Ca^{2+} wave initiation in striatal glia differ from those in cortical rat glia, probably due to differences in the expression of membrane channels and receptors (Giaume and Venance, 1998; Venance et al., 1997). The experiments in this and previous studies, suggest that for a majority of cell types Ca^{2+} activation of PLC does not seem to be a necessary step in initiation of intercellular Ca^{2+} waves because a robust mechanical stimulation in a Ca^{2+}-free environment may cause no change or a decrease in $[Ca^{2+}]_i$ in the stimulated cell, and still successfully initiate a Ca^{2+} wave (Sanderson et al., 1990). Therefore, Ca^{2+}-dependent activation of PLC most likely potentiates, but is not necessary for, the initiation of intercellular Ca^{2+} wave in rat cortical glia.

The suggested effect of $[Ca^{2+}]_i$ increases on IP_3 generation in the stimulated cell, but not in the cells that propagate a Ca^{2+} wave, may seem contradictory. Two properties distinguish a stimulated cell from the cells that propagate Ca^{2+} wave. First, $[Ca^{2+}]_i$ in the stimulated cell approaches values that have been reported to activate PLC, while $[Ca^{2+}]_i$ in cells that propagate Ca^{2+} waves is lower. Second, $[Ca^{2+}]_i$ increases and mechanical stimulus act synergistically in the stimulated cell, while in cells that propagate Ca^{2+} waves $[Ca^{2+}]_i$ increase occurs alone. Both of these factors may contribute to the difference between Ca^{2+}-mediated activation of PLC between these two groups of cells.

III-13.ix. Relevance.

A striking cell type- and species-related differences emerge from a number of studies in the Ca^{2+} signaling field, and while demonstrating the diversity of controlling and utilization mechanisms of Ca^{2+} signals, also calls for caution in the generalization of mechanisms contributing to Ca^{2+} handling. Adding to the complexity of the problem, the sensitivity of glial cells to neurotransmitters, as well as connexin expression, appear to be developmentally regulated, and can be altered by specific pathological conditions (Enkvist et al., 1996; McCarthy and Salm, 1991; Messamore et al., 1994; Nitsch et al., 1992; Pearce et al., 1985; Pearce et al., 1988; Petryniak et al., 1996; Porter and McCarthy, 1997; Shao and McCarthy, 1995). Comparative studies of Ca^{2+} signaling in human glial cultures are becoming necessary in order to determine the dominant mechanism of Ca^{2+} signaling in healthy and diseased nervous tissue. These experiments will enable determination of the ideal animal model of Ca^{2+} handling in human glial cells.

III-14. Conclusions of the Specific Aim 1

Studies conducted in the Specific Aim 1 have focused on the mechanisms of initiation and propagation of intercellular Ca^{2+} waves in rat cortical glia. The catalytic activity of PLC was found to be necessary for the initiation of intercellular Ca^{2+} waves. In the cell of the Ca^{2+} wave origin, mechanical stimulation activates PLC and induces an increase in $[Ca^{2+}]_i$ due to the influx of extracellular Ca^{2+} and the release of Ca^{2+} from IP_3- and Ry-sensitive Ca^{2+} stores. The increase in $[Ca^{2+}]_i$ in the mechanically-stimulated cells appears to enhance PLC activity. Furthermore, both functional IP_3-sensitive intracellular Ca^{2+} stores and gap junction-mediated connectivity are necessary for the initiation and propagation of intercellular Ca^{2+} waves in rat glia. Release of Ca^{2+} from Ry-sensitive Ca^{2+} stores, although occurring during both initiation and propagation of intercellular Ca^{2+} waves, is not necessary element of these processes.

The results presented are consistent with the hypothesis that the propagation of intercellular Ca^{2+} waves predominantly occurs due to the diffusion of IP_3 from the stimulated cell through the gap junctions of neighboring cells. Ca^{2+} ions are not a major messenger in Ca^{2+} wave propagation. Furthermore, Ca^{2+} ions do not appear to co-diffuse with IP_3 molecules during Ca^{2+} wave propagation.

CHAPTER IV

SPECIFIC AIM 2

Specific Aim 2 investigates how intercellular Ca^{2+} waves induce spatio-temporally distinct intracellular Ca^{2+} oscillations. Specifically, the experiments of Specific Aim 2 are designed to test whether intercellular Ca^{2+} waves induce Ca^{2+} oscillations by establishing a specific range of oscillation-promoting $[IP_3]_i$ within the glial syncytium. The dependence of the initiation of Ca^{2+} oscillations on the distance from the origin of Ca^{2+} wave, cell type, and $[IP_3]_i$ are investigated.

IV-1. Intercellular Ca^{2+} waves induce intracellular Ca^{2+} oscillations

Following the passage of an intercellular Ca^{2+} wave, repetitive increases and decreases in $[Ca^{2+}]_i$ (i.e., Ca^{2+} oscillations) were initiated in 34% of the cells that propagated a Ca^{2+} wave (35 experiments, 692 cells, **Fig. 5c, d**, **Fig. 35a, b**). These Ca^{2+} oscillations occurred independently of the changes in $[Ca^{2+}]_i$ of adjacent cells and were considered to occur asynchronously. Asynchronous Ca^{2+} oscillations did not initiate intercellular Ca^{2+} waves, but instead were confined to single cells in culture (**Fig. 35a, b**). This was not due to the lack of intercellular communication, since further experiments showed that a Ca^{2+} wave, initiated in a culture that contained oscillating cells, propagated

through both non-oscillating and oscillating cells.

IV-2. Spatial distribution of Ca^{2+} oscillations

A normalized distribution of the cells participating in a Ca^{2+} wave with respect to the distance from the wave origin was obtained by dividing the number of cells showing a Ca^{2+} response by the total number of cells present at the same distance from the wave origin (**Fig. 35 c and d**). This normalization was necessary to eliminate the sampling bias imposed by the rectangular field of view. A normalized distribution of cells showing Ca^{2+} oscillations after the passage of a Ca^{2+} wave was obtained in a similar manner (**Fig. 35 c and d**). The number of cells passing a Ca^{2+} wave declined from 98% near the point of stimulation, to 0%, 310 μm away. The number of cells showing Ca^{2+} oscillations rose from 0% to 32% within 80-100 μm from the Ca^{2+} wave origin. 45% of all the cells showing Ca^{2+} oscillations were in a zone 60-120 μm away from the Ca^{2+} wave origin (**Fig. 35 d**). This spatial distribution of the cells showing Ca^{2+} oscillations after the passage of an intercellular Ca^{2+} wave indicated that the cells' response is a function of the cells' distance from the Ca^{2+} wave origin.

IV-3. Types of the intracellular Ca^{2+} oscillations

To simplify the analysis of the induced Ca^{2+} oscillations, the Ca^{2+} oscillatory behaviors observed were classified on the basis of their periodicity, duration, and onset

Figure 35: Analysis of the spatial distribution of the Ca^{2+} oscillations induced by an intercellular Ca^{2+} wave. a) and b) Each graph represents the variation in $[Ca^{2+}]_i$ with respect to time of a different cell in the same area of 16-day old cell culture. Mechanical stimulation was applied to a nearby cell at time zero. The communicated intercellular Ca^{2+} wave is indicated in each tracing by the label "w". The subsequent Ca^{2+} oscillations induced in each cell occurred with different frequencies. c) A graph showing the total number of cells that propagated an intercellular Ca^{2+} wave (circles), the total number of cells induced to display Ca^{2+} oscillations by the Ca^{2+} wave (triangles) and the total number of cells (squares) within the field of view (35 experiments, 1988 cells field size 283 × 213 μm). d) The normalized percentage of cells that propagated an intercellular Ca^{2+} wave (circles) and were induced to display Ca^{2+} oscillations (triangles) with respect to distance from the origin of the intercellular Ca^{2+} wave.

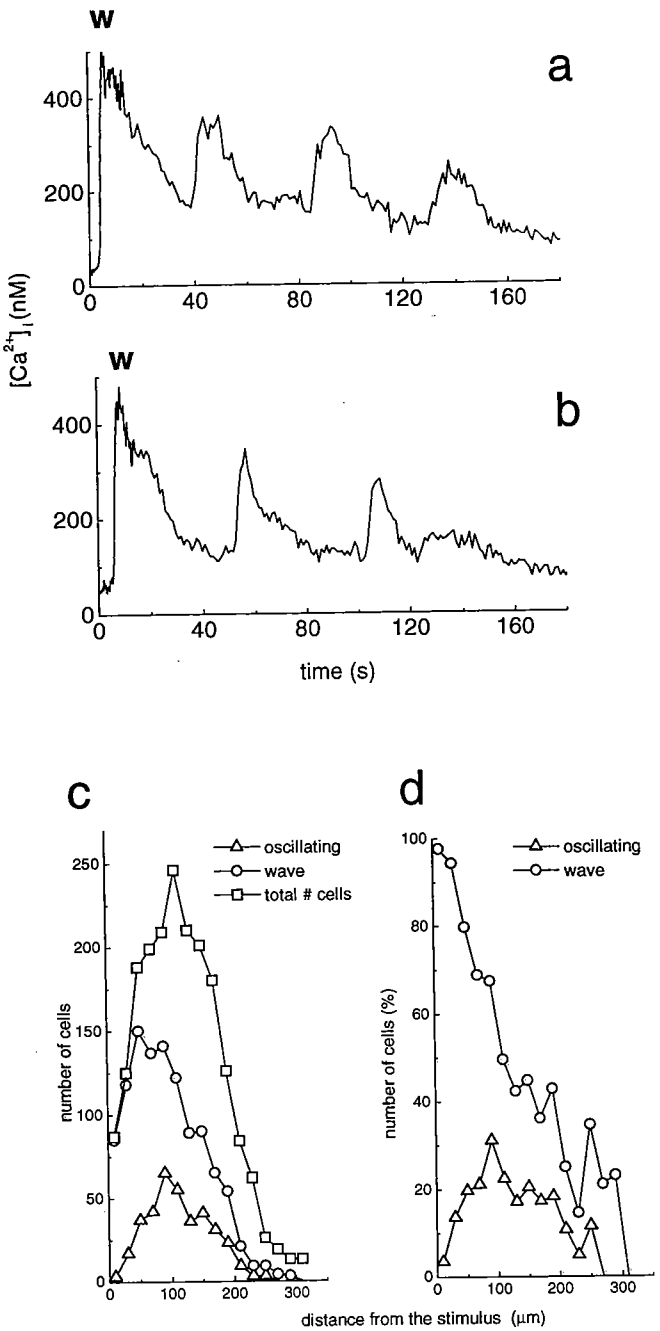
w
a
400
200
0
0
40
80
120
160
[Ca2+]i (nM)
w
b
400
200
0
0
40
80
120
160
time (s)
c
d
oscillating
wave
total # cells
number of cells
250
200
150
100
50
0
0
100
200
300
oscillating
wave
number of cells (%)
100
80
60
40
20
0
0
100
200
300
distance from the stimulus (μm)

Figure 35

time (monitoring period 160-200 s, **Fig. 36, Table 3**). According to these criteria, four different types of oscillatory patterns were discerned. The first, **spike type** (S-type) oscillations, which occurred while the wave-induced $[Ca^{2+}]_i$ was still elevated, were characterized by the quick onset of a rapid burst of spikes in $[Ca^{2+}]_i$ (**Fig. 36 a, Table 3**). The second, **continuous type** (C-type) oscillations, were characterized by a continued activity throughout the monitoring period, a slower periodicity than the S-type oscillations and were initiated when the wave-induced $[Ca^{2+}]_i$ increase had been significantly reduced (**Table 3**). C-type oscillations were further classified into two groups, **immediate** and **delayed**, based on the onset time of the first Ca^{2+} oscillation (**Table 3, Fig. 36 b, c**). The third, **brief type** (B-type) oscillations, although having a similar average periodicity to the C-type, were differentiated from the C-type oscillations by their short duration or early termination before the end of monitoring period (**Fig. 36 d, Table 3**). In addition, the periodicity of the B-type oscillations was not constant and increased from 25 s to 42 s before termination. Similarly, the peak elevations in $[Ca^{2+}]_i$ of each oscillation declined with time from 125 nM to 75 nM. The forth, **recovered type** (R-type) oscillations, were similar to B-type oscillations except that, after a lag time, the oscillatory behavior recovered with a different periodicity within the monitoring period (**Fig. 36 e, Table 3**). The C-type oscillations were the most commonly observed (4.9 cells per experiment) while the R-type oscillations were the least commonly observed (0.8 cells per experiment, **Table 3**).

IV-4. Types of intracellular Ca^{2+} oscillations are not dependent on the cell identity

To determine if all the cell types in the primary glial cell cultures equally contributed to the population of cells displaying Ca^{2+} oscillations, immunocytochemically-determined cell identity was correlated with the changes in $[Ca^{2+}]_i$ (**Fig. 37 a,b,c**). Initial single staining experiments demonstrated that majority of the cells in cultures were GFAP+ or GalC+ (**Fig. 37 d**). Double-staining experiments identified three major groups of cells: 23 ± 8% of the cells were only GFAP+ and were identified as astrocytes (white arrows, **Fig. 37 a**), 39 ± 14 % of the cells were only GalC+ and were identified as oligodendrocytes (gray arrows, **Fig. 37 b**), while 38 ± 9 % were both GFAP+ and GalC+ and were identified as mixed phenotype or precursor cells (black arrows, **Fig. 37 a and b**). The cell density was 1216 ± 224 cells/mm^2. This identification scheme follows that described by Ranscht et al., (1982), Raff et al., (1983) and Frotter and Schachner, (1989). Phase-contrast images acquired after the staining process confirmed that cells were not washed off during immunochemistry procedures (**Fig. 37 c**). There was no cross-reactivity between the secondary antibody conjugated to FITC and the primary antibody for GFAP.

Table 3. Properties and occurrence of different types of Ca^{2+} oscillation induced by intercellular Ca^{2+} waves

oscillation type	periodicity (s)	duration (s)	onset time (range, s)	peak $\Delta [Ca^{2+}]_i$ (nM)	observation frequency (#cells/# experiments)
S-type[1]	6 ± 2	20 ± 9	3-7	44 ± 26	1.3
C-type[2]	28 ± 15	>160	**immediate** 10-34 **delayed** 40-95	91 ± 26	4.9
B-type[3]	29 ± 19	66 ± 35	18 - 58	85 ± 37	3.4
R-type[4]	**initial**[5] 14 ± 7 **recovered**[5] 27 ± 11	-	13 - 47	83 ± 29	0.8

[1] mean ± SD, n = 26 cells, 14 exp. [2] mean ± SD, n = 50 cells, 14 exp. [3]mean ± SD, n = 38 cells, 14 exp. [4]mean ± SD, n = 19 cells, 14 exp.
[5] initial oscillations stopped and, after a lag time of 75 ± 25 seconds, recovered with the second periodicity.
Periodicity: average time of each oscillation.
Duration: average time during which oscillations occurred.
Onset time: average time between the propagation of a Ca^{2+} wave and the initiation of the first Ca^{2+} oscillation.

Peak $\Delta[Ca^{2+}]_i$: maximal change in $[Ca^{2+}]_i$ attained during each oscillation.

Figure 36: The types of intracellular Ca^{2+} oscillations induced by an intercellular Ca^{2+} wave. Each tracing represents the changes in $[Ca^{2+}]_i$ with respect to time of single cells in a 17-day old culture. The intercellular Ca^{2+} wave is indicated by the label "w". Cells are displaying a) a spike or S-type Ca^{2+} oscillations, b) an continuous immediate or C-type oscillations, c) a continuous delayed (C-type) oscillations, d) a brief or B-type oscillations and e) a recovered or R-type oscillations.

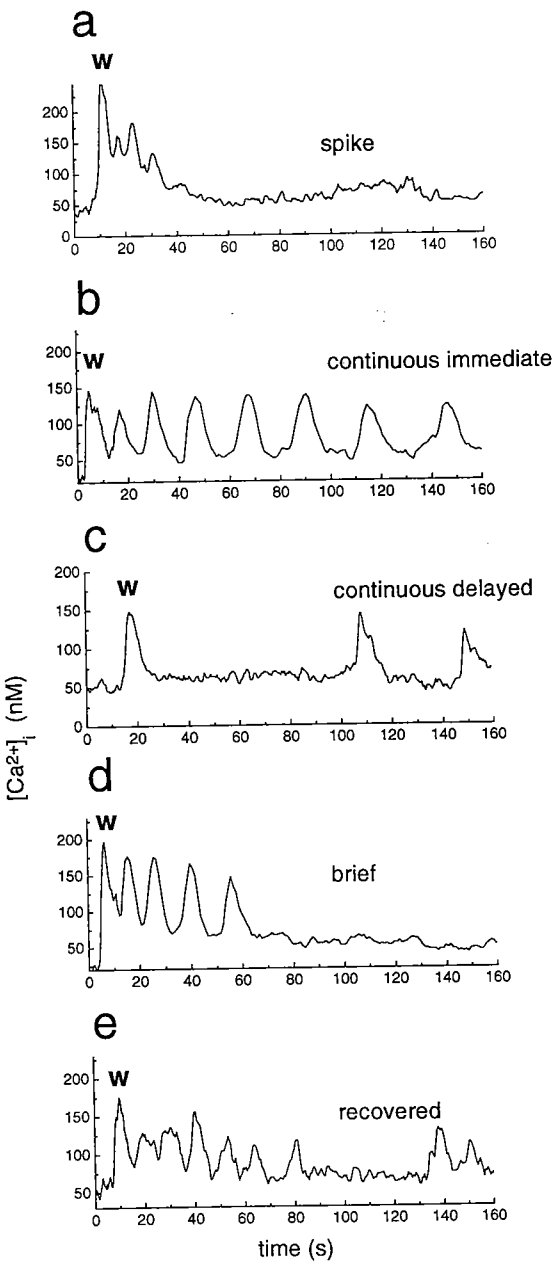
a
w
spike
b
w
continuous immediate
c
w
continuous delayed
d
w
brief
e
w
recovered
[Ca2+]i (nM)
time (s)

Figure 36

Figure 37: Analysis of different cell types found in culture. Glial cells within the same field are visualized by fluorescent immunocytochemistry using a) antibodies to GFAP, b) antibodies to GalC as well as c) viewed with the phase-contrast optics. White arrows indicate cells that were only GFAP+ and were identified as astrocytes, gray arrows indicate cells that were only GalC+ and were identified as oligodendrocytes, and black arrows indicate cells positive for both GFAP and GalC, that were identified as precursor cells. d) The number of different immunopositive cells per 0.01 mm^2 (10 experiments): neurofilament, i.e., NF+, GFAP+, and GalC+. e) The percentage of different types of cells displaying Ca^{2+} oscillations induced by an intercellular Ca^{2+} wave; astrocytes (A), oligodendrocytes (O) and precursor cells (P). Bars represent mean ± SD (n=380 cells, 7 experiments).

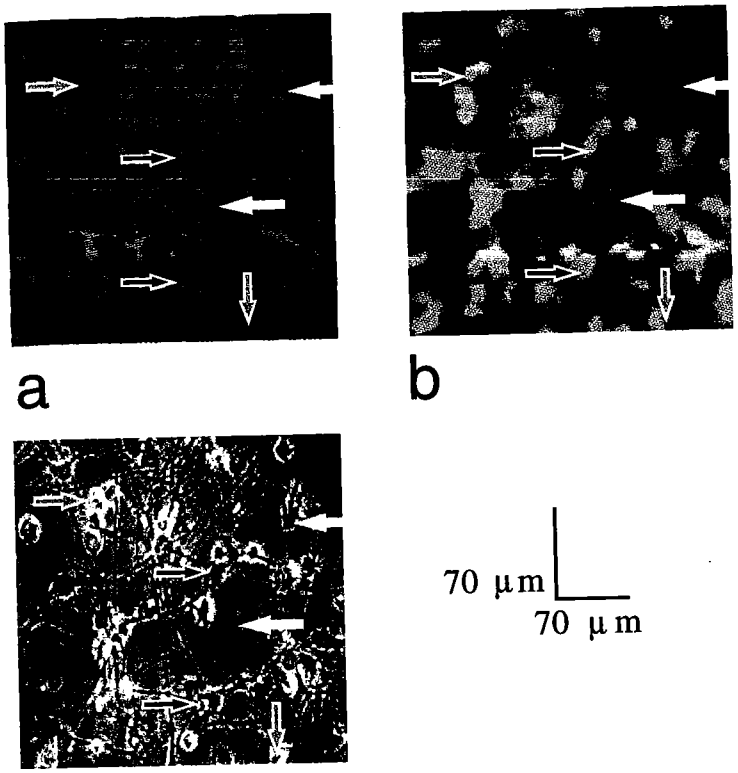
a
b
c
70 µm
70 µm
d
10
5
0
cells \ 0.01 mm²
NF+
GFAP+
GalC+
e
80
70
60
50
40
30
20
10
0
cells oscillating after Ca²⁺ wave (%)
A
P
O

Figure 37

Cell type identification coupled with $[Ca^{2+}]_i$ imaging revealed that intercellular Ca^{2+} waves were initiated from and passed between astrocytes, oligodendrocytes, and precursor cells, as well as from one cell type to another. All the glial cell types recognized by immunocytochemistry were equally capable of displaying Ca^{2+} oscillations after propagating an intercellular Ca^{2+} wave (**Fig. 37 e** ANOVA $F = 0.401$, $p > 0.05$). Furthermore, all the glial cell types were capable of displaying, to the same extent, the general characteristics of the four major types of Ca^{2+} oscillatory behavior (**Fig. 38,** ANOVA between cell types for C-, B-, R- and S-oscillations was $F= 2.425$, 0.343, 0.716, and 2.25 respectively, $p > 0.05$). This analysis demonstrated that specific oscillatory types do not represent specific oscillatory behaviors of different glial cell types.

IV-5. Cell type-dependent specifics of Ca^{2+} oscillations

Not surprisingly, some specific characteristics of each type of Ca^{2+} oscillatory behavior were observed for the different cell types. A comparison of the oscillatory periodicity of C- and B-type oscillations in astrocytes and oligodendrocytes was conducted because these are the most frequent oscillatory types observed and they differ only in the duration of their oscillatory activity. Analysis of the initiation of the first, second, and third $[Ca^{2+}]_i$ rise during the C- and B- type oscillations demonstrated slower periodicity of oscillations in oligodendrocytes than in astrocytes (**Fig. 39 a**). Furthermore, time periods between $[Ca^{2+}]_i$ elevations increased more in oligodendrocyte oscillations than astrocyte oscillations. In order to analyze the cell type-specific kinetics of $[Ca^{2+}]_i$

Figure 38: The distribution of the different types of Ca^{2+} oscillations with respect to the cell type. C-type (C), B-type (B), R-type (R) and S-type (S). Astrocytes (white bars), oligodendrocytes (gray bars) and precursor cells (black bars). Bars represent mean ± SD (n=102 cells, 5 experiments).

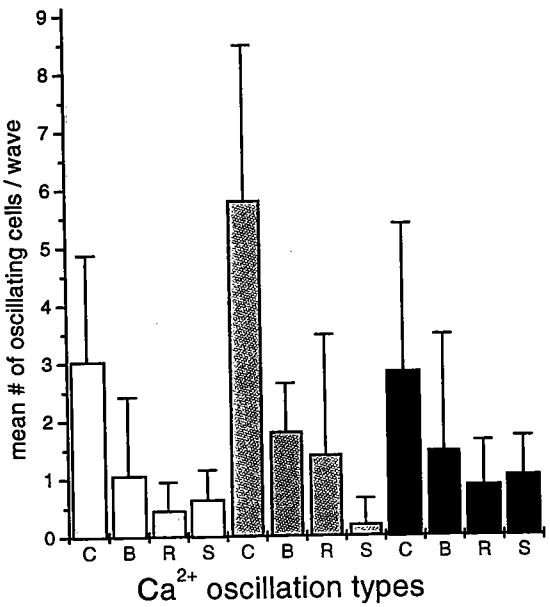
mean # of oscillating cells / wave
0
1
2
3
4
5
6
7
8
9
C B R S C B R S C B R S
Ca2+ oscillation types

Figure 38

Figure 39: Characteristics of Ca^{2+} oscillation of different cell types. a) A comparison of start times of the first , second and third $[Ca^{2+}]_i$ increases during C- and B-type oscillations between astrocytes (black circles) and oligodendrocytes (white circles). b) A comparison of the kinetics of Ca^{2+} release during S-type and C-type Ca^{2+} oscillations in astrocytes (black bars) and oligodendrocytes (white bars). Bars represent mean values and lines represent standard deviation. c) comparison of $[Ca^{2+}]_i$ changes during propagation of Ca^{2+} wave and the first, second and third $[Ca^{2+}]_i$ rise of the early onset types of Ca^{2+} oscillations between astrocytes (black circles) and oligodendrocytes (white circles), d) comparison of $[Ca^{2+}]_i$ changes during propagation of Ca^{2+} wave and the first , second and third $[Ca^{2+}]_i$ rise of the late onset types of Ca^{2+} oscillations between astrocytes (black circles) and oligodendrocytes (white circles).

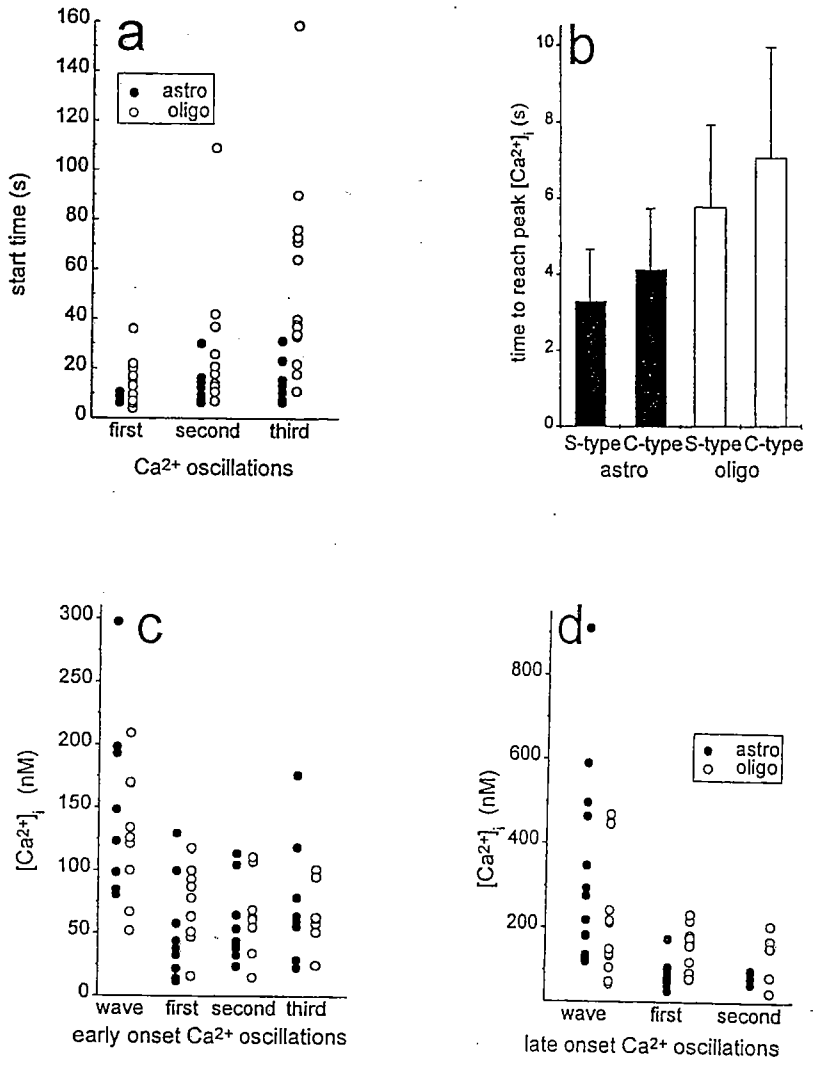
a
start time (s)
160
140
120
100
80
60
40
20
0
astro
oligo
first
second
third
Ca2+ oscillations
b
time to reach peak [Ca2+]i (s)
10
8
6
4
2
0
S-type C-type S-type C-type
astro
oligo
c
[Ca2+]i (nM)
300
250
200
150
100
50
0
wave
first
second
third
early onset Ca2+ oscillations
d
[Ca2+]i (nM)
800
600
400
200
astro
oligo
wave
first
second
late onset Ca2+ oscillations

Figure 39

elevations during oscillatory activity, the times to reach the maximum $[Ca^{2+}]_i$ during S-type and C-type oscillations were measured. These two oscillatory types were chosen because they are characterized by a striking difference in oscillatory frequency, a parameter that is closely dependent on the kinetics of individual oscillatory $[Ca^{2+}]_i$ elevations. The kinetics of $[Ca^{2+}]_i$ elevation during both S- and C-type Ca^{2+} oscillations was significantly faster in astrocytes than in oligodendrocytes (**Fig. 39 b**).

The cell type-specifics of $[Ca^{2+}]_i$ increases during Ca^{2+} wave and Ca^{2+} oscillations were analyzed. This parameter was chosen as it quantifies the recovery of a cell to its steady-state $[Ca^{2+}]_i$ after the Ca^{2+} wave propagation. Astrocytes and oligodendrocytes exhibited comparable magnitudes of $[Ca^{2+}]_i$ during the propagation of a Ca^{2+} wave that induced early onset oscillations (i.e., S-, C- and B-type oscillations) (**Fig. 39 c**). In astrocytes, $[Ca^{2+}]_i$ elevations during the early onset oscillations appeared initially smaller than elevations measured for oligodendrocytes. Interestingly, the magnitudes of astrocytic $[Ca^{2+}]_i$ increased from the first to the third $[Ca^{2+}]_i$ elevations and were ultimately comparable and/or higher than oligodendrocytic $[Ca^{2+}]_i$ elevations. One explanation of this result can probably be found in the fast oscillatory activity of astrocytes that is initiated by Ca^{2+} wave propagation before the complete recovery of $[Ca^{2+}]_i$ regulatory proteins. A comparison of $[Ca^{2+}]_i$ changes during the propagation of a Ca^{2+} wave and the first and second $[Ca^{2+}]_i$ increases during late onset oscillations (i.e., continuous delayed type) between astrocytes and oligodendrocytes showed that the magnitude of $[Ca^{2+}]_i$ elevation during the propagation of a Ca^{2+} wave was larger in astrocytes than in oligodendrocytes and $[Ca^{2+}]_i$ rises during oscillations were specific for the two cell types (**Fig. 39 d**).

Although different oscillatory types showed cell type-related characteristics, it should be emphasized that these cell-specific features were minor in comparison to the general classification described earlier.

IV-6. The specifics of induced intracellular Ca^{2+} oscillations varies with distance from the Ca^{2+} wave origin

The expression of a particular Ca^{2+} oscillation type was related to the distance of the cell from the origin of the intercellular Ca^{2+} wave (**Fig. 40**). To account for the variability in the strength of the mechanical stimulation between experiments, the distributions of the different oscillatory types were normalized with respect to the distribution of C-type oscillations, the most prominent oscillation type observed in all experiments. This relative analysis was performed by aligning the distributions of the C-type oscillations from each experiment.

C-type oscillations occurred in cells in a zone approximately 150 μm wide, centered around a distribution peak at 102 ± 46 μm away from the origin of the Ca^{2+} wave (**Fig. 40 a**). Cells displaying S-type oscillations were found at approximately 60 μm from the Ca^{2+} wave origin, in a zone 80 μm wide (**Fig. 40 b**). B-type oscillations occurred in a zone 160 μm wide, with a distribution peak further away from the Ca^{2+} wave origin than the distribution peak of the C-type oscillations (**Fig. 40 c**). R-type

Figure 40: The spatial distribution of the different types of Ca^{2+} oscillations induced by an intercellular Ca^{2} wave. For comparison, the distribution profiles of each oscillatory type are aligned with respect to the mode of the distribution of C-type oscillations. The distribution profiles of a) aligned C-type oscillations, b) S-type oscillations, c) B-type oscillations and d) R-type oscillations. X axis represents relative distance from the origin of the intercellular Ca^{2+} wave. Vertical line represents the averaged mode (102 ± 46 μm) of the C-type oscillation distribution profiles. Total number of cells analyzed = 257, from 16 experiments.

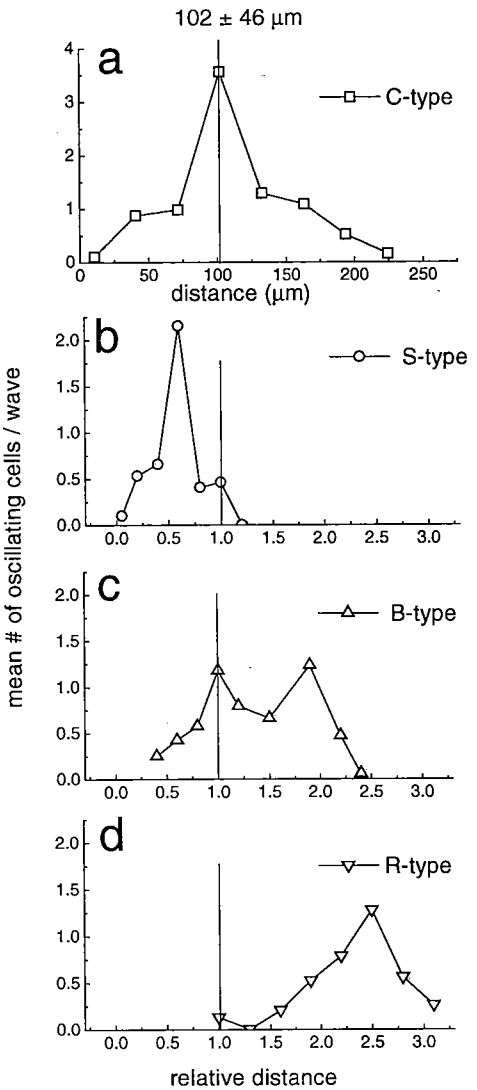
102 ± 46 µm
a
C-type
distance (µm)
b
S-type
c
B-type
d
R-type
mean # of oscillating cells / wave
relative distance

Figure 40

oscillations were found in cells furthest away from the Ca^{2+} wave origin, in a zone 90 μm wide with a distribution peak 250 μm away from the Ca^{2+} wave origin (**Fig. 40 d**).

To further test the hypothesis that oscillatory behavior induced by an intercellular Ca^{2+} wave is a function of distance but not of cell type, intercellular Ca^{2+} waves were sequentially initiated from two sites such that each Ca^{2+} wave propagated from different distances in opposite directions before arriving at a cell (**Fig. 5 a and b**). Two intercellular Ca^{2+} waves, initiated at different sites, evoked oscillations in 39% of the cells that propagated one or both Ca^{2+} waves. 30% of these cells oscillated in response to both Ca^{2+} waves, and this group of cells displayed a change in oscillatory behavior in response to the first and the second Ca^{2+} wave (45 cells, 14 paired experiments, **Fig. 5 c, d**). The nature of the oscillatory change was determined by the difference in distance of the oscillating cell from each Ca^{2+} wave origin. Ca^{2+} waves traveling distances that differed by an average value of 69 ± 17 μm (mean ± SD, 25 cells) converted the oscillatory behavior displayed by a cell from one oscillation type to another. If the second Ca^{2+} wave propagated a shorter distance to reach the cell, Ca^{2+} oscillations were converted from B- or R-type to S- or C-type (**Fig. 41 a**). On the other hand, if the second Ca^{2+} wave propagated further to reach the cell, S- and C-type oscillations were converted to B- and R-type oscillations (**Fig. 41 b**). Cells that passed Ca^{2+} waves arriving from distances that differed by an average of 35 ± 14 μm (mean ± SD, 20 cells) did not alter the type of Ca^{2+} oscillation, but instead showed a change in oscillatory frequency. If the second Ca^{2+} wave propagated a shorter distance to the oscillating cell, the frequency of

Figure 41: The conversion of the oscillatory pattern and the alteration of the frequency of Ca^{2+} oscillations of a single cell by two intercellular Ca^{2+} waves which differ in their propagation distance to the cell. Each tracing represents the change in $[Ca^{2+}]_i$ with respect to time of the same cell in a 19-day old culture after the first Ca^{2+} wave (black line) and after the second Ca^{2+} wave (red line). a) and b) The cells experienced two waves with a large (69 ± 17 μm, mean ± SD, 25 cells) difference in their propagation distance. a) The cell initially showed a C-type oscillations in response to the first Ca^{2+} wave that was converted to an S-type oscillation after the second wave. b) Another cell showing C-type oscillations after the first Ca^{2+} wave that are converted to a B-type oscillations after the second Ca^{2+} wave. c) and d) The cells experienced two waves with a small (35 ± 14 μm, mean ± SD, 20 cells) difference in their propagation distance. c) A cell displaying Ca^{2+} oscillations with an initial periodicity of about 125 seconds in response to the first Ca^{2+} wave. The periodicity of the Ca^{2+} oscillations induced by the second wave was reduced to 39 seconds. d) A different cell displaying an increase in the periodicity of the initial Ca^{2+} oscillation in response to a second Ca^{2+} wave. e) A cell propagating two Ca^{2+} waves initiated from the same origin does not alter its oscillatory behavior.

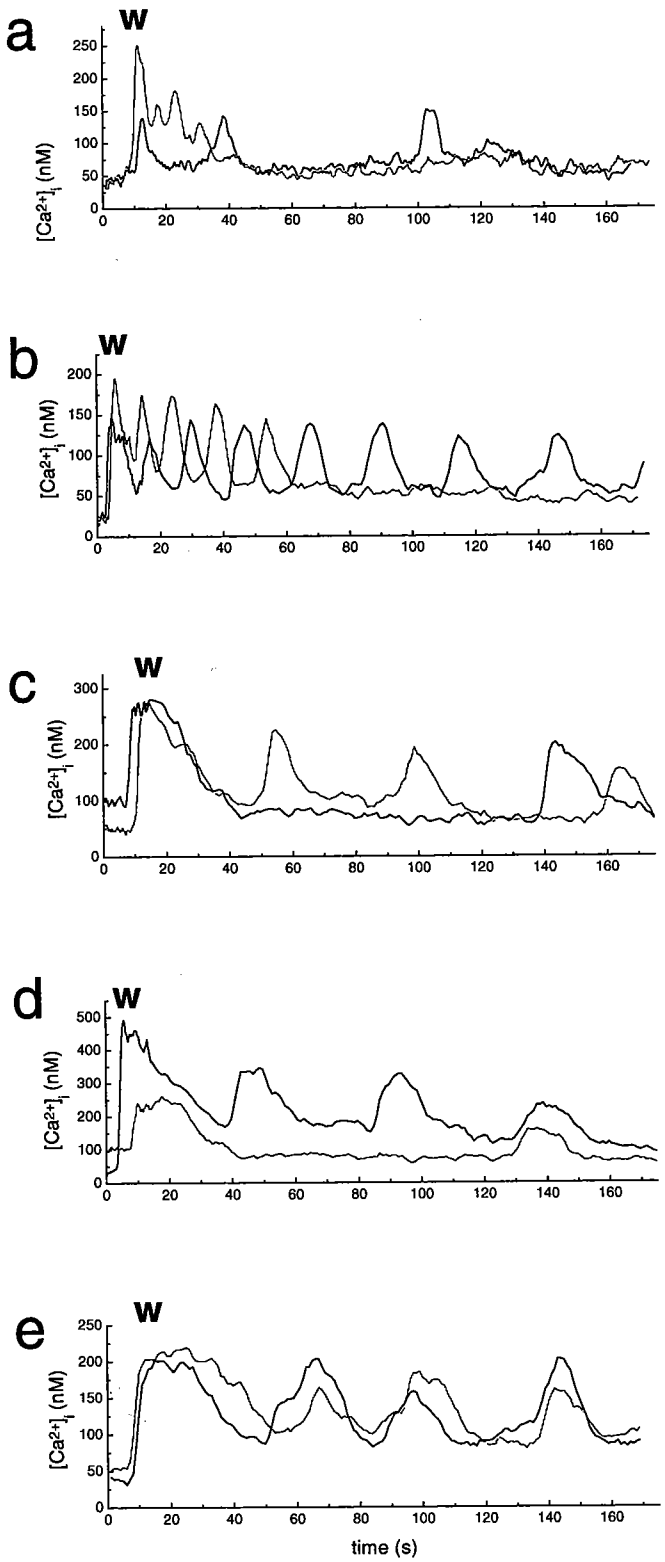

Figure 41

Ca^{2+} oscillations increased (**Fig. 41 c**). Conversely, if the second Ca^{2+} wave propagated further to reach the cell, the frequency of Ca^{2+} oscillations decreased (**Fig. 41 d**).

The Ca^{2+} oscillatory behavior of cells induced by pairs of Ca^{2+} waves was not biased by the properties of the first Ca^{2+} wave because the spatial distribution of oscillating cells induced by each wave was similar (**Fig. 42**). Furthermore, in control experiments, cells showed the same oscillatory response after propagation of two Ca^{2+} waves that were initiated from the same cell in culture, and therefore propagated the same distance to reach the cell (**Fig. 41 e**). The dual stimulation protocol also revealed that almost all cells are capable of displaying Ca^{2+} oscillations if adequately stimulated. For example, 22% of the cells that did not oscillate in response to the first Ca^{2+} wave, did oscillate in response to the second Ca^{2+} wave. Conversely, 42% of the cells induced to oscillate by the first wave did not oscillate in response to the second wave.

Collectively, these results demonstrated that glial cells can decode multiple mechanical stimuli that generate intercellular Ca^{2+} waves by expressing specific Ca^{2+} oscillations, whose characteristics are a function of the distance traveled by the Ca^{2+} waves.

IV-7. Acetylcholine and acetylmethilcholine induce Ca^{2+} oscillations in glia

The search for an experimental procedure that would allow for the analysis of the effects of a uniform increase in the $[IP_3]_i$ throughout the glial culture was guided by the

Figure 42: The spatial distribution of cells displaying Ca^{2+} oscillations in response to two Ca^{2+} waves. Two distributions are almost identical (first Ca^{2+} wave, 16 experiments; second Ca^{2+} wave, 15 experiments).

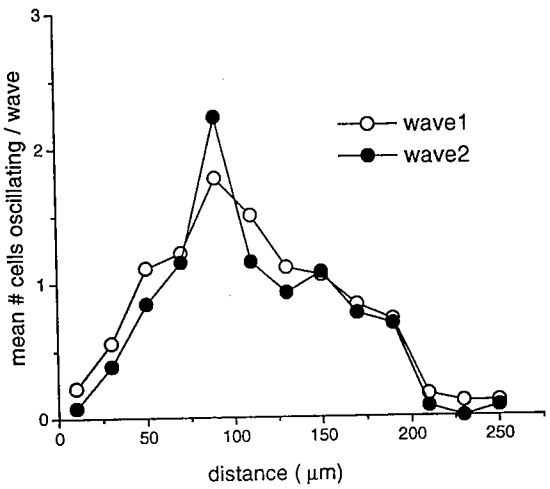
mean # cells oscillating / wave
distance (μm)
wave1
wave2
0
1
2
3
0
50
100
150
200
250

Figure 42

observation that the neurotransmitter ACh and muscarinic agonist AMCh induce a response in glial cells in the form of intracellular Ca^{2+} oscillations (muscarinic, or 'MR-induced Ca^{2+} oscillations'). Previous studies demonstrated that glial cells respond to cholinergic stimulus by accumulation of IP_3 (Pearce et al., 1985; Pearce et al., 1986) that induces a rise in $[Ca^{2+}]_i$ by causing the release of Ca^{2+} from IP_3-sensitive intracellular calcium stores in both astrocytes and oligodendrocytes (Shao and McCarthy, 1995; Takeda et al., 1995). A series of experiments was conducted in order to analyze the oscillatory activity of glia in response to different concentrations of ACh and AMCh. Dose-response curves generated for ACh and AMCh showed that oscillatory responses reached their plateau for concentrations above 100μM, where 40 % and 65 % of the cells responded per visualized cell field (**Fig. 43**). MR-induced Ca^{2+} oscillations occurred in a Ca^{2+}-free extracellular solution, thus supporting previous findings that these oscillations occur due to the release of Ca^{2+} from the intracellular Ca^{2+} stores. Although Ca^{2+} oscillations remained confined to individual cells and did not spread through the culture in the form of Ca^{2+} waves, this confinement was not due to the inhibition of intercellular gap junctions, since mechanically-induced intercellular Ca^{2+} waves propagated through the oscillating cells (**Fig. 44**).

In order for a repeated exposure of glial cells to ACh or AMCh to result in identical oscillatory activity of individual cells, cells needed to recover for a minimum of 5 minutes in an HBSS-agonist free extracellular solution (**Fig. 45**). Therefore, in experiments designed to analyze MR-induced $[Ca^{2+}]_i$ changes, cell cultures were always allowed to recover for 5 min in agonist-free solution before an application of a drug.

Figure 43: Dose-response curves demonstrate the dependence of the number of cells responding on the concentration of ACh and AMCh. The number of cells responding to agonist was normalized to the total number of cells present in the field of view. Squares (ACh, blue line) and circles (AMCh, black dotted line) represent mean values and lines represent standard deviation. $N \geq 5$ experiments for each agonist concentration. Total number of cells analyzed = 2144.

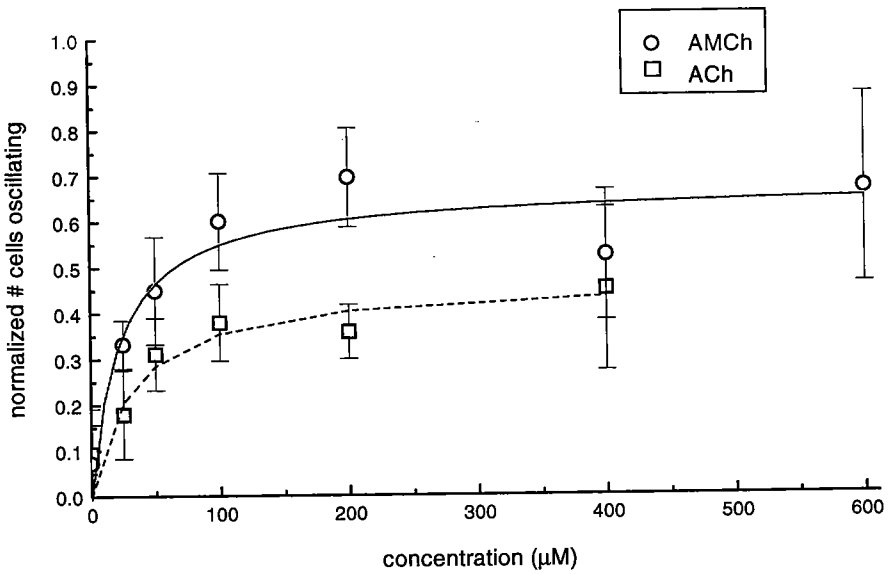
AMCh
ACh
normalized # cells oscillating
1.0
0.9
0.8
0.7
0.6
0.5
0.4
0.3
0.2
0.1
0.0
0
100
200
300
400
500
600
concentration (μM)

Figure 43

Figure 44: Ca^{2+} wave propagates through glial cells that oscillate in response to ACh (100 μM). a) and b) Each tracing represents the change in $[Ca^{2+}]_i$ with respect to time of the same cell in a 16-day old culture. Note that Ca^{2+} waves of different magnitude propagate through cells oscillating with different frequencies. Line above the trace indicates exposure to ACh. Black arrow marks the increase in $[Ca^{2+}]_i$ associated with the propagation of an intercellular Ca^{2+} wave initiated from a cell at a given distance from the oscillating cell.

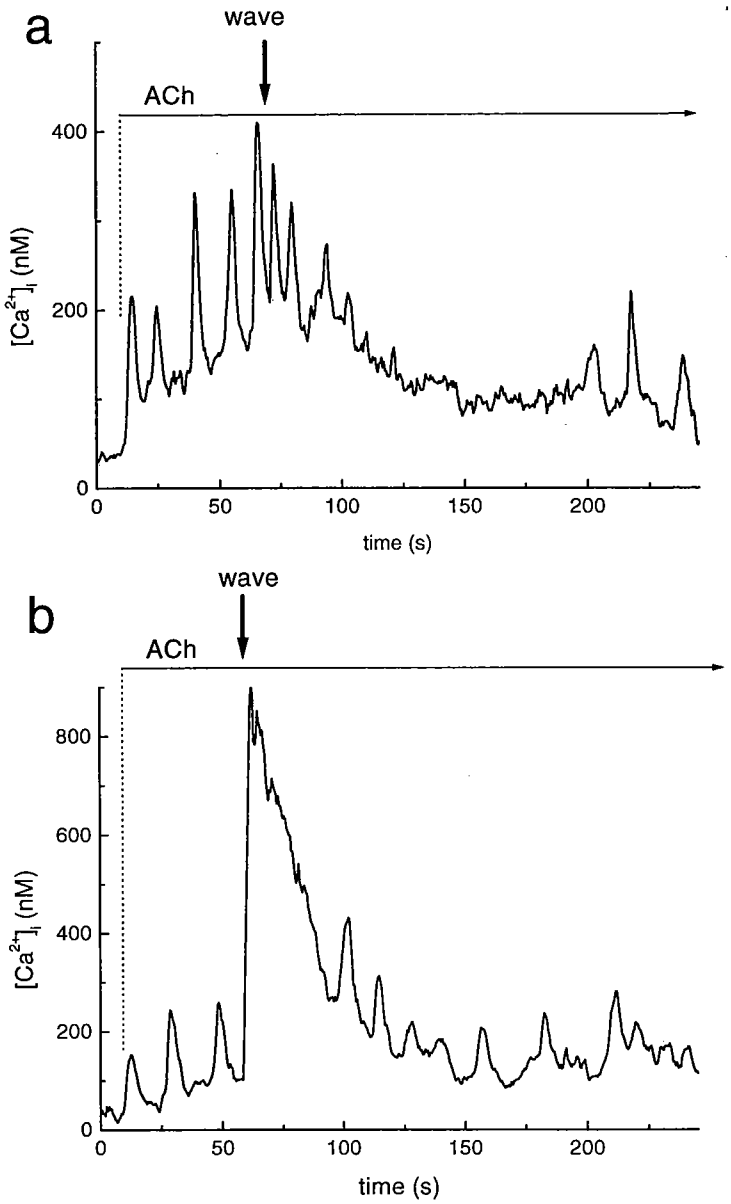
a
wave
ACh
400
200
0
[Ca2+]i (nM)
0
50
100
150
200
time (s)
b
wave
ACh
800
600
400
200
0
[Ca2+]i (nM)
0
50
100
150
200
time (s)

Figure 44

Figure 45: Exposure to AMCh repeated after 5 min of recovery induces a very similar pattern of Ca^{2+} oscillations in a cell. Tracings represent the change in $[Ca^{2+}]_i$ with respect to time of the same cell in a 19-day old culture. Black bar indicates exposure to AMCh, The scale bar indicates exposure to the control, HBSS solution.

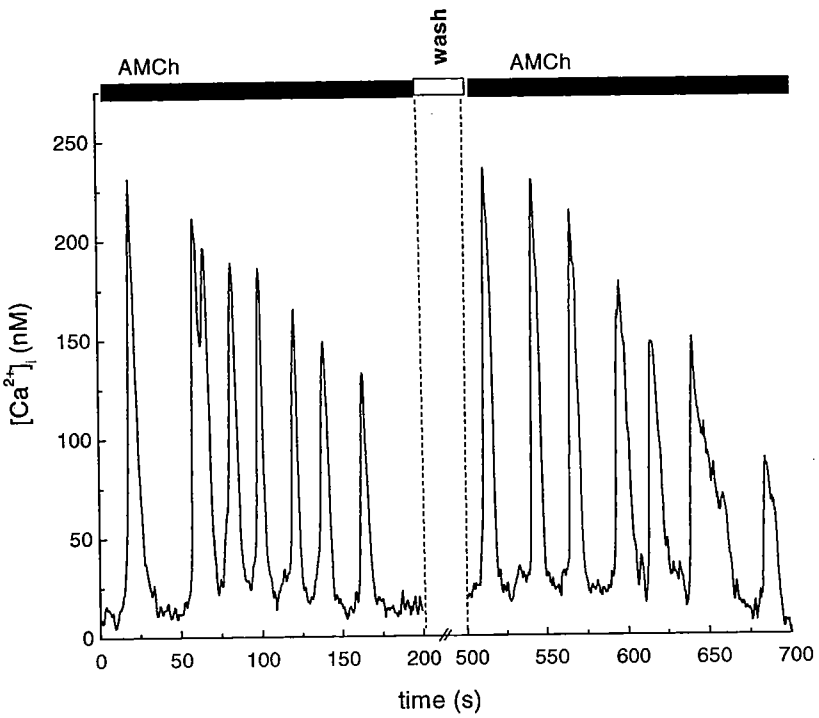
AMCh
wash
AMCh
250
200
150
100
50
0
[Ca2+]i (nM)
0
50
100
150
200
500
550
600
650
700
time (s)

Figure 45

IV-7.i. The effect of PLC inhibitors on MR-induced oscillations.

To further test whether MR-induced Ca^{2+} oscillations are generated by PLC activation and mobilization of Ca^{2+} by IP_3, different inhibitors of PLC were used. Treatment of cultures with PLC inhibitor neomycin sulfate (200μM, 30 min incubation) (Prentki et al., 1986) blocked oscillations in 70% of the cells that oscillated after the control exposure to AMCh (200μM, n = 4, **Fig. 46, Fig. 48 c**). The remaining cells in the group that oscillated in response to AMCh did not cease to oscillate after exposure to neomycin, but instead, decreased the frequency of their oscillations (**Fig. 47**). The initial oscillatory behavior was restored in 62% of cells after a 30 minutes recovery period in neomycin-free extracellular solution (n = 4 experiments, **Fig. 46, Fig. 47, Fig. 48 c**).

Preincubation with LiCl (10 mM, 30 min) inhibited MR-induced oscillations in 98 % of glial cells. MR-induced oscillations (100μM AMCh) were recovered after a 45 min incubation in LiCl-free extracellular solution (**Fig. 48 a**, n = 7 experiments).

U-73122 (5 μM, 1 min incubation) blocked the response to AMCh (100μM) in 92 % of treated cells (**Fig. 48 b**, n = 4). Preincubation with inactive U-73343 however, did not significantly change cells' oscillatory responses to AMCh (n = 3).

Figure 46: Complete block of AMCh-induced Ca^{2+} oscillations by neomycin sulfate (200 μM). Tracings represent the change in $[Ca^{2+}]_i$ with respect to time of a single cell in a 19-day old culture. Application of AMCh (200 μM, black bar) induces Ca^{2+} oscillations in a cell. Following 5 min wash in control HBSS solution and 30 min incubation in neomycin sulfate (200μM, gray bar), exposure to AMCh is repeated (black bar), but Ca^{2+} oscillations are not induced. After 30 min wash in HBSS, the same concentration of AMCh induces an oscillatory pattern similar to initial Ca^{2+} oscillations in control conditions. The scale bar indicates wash in control HBSS extracellular solution, gray bar indicates incubation in neomycin solution, black bar indicates exposure to AMCh.

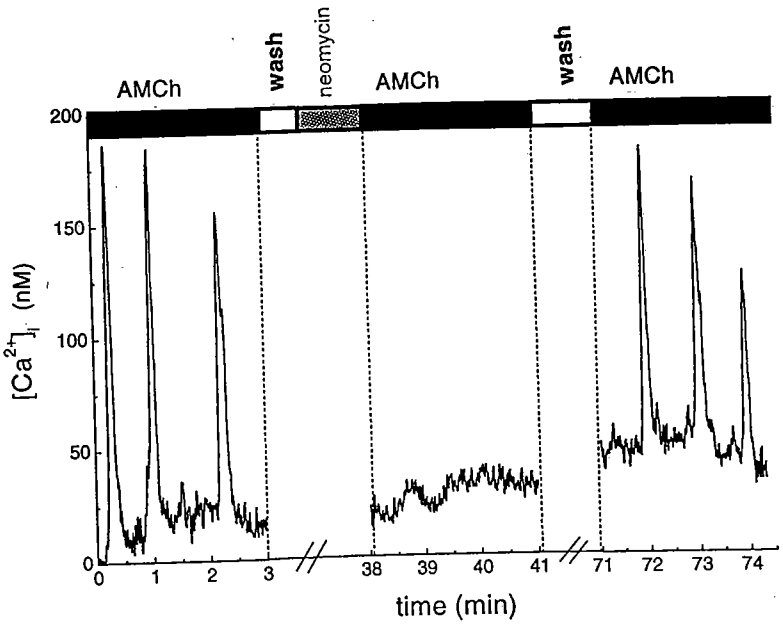
AMCh
wash
neomycin
AMCh
wash
AMCh
200
150
100
50
0
[Ca2+]i (nM)
0
1
2
3
38
39
40
41
71
72
73
74
time (min)

Figure 46

Figure 47: Partial block of AMCh-induced Ca^{2+} oscillations by neomycin sulfate. Tracings represent the change in $[Ca^{2+}]_i$ with respect to time for a single cell in a 19-day old culture. Exposure to AMCh (200 μM) induces Ca^{2+} oscillations in a cell. Note that the frequency of these oscillations is faster than the frequency of oscillations in Fig 46. Following a wash in HBSS and incubation in neomycin sulfate (200μM), exposure to AMCh is repeated and slower oscillations are induced. After a period of recovery, AMCh stimulus is repeated and Ca^{2+} oscillations, similar to initial, control Ca^{2+} oscillations, are induced. The scale bar indicates wash in control extracellular solution, gray bar indicates incubation in neomycin solution, black bar indicates exposure to AMCh.

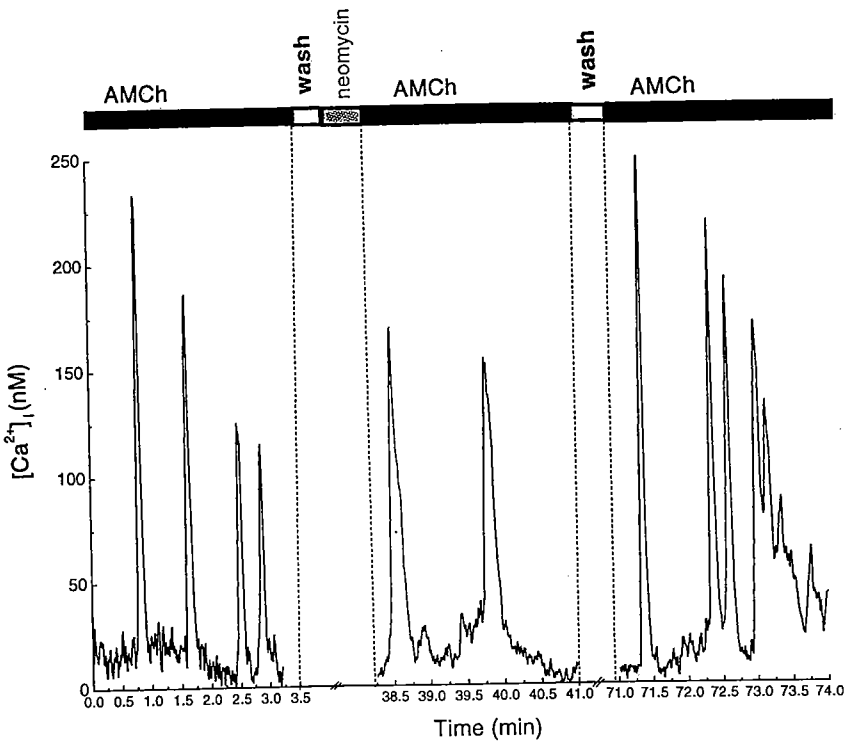
AMCh
wash
neomycin
AMCh
wash
AMCh
250
200
150
100
50
0
[Ca2+]i (nM)
0.0 0.5 1.0 1.5 2.0 2.5 3.0 3.5
38.5 39.0 39.5 40.0 40.5 41.0
71.0 71.5 72.0 72.5 73.0 73.5 74.0
Time (min)

Figure 47

Similar results were also observed for other concentrations of agonists tested (50 - 200 μM AMCh and ACh) in the presence of PLC and IP_3 recycling inhibitors.

IV-7.ii. The effect of heparin on MR-induced oscillations.

The role of Ca^{2+} release from IP_3-sensitive Ca^{2+} stores in MR-induced oscillations was investigated. Cells were grown on the conductive side of half-etched coverslips and loaded with IP_3 receptor blocker heparin. In response to AMCh (100μM), Ca^{2+} oscillations occurred predominantly on the non-loaded half of the coverslip (**Fig. 49 a**). Analyses of multiple experiments showed that heparin significantly reduced the number of cells that responded to AMCh (**Fig. 49 b**, n = 5).

This study supports the conclusion that ACh and AMCh induce Ca^{2+} oscillations in glial cells by activation of PLC, production of IP_3, binding of IP_3 to intracellular IP_3 receptors, and subsequent release of Ca^{2+} from IP_3-sensitive intracellular calcium stores. In keeping with previous studies (Andre et al., 1994; Cohen and Almazan, 1994; Cohen et al., 1996; Pearce et al., 1986; Repke and Maderspach, 1982) these results indicate that the application of muscarinic agonists can be used to uniformly increase $[IP_3]_i$ in a population of glial cells.

Figure 48: Effect of PLC blockers on AMCh-induced Ca^{2+} oscillations. Each cell oscillating after initial exposure to AMCh was monitored, and its responses to repeated exposures to AMCh after different treatments with PLC blockers were measured. Mean number of cells oscillating after each treatment were represented as the percentage of the total number of cells oscillating in control conditions. a) Neomycin sulfate (200μM, 30 min incubation) inhibited Ca^{2+} oscillations (black bar) in cells responding to AMCh (200μM, n = 4 experiments). Oscillatory activity partially recovered following the wash in control solution (checked bar). b) The effect of LiCl on AMCh-induced (100μM) Ca^{2+} oscillations. LiCl (10 mM, 30 min, n = 7experiments) inhibited Ca^{2+} oscillations (black bars) that recovered following wash in control solution (checked bar). c) U-73122 (5 μM, 1 min incubation, n = 4 experiments) blocked AMCh-induced (100μM) oscillations (black bar), while U-73343 (5 μM, 1 min incubation, n = 3 experiments) did not block Ca^{2+} oscillations (checked bar). Bars represent mean values and lines represent standard deviations.

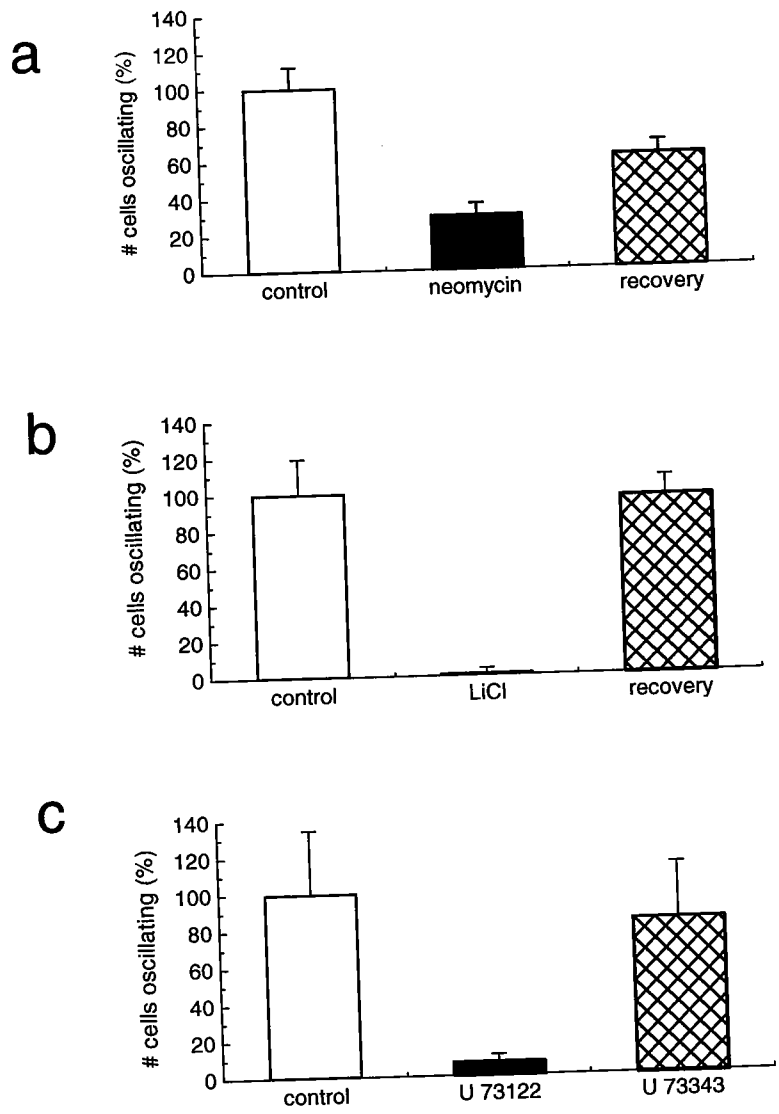
a
cells oscillating (%)
140
120
100
80
60
40
20
0
control
neomycin
recovery
b
cells oscillating (%)
140
120
100
80
60
40
20
0
control
LiCl
recovery
c
cells oscillating (%)
140
120
100
80
60
40
20
0
control
U 73122
U 73343

Figure 48

Figure 49: Acetylmethylcholine-induced Ca^{2+} oscillations depend on the functional IP_3 receptors. a) First image is a pseudocolored image of Texas Red fluorescence representing the area loaded with IP_3R blocker heparin. AMCh induces Ca^{2+} oscillations in the non-loaded zone of cells (white arrows). Note that the cell within the loaded zone responding to AMCh has not been loaded (striped arrow in Texas Red and 5 s images). The acquisition times are indicated below each image. Color calibration bar indicates changes in $[Ca^{2+}]_i$. b) Difference in the number of cells responding to AMCh between non-loaded and loaded zone, calculated as the percentage of the total number of cells present in the zone. Bars represent mean values and lines represent standard deviations, n = 5 experiments.

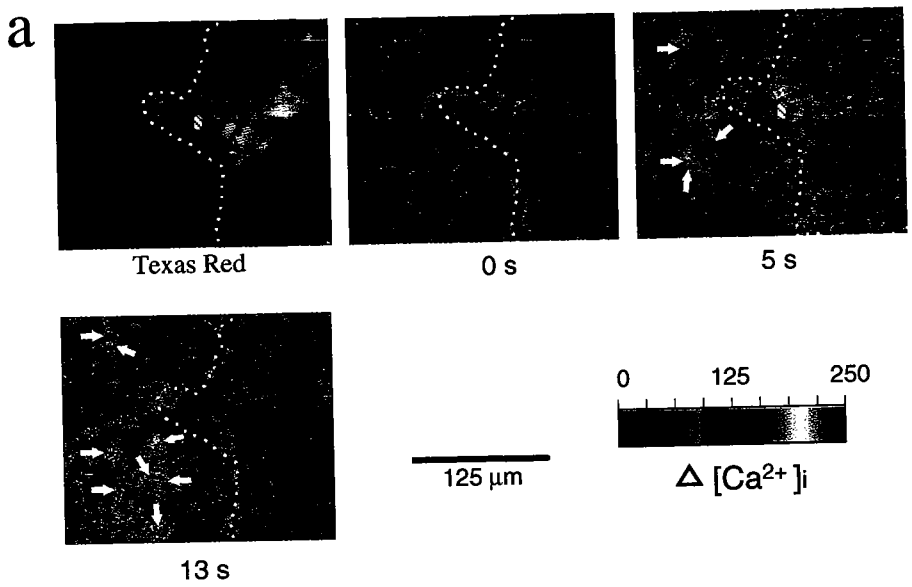
a
Texas Red
0 s
5 s
13 s
125 µm
0
125
250
Δ [Ca2+]i

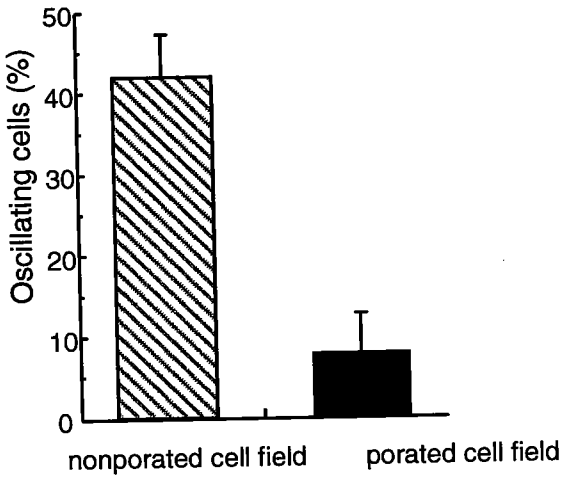
b
Oscillating cells (%)
50
40
30
20
10
0
nonporated cell field
porated cell field

Figure 49

IV-8. Acetylcholine-induced increase in $[IP_3]_i$ alters the oscillatory responses of glial cells to intercellular Ca^{2+} waves

Temporo-spatial patterns of Ca^{2+} wave-induced Ca^{2+} oscillations may be a function of the $[IP_3]_i$ gradient that was generated during the propagation of intercellular Ca^{2+} waves. If Ca^{2+} oscillations depend on $[IP_3]_i$ gradient, the distribution of cells displaying Ca^{2+} oscillations should be altered by manipulating $[IP_3]_i$. This hypothesis was tested by examining the effects of the neurotransmitter ACh on the distribution of Ca^{2+} oscillations induced by intercellular Ca^{2+} waves. ACh (400 μM), applied extracellularly 100-120 seconds after the initiation of an intercellular Ca^{2+} wave, increased the number of oscillating cells by 35 % relative to the number of cells oscillating only due to the Ca^{2+} wave. In addition, ACh shifted the distribution peak of Ca^{2+} oscillations 50 μm further away from the distribution peak of Ca^{2+} wave-induced oscillations (**Fig. 50**).

The responses of single glial cells to ACh, applied after the initiation of an intercellular Ca^{2+} wave, were analyzed in order to determine how ACh modulates individual Ca^{2+} oscillations. Following the addition of ACh, 87% of the cells changed the temporal characteristics of the Ca^{2+} oscillations induced by the Ca^{2+} wave. ACh either: 1) increased the frequency of Ca^{2+} oscillations (**Fig. 51 a**), 2) initiated Ca^{2+} oscillations in cells that had not been induced to oscillate by the Ca^{2+} wave alone (**Fig. 51 b**), 3) stopped the Ca^{2+} oscillations (**Fig. 51 c**), or 4) initiated Ca^{2+} oscillations in cells that were not reached by Ca^{2+} wave (**Fig. 51 d**). ACh most commonly increased the frequency of Ca^{2+}

Figure 50: The spatial distribution of cells displaying Ca^{2+} oscillations in response to a propagating intercellular Ca^{2+} wave alone (open squares, n = 35 experiments) and an intercellular Ca^{2+} wave with the addition of ACh (open circles, n = 9 experiments). Both data sets were fitted with Gaussian curve.

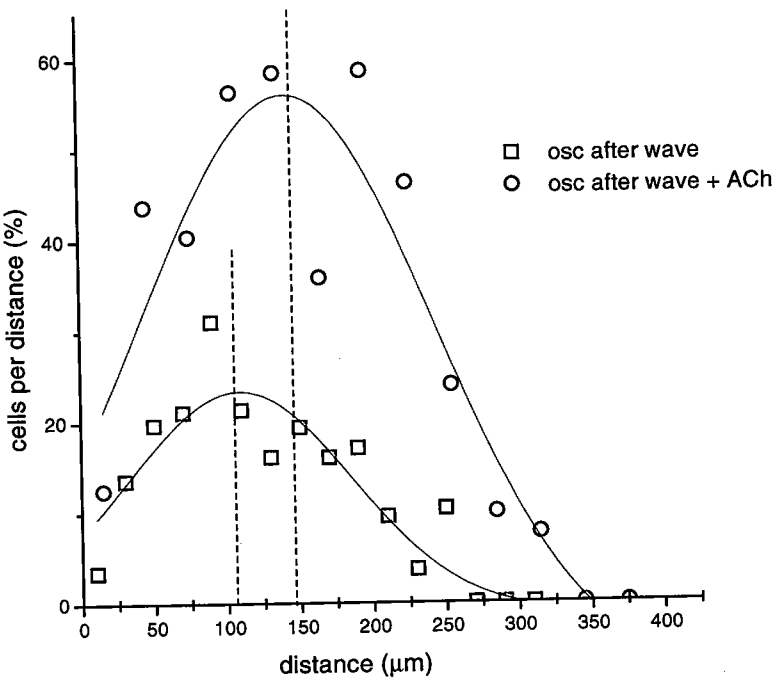
60
40
20
0
cells per distance (%)
0
50
100
150
200
250
300
350
400
distance (µm)
osc after wave
osc after wave + ACh

Figure 50

Figure 51: Acetylcholine modifies the patterns of Ca^{2+} oscillations induced by propagating intercellular Ca^{2+} waves. Each graph represents the variation in $[Ca^{2+}]_i$ with respect to time of a single cell in an 18-day old culture. The label "w" indicates intercellular Ca^{2+} wave and the bar labeled "ACh" indicates the addition of 400 μM ACh. Application of ACh after inducing an intercellular wave a) increases the frequency of the Ca^{2+} oscillations, b) initiates Ca^{2+} oscillations in cells that did not oscillate in response to a propagating Ca^{2+} wave, c) inhibits Ca^{2+} oscillations and d) stimulates Ca^{2+} oscillations in cells that had not propagated an intercellular Ca^{2+} wave.

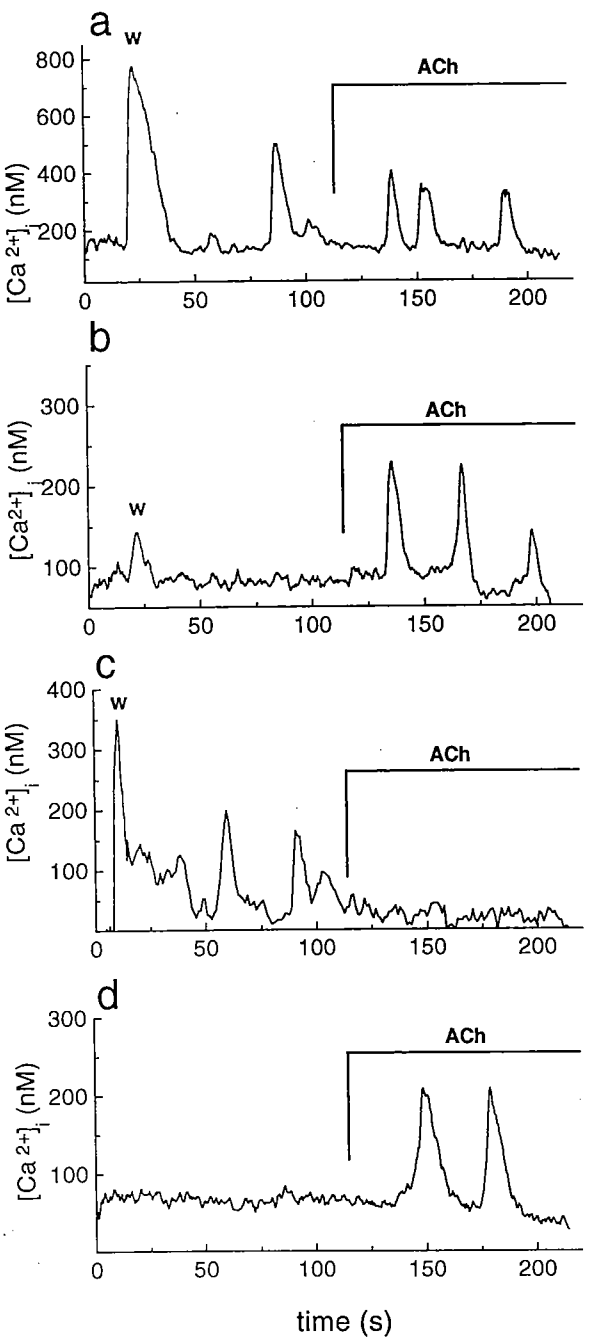
a
w
ACh
800
600
400
200
[Ca 2+]i (nM)
0
50
100
150
200
b
300
200
100
[Ca2+]i (nM)
w
ACh
c
400
300
200
100
[Ca 2+]i (nM)
w
ACh
d
300
200
100
[Ca 2+]i (nM)
ACh
time (s)

Figure 51

oscillations (8.6 cells per experiment) rather than initiated or stopped the Ca^{2+} oscillations (4.1 and 2.8 cells per experiment respectively, average of 9 experiments).

These ACh-induced modulations of Ca^{2+} oscillations occurred in cells at different distances from the Ca^{2+} wave origin. To account for the variability of mechanical stimuli between experiments, each experiment was analyzed such that the spatial distributions of different ACh-induced modulations were normalized with respect to the distribution of the most prominent group, i.e., the cells that in response to ACh increased the frequency of Ca^{2+} oscillations (**Fig. 52 a**). ACh stopped oscillations in cells closest to the Ca^{2+} wave origin (**Fig. 52 b**). More distally, ACh increased the frequency of the oscillations. The peak number of cells in this group were 105 μm away from the Ca^{2+} wave origin (**Fig. 52 a**). Cells furthest away from the intercellular Ca^{2+} wave origin were induced to oscillate by ACh (zone peak 160 μm from the Ca^{2+} wave origin, **Fig. 52 c**).

IV-9. Intracellular photorelease of IP_3 alters the oscillatory responses of glial cells to intercellular Ca^{2+} waves

The role of $[IP_3]_i$ in the induction of specific Ca^{2+} oscillations was further tested by a direct increase in the $[IP_3]_i$ of glia via intracellular photorelease of IP_3 from its photolabile carrier D-myo-inositol 1,4,5-trisphosphate, P4(5)-(1-(2-nitrophenyl)ethyl) ester trisodium salt (i.e., "caged IP_3"). In these experiments, Ca^{2+} waves were initiated by mechanical stimulation to propagate through the glial cultures loaded with caged IP_3 (200μM). 120 seconds after the initiation of an intercellular

Figure 52: The responses of cells to ACh after the propagation of an intercellular Ca^{2+} wave are dependent on the position of the cell relative to the wave origin. For comparison, the distribution profiles of responses from 9 experiments were aligned with respect to the mode of the spatial distribution of cells that increased the frequency of oscillations. The spatial distribution of cells that a) increased oscillatory frequency (open squares), b) stop oscillating (open circles) and c) initiated Ca^{2+} oscillations in response to ACh. Vertical line represents the averaged mode (105 ± 56 μm) of the distribution of cells that continued to oscillate. X axis represents the normalized distance, with value of 1 representing the averaged distance of cells that continued to oscillate from the origin of the intercellular Ca^{2+} wave.

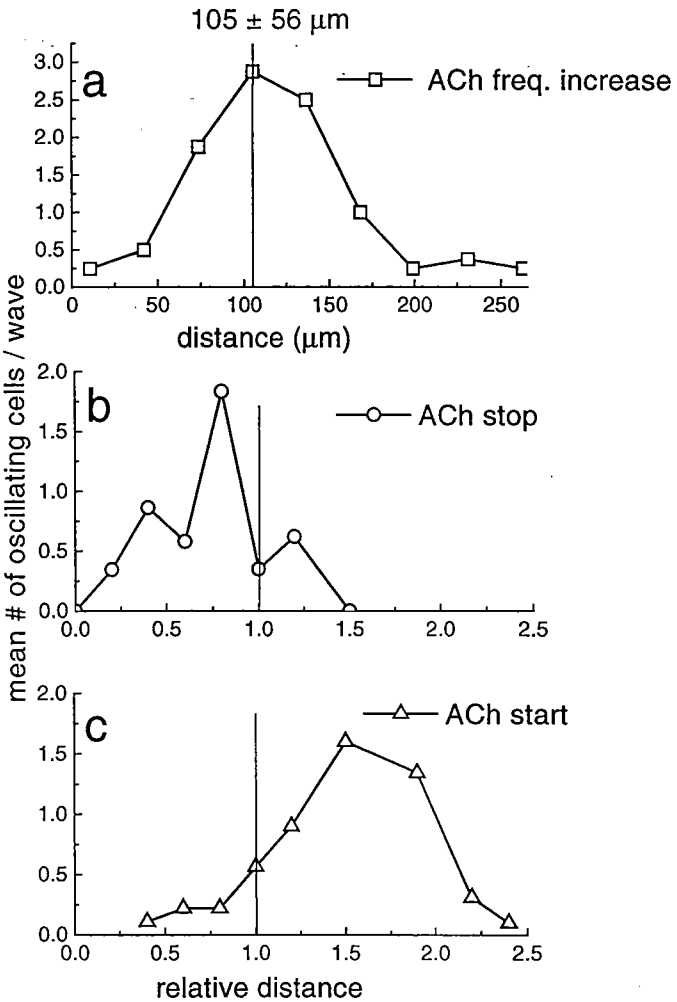
105 ± 56 µm
a
ACh freq. increase
distance (µm)
b
ACh stop
mean # of oscillating cells / wave
c
ACh start
relative distance

Figure 52

Ca^{2+} wave, a simultaneous photorelease of IP_3 within all the cells in the field of view was achieved by exposing the culture to a UV flash. Following the photorelease of IP_3, the changes in the oscillatory behavior were analyzed. Ca^{2+} oscillations within individual glial cells either a) ceased to oscillate (**Fig. 53 a**), b) increased their oscillatory frequency (**Fig. 53 b**), c) were initiated in cells that did not oscillate following a propagation of a Ca^{2+} wave (**Fig. 53 c**), and d) were initiated in cells that were not on the Ca^{2+} wave path (**Fig. 53 d**). IP_3 release-induced modulations of Ca^{2+} oscillations also occurred in cells at different distances from the Ca^{2+} wave origin. Cells showing Ca^{2+} oscillations that were closest to the origin of intercellular Ca^{2+} waves stopped oscillating in response to IP_3 release (76 μm ± 51, n = 39 cells, 9 experiments). Cells that increased oscillatory frequency were positioned further away from the Ca^{2+} wave origin (143 μm ± 57, n= 61 cells, 9 experiments). Finally, cells that propagated a Ca^{2+} wave, but started to oscillate only in response to the photorelease of IP_3 were furthest away from the Ca^{2+} wave origin (203 μm ± 69, n=70 cells, 9 experiments) (**Fig. 54**).

These experiments demonstrated that a direct increase of $[IP_3]_i$ shifts the zone of Ca^{2+} wave-induced Ca^{2+} oscillations further away from the origin of the wave.

Figure 53: Intracellular release of IP_3 from its photolabile carrier modifies the patterns of Ca^{2+} oscillations induced by propagating intercellular Ca^{2+} waves. Each graph represents the variation in $[Ca^{2+}]_i$ with respect to time of a single cell in an 16-day old culture. The variation in $[Ca^{2+}]_i$ is presented as (Ft-F0)/F0, where F0 is fluorescence intensity of fluo-3 at 0 seconds and Ft is fluorescence intensity of fluo-3 at a time t. The label "w" indicates intercellular Ca^{2+} wave and the vertical arrow indicates the flash of UV light that releases IP_3. The distance of the oscillating cell from the origin of intercellular Ca^{2+} wave is shown in the right top corner of each graph.

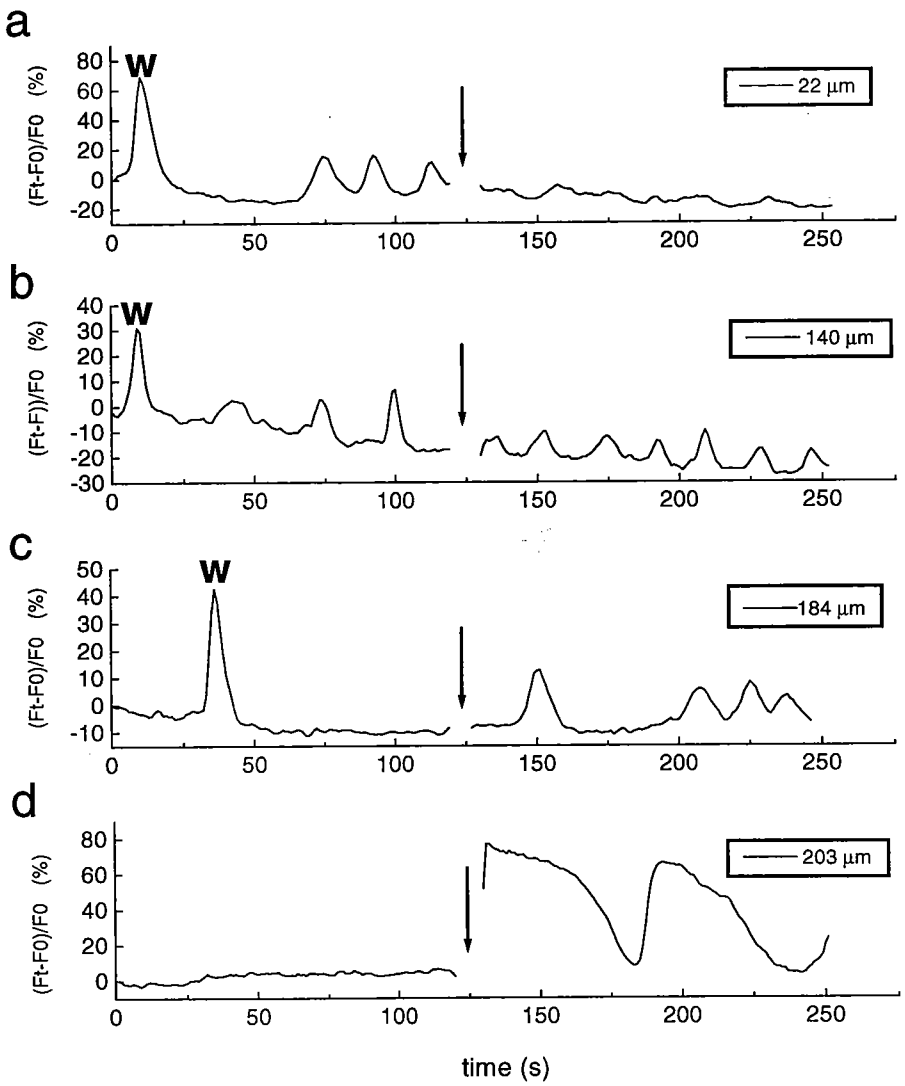

Figure 53

Figure 54: The responses of cells to intracellular release of IP_3 after the propagation of an intercellular Ca^{2+} wave are dependent on the position of the cell relative to the wave origin. The distances of cells that: started to oscillate, increased the frequency of oscillations, and stopped Ca^{2+} oscillations were measured, and the mean values of these measurements compared. Closest to the Ca^{2+} wave origin cells stopped oscillating (n = 39 cells), further away, cells increased the frequency of oscillations (n= 61 cells) while the zone of cells that started to oscillate in response to $[IP_3]_i$ increase was the furthest away from the origin of the Ca^{2+} wave (n = 70 cells). Squares represent the means, while horizontal lines represent standard deviations; n = 9 experiments. X axis represents distance from the origin of the intercellular Ca^{2+} wave.

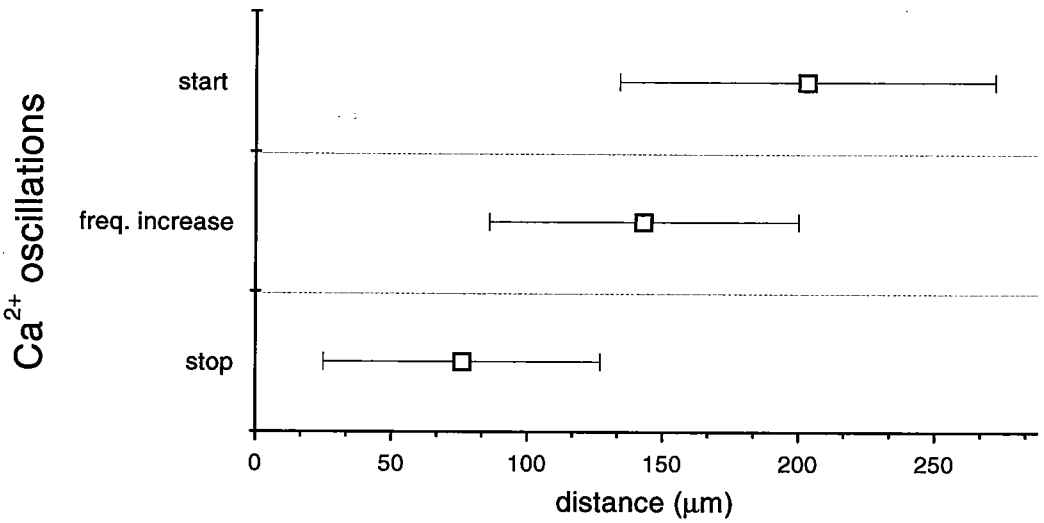
Ca2+ oscillations
start
freq. increase
stop
0
50
100
150
200
250
distance (µm)

Figure 54

Comparisons of the spatial distribution of cells displaying Ca^{2+} oscillations in response to a Ca^{2+} wave (**Fig. 55 a**), a Ca^{2+} wave followed by exposure to ACh (**Fig. 55 b**), and a Ca^{2+} wave followed by intracellular release of IP_3 (**Fig. 55 c**), showed that both exposure to ACh and release of IP_3 shifted the zone of oscillating cells further away from the origin of Ca^{2+} wave (**Fig. 55 d**).

Collectively, these results suggest that the initiation and characteristics of Ca^{2+} wave-induced Ca^{2+} oscillations strongly depend on a specific range of $[IP_3]_i$.

IV-10. The effects of $[Ca^{2+}]_i$ on intracellular Ca^{2+} oscillations

To test whether a specific increase in $[Ca^{2+}]_i$ causes the expression of the specific type of oscillations, a correlation analysis was carried out. The magnitude of the increase in $[Ca^{2+}]_i$ associated with the Ca^{2+} oscillations was found to be linearly correlated with the increase in $[Ca^{2+}]_i$ associated with intercellular Ca^{2+} wave (**Fig. 56 a**). One explanation of this result is the dependence of the magnitude of both types of Ca^{2+} signals on the capacity of a cell's intracellular Ca^{2+} store and CICR mechanism. On the other hand, no correlation between the increase in $[Ca^{2+}]_i$ during propagation of intercellular Ca^{2+} wave and the major defining parameter of different oscillatory behaviors, i.e., the onset time of Ca^{2+} oscillations was found (**Fig. 56 b**). This suggested that the increase in $[Ca^{2+}]_i$ does not induce specific types of Ca^{2+} oscillations.

Figure 55: The spatial distribution of cells displaying Ca^{2+} oscillations in response to: a) a propagating intercellular Ca^{2+} wave alone (black bars, n = 35 experiments), b) intercellular Ca^{2+} wave with the addition of ACh (stripped bars, n = 9 experiments), and c) intercellular Ca^{2+} wave that was followed by photorelease of IP_3 (gray bars, n = 6 experiments). d) Distributions of oscillations for different data sets were fitted with Gaussian curves.

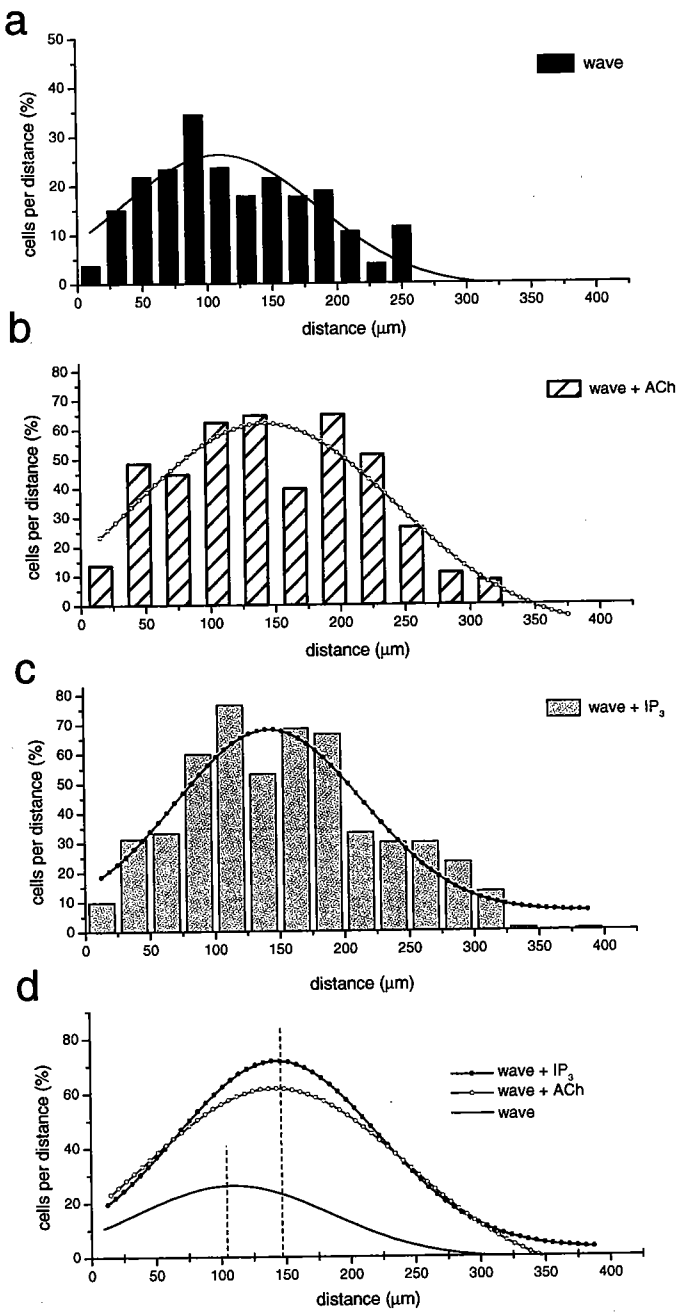
a
wave
cells per distance (%)
distance (µm)
b
wave + ACh
cells per distance (%)
distance (µm)
c
wave + IP3
cells per distance (%)
distance (µm)
d
wave + IP3
wave + ACh
wave
cells per distance (%)
distance (µm)

Figure 55

Figure 56: The relationship between the increase in $[Ca^{2+}]_i$ associated with the intercellular Ca^{2+} wave and properties of Ca^{2+} oscillations. Correlation analysis between $[Ca^{2+}]_i$ during wave propagation and a) the increase in $[Ca^{2+}]_i$ and b) the onset of Ca^{2+} oscillations. A significant correlation ($p < 0.0001$) was found between the magnitudes of the increases in $[Ca^{2+}]_i$ of each response, but not between the $[Ca^{2+}]_i$ associated with Ca^{2+} wave and the onset time of Ca^{2+} oscillations ($p > 0.05$).

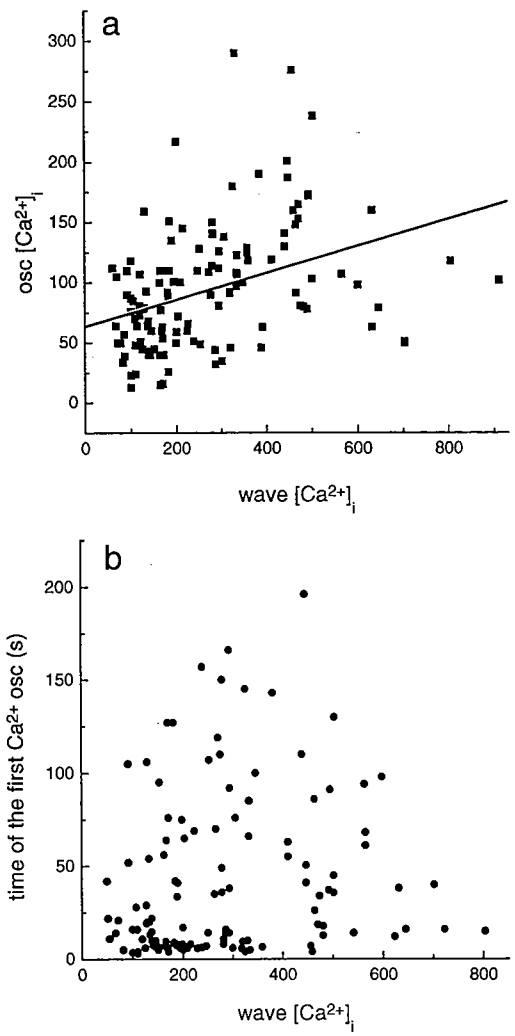
a
300
250
200
150
100
50
0
osc [Ca2+]i
0
200
400
600
800
wave [Ca2+]i
b
200
150
100
50
0
time of the first Ca2+ osc (s)
0
200
400
600
800
wave [Ca2+]i

Figure 56

It is important to emphasize that different oscillatory types did not significantly vary in the magnitude of $[Ca^{2+}]_i$ elevations, and the magnitude of $[Ca^{2+}]_i$ increase was not one of the defining parameters of the different oscillatory types in glia (**Table 3**).

An increase in $[Ca^{2+}]_i$ achieved by photorelease of Ca^{2+} did not induce intracellular Ca^{2+} oscillations demonstrating that Ca^{2+} oscillations are not initiated via release of Ca^{2+} through RyRs. These experiments suggest that increases in $[Ca^{2+}]_i$ do not initiate specific oscillatory activity in glia and reinforce the dependence of the induction of specific Ca^{2+} oscillations on $[IP_3]_i$ and release of Ca^{2+} through intracellular IP_3Rs.

IV-11. Mathematical model simulations support passive IP_3 diffusion as the common mechanism of Ca^{2+} waves and Ca^{2+} oscillations

In order to quantitatively evaluate the IP_3 diffusion hypothesis as the predominant mechanism for the generation of Ca^{2+} signals in glia, a mathematical model that simulates Ca^{2+} wave propagation via passive diffusion of IP_3 was tested (Sneyd et al., 1995; Sneyd et al., 1998). This model correctly predicted the experimental Ca^{2+} wave parameters of arrival time and intercellular delay as well as the peak $[Ca^{2+}]_i$ achieved. The model assumes that: a) mechanical stimulation initiates the production of IP_3 only in the stimulated cell and that this IP_3 diffuses from cell to cell; b) the diffusion of IP_3 and Ca^{2+} between two cells is proportional to their concentration difference across the adjacent cell membranes; c) the Ca^{2+} release via IP_3Rs is dependent on the $[Ca^{2+}]_i$; d) IP_3 is degraded with saturable kinetics, and the Ca^{2+} released from the ER is pumped either back into the

ER or out of the cell.

To simulate a mechanical stimulation, IP_3 was added at a rate of 1 μMs^{-1} to the first simulated cell in mathematical model. Solving model equations for $[IP_3]_i$ and $[Ca^{2+}]_i$ dynamics revealed that intracellular Ca^{2+} oscillations exist only when $[IP_3]_i$ is between 0.06 and 0.18 μM. Thus, an intercellular Ca^{2+} wave generated by the diffusion of IP_3 would evoke Ca^{2+} oscillations only in a zone of cells at a specific diffusion distance from the stimulated cell, just as was demonstrated in the experimental data. To evaluate the role of intercellular Ca^{2+} diffusion on the Ca^{2+} waves and oscillations, simulations were performed with different intercellular Ca^{2+} permeability values. As Ca^{2+} permeability increased, the synchronization of the simulated Ca^{2+} oscillations within different simulation cells was achieved. Only the low values for the intercellular Ca^{2+} permeability (1 μms^{-1}, 0.1μms^{-1}) however, agreed with experimentally observed asynchronous oscillations in glia and the inability of experimental increases in $[Ca^{2+}]_i$ to evoke intercellular Ca^{2+} waves. Furthermore, the IP_3 passive diffusion model successfully predicted spatial organization of different oscillatory types. The model also predicted that the addition of 0.3 μM $[IP_3]_i$ uniformly across the culture after mechanical stimulation changes the oscillatory behavior of glial cells in a manner demonstrated by the global addition of ACh and IP_3 uncaging.

In conclusion, the mathematical model of IP_3 passive diffusion accurately predicted spatial organization of oscillatory types, the modulation of this organization by an increase in $[IP_3]_i$, and estimated the diffusion parameters of Ca^{2+} and minimal increase in $[IP_3]_i$ necessary for experimentally observed oscillatory modulations.

IV-12. The orientations of intra- and intercellular Ca^{2+} waves are independent

To determine if the spatial characteristics of the intracellular Ca^{2+} waves associated with each Ca^{2+} oscillation were dependent on the orientation of the intercellular Ca^{2+} waves that induced oscillations, the temporal-spatial changes of $[Ca^{2+}]_i$ within single cells during and after the passage of two intercellular Ca^{2+} waves were analyzed (**Fig. 57**). Of particular interest was determining whether Ca^{2+} waves propagating in different directions may alter the intracellular origin and orientation of Ca^{2+} oscillations. In these experiments, 88 % of the intracellular Ca^{2+} oscillations were found to be initiated repeatedly from the same intracellular site and propagated in the same direction across the cell, regardless of the orientation of the two intercellular Ca^{2+} waves (**Fig. 57**). In addition, the Ca^{2+} oscillations continued to occur with a similar frequency and spatial orientation when an extracellular perfusion of fluid was applied after the propagation of one Ca^{2+} wave.

To control for the possibility that Ca^{2+} waves established an intracellular site to serve as the origin for the subsequent Ca^{2+} oscillations, the origin and orientation of the Ca^{2+} oscillations were compared with the entry point and orientation of the first and the second intercellular Ca^{2+} wave. No correlation was found between the orientation and origin of the first ($\chi^2 = 2.3$, $p > 0.05$, $n = 55$) or second ($\chi^2 = 2.1$, $p > 0.05$) intercellular Ca^{2+} waves and the orientation of the subsequent intracellular Ca^{2+} oscillations. Similarly, the origin and orientation of intracellular Ca^{2+} waves associated with spontaneous Ca^{2+}

oscillations were unchanged by the propagation of intercellular Ca^{2+} waves. For 74% of cells analyzed, the addition of neurotransmitter ACh did not change the origin or the orientation of intracellular Ca^{2+} waves associated with either spontaneous or intercellular wave-induced Ca^{2+} oscillations. These results suggested that Ca^{2+} oscillations are driven by a different messenger than the intercellular Ca^{2+} waves. Furthermore, the origin and orientation of the intracellular Ca^{2+} waves were consistent for each cell but random between cells, probably reflecting a unique distribution of intracellular calcium stores and store-forming proteins.

Figure 57: A comparison of the orientation of the propagating intercellular Ca^{2+} waves and the intracellular Ca^{2+} waves associated with Ca^{2+} oscillations. All images are from the same cell (dotted line). a) The first propagating intercellular Ca^{2+} wave (long arrow) and b) a subsequent intracellular Ca^{2+} wave associated with the induced Ca^{2+} oscillation (short arrow). c) The second propagating intercellular Ca^{2+} wave (long arrow) and d) a subsequent intracellular Ca^{2+} wave associated with the induced Ca^{2+} oscillation (short arrow). Note that the intracellular Ca^{2+} waves associated with the Ca^{2+} oscillations have the same origin and orientation irrespective of the orientation of the inducing intercellular Ca^{2+} waves. The acquisition times are indicated below each image. Color calibration bar indicates changes in $[Ca^{2+}]_i$.

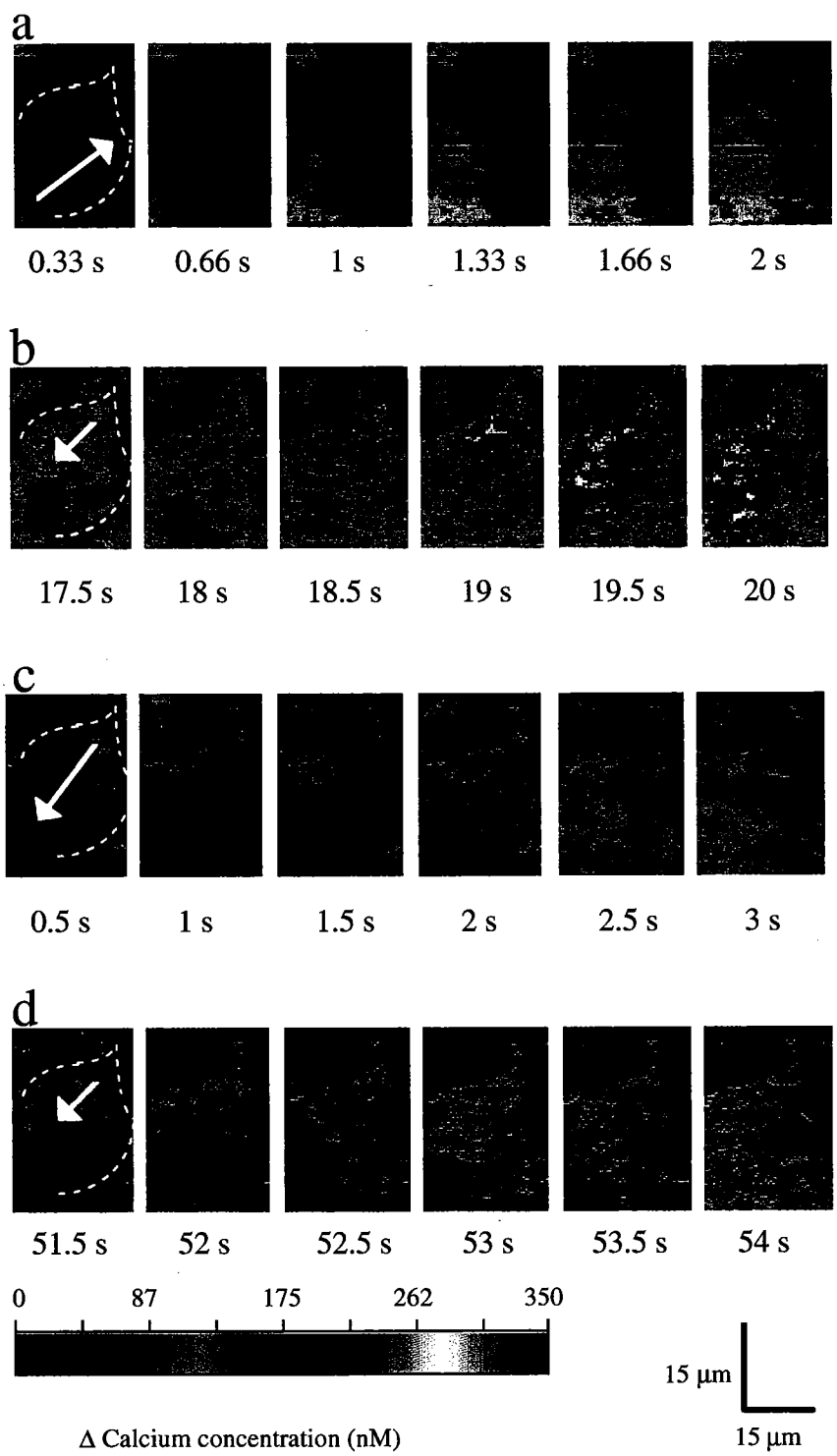
a
0.33 s
0.66 s
1 s
1.33 s
1.66 s
2 s
b
17.5 s
18 s
18.5 s
19 s
19.5 s
20 s
c
0.5 s
1 s
1.5 s
2 s
2.5 s
3 s
d
51.5 s
52 s
52.5 s
53 s
53.5 s
54 s
0
87
175
262
350
Δ Calcium concentration (nM)
15 µm
15 µm

Figure 57

IV-13. Discussion of the Specific Aim 2

The studies of Specific Aim 2 demonstrate that mechanically-induced intercellular Ca^{2+} waves initiate specific intracellular Ca^{2+} oscillations. The results indicate that a common link, increase in $[IP_3]_i$, exists between the propagation of intercellular Ca^{2+} waves and initiation of intracellular Ca^{2+} oscillations.

Previous studies hypothesized that mechanically-induced intercellular Ca^{2+} waves in glia are mediated by the diffusion of IP_3 through the gap junctions (Charles et al., 1991; Charles et al., 1992; Finkbeiner, 1992; Giaume and Venance, 1998; Leybaert et al., 1998; Newman and Zahs, 1997). This hypothesis was further supported by the results of Specific Aim 1 that demonstrated that Ca^{2+} wave initiation and propagation require PLC activation, generation of IP_3, gap junction-mediated diffusion of IP_3 to neighboring cells, binding of IP_3 to IP_3Rs, and release of Ca^{2+} from intracellular calcium stores.

The appearance of Ca^{2+} oscillations in glia depends on agonist concentration: glia stimulated with low doses of metabotropic agonists, glutamate, histamine, norepinephrine and endothelin respond with single rise in $[Ca^{2+}]_i$, moderate doses lead to Ca^{2+} oscillation, and high doses of these agonists result in a plateau $[Ca^{2+}]_i$ increase (Cornell-Bell and Finkbeiner, 1991; Fukui et al., 1991; Goldman et al., 1991; Salm and McCarthy, 1990). Agonists initiate Ca^{2+} oscillations by increasing $[IP_3]_i$ that promotes cycles of CICR via IP_3Rs followed by the re-uptake of Ca^{2+} into the ER (Bezprozvanny et al., 1991; Iino and

Endo, 1992; Pozzan et al., 1994; Verkhratsky and Kettenmann, 1996). The temporal properties of Ca^{2+} oscillations, i.e., the initiation time and periodicity, are dependent on $[IP_3]_i$ (Berridge, 1993; Berridge, 1993; Berridge and Dupont, 1994).

The experiments of Specific Aim 2 support the concept that an $[IP_3]_i$ gradient formed within the cell population is responsible for both intercellular Ca^{2+} wave propagation and Ca^{2+} oscillations. Unfortunately, this intercellular $[IP_3]_i$ gradient cannot be directly visualized by current imaging technologies. Similarly, the $[Ca^{2+}]_i$ cannot be used as an indicator of $[IP_3]_i$ because, in the presence of variable amounts of IP_3, the IP_3Rs release Ca^{2+} until a specific inhibitory $[Ca^{2+}]_i$ has been reached (Iino and Endo, 1992; Kaftan et al., 1997). Due to the dependence of Ca^{2+} oscillations on the $[IP_3]_i$ however, a gradient of $[IP_3]_i$ may be represented in a population of cells by the spatial distribution of specific Ca^{2+} oscillations.

IV-13.i. Ca^{2+} waves induce temporally and spatially specific Ca^{2+} oscillations.

Ca^{2+} oscillations induced by a Ca^{2+} wave occurred predominantly in cells in a zone 60-120 μm from the wave origin. Based on the analysis of oscillations for their onset time, periodicity, and duration during the finite experimental time interval, Ca^{2+} oscillations were classified into four types: spike, continuous, brief and recovered. A similar classification of different oscillatory behaviors was also reported by Cornell-Bell et al. (1990). In response to glutamate, astrocytes showed continuous, decreasing frequency, and damped Ca^{2+} oscillations. These oscillations are similar to continuous, brief, and spike oscillations

observed after Ca^{2+} wave propagation. The difference in duration between mechanically- and glutamate-stimulated oscillations probably reflects the duration of stimulation: glutamate exposure is a prolonged stimulus whereas Ca^{2+} wave is a transient stimulus.

In this study, the various types of Ca^{2+} oscillations had different spatial distributions and occurred in approximately concentric zones around the cell of wave origin. Cells that were close to, or a long distance from, the wave origin (with predictably either too high, or too low $[IP_3]_i$, respectively) did not display Ca^{2+} oscillations. This spatial sequence of inhibition, specific type initiation, and inability to display Ca^{2+} oscillation, reflects the specific oscillatory behavior-$[IP_3]_i$ relationship (Berridge, 1997; Berridge and Dupont, 1994) that was recently modeled (Sneyd et al., 1995a; Sneyd et al., 1998).

IV-13.ii. An intercellular $[IP_3]_i$ gradient initiates Ca^{2+} oscillations.

The suggestion that the distribution of Ca^{2+} oscillations depends on an $[IP_3]_i$ gradient is further emphasized by the conversion or modulation of the Ca^{2+} oscillations displayed by cells responding to two different Ca^{2+} waves. When a cell experienced a second Ca^{2+} wave that originated from a site that was, on average more than 60 μm further from the origin of the first Ca^{2+} wave, the cell displayed a different type of oscillatory behavior. If the difference in distance between the two waves was about 30 μ m, the cell modulated only the oscillatory frequency. This effect was not due to the difference in the strength of stimuli or a change in sensitivity of the cells, because the

spatial distribution of the induced oscillations was highly reproducible after each Ca^{2+} wave, and cells responded to Ca^{2+} waves initiated from the same place with identical Ca^{2+} oscillations. Finally, the presence of different oscillatory types and their spatial distribution were not related to the different cell types, since all glial types were uniformly distributed throughout the culture, and capable of displaying all types of Ca^{2+} oscillations. Glial Ca^{2+} oscillations behaved as highly plastic signals that change depending on the different propagation distances of intercellular Ca^{2+} waves. A similar plasticity of glial Ca^{2+} oscillations was observed by (Pasti et al., 1997).

The hypothesis that the spatial distribution of the Ca^{2+} wave-induced Ca^{2+} oscillations depends on a gradient of $[IP_3]_i$ was tested by the elevation of the $[IP_3]_i$ in all cells by the extracellular application of ACh or by the intracellular photorelease of IP_3.

ACh was used since ACh binding to muscarinic receptors induces PLC activation and IP_3 production in both astrocytes and oligodendrocytes (Cohen and Almazan, 1994; Cohen et al., 1996; Pearce et al., 1985; Pearce et al., 1986). This effect was confirmed by the inhibition of MR-induced Ca^{2+} oscillations by PLC inhibitors and heparin. Although PLC inhibitors predominantly inhibited MR-induced oscillations, in a subset of cells that were characterized by a robust response to MR-stimuli, PLC inhibitors did not abolish Ca^{2+} oscillations, but instead decreased the oscillation frequency. This may be explained by each cell having a slightly different sensitivity to the agonist, a different number of metabotropic receptors, or different number of IP_3Rs associated with intracellular Ca^{2+} stores. A variability in the number of surface receptors has been demonstrated in astrocytes for alpha1-adrenergic and muscarinic receptors (Venance et al., 1998).

ACh displaced the zone of oscillating cells away from the Ca^{2+} wave origin by inducing changes in the oscillatory behavior of individual cells. In response to ACh, Ca^{2+} oscillations were terminated in cells closer to the wave origin, increased in frequency in cells in the central part of the zone, and were initiated at the distal end of the zone. All three responses are compatible with an increase in $[IP_3]_i$ that offsets the gradient established by a Ca^{2+} wave. The assumption that ACh increased $[IP_3]_i$ approximately uniformly throughout the culture is strongly supported by the initiation of Ca^{2+} oscillations on the outer edge of the zone and by the fact ACh initiated oscillations in glial cells that were not involved in propagating a Ca^{2+} wave.

A similar offset of the wave-generated $[IP_3]_i$ gradient was also achieved by photorelease of IP_3. This direct increase in $[IP_3]_i$ caused a cessation of oscillations closest to the wave origin, increased oscillatory frequency in cells further away from the wave origin, and initiated oscillations in cells that were furthest from the wave origin. The assumption that the photorelease of IP_3 resulted in approximately uniform increase of $[IP_3]_i$ throughout the culture is strongly supported by the fact that uncaging initiated oscillations in glial cells that were not involved in propagating a Ca^{2+} wave.

The spatial distribution of specific changes in oscillatory behavior induced by photolysis of IP_3 was slightly different from that induced by ACh. First, when different types of responses to IP_3 were analyzed, the group of cells that showed increased oscillatory frequency was 38 μm further away from the wave origin than the peak of the same group in ACh experiments. Also, in contrast to the ACh application, the photorelease of IP_3 predominantly induced Ca^{2+} oscillations in cells that did not oscillate in

response to a Ca^{2+} wave making the zone of cells with this response the widest of the three response zones. Although both ACh application and the uncaging of IP_3 increased the total number of oscillating cells, the uncaging of IP_3 was more efficient. These results suggest that the photolysis of IP_3 was more effective in increasing $[IP_3]_i$ when compared to ACh application. The analysis of the spatial distribution of Ca^{2+} oscillations revealed that ACh and photorelease of IP_3 shifted the zone of oscillating cells by a comparable distance. Thus, $[IP_3]_i$ increases achieved by ACh or photorelease of IP_3 demonstrated that Ca^{2+} oscillations are initiated by an interval of $[IP_3]_i$ and support hypothesis that propagation of intercellular Ca^{2+} wave generates an intercellular gradient of $[IP_3]_i$, and consequently an oscillation-inducing $[IP_3]_i$ interval at the specific distance from the Ca^{2+} wave origin.

IV-13.iii. The role of $[Ca^{2+}]_i$ and RyRs in Ca^{2+} oscillations.

Ryanodine receptors (RyRs) respond to increases of $[Ca^{2+}]_i$ by CICR mechanism, and might contribute to initiation or maintenance of Ca^{2+} oscillations. For example, although the release of Ca^{2+} through IP_3Rs is necessary for the initiation of ACh-induced Ca^{2+} oscillations, Ca^{2+} release through RyRs sustains Ca^{2+} oscillations in tracheal smooth muscle cells (Kannan et al., 1997). In some non-excitable cells, reuptake rate of Ca^{2+} by intracellular Ca^{2+} pumps determines Ca^{2+} oscillatory frequency by regulating the level of free cytosolic Ca^{2+} that initiates CICR (Petersen et al., 1993; Pozzan et al., 1994). An increase in $[Ca^{2+}]_i$ however, does not seem to induce Ca^{2+} oscillations in glia. First, the

photorelease of Ca^{2+} does not induce Ca^{2+} oscillations. Second, there was no correlation between the magnitude of $[Ca^{2+}]_i$ of an intercellular Ca^{2+} wave and the onset time of the Ca^{2+} oscillations, indicating the lack of a specific oscillatory behavior-$[Ca^{2+}]_i$ relationship. These findings suggest that increases in $[Ca^{2+}]_i$ during Ca^{2+} wave propagation do not induce Ca^{2+} oscillations. These findings however, do not exclude the possibility that CICR through RyRs occurs during glial oscillatory activity, secondary to the release of Ca^{2+} from IP_3-sensitive Ca^{2+} stores.

IV-13.iv. Necessary and sufficient requirements for initiation and maintenance of Ca^{2+} oscillations

This study demonstrated that Ca^{2+} oscillations are initiated by the elevation of $[IP_3]_i$ achieved by propagation of an intercellular Ca^{2+} wave. A specific range of $[IP_3]_i$ was necessary and sufficient for initiation of Ca^{2+} oscillations, as demonstrated by Ca^{2+} oscillations which occurred only within a narrow zone at a particular distance from the origin of intercellular Ca^{2+} waves. Furthermore, the hypothesis that a specific range of $[IP_3]_i$ is a necessary factor for initiation of Ca^{2+} oscillations was supported by the findings that increasing the concentrations of neurotransmitters that induce IP_3 production, i.e., ACh, AMCh, and ATP, result in a) single $[Ca^{2+}]_i$ elevation for lower agonist concentrations, b) Ca^{2+} oscillations in response to intermediate concentrations, and c) sustained, slowly recovering $[Ca^{2+}]_i$ elevation for high agonist concentrations. Similar $[Ca^{2+}]_i$ responses of glia to increasing glutamate concentrations was also reported by Cornell-Bell et al. (1990). Furthermore, the same sequence of inability to oscillate, Ca^{2+}

oscillations, and sustained $[Ca^{2+}]_i$ increase was observed for increasing levels of photoreleased IP_3 (data not shown). On the other hand, increasing levels of photoreleased Ca^{2+} alone were not sufficient to initiate Ca^{2+} oscillations.

Furthermore, a specific $[IP_3]_i$ was a sufficient and necessary element in the initiation of different types of Ca^{2+} oscillations, since altering $[IP_3]_i$ by ACh, photorelease of IP_3, or distance from the origin of Ca^{2+} wave were all sufficient in altering the type of oscillatory behavior. On the other hand, the level of $[Ca^{2+}]_i$ elevation in cells that propagated Ca^{2+} wave did not determine the type of oscillatory activity, as demonstrated by the correlation analysis.

This study supports the hypothesis that Ca^{2+} oscillations are maintained by calcium induced calcium release via IP_3Rs, a process during which Ca^{2+} released initially via IP_3-bound IP_3Rs acts as a co-agonist of Ca^{2+} release, while high $[Ca^{2+}]_i$ (i.e., concentrations achieved at the peak of a single oscillatory elevation) inhibit further Ca^{2+} release via IP_3Rs, thus causing $[Ca^{2+}]_i$ to return to the baseline (Bezprozvanny, 1991; 1995; Berridge, 1993). The hypothesis that Ca^{2+} oscillations are maintained by CICR is supported by finding that Ca^{2+} oscillations spread through single cells in orientation independent of the orientation of Ca^{2+} wave propagation, and consequently, independent of the $[IP_3]_i$ gradient established by intercellular Ca^{2+} wave. Furthermore, the origin and propagation direction of intracellular Ca^{2+} oscillations did not change upon the propagation of second intercellular Ca^{2+} wave that had a different propagation direction. Ca^{2+}-mediated intracellular propagation of individual Ca^{2+} oscillations is supported by the finding that oscillations were initiated repeatedly from a single, intracellular site of origin. Interestingly, Sheppard

et al. (1997) correlated the intracellular origin of Ca^{2+} oscillations with clusters of IP_3Rs within glial ER, sites with increased sensitivity to CICR mechanism.

IV-13.v. The spatial organization of Ca^{2+} oscillations.

While the passage of an intercellular Ca^{2+} wave initiated Ca^{2+} oscillations, the propagation direction of the subsequent intracellular Ca^{2+} waves associated with each oscillation was totally independent of the spatial properties of the initial intercellular Ca^{2+} wave. This behavior suggests that the oscillation-associated intracellular Ca^{2+} waves are propagated by a separate messenger other than the $[IP_3]_i$ gradient, since oscillations do not propagate in the radial direction of the IP_3 diffusion as do intercellular Ca^{2+} waves. Intracellular Ca^{2+} waves associated with each oscillation were also not propagated by extracellular IP_3-producing messenger, since Ca^{2+} oscillations continue undisturbed by extracellular perfusion. Furthermore, the origin and propagation direction of intracellular Ca^{2+} oscillations did not change upon the propagation of second intercellular Ca^{2+} wave that had different propagation direction. Therefore, these results are compatible with the idea that Ca^{2+} diffusion and CICR through sensitized IP_3 receptors is the dominant mechanism of propagation for oscillation-associated intracellular Ca^{2+} waves. Ca^{2+} waves predominantly activated intracellular Ca^{2+} oscillations repeatedly from a single, intracellular site of origin, a finding consistent with the report of Yagodin et al. (Yagodin et al., 1994), that may be explained by the unique distribution and clustering of intracellular Ca^{2+} stores and stores-constituting proteins within individual cells

(Bourguignon et al., 1993; Pozzan et al., 1994). Still, these experiments do not exclude the existence of multiple intracellular pacemakers suggested by Inagaki et al. (Inagaki and Wada, 1994) that may be, due to their unique ratio of intracellular Ca^{2+} channels, Ca^{2+} buffer molecules and Ca^{2+} pumps, sensitive to a specific range of $[IP_3]_i$ and $[Ca^{2+}]_i$. An increasing number of studies in glia and other cell types suggests that the specific intracellular position of increases in $[Ca^{2+}]_i$ determines the specificity of a Ca^{2+} signal, since it permits Ca^{2+} to interact with Ca^{2+}-sensitive proteins located in a particular subcellular zone (Finkbeiner and Greenberg, 1997; Inagaki et al., 1997; Yagodin et al., 1995). Finally, the difference in the capacity of Ca^{2+} stores between cells may explain the correlation observed between the increases in $[Ca^{2+}]_i$ seen in the intercellular Ca^{2+} wave and the subsequent intracellular Ca^{2+} oscillations.

IV-13.vi. Relevance.

In view of these findings, it may be proposed that a glial syncytium utilizes specific intracellular Ca^{2+} oscillations to encode spatio-temporal information reflecting the position and strength of a stimulus that induces intercellular Ca^{2+} waves. A recent advance in the understanding of how cells decode specific intracellular Ca^{2+} oscillations was achieved by De Koninck and Shulman (1998) who found that the activation kinetics of CaM kinase depends on pulse duration and oscillatory frequency of Ca^{2+} spikes (De Koninck and Schulman, 1998). The amplitude and duration of calcium signals were shown to control differential activation of the pro-inflammatory transcriptional regulators in B lymphocytes

(Dolmetsch et al., 1997). Oscillating calcium signals may also be decoded by mitochondria that can sense and integrate Ca^{2+} oscillations by Ca^{2+} uptake (Hajnoczky et al., 1995). Finally, cellular output response may also retain the oscillatory behavior of initial Ca^{2+} oscillations, similar to pituitary cell secretory rates in response to hormone-induced oscillations (Tse et al., 1993). Future studies are expected to bring a further understanding of how specific glial cell types decode intracellular Ca^{2+} oscillations. It will be of tremendous importance to determine how downstream effectors in glia decode information contained in the amplitude and duration of Ca^{2+} signals, and thus reveal the mechanisms by which a multifunctional second messenger such as Ca^{2+} achieves specificity in signaling to the cell infrastructure and nucleus.

IV-14. Conclusions of the Specific Aim 2

Experimental results of the Specific Aim 2 show that intracellular Ca^{2+} waves induce intracellular Ca^{2+} oscillations predominantly within a zone of cells 60-120 μm away from the origin of the Ca^{2+} wave. Within the zone of oscillating cells four different oscillatory behaviors can be observed, and these occur at specific distances from the Ca^{2+} wave origin. Different glial cell types have the same potential to oscillate after Ca^{2+} wave propagation, and express, to the same extent, all four types of oscillatory behavior. Therefore, the clustering of oscillations within a zone of cells and different oscillatory types observed within the oscillatory zone, suggests that the specific oscillatory activity of

a cell is dependent on the position of a cell in relation to the origin of the Ca^{2+} wave. This idea is supported by the finding that oscillatory behavior can be altered following the propagation of Ca^{2+} waves which originate from different distances to reach the oscillating cell.

The hypothesis that intercellular Ca^{2+} waves induce Ca^{2+} oscillations by generating an intercellular gradient of $[IP_3]_i$ is supported by the finding that both ACh-induced and photorelease-induced increases in $[IP_3]_i$ were able to shift the zone of oscillating cells further away from the origin of the mechanically-induced Ca^{2+} wave. On the other hand, the magnitude of a Ca^{2+} wave did not correlate with the onset time of Ca^{2+} oscillations and intracellular photorelease of Ca^{2+} did not initiate Ca^{2+} oscillations. Therefore, Ca^{2+} wave-induced Ca^{2+} oscillations are generated by a specific, oscillation-inducing range of $[IP_3]_i$ that is generated in a population of glial cells during Ca^{2+} wave propagation.

The origin and orientation of intracellular Ca^{2+} waves associated with Ca^{2+} oscillations are independent of the spatial properties of the intercellular Ca^{2+} wave. This finding suggests that oscillation-associated intracellular Ca^{2+} waves are propagated by a messenger other than the $[IP_3]_i$ gradient, and is consistent with the hypothesis that the intracellular diffusion of Ca^{2+} and the CICR mechanism are involved in intracellular Ca^{2+} waves associated with Ca^{2+} oscillations.

CHAPTER V

CONCLUSIONS OF THE STUDY

The results of the Specific Aim 1 support the hypothesis that mechanically - induced intercellular Ca^{2+} waves in glia are initiated by the generation of IP_3 within the stimulated cell, and propagated by the diffusion of IP_3 molecules between neighboring cells via gap junctions. The results of the Specific Aim 2 suggest that the propagation of an intercellular Ca^{2+} wave results in the generation of an intercellular gradient of $[IP_3]_i$ throughout the culture, and initiates distinct intracellular Ca^{2+} oscillations only in cells that, being at a specific distance from the wave origin, have a specific $[IP_3]_i$. In conclusion, the results of Specific Aim 1 and Specific Aim 2 have proven the hypothesis that passive diffusion of IP_3 from the stimulated cell is the mechanism responsible for both propagation of intercellular Ca^{2+} waves and generation of intracellular Ca^{2+} oscillations.

Ca^{2+} wave -induced Ca^{2+} oscillations may serve to resolve information contained in the position and strength of a local stimulus that induces intercellular Ca^{2+} wave propagation. Intercellular Ca^{2+} waves and wave-induced Ca^{2+} oscillations may serve as mechanisms for the integration and coordination of multicellular glial functions in the CNS.

CHAPTER VI

BIBLIOGRAPHY

Abbott, N. J., Hughes, C. C., Revest, P. A., and Greenwood, J. (1992). Development and characterisation of a rat brain capillary endothelial culture: towards an in vitro blood-brain barrier. J Cell Sci *103*, 23-37.

Abbott, N. J., Revest, P. A., and Romero, I. A. (1992). Astrocyte-endothelial interaction: physiology and pathology. Neuropathol Appl Neurobiol *18*, 424-33.

Akopian, G., Kressin, K., Derouiche, A., and Steinhauser, C. (1996). Identified glial cells in the early postnatal mouse hippocampus display different types of Ca2+ currents. Glia *17*, 181-94.

Allbritton, N. L., Meyer, T., and Stryer, L. (1992). Range of messenger action of calcium ion and inositol 1,4,5- trisphosphate. Science *258*, 1812-5.

Amundson, J., and Clapham, D. (1993). Calcium waves. Curr Opin Neurobiol *3*, 375-82.

Anders, J. J. (1988). Lactic acid inhibition of gap junctional intercellular communication in in vitro astrocytes as measured by fluorescence recovery after laser photobleaching. Glia *1*, 371-9.

Andre, C., Dos Santos, G., and Koulakoff, A. (1994). Muscarinic receptor profiles of mouse brain astrocytes in culture vary with their tissue of origin but differ from those of neurons. Eur J Neurosci *6*, 1702-9.

Araque, A., Sanzgiri, R. P., Parpura, V., and Haydon, P. G. (1998). Calcium elevation in astrocytes causes an NMDA receptor-dependent increase in the frequency of miniature synaptic currents in cultured hippocampal neurons. J Neurosci *18*, 6822-9.

Baird, J. G., and Nahorski, S. R. (1990). Increased intracellular calcium stimulates 3H-inositol polyphosphate accumulation in rat cerebral cortical slices. J Neurochem *54*, 555-61.

Bakardjiev, A. (1998). Carnosine and beta-alanine release is stimulated by glutamatergic receptors in cultured rat oligodendrocytes. Glia *24*, 346-51.

Balazs, R., Miller, S., Chun, Y., and Cotman, C. W. (1998). Receptor-coupled phospholipase C and adenylyl cyclase function with different calcium pools in astrocytes. Neuroreport *9*, 1397-401.

Bambrick, L. L., Golovina, V. A., Blaustein, M. P., Yarowsky, P. J., and Krueger, B. K. (1997). Abnormal calcium homeostasis in astrocytes from the trisomy 16 mouse. Glia *19*, 352-8.

Barish, M. E. (1995). Modulation of the electrical differentiation of neurons by interactions with glia and other non-neuronal cells. Perspect Dev Neurobiol *2*, 357-70.

Barres, B. A., Chun, L. L., and Corey, D. P. (1988). Ion channel expression by white matter glia: I. Type 2 astrocytes and oligodendrocytes. Glia *1*, 10-30.

Barres, B. A., Chun, L. L., and Corey, D. P. (1990). Ion channels in vertebrate glia. Annu Rev Neurosci *13*, 441-74.

Barres, B. A., Koroshetz, W. J., Chun, L. L., and Corey, D. P. (1990). Ion channel expression by white matter glia: the type-1 astrocyte. Neuron *5*, 527-44.

Barres, B. A., Lazar, M. A., and Raff, M. C. (1994). A novel role for thyroid hormone, glucocorticoids and retinoic acid in timing oligodendrocyte development. Development *120*, 1097-108.

Barres, B. A., and Raff, M. C. (1993). Proliferation of oligodendrocyte precursor cells depends on electrical activity in axons. Nature *361*, 258-60.

Belachew, S., Malgrange, B., Rigo, J. M., Rogister, B., Coucke, P., Mazy-Servais, C., and Moonen, G. (1998). Developmental regulation of neuroligand-induced responses in cultured oligodendroglia. Neuroreport *9*, 973-80.

Bender, A. S., Schousboe, A., Reichelt, W., and Norenberg, M. D. (1998). Ionic mechanisms in glutamate-induced astrocyte swelling: role of K+ influx. J Neurosci Res *52*, 307-21.

Benninger, C., Kadis, J., and Prince, D. A. (1980). Extracellular calcium and potassium changes in hippocampal slices. Brain Res *187*, 165-82.

Benos, D. J., Hahn, B. H., Bubien, J. K., Ghosh, S. K., Mashburn, N. A., Chaikin, M. A., Shaw, G. M., and Benveniste, E. N. (1994). Envelope glycoprotein gp120 of human immunodeficiency virus type 1 alters ion transport in astrocytes: implications for AIDS dementia complex. Proc Natl Acad Sci U S A *91*, 494-8.

Berridge, M. J. (1997). The AM and FM of calcium signalling. Nature *386*, 759-60.

Berridge, M. J. (1993). Cell signalling. A tale of two messengers [news; comment]. Nature *365*, 388-9.

Berridge, M. J. (1993). Inositol trisphosphate and calcium signalling. Nature *361*, 315-25.

Berridge, M. J., Downes, C. P., and Hanley, M. R. (1989). Neural and developmental actions of lithium: a unifying hypothesis. Cell *59*, 411-9.

Berridge, M. J., and Dupont, G. (1994). Spatial and temporal signalling by calcium. Curr Opin Cell Biol *6*, 267-74.

Bezprozvanny, I., and Ehrlich, B. E. (1993). ATP modulates the function of inositol 1,4,5-trisphosphate-gated channels at two sites. Neuron *10*, 1175-84.

Bezprozvanny, I., Watras, J., and Ehrlich, B. E. (1991). Bell-shaped calcium-response curves of Ins(1,4,5)P3- and calcium-gated channels from endoplasmic reticulum of cerebellum. Nature *351*, 751-4.

Bezzi, P., Carmignoto, G., Pasti, L., Vesce, S., Rossi, D., Rizzini, B. L., Pozzan, T., and Volterra, A. (1998). Prostaglandins stimulate calcium-dependent glutamate release

in astrocytes. Nature *391*, 281-5.

Blakemore, W. F., and Franklin, R. J. (1991). Transplantation of glial cells into the CNS. Trends Neurosci *14*, 323-7.

Blanc, E. M., Bruce-Keller, A. J., and Mattson, M. P. (1998). Astrocytic gap junctional communication decreases neuronal vulnerability to oxidative stress-induced disruption of Ca2+ homeostasis and cell death. J Neurochem *70*, 958-70.

Boitano, S., Dirksen, E. R., and Sanderson, M. J. (1992). Intercellular propagation of calcium waves mediated by inositol trisphosphate. Science *258*, 292-5.

Bourguignon, L. Y., Jin, H., Iida, N., Brandt, N. R., and Zhang, S. H. (1993). The involvement of ankyrin in the regulation of inositol 1,4,5- trisphosphate receptor-mediated internal Ca2+ release from Ca2+ storage vesicles in mouse T-lymphoma cells. J Biol Chem *268*, 7290-7.

Breer, H., Boekhoff, I., and Tareilus, E. (1990). Rapid kinetics of second messenger formation in olfactory transduction. Nature *345*, 65-8.

Brophy, C. M., Mills, I., Rosales, O., Isales, C., and Sumpio, B. E. (1993). Phospholipase C: a putative mechanotransducer for endothelial cell response to acute

hemodynamic changes. Biochem Biophys Res Commun *190*, 576-81.

Bruner, G., and Murphy, S. (1993). Purinergic P2Y receptors on astrocytes are directly coupled to phospholipase A2. Glia *7*, 219-24.

Bruner, G., and Murphy, S. (1993). UTP activates multiple second messenger systems in cultured rat astrocytes. Neurosci Lett *162*, 105-8.

Burt, J. M., and Spray, D. C. (1989). Volatile anesthetics block intercellular communication between neonatal rat myocardial cells. Circ Res *65*, 829-37.

Canzoniero, L. M., Taglialatela, M., Di Renzo, G., and Annunziato, L. (1993). Gadolinium and neomycin block voltage-sensitive Ca2+ channels without interfering with the Na(+)-Ca2+ antiporter in brain nerve endings. Eur J Pharmacol *245*, 97-103.

Cardy, T. J., and Taylor, C. W. (1998). A novel role for calmodulin: Ca2+-independent inhibition of type-1 inositol trisphosphate receptors. Biochem J *334*, 447-55.

Cardy, T. J., Traynor, D., and Taylor, C. W. (1997). Differential regulation of types-1 and -3 inositol trisphosphate receptors by cytosolic Ca2+. Biochem J *328*, 785-93.

Carter, T. D., Chen, X. Y., Carlile, G., Kalapothakis, E., Ogden, D., and Evans, W. H. (1996). Porcine aortic endothelial gap junctions: identification and permeation by caged InsP3. J Cell Sci *109*, 1765-73.

Centemeri, C., Bolego, C., Abbracchio, M. P., Cattabeni, F., Puglisi, L., Burnstock, G., and Nicosia, S. (1997). Characterization of the Ca2+ responses evoked by ATP and other nucleotides in mammalian brain astrocytes. Br J Pharmacol *121*, 1700-6.

Chamberlain, B. K., Volpe, P., and Fleischer, S. (1984). Inhibition of calcium-induced calcium release from purified cardiac sarcoplasmic reticulum vesicles. J Biol Chem *259*, 7547-53.

Chandler, L. J., and Crews, F. T. (1990). Calcium- versus G protein-mediated phosphoinositide. Hydrolysis in rat cerebral cortical synaptoneurosomes. J Neurochem *55*, 1022-30.

Charles, A. (1998). Intercellular calcium waves in glia. Glia *24*, 39-49.

Charles, A. C. (1994). Glia-neuron intercellular calcium signaling. Dev Neurosci *16*, 196-206.

Charles, A. C., Dirksen, E. R., Merrill, J. E., and Sanderson, M. J. (1993). Mechanisms of intercellular calcium signaling in glial cells studied with dantrolene and thapsigargin. Glia *7*, 134-45.

Charles, A. C., Merrill, J. E., Dirksen, E. R., and Sanderson, M. J. (1991). Intercellular signaling in glial cells: calcium waves and oscillations in response to mechanical stimulation and glutamate. Neuron *6*, 983-92.

Charles, A. C., Naus, C. C., Zhu, D., Kidder, G. M., Dirksen, E. R., and Sanderson, M. J. (1992). Intercellular calcium signaling via gap junctions in glioma cells. J Cell Biol *118*, 195-201.

Chen, C. C., and Chen, W. C. (1996). ATP-evoked inositol phosphates formation through activation of P2U purinergic receptors in cultured astrocytes: regulation by PKC subtypes alpha, delta, and theta. Glia *17*, 63-71.

Chen, Z. P., Levy, A., and Lightman, S. L. (1995). Nucleotides as extracellular signalling molecules. J Neuroendocrinol *7*, 83-96.

Chiu, S. Y., and Kriegler, S. (1994). Neurotransmitter-mediated signaling between axons and glial cells. Glia *11*, 191-200.

Churchill, G., and Louis, C. (1998). Roles of Ca2+, inositol trisphosphate and cyclic ADP-ribose in mediating intercellular Ca2+ signaling in sheep lens cells. J Cell Sci *111*, 1217-25.

Clementi, E., and Meldolesi, J. (1996). Pharmacological and functional properties of voltage-independent Ca2+ channels. Cell Calcium *19*, 269-79.

Cohen, R. I., and Almazan, G. (1993). Norepinephrine-stimulated PI hydrolysis in oligodendrocytes is mediated by alpha 1A-adrenoceptors. Neuroreport *4*, 1115-8.

Cohen, R. I., and Almazan, G. (1994). Rat oligodendrocytes express muscarinic receptors coupled to phosphoinositide hydrolysis and adenylyl cyclase. Eur J Neurosci *6*, 1213-24.

Cohen, R. I., Molina-Holgado, E., and Almazan, G. (1996). Carbachol stimulates c-fos expression and proliferation in oligodendrocyte progenitors. Brain Res Mol Brain Res *43*, 193-201.

Cole, R., and de Vellis, J. (1989). Preparation of astrocyte and oligodendrocyte cultures from primary rat glial cultures, d. V. Sahar, Vernadakis, Haber, ed. (NY: Wiley-Liss).

Compston, A. (1995). Brain repair. J Intern Med *237*, 127-34.

Connors, B. W., Benardo, L. S., and Prince, D. A. (1984). Carbon dioxide sensitivity of dye coupling among glia and neurons of the neocortex. J Neurosci *4*, 1324-30.

Cooper, M. S. (1995). Intercellular signaling in neuronal-glial networks. Biosystems *34*, 65-85.

Cornell-Bell, A. H., and Finkbeiner, S. M. (1991). Ca2+ waves in astrocytes. Cell Calcium *12*, 185-204.

Cornell-Bell, A. H., Finkbeiner, S. M., Cooper, M. S., and Smith, S. J. (1990). Glutamate induces calcium waves in cultured astrocytes: long-range glial signaling. Science *247*, 470-3.

Cotrina, M. L., Lin, J. H., Alves-Rodrigues, A., Liu, S., Li, J., Azmi-Ghadimi, H., Kang, J., Naus, C. C., and Nedergaard, M. (1998). Connexins regulate calcium signaling by controlling ATP release. Proc Natl Acad Sci U S A *95*, 15735-40.

Cotrina, M. L., Lin, J. H., and Nedergaard, M. (1998). Cytoskeletal assembly and ATP release regulate astrocytic calcium signaling. J Neurosci *18*, 8794-804.

Dandrea, P., Calabrese, A., and Grandolfo, M. (1998). Intercellular calcium signalling between chondrocytes and synovial cells in co-culture. Biochem J *329*, 681-7.

Dani, J. W., Chernjavsky, A., and Smith, S. J. (1992). Neuronal activity triggers calcium waves in hippocampal astrocyte networks. Neuron *8*, 429-40.

Dani, J. W., and Smith, S. J. (1995). The triggering of astrocytic calcium waves by NMDA-induced neuronal activation. Ciba Found Symp *188*, 195-205; discussion 205-9.

Dasso, L. L., and Taylor, C. W. (1991). Heparin and other polyanions uncouple alpha 1-adrenoceptors from G- proteins. Biochem J *280*, 791-5.

Dave, V., Gordon, G. W., and McCarthy, K. D. (1991). Cerebral type 2 astroglia are heterogeneous with respect to their ability to respond to neuroligands linked to calcium mobilization. Glia *4*, 440-7.

David, J. C., Yamada, K. A., Bagwe, M. R., and Goldberg, M. P. (1996). AMPA receptor activation is rapidly toxic to cortical astrocytes when desensitization is blocked. J Neurosci *16*, 200-9.

Davidson, J. S., Baumgarten, I. M., and Harley, E. H. (1986). Reversible inhibition of intercellular junctional communication by glycyrrhetinic acid. Biochem Biophys Res Commun *134*, 29-36.

De Koninck, P., and Schulman, H. (1998). Sensitivity of CaM kinase II to the frequency of Ca2+ oscillations. Science *279*, 227-30.

Deitmer, J. W., Verkhratsky, A. J., and Lohr, C. (1998). Calcium signalling in glial cells. Cell Calcium *24*, 405-16.

Delaunoy, J. P., Hog, F., Devilliers, G., Bansart, M., Mandel, P., and Sensenbrenner, M. (1980). Developmental changes and localization of carbonic anhydrase in cerebral hemispheres of the rat and in rat glial cell cultures. Cell Mol Biol *26*, 235-40.

Delgado-Escueta, A. V., Ward, A. A., Jr., Woodbury, D. M., and Porter, R. J. (1986). New wave of research in the epilepsies. Adv Neurol *44*, 3-55.

Dent, M. A., Raisman, G., and Lai, F. A. (1996). Expression of type 1 inositol 1,4,5-trisphosphate receptor during axogenesis and synaptic contact in the central and peripheral nervous system of developing rat. Development *122*, 1029-39.

Dermietzel, R. (1998). Gap junction wiring: a 'new' principle in cell-to-cell communication in the nervous system? Brain Res Brain Res Rev *26*, 176-83.

Dermietzel, R., Hertberg, E. L., Kessler, J. A., and Spray, D. C. (1991). Gap junctions between cultured astrocytes: immunocytochemical, molecular, and electrophysiological analysis. J Neurosci *11*, 1421-32.

Dermietzel, R., and Spray, D. C. (1998). From neuro-glue ('Nervenkitt') to glia: a prologue. Glia *24*, 1-7.

Dermietzel, R., and Spray, D. C. (1993). Gap junctions in the brain: where, what type, how many and why? Trends Neurosci *16*, 186-92.

Derouiche, A., and Frotscher, M. (1991). Astroglial processes around identified glutamatergic synapses contain glutamine synthetase: evidence for transmitter degradation. Brain Res *552*, 346-50.

Deutsch, D. E., Williams, J. A., and Yule, D. I. (1995). Halothane and octanol block Ca2+ oscillations in pancreatic acini by multiple mechanisms. Am J Physiol *269*, G779-88.

Diamond, J. S., Bergles, D. E., and Jahr, C. E. (1998). Glutamate release monitored with astrocyte transporter currents during LTP. Neuron *21*, 425-33.

Dolmetsch, R. E., Lewis, R. S., Goodnow, C. C., and Healy, J. I. (1997). Differential activation of transcription factors induced by Ca2+ response amplitude and duration. Nature *386*, 855-8.

Domenighetti, A. A., Beny, J. L., Chabaud, F., and Frieden, M. (1998). An intercellular regenerative calcium wave in porcine coronary artery endothelial cells in primary culture. J Physiol (Lond) *513*, 103-16.

Duffy, S., and MacVicar, B. A. (1995). Adrenergic calcium signaling in astrocyte networks within the hippocampal slice. J Neurosci *15*, 5535-50.

Duffy, S., and MacVicar, B. A. (1996). In vitro ischemia promotes calcium influx and intracellular calcium release in hippocampal astrocytes. J Neurosci *16*, 71-81.

Duffy, S., and MacVicar, B. A. (1994). Potassium-dependent calcium influx in acutely isolated hippocampal astrocytes. Neuroscience *61*, 51-61.

Dunina-Barkovskaya, A. (1998). pH dependence of junctional conductance. Membr Cell Biol *11*, 793-801.

Eberhard, D. A., and Holz, R. W. (1988). Intracellular Ca2+ activates phospholipase C. Trends Neurosci *11*, 517-20.

Ehrlich, B. E. (1995). Functional properties of intracellular calcium-release channels. Curr Opin Neurobiol *5*, 304-9.

Ehrlich, B. E., Kaftan, E., Bezprozvannaya, S., and Bezprozvanny, I. (1994). The pharmacology of intracellular Ca(2+)-release channels. Trends Pharmacol Sci *15*, 145-9.

Ek-Vitorin, J. F., Calero, G., Morley, G. E., Coombs, W., Taffet, S. M., and Delmar, M. (1996). PH regulation of connexin43: molecular analysis of the gating particle. Biophys J *71*, 1273-84.

Enkvist, M. O., Hamalainen, H., Jansson, C. C., Kukkonen, J. P., Hautala, R., Courtney, M. J., and Akerman, K. E. (1996). Coupling of astroglial alpha 2-adrenoreceptors to second messenger pathways. J Neurochem *66*, 2394-401.

Enkvist, M. O., and McCarthy, K. D. (1992). Activation of protein kinase C blocks astroglial gap junction communication and inhibits the spread of calcium waves. J

Neurochem *59*, 519-26.

Enkvist, M. O., and McCarthy, K. D. (1994). Astroglial gap junction communication is increased by treatment with either glutamate or high K+ concentration. J Neurochem *62*, 489-95.

Evans, W. H. (1994). Assembly of gap junction intercellular communication channels. Biochem Soc Trans *22*, 788-92.

Exton, J. H. (1996). Regulation of phosphoinositide phospholipases by hormones, neurotransmitters, and other agonists linked to G proteins. Annu Rev Pharmacol Toxicol *36*, 481-509.

Fatatis, A., and Russell, J. T. (1992). Spontaneous changes in intracellular calcium concentration in type I astrocytes from rat cerebral cortex in primary culture. Glia *5*, 95-104.

Felix, J. A., Woodruff, M. L., and Dirksen, E. R. (1996). Stretch increases inositol 1,4,5-trisphosphate concentration in airway epithelial cells. Am J Respir Cell Mol Biol *14*, 296-301.

Finch, E. A., Turner, T. J., and Goldin, S. M. (1991). Calcium as a coagonist of inositol 1,4,5-trisphosphate-induced calcium release. Science *252*, 443-6.

Finkbeiner, S. (1992). Calcium waves in astrocytes-filling in the gaps. Neuron *8*, 1101-8.

Finkbeiner, S., and Greenberg, M. E. (1998). Ca2+ channel-regulated neuronal gene expression. J Neurobiol *37*, 171-89.

Finkbeiner, S., and Greenberg, M. E. (1996). Ca(2+)-dependent routes to Ras: mechanisms for neuronal survival, differentiation, and plasticity? Neuron *16*, 233-6.

Finkbeiner, S., and Greenberg, M. E. (1997). Spatial features of calcium-regulated gene expression. Bioessays *19*, 657-60.

Finkbeiner, S. M. (1993). Glial calcium. Glia *9*, 83-104.

Flint, A. C., and Kriegstein, A. R. (1997). Mechanisms underlying neuronal migration disorders and epilepsy. Curr Opin Neurol *10*, 92-7.

Florio, T., Grimaldi, M., Scorziello, A., Salmona, M., Bugiani, O., Tagliavini, F., Forloni, G., and Schettini, G. (1996). Intracellular calcium rise through L-type calcium

channels, as molecular mechanism for prion protein fragment 106-126-induced astroglial proliferation. Biochem Biophys Res Commun *228*, 397-405.

Frame, M. K., and de Feijter, A. W. (1997). Propagation of mechanically induced intercellular calcium waves via gap junctions and ATP receptors in rat liver epithelial cells. Exp Cell Res *230*, 197-207.

Franck, G., Grisar, T., Moonen, G., and Schoffeniels, E. (1978). Potassium transport in mammalian astroglia. pp. 315-25. In: Schoffeniels E, et al., ed. Dynamic properties of glia cells. Oxford, Pergamon Press,.

Franklin, R. J., and Blakemore, W. F. (1995). Glial-cell transplantation and plasticity in the O-2A lineage-- implications for CNS repair. Trends Neurosci *18*, 151-6.

Fukui, H., Inagaki, N., Ito, S., Kubo, A., Kondoh, H., Yamatodani, A., and Wada, H. (1991). Histamine H1-receptors on astrocytes in primary cultures: a possible target for histaminergic neurones. Agents Actions Suppl *33*, 161-80.

Fulton, B. P. (1995). Gap junctions in the developing nervous system. Perspect Dev Neurobiol *2*, 327-34.

Furuichi, T., Furutama, D., Hakamata, Y., Nakai, J., Takeshima, H., and Mikoshiba, K. (1994). Multiple types of ryanodine receptor/Ca2+ release channels are differentially expressed in rabbit brain. J Neurosci *14*, 4794-805.

Furuichi, T., Kohda, K., Miyawaki, A., and Mikoshiba, K. (1994). Intracellular channels [published erratum appears in Curr Opin Neurobiol 1994 Oct;4(5):758]. Curr Opin Neurobiol *4*, 294-303.

Gafni, J., Munsch, J. A., Lam, T. H., Catlin, M. C., Costa, L. G., Molinski, T. F., and Pessah, I. N. (1997). Xestospongins: potent membrane permeable blockers of the inositol 1,4,5- trisphosphate receptor. Neuron *19*, 723-33.

Garcia-Segura, L. M., Chowen, J. A., Parducz, A., and Naftolin, F. (1994). Gonadal hormones as promoters of structural synaptic plasticity: cellular mechanisms. Prog Neurobiol *44*, 279-307.

Garcia-Segura, L. M., Duenas, M., Busiguina, S., Naftolin, F., and Chowen, J. A. (1995). Gonadal hormone regulation of neuronal-glial interactions in the developing neuroendocrine hypothalamus. J Steroid Biochem Mol Biol *53*, 293-8.

Gardner, P. (1989). Calcium and T lymphocyte activation. Cell *59*, 15-20.

Giaume, C., and Venance, L. (1995). Gap junctions in brain glial cells and development. Perspect Dev Neurobiol *2*, 335-45.

Giaume, C., and Venance, L. (1998). Intercellular calcium signaling and gap junctional communication in astrocytes. Glia *24*, 50-64.

Goldman, R. S., Finkbeiner, S. M., and Smith, S. J. (1991). Endothelin induces a sustained rise in intracellular calcium in hippocampal astrocytes. Neurosci Lett *123*, 4-8.

Golovina, V. A., Bambrick, L. L., Yarowsky, P. J., Krueger, B. K., and Blaustein, M. P. (1996). Modulation of two functionally distinct Ca2+ stores in astrocytes: role of the plasmalemmal Na/Ca exchanger. Glia *16*, 296-305.

Golovina, V. A., and Blaustein, M. P. (1997). Spatially and functionally distinct Ca2+ stores in sarcoplasmic and endoplasmic reticulum. Science *275*, 1643-8.

Goodenough, D. A., Goliger, J. A., and Paul, D. L. (1996). Connexins, connexons, and intercellular communication. Annu Rev Biochem *65*, 475-502.

Grima, G., Benz, B., and Do, K. Q. (1997). Glutamate-induced release of the nitric oxide precursor, arginine, from glial cells. Eur J Neurosci *9*, 2248-58.

Grynkiewicz, G., Poenie, M., and Tsien, R. Y. (1985). A new generation of Ca2+ indicators with greatly improved fluorescence properties. J Biol Chem *260*, 3440-50.

Guan, X., Cravatt, B. F., Ehring, G. R., Hall, J. E., Boger, D. L., Lerner, R. A., and Gilula, N. B. (1997). The sleep-inducing lipid oleamide deconvolutes gap junction communication and calcium wave transmission in glial cells. J Cell Biol *139*, 1785-92.

Guan, Y. Y., Quastel, D. M., and Saint, D. A. (1988). Single Ca2+ entry and transmitter release systems at the neuromuscular synapse. Synapse *2*, 558-64.

Guthrie, P. B., Knappenberger, J., Segal, M., Bennett, M. V. L., Charles, A. C., and Kater, S. B. (1999). ATP released from astrocytes mediates glial calcium waves. J Neurosci *19*, 520-8.

Hajnoczky, G., Gao, E., Nomura, T., Hoek, J. B., and Thomas, A. P. (1993). Multiple mechanisms by which protein kinase A potentiates inositol 1,4,5-trisphosphate-induced Ca2+ mobilization in permeabilized hepatocytes. Biochem J *293*, 413-22.

Hajnoczky, G., Robb-Gaspers, L. D., Seitz, M. B., and Thomas, A. P. (1995). Decoding of cytosolic calcium oscillations in the mitochondria. Cell *82*, 415-24.

Hajnoczky, G., and Thomas, A. P. (1997). Minimal requirements for calcium oscillations driven by the IP3 receptor. Embo J *16*, 3533-43.

Hampson, E. C., Vaney, D. I., and Weiler, R. (1992). Dopaminergic modulation of gap junction permeability between amacrine cells in mammalian retina. J Neurosci *12*, 4911-22.

Hansen, M., Boitano, S., Dirksen, E. R., and Sanderson, M. J. (1993). Intercellular calcium signaling induced by extracellular adenosine 5'- triphosphate and mechanical stimulation in airway epithelial cells. J Cell Sci *106*, 995-1004.

Hassinger, T. D., Atkinson, P. B., Strecker, G. J., Whalen, L. R., Dudek, F. E., Kossel, A. H., and Kater, S. B. (1995). Evidence for glutamate-mediated activation of hippocampal neurons by glial calcium waves. J Neurobiol *28*, 159-70.

Hassinger, T. D., Guthrie, P. B., Atkinson, P. B., Bennett, M. V., and Kater, S. B. (1996). An extracellular signaling component in propagation of astrocytic calcium waves. Proc Natl Acad Sci U S A *93*, 13268-73.

Haun, S. E., Murphy, E. J., Bates, C. M., and Horrocks, L. A. (1992). Extracellular calcium is a mediator of astroglial injury during combined glucose-oxygen

deprivation. Brain Res *593*, 45-50.

He, M., Howe, D. G., and McCarthy, K. D. (1996). Oligodendroglial signal transduction systems are regulated by neuronal contact. J Neurochem *67*, 1491-9.

Hildebrandt, J. P., and Hildebrandt, P. (1997). Lysophosphatidic acid depletes intracellular calcium stores different from those mediating capacitative calcium entry in C6 rat glioma cells. Glia *19*, 67-73.

Ho, C., Hicks, J., and Salter, M. W. (1995). A novel P2-purinoceptor expressed by a subpopulation of astrocytes from the dorsal spinal cord of the rat. Br J Pharmacol *116*, 2909-18.

Hofer, A. M., Fasolato, C., and Pozzan, T. (1998). Capacitative Ca2+ entry is closely linked to the filling state of internal Ca2+ stores: a study using simultaneous measurements of ICRAC and intraluminal [Ca2+]. J Cell Biol *140*, 325-34.

Hossain, M. Z., Murphy, L. J., Hertzberg, E. L., and Nagy, J. I. (1994). Phosphorylated forms of connexin43 predominate in rat brain: demonstration by rapid inactivation of brain metabolism. J Neurochem *62*, 2394-403.

Iino, M., and Endo, M. (1992). Calcium-dependent immediate feedback control of inositol 1,4,5- triphosphate-induced Ca2+ release. Nature *360*, 76-8.

Inagaki, N., Goto, H., Ogawara, M., Nishi, Y., Ando, S., and Inagaki, M. (1997). Spatial patterns of Ca2+ signals define intracellular distribution of a signaling by Ca2+/Calmodulin-dependent protein kinase II. J Biol Chem *272*, 25195-9.

Inagaki, N., and Wada, H. (1994). Histamine and prostanoid receptors on glial cells. Glia *11*, 102-9.

Ishida, T., Takahashi, M., Corson, M. A., and Berk, B. C. (1997). Fluid shear stress-mediated signal transduction: how do endothelial cells transduce mechanical force into biological responses? Ann N Y Acad Sci *811*, 12-23; discussion 23-4.

Jahromi, B. S., Robitaille, R., and Charlton, M. P. (1992). Transmitter release increases intracellular calcium in perisynaptic Schwann cells in situ. Neuron *8*, 1069-77.

James, S. R., and Downes, C. P. (1997). Structural and mechanistic features of phospholipases C: effectors of inositol phospholipid-mediated signal transduction. Cell Signal *9*, 329-36.

James, S. R., Paterson, A., Harden, T. K., Demel, R. A., and Downes, C. P. (1997). Dependence of the activity of phospholipase C beta on surface pressure and surface composition in phospholipid monolayers and its implications for their regulation. Biochemistry *36*, 848-55.

Jeftinija, S. D., and Jeftinija, K. V. (1998). ATP stimulates release of excitatory amino acids from cultured Schwann cells. Neuroscience *82*, 927-34.

Johnston, M. V. (1996). Developmental aspects of epileptogenesis. Epilepsia *37 Suppl 1*, S2-9.

Jou, M. J., Peng, T. I., and Sheu, S. S. (1996). Histamine induces oscillations of mitochondrial free Ca2+ concentration in single cultured rat brain astrocytes. J Physiol (Lond) *497*, 299-308.

Kaftan, E. J., Ehrlich, B. E., and Watras, J. (1997). Inositol 1,4,5-trisphosphate (InsP3) and calcium interact to increase the dynamic range of InsP3 receptor-dependent calcium signaling. J Gen Physiol *110*, 529-38.

Kanai, Y., Smith, C. P., and Hediger, M. A. (1993). The elusive transporters with a high affinity for glutamate. Trends Neurosci *16*, 365-70.

Kannan, M. S., Prakash, Y. S., Brenner, T., Mickelson, J. R., and Sieck, G. C. (1997). Role of ryanodine receptor channels in Ca2+ oscillations of porcine tracheal smooth muscle. Am J Physiol *272*, L659-64.

Kastritsis, C. H., and McCarthy, K. D. (1993). Oligodendroglial lineage cells express neuroligand receptors. Glia *8*, 106-13.

Keyser, D. O., and Pellmar, T. C. (1994). Synaptic transmission in the hippocampus: critical role for glial cells. Glia *10*, 237-43.

Khodakhah, K., and Ogden, D. (1993). Functional heterogeneity of calcium release by inositol trisphosphate in single Purkinje neurones, cultured cerebellar astrocytes, and peripheral tissues. Proc Natl Acad Sci U S A *90*, 4976-80.

Kiedrowski, L., Brooker, G., Costa, E., and Wroblewski, J. T. (1994). Glutamate impairs neuronal calcium extrusion while reducing sodium gradient. Neuron *12*, 295-300.

Kim, W. T., Rioult, M. G., and Cornell-Bell, A. H. (1994). Glutamate-induced calcium signaling in astrocytes. Glia *11*, 173-84.

King, B. F., Neary, J. T., Zhu, Q., Wang, S., Norenberg, M. D., and Burnstock, G. (1996). P2 purinoceptors in rat cortical astrocytes: expression, calcium- imaging and signalling studies. Neuroscience *74*, 1187-96.

Kirischuk, S., Moller, T., Voitenko, N., Kettenmann, H., and Verkhratsky, A. (1995). ATP-induced cytoplasmic calcium mobilization in Bergmann glial cells. J Neurosci *15*, 7861-71.

Kirischuk, S., Scherer, J., Kettenmann, H., and Verkhratsky, A. (1995). Activation of P2-purinoreceptors triggered Ca2+ release from InsP3- sensitive internal stores in mammalian oligodendrocytes. J Physiol (Lond) *483*, 41-57.

Kirischuk, S., Scherer, J., Moller, T., Verkhratsky, A., and Kettenmann, H. (1995). Subcellular heterogeneity of voltage-gated Ca2+ channels in cells of the oligodendrocyte lineage. Glia *13*, 1-12.

Kirischuk, S., Tuschick, S., Verkhratsky, A., and Kettenmann, H. (1996). Calcium signalling in mouse Bergmann glial cells mediated by alpha1- adrenoreceptors and H1 histamine receptors. Eur J Neurosci *8*, 1198-208.

Kostyuk, P., and Verkhratsky, A. (1994). Calcium stores in neurons and glia. Neuroscience *63*, 381-404.

Kunzelmann, P., Blumcke, I., Traub, O., Dermietzel, R., and Willecke, K. (1997). Coexpression of connexin45 and -32 in oligodendrocytes of rat brain. J Neurocytol *26*, 17-22.

Kuraoka, A., Iida, H., Hatae, T., Shibata, Y., Itoh, M., and Kurita, T. (1993). Localization of gap junction proteins, connexins 32 and 26, in rat and guinea pig liver as revealed by quick-freeze, deep-etch immunoelectron microscopy. J Histochem Cytochem *41*, 971-80.

Kwak, B. R., Hermans, M. M., De Jonge, H. R., Lohmann, S. M., Jongsma, H. J., and Chanson, M. (1995a). Differential regulation of distinct types of gap junction channels by similar phosphorylating conditions. Mol Biol Cell *6*, 1707-19.

Kwak, B. R., Saez, J. C., Wilders, R., Chanson, M., Fishman, G. I., Hertzberg, E. L., Spray, D. C., and Jongsma, H. J. (1995b). Effects of cGMP-dependent phosphorylation on rat and human connexin43 gap junction channels. Pflugers Arch *430*, 770-8.

Lamb, R. G., Harper, C. C., McKinney, J. S., Rzigalinski, B. A., and Ellis, E. F. (1997). Alterations in phosphatidylcholine metabolism of stretch-injured cultured rat astrocytes. J Neurochem *68*, 1904-10.

Lamont, C., Luther, P. W., Balke, C. W., and Wier, W. G. (1998). Intercellular Ca2+ waves in rat heart muscle. J Physiol (Lond) *512*, 669-76.

Langley, D., and Pearce, B. (1994). Ryanodine-induced intracellular calcium mobilisation in cultured astrocytes. Glia *12*, 128-34.

Lauritzen, M., and Fabricius, M. (1995). Real time laser-Doppler perfusion imaging of cortical spreading depression in rat neocortex. Neuroreport *6*, 1271-3.

Lee, H. C. (1993). Potentiation of calcium- and caffeine-induced calcium release by cyclic ADP-ribose. J Biol Chem *268*, 293-9.

Lee, S. H., Kim, W. T., Cornell-Bell, A. H., and Sontheimer, H. (1994). Astrocytes exhibit regional specificity in gap-junction coupling. Glia *11*, 315-25.

Lee, S. H., Magge, S., Spencer, D. D., Sontheimer, H., and Cornell-Bell, A. H. (1995). Human epileptic astrocytes exhibit increased gap junction coupling. Glia *15*, 195-202.

Leibowitz, D. H. (1992). The glial spike theory. I. On an active role of neuroglia in spreading depression and migraine. Proc R Soc Lond B Biol Sci *250*, 287-95.

Leybaert, L., Paemeleire, K., Strahonja, A., and Sanderson, M. J. (1998). Inositol-trisphosphate-dependent intercellular calcium signaling in and between astrocytes and endothelial cells. Glia *24*, 398-407.

Leybaert, L., Sneyd, J., and Sanderson, M. J. (1998). A simple method for high temporal resolution calcium imaging with dual excitation dyes. Biophys J *75*, 2025-9.

Li, J., Hertzberg, E. L., and Nagy, J. I. (1997). Connexin32 in oligodendrocytes and association with myelinated fibers in mouse and rat brain. J Comp Neurol *379*, 571-91.

Li, Z., and Hatton, G. I. (1996). Oscillatory bursting of phasically firing rat supraoptic neurones in low-Ca2+ medium: Na+ influx, cytosolic Ca2+ and gap junctions. J Physiol (Lond) *496*, 379-94.

Lipton, S. A. (1994). AIDS-related dementia and calcium homeostasis. Ann N Y Acad Sci *747*, 205-24.

Lipton, S. A. (1994). Neuronal injury associated with HIV-1 and potential treatment with calcium-channel and NMDA antagonists. Dev Neurosci *16*, 145-51.

Liu, H. N., Molina-Holgado, E., and Almazan, G. (1997). Glutamate-stimulated production of inositol phosphates is mediated by Ca2+ influx in oligodendrocyte progenitors. Eur J Pharmacol *338*, 277-87.

Longuemare, M. C., and Swanson, R. A. (1995). Excitatory amino acid release from astrocytes during energy failure by reversal of sodium-dependent uptake. J Neurosci Res *40*, 379-86.

Lupu, V. D., Kaznacheyeva, E., Krishna, U. M., Falck, J. R., and Bezprozvanny, I. (1998). Functional coupling of phosphatidylinositol 4,5-bisphosphate to inositol 1,4,5-trisphosphate receptor. J Biol Chem *273*, 14067-70.

Luzzi, V., Sims, C. E., Soughayer, J. S., and Allbritton, N. L. (1998). The physiologic concentration of inositol 1,4,5-trisphosphate in the oocytes of Xenopus laevis. J Biol Chem *273*, 28657-62.

Magistretti, P. J., Sorg, O., Yu, N., Martin, J. L., and Pellerin, L. (1993). Neurotransmitters regulate energy metabolism in astrocytes: implications for the metabolic trafficking between neural cells. Dev Neurosci *15*, 306-12.

Mak, D. O., and Foskett, J. K. (1997). Single-channel kinetics, inactivation, and spatial distribution of inositol trisphosphate (IP3) receptors in Xenopus oocyte nucleus. J Gen Physiol *109*, 571-87.

Mangoura, D., Sogos, V., Pelletiere, C., and Dawson, G. (1995). Differential regulation of phospholipases C and D by phorbol esters and the physiological activators carbachol and glutamate in astrocytes from chicken embryo cerebrum and cerebellum. Brain Res Dev Brain Res *87*, 12-21.

Manning, T. J., Jr., and Sontheimer, H. (1997). Spontaneous intracellular calcium oscillations in cortical astrocytes from a patient with intractable childhood epilepsy (Rasmussen's encephalitis). Glia *21*, 332-7.

Marchant, J. S., and Taylor, C. W. (1997). Cooperative activation of IP3 receptors by sequential binding of IP3 and Ca2+ safeguards against spontaneous activity. Curr Biol *7*, 510-8.

Marchant, J. S., and Taylor, C. W. (1998). Rapid activation and partial inactivation of inositol trisphosphate receptors by inositol trisphosphate. Biochemistry *37*, 11524-33.

Martin, D. L. (1992). Synthesis and release of neuroactive substances by glial cells. Glia *5*, 81-94.

Matsuda, T., Takuma, K., Asano, S., Kishida, Y., Nakamura, H., Mori, K., Maeda, S., and Baba, A. (1998). Involvement of calcineurin in Ca2+ paradox-like injury of cultured rat astrocytes. J Neurochem *70*, 2004-11.

McCarthy, K. D., and Salm, A. K. (1991). Pharmacologically-distinct subsets of astroglia can be identified by their calcium response to neuroligands. Neuroscience *41*, 325-33.

McDonald, F., Somasundaram, B., McCann, T. J., Mason, W. T., and Meikle, M. C. (1996). Calcium waves in fluid flow stimulated osteoblasts are G protein mediated. Arch Biochem Biophys *326*, 31-8.

McKay, R. (1997). Stem cells in the central nervous system. Science *276*, 66-71.

McMillian, M. K., and Hong, J. S. (1994). Regulation of preproenkephalin expression in astrocytes: is there a role for glia-derived opioid peptides in reactive gliosis? Crit Rev Neurobiol *9*, 91-103.

McMillian, M. K., Thai, L., Hong, J. S., JP, O. C., and Pennypacker, K. R. (1994). Brain injury in a dish: a model for reactive gliosis. Trends Neurosci *17*, 138-42.

Meda, P. (1996). Gap junction involvement in secretion: the pancreas experience. Clin Exp Pharmacol Physiol *23*, 1053-7.

Messamore, E., Bogdanovich, N., Schroder, H., and Winblad, B. (1994). Astrocytes associated with senile plaques possess muscarinic acetylcholine receptors. Neuroreport *5*, 1473-6.

Michikawa, T., Miyawaki, A., Furuichi, T., and Mikoshiba, K. (1996). Inositol 1,4,5-trisphosphate receptors and calcium signaling. Crit Rev Neurobiol *10*, 39-55.

Miele, M., Boutelle, M. G., and Fillenz, M. (1996). The source of physiologically stimulated glutamate efflux from the striatum of conscious rats. J Physiol (Lond) *497*, 745-51.

Mikoshiba, K. (1997). The InsP3 receptor and intracellular Ca2+ signaling. Curr Opin Neurobiol *7*, 339-45.

Mikoshiba, K., Furuichi, T., Miyawaki, A., Yoshikawa, S., Nakade, S., Michikawa, T., Nakagawa, T., Okano, H., Kume, S., Muto, A., and et al. (1993). Structure and function of inositol 1,4,5-trisphosphate receptor. Ann N Y Acad Sci *707*, 178-97.

Miragall, F., Albiez, P., Bartels, H., de Vries, U., and Dermietzel, R. (1997). Expression of the gap junction protein connexin43 in the subependymal layer and the rostral migratory stream of the mouse: evidence for an inverse correlation between intensity of connexin43 expression and cell proliferation activity. Cell Tissue Res *287*, 243-53.

Mollace, V., and Nistico, G. (1995). Release of nitric oxide from astroglial cells: a key mechanism in neuroimmune disorders. Adv Neuroimmunol *5*, 421-30.

Morley, G. E., Ek-Vitorin, J. F., Taffet, S. M., and Delmar, M. (1997). Structure of connexin43 and its regulation by pHi. J Cardiovasc Electrophysiol *8*, 939-51.

Mouillac, B., Balestre, M. N., and Guillon, G. (1990). Positive feedback regulation of phospholipase C by vasopressin-induced calcium mobilization in WRK1 cells. Cell Signal *2*, 497-507.

Murphy, T. H., Blatter, L. A., Wier, W. G., and Baraban, J. M. (1993). Rapid communication between neurons and astrocytes in primary cortical cultures. J Neurosci *13*, 2672-9.

Nadal, A., Fuentes, E., Pastor, J., and McNaughton, P. A. (1997). Plasma albumin induces calcium waves in rat cortical astrocytes. Glia *19*, 343-51.

Nagy, J. I., Ochalski, P. A., Li, J., and Hertzberg, E. L. (1997). Evidence for the co-localization of another connexin with connexin-43 at astrocytic gap junctions in rat brain. Neuroscience *78*, 533-48.

Naus, C. C., Bechberger, J. F., Zhang, Y., Venance, L., Yamasaki, H., Juneja, S. C., Kidder, G. M., and Giaume, C. (1997). Altered gap junctional communication, intercellular signaling, and growth in cultured astrocytes deficient in connexin43. J Neurosci Res *49*, 528-40.

Nedergaard, M. (1994). Direct signaling from astrocytes to neurons in cultures of mammalian brain cells. Science *263*, 1768-71.

Nedergaard, M., Cooper, A. J., and Goldman, S. A. (1995). Gap junctions are required for the propagation of spreading depression. J Neurobiol *28*, 433-44.

Negishi, K., Teranishi, T., and Kato, S. (1985). Opposite effects of ammonia and carbon dioxide on dye coupling between horizontal cells in the carp retina. Brain Res *342*, 330-9.

New, K. C., and Rabkin, S. D. (1998). GABA synthesis in astrocytes after infection with defective herpes simplex virus vectors expressing glutamic acid decarboxylase 65 or 67. J Neurochem *71*, 2304-12.

Newman, E. A., and Zahs, K. R. (1997). Calcium waves in retinal glial cells. Science *275*, 844-7.

Newman, E. A., and Zahs, K. R. (1998). Modulation of neuronal activity by glial cells in the retina. J Neurosci *18*, 4022-8.

Nilsson, M., Hansson, E., and Ronnback, L. (1991). Adrenergic and 5-HT2 receptors on the same astroglial cell. A microspectrofluorimetric study on cytosolic Ca2+ responses in single cells in primary culture. Brain Res Dev Brain Res *63*, 33-41.

Nitsch, R. M., Slack, B. E., Wurtman, R. J., and Growdon, J. H. (1992). Release of Alzheimer amyloid precursor derivatives stimulated by activation of muscarinic acetylcholine receptors. Science *258*, 304-7.

Oberdorf, J., Vallano, M. L., and Wojcikiewicz, R. J. (1997). Expression and regulation of types I and II inositol 1,4,5- trisphosphate receptors in rat cerebellar granule cell preparations. J Neurochem *69*, 1897-903.

Ochalski, P. A., Frankenstein, U. N., Hertzberg, E. L., and Nagy, J. I. (1997). Connexin-43 in rat spinal cord: localization in astrocytes and identification of heterotypic astro-oligodendrocytic gap junctions. Neuroscience *76*, 931-45.

Okada, M., Matsumori, A., Ono, K., Furukawa, Y., Shioi, T., Iwasaki, A., Matsushima, K., and Sasayama, S. (1998). Cyclic stretch upregulates production of interleukin-8 and monocyte chemotactic and activating factor/monocyte chemoattractant protein-1 in human endothelial cells. Arterioscler Thromb Vasc Biol *18*, 894-901.

Pappas, C. A., Rioult, M. G., and Ransom, B. R. (1996). Octanol, a gap junction uncoupling agent, changes intracellular [H+] in rat astrocytes. Glia *16*, 7-15.

Parpura, V., Basarsky, T. A., Liu, F., Jeftinija, K., Jeftinija, S., and Haydon, P. G. (1994). Glutamate-mediated astrocyte-neuron signalling. Nature *369*, 744-7.

Parpura, V., Liu, F., Jeftinija, K. V., Haydon, P. G., and Jeftinija, S. D. (1995). Neuroligand-evoked calcium-dependent release of excitatory amino acids from Schwann cells. J Neurosci *15*, 5831-9.

Pasti, L., Pozzan, T., and Carmignoto, G. (1995). Long-lasting changes of calcium oscillations in astrocytes. A new form of glutamate-mediated plasticity. J Biol Chem *270*,

15203-10.

Pasti, L., Volterra, A., Pozzan, T., and Carmignoto, G. (1997). Intracellular calcium oscillations in astrocytes: a highly plastic, bidirectional form of communication between neurons and astrocytes in situ. J Neurosci *17*, 7817-30.

Pawlikowska, L., Cottrell, S. E., Harms, M. B., Li, Y., and Rosenberg, P. A. (1996). Extracellular synthesis of cADP-ribose from nicotinamide-adenine dinucleotide by rat cortical astrocytes in culture. J Neurosci *16*, 5372-81.

Pearce, B., Cambray-Deakin, M., Morrow, C., Grimble, J., and Murphy, S. (1985). Activation of muscarinic and of alpha 1-adrenergic receptors on astrocytes results in the accumulation of inositol phosphates. J Neurochem *45*, 1534-40.

Pearce, B., Morrow, C., and Murphy, S. (1988). Characteristics of phorbol ester- and agonist-induced down-regulation of astrocyte receptors coupled to inositol phospholipid metabolism. J Neurochem *50*, 936-44.

Pearce, B., Morrow, C., and Murphy, S. (1986). Receptor-mediated inositol phospholipid hydrolysis in astrocytes. Eur J Pharmacol *121*, 231-43.

Petersen, C. C., Petersen, O. H., and Berridge, M. J. (1993). The role of endoplasmic reticulum calcium pumps during cytosolic calcium spiking in pancreatic acinar cells. J Biol Chem *268*, 22262-4.

Petryniak, M. A., Wurtman, R. J., and Slack, B. E. (1996). Elevated intracellular calcium concentration increases secretory processing of the amyloid precursor protein by a tyrosine phosphorylation-dependent mechanism. Biochem J *320*, 957-63.

Peuchen, S., Clark, J. B., and Duchen, M. R. (1996). Mechanisms of intracellular calcium regulation in adult astrocytes. Neuroscience *71*, 871-83.

Pfrieger, F. W., and Barres, B. A. (1996). New views on synapse-glia interactions. Curr Opin Neurobiol *6*, 615-21.

Pfrieger, F. W., and Barres, B. A. (1997). Synaptic efficacy enhanced by glial cells in vitro. Science *277*, 1684-7.

Porter, J. T., and McCarthy, K. D. (1997). Astrocytic neurotransmitter receptors in situ and in vivo. Prog Neurobiol *51*, 439-55.

Porter, J. T., and McCarthy, K. D. (1996). Hippocampal astrocytes in situ respond to glutamate released from synaptic terminals. J Neurosci *16*, 5073-81.

Pozzan, T., Rizzuto, R., Volpe, P., and Meldolesi, J. (1994). Molecular and cellular physiology of intracellular calcium stores. Physiol Rev *74*, 595-636.

Prentki, M., Deeney, J. T., Matschinsky, F. M., and Joseph, S. K. (1986). Neomycin: a specific drug to study the inositol-phospholipid signalling system? FEBS Lett *197*, 285-8.

Prothero, L. S., Richards, C. D., and Mathie, A. (1998). Inhibition by inorganic ions of a sustained calcium signal evoked by activation of mGlu5 receptors in rat cortical neurons and glia. Br J Pharmacol *125*, 1551-61.

Qi, Y., and Dawson, G. (1993). Effects of hypoxia on oligodendrocyte signal transduction. J Neurochem *61*, 1097-104.

Rahman, S., Carlile, G., and Evans, W. H. (1993). Assembly of hepatic gap junctions. Topography and distribution of connexin 32 in intracellular and plasma membranes determined using sequence-specific antibodies. J Biol Chem *268*, 1260-5.

Ranscht, B., Clapshaw, P. A., Price, J., Noble, M., and Seifert, W. (1982). Development of oligodendrocytes and Schwann cells studied with a monoclonal antibody against galactocerebroside. Proc Natl Acad Sci U S A *79*, 2709-13.

Raptis, L. H., Brownell, H. L., Firth, K. L., and Mackenzie, L. W. (1994). A novel technique for the study of intercellular, junctional communication: electroporation of adherent cells on a partly conductive slide. DNA Cell Biol *13*, 963-75.

Raptis, L. H., Brownell, H. L., Liu, S. K., Firth, K. L., MacKenzie, L. W., Stiles, C. D., and Alberta, J. A. (1995). Applications of electroporation of adherent cells in situ, on a partly conductive slide. Mol Biotechnol *4*, 129-38.

Raptis, L. H., Liu, S. K., Firth, K. L., Stiles, C. D., and Alberta, J. A. (1995). Electroporation of peptides into adherent cells in situ. Biotechniques *18*, 104, 106, 108, 110 passim.

Rebecchi, M. J., and Rosen, O. M. (1987). Stimulation of polyphosphoinositide hydrolysis by thrombin in membranes from human fibroblasts. Biochem J *245*, 49-57.

Reetz, G., and Reiser, G. (1996). [Ca2+]i oscillations induced by bradykinin in rat glioma cells associated with Ca2+ store-dependent Ca2+ influx are controlled by cell volume and by membrane potential. Cell Calcium *19*, 143-56.

Reeves, R. H., Yao, J., Crowley, M. R., Buck, S., Zhang, X., Yarowsky, P., Gearhart, J. D., and Hilt, D. C. (1994). Astrocytosis and axonal proliferation in the

hippocampus of S100b transgenic mice. Proc Natl Acad Sci U S A *91*, 5359-63.

Repke, H., and Maderspach, K. (1982). Muscarinic acetylcholine receptors on culture glia cells. Brain Res *232*, 206-11.

Rhee, S. G., and Bae, Y. S. (1997). Regulation of phosphoinositide-specific phospholipase C isozymes. J Biol Chem *272*, 15045-8.

Robb-Gaspers, L. D., Rutter, G. A., Burnett, P., Hajnoczky, G., Denton, R. M., and Thomas, A. P. (1998). Coupling between cytosolic and mitochondrial calcium oscillations: role in the regulation of hepatic metabolism. Biochim Biophys Acta *1366*, 17-32.

Robb-Gaspers, L. D., and Thomas, A. P. (1995). Coordination of Ca2+ signaling by intercellular propagation of Ca2+ waves in the intact liver. J Biol Chem *270*, 8102-7.

Rorig, B., and Sutor, B. (1996). Regulation of gap junction coupling in the developing neocortex. Mol Neurobiol *12*, 225-49.

Rorig, B., and Sutor, B. (1996). Serotonin regulates gap junction coupling in the developing rat somatosensory cortex. Eur J Neurosci *8*, 1685-95.

Ryu, S. H., Cho, K. S., Lee, K. Y., Suh, P. G., and Rhee, S. G. (1987). Purification and characterization of two immunologically distinct phosphoinositide-specific phospholipases C from bovine brain. J Biol Chem *262*, 12511-8.

Rzigalinski, B. A., Weber, J. T., Willoughby, K. A., and Ellis, E. F. (1998). Intracellular free calcium dynamics in stretch-injured astrocytes. J Neurochem *70*, 2377-85.

Sacchettoni, S. A., Benchaibi, M., Sindou, M., Belin, M. F., and Jacquemont, B. (1998). Glutamate-modulated production of GABA in immortalized astrocytes transduced by a glutamic acid decarboxylase-expressing retrovirus. Glia *22*, 86-93.

Salm, A. K., and McCarthy, K. D. (1990). Norepinephrine-evoked calcium transients in cultured cerebral type 1 astroglia. Glia *3*, 529-38.

Salter, M. W., and Hicks, J. L. (1995). ATP causes release of intracellular Ca2+ via the phospholipase C beta/IP3 pathway in astrocytes from the dorsal spinal cord. J Neurosci *15*, 2961-71.

Sandberg, K., Ji, H., Iida, T., and Catt, K. J. (1992). Intercellular communication between follicular angiotensin receptors and Xenopus laevis oocytes: medication by an

inositol 1,4,5- trisphosphate-dependent mechanism. J Cell Biol *117*, 157-67.

Sanderson, M. J. (1995). Intercellular calcium waves mediated by inositol trisphosphate. Ciba Found Symp *188*, 175-89.

Sanderson, M. J., Charles, A. C., Boitano, S., and Dirksen, E. R. (1994). Mechanisms and function of intercellular calcium signaling. Mol Cell Endocrinol *98*, 173-87.

Sanderson, M. J., Charles, A. C., and Dirksen, E. R. (1990). Mechanical stimulation and intercellular communication increases intracellular Ca2+ in epithelial cells. Cell Regul *1*, 585-96.

Scemes, E., Dermietzel, R., and Spray, D. C. (1998). Calcium waves between astrocytes from Cx43 knockout mice. Glia *24*, 65-73.

Scemes, E., and Spray, D. C. (1998). Increased intercellular communication in mouse astrocytes exposed to hyposmotic shocks. Glia *24*, 74-84.

Schlue, W. R., Dorner, R., Rempe, L., and Riehl, B. (1991). Glial H+ transport and control of pH. Ann N Y Acad Sci *633*, 287-305.

Seregi, A., Doll, S., Schobert, A., and Hertting, G. (1992). Functionally diverse purinergic P2Y-receptors mediate prostanoid synthesis in cultured rat astrocytes: the role of ATP-induced phosphatidyl-inositol breakdown. Eicosanoids *5*, S19-22.

Shao, Y., and McCarthy, K. D. (1994). Plasticity of astrocytes. Glia *11*, 147-55.

Shao, Y., and McCarthy, K. D. (1995). Receptor-mediated calcium signals in astroglia: multiple receptors, common stores and all-or-nothing responses. Cell Calcium *17*, 187-96.

Sheppard, C. A., Simpson, P. B., Sharp, A. H., Nucifora, F. C., Ross, C. A., Lange, G. D., and Russell, J. T. (1997). Comparison of type 2 inositol 1,4,5-trisphosphate receptor distribution and subcellular Ca2+ release sites that support Ca2+ waves in cultured astrocytes. J Neurochem *68*, 2317-27.

Silver, J. (1993). Glia-neuron interactions at the midline of the developing mammalian brain and spinal cord. Perspect Dev Neurobiol *1*, 227-36.

Simpson, P. B., Holtzclaw, L. A., Langley, D. B., and Russell, J. T. (1998). Characterization of ryanodine receptors in oligodendrocytes, type 2 astrocytes, and O-2A progenitors. J Neurosci Res *52*, 468-82.

Simpson, P. B., Mehotra, S., Langley, D., Sheppard, C. A., and Russell, J. T. (1998). Specialized distributions of mitochondria and endoplasmic reticulum proteins define Ca2+ wave amplification sites in cultured astrocytes. J Neurosci Res *52*, 672-83.

Sims, C. E., and Allbritton, N. L. (1998). Metabolism of inositol 1,4,5-trisphosphate and inositol 1,3,4,5- tetrakisphosphate by the oocytes of Xenopus laevis. J Biol Chem *273*, 4052-8.

Smith, R. J., Sam, L. M., Justen, J. M., Bundy, G. L., Bala, G. A., and Bleasdale, J. E. (1990). Receptor-coupled signal transduction in human polymorphonuclear neutrophils: effects of a novel inhibitor of phospholipase C-dependent processes on cell responsiveness. J Pharmacol Exp Ther *253*, 688-97.

Smith, S. J. (1994). Neural signalling. Neuromodulatory astrocytes. Curr Biol *4*, 807-10.

Sneyd, J., Charles, A. C., and Sanderson, M. J. (1994). A model for the propagation of intercellular calcium waves. Am J Physiol *266*, C293-302.

Sneyd, J., Keizer, J., and Sanderson, M. J. (1995a). Mechanisms of calcium oscillations and waves: a quantitative analysis. Faseb J *9*, 1463-72.

Sneyd, J., Wetton, B. T., Charles, A. C., and Sanderson, M. J. (1995b). Intercellular calcium waves mediated by diffusion of inositol trisphosphate: a two-dimensional model. Am J Physiol *268*, C1537-45.

Sneyd, J., Wilkins, M., Strahonja, A., and Sanderson, M. J. (1998). Calcium waves and oscillations driven by an intercellular gradient of inositol (1,4,5)-trisphosphate. Biophys Chem *72*, 101-9.

Sontheimer, H. (1994). Voltage-dependent ion channels in glial cells. Glia *11*, 156-72.

Spicer, S. S., Stoward, P. J., and Tashian, R. E. (1979). The immunohistolocalization of carbonic anhydrase in rodent tissues. J Histochem Cytochem *27*, 820-31.

Spray, D. C., White, R. L., Mazet, F., and Bennett, M. V. (1985). Regulation of gap junctional conductance. Am J Physiol *248*, H753-64.

Striggow, F., and Ehrlich, B. E. (1996). Ligand-gated calcium channels inside and out. Curr Opin Cell Biol *8*, 490-5.

Stutenkemper, R., Geisse, S., Schwarz, H. J., Look, J., Traub, O., Nicholson, B. J., and Willecke, K. (1992). The hepatocyte-specific phenotype of murine liver cells correlates with high expression of connexin32 and connexin26 but very low expression of connexin43. Exp Cell Res *201*, 43-54.

Takeda, M., Nelson, D. J., and Soliven, B. (1995). Calcium signaling in cultured rat oligodendrocytes. Glia *14*, 225-36.

Taylor, C. W., and Broad, L. M. (1998). Pharmacological analysis of intracellular Ca2+ signalling: problems and pitfalls. Trends Pharmacol Sci *19*, 370-5.

Thomson, C. E., Griffiths, I. R., McCulloch, M. C., Kyriakides, E., Barrie, J. A., and Montague, P. (1993). In vitro studies of axonally-regulated Schwann cell genes during Wallerian degeneration. J Neurocytol *22*, 590-602.

Tordjmann, T., Berthon, B., Claret, M., and Combettes, L. (1997). Coordinated intercellular calcium waves induced by noradrenaline in rat hepatocytes: dual control by gap junction permeability and agonist. Embo J *16*, 5398-407.

Tsacopoulos, M., and Magistretti, P. J. (1996). Metabolic coupling between glia and neurons. J Neurosci *16*, 877-85.

Tse, A., Tse, F. W., Almers, W., and Hille, B. (1993). Rhythmic exocytosis stimulated by GnRH-induced calcium oscillations in rat gonadotropes. Science *260*, 82-4.

Tuschick, S., Kirischuk, S., Kirchhoff, F., Liefeldt, L., Paul, M., Verkhratsky, A., and Kettenmann, H. (1997). Bergmann glial cells in situ express endothelinB receptors linked to cytoplasmic calcium signals. Cell Calcium *21*, 409-19.

van den Pol, A. N., Finkbeiner, S. M., and Cornell-Bell, A. H. (1992). Calcium excitability and oscillations in suprachiasmatic nucleus neurons and glia in vitro. J Neurosci *12*, 2648-64.

Venance, L., Cordier, J., Monge, M., Zalc, B., Glowinski, J., and Giaume, C. (1995). Homotypic and heterotypic coupling mediated by gap junctions during glial cell differentiation in vitro. Eur J Neurosci *7*, 451-61.

Venance, L., Piomelli, D., Glowinski, J., and Giaume, C. (1995). Inhibition by anandamide of gap junctions and intercellular calcium signalling in striatal astrocytes. Nature *376*, 590-4.

Venance, L., Premont, J., Glowinski, J., and Giaume, C. (1998). Gap junctional communication and pharmacological heterogeneity in astrocytes cultured from the rat

striatum. J Physiol (Lond) *510*, 429-40.

Venance, L., Stella, N., Glowinski, J., and Giaume, C. (1997). Mechanism involved in initiation and propagation of receptor-induced intercellular calcium signaling in cultured rat astrocytes. J Neurosci *17*, 1981-92.

Verkhratsky, A., and Kettenmann, H. (1996). Calcium signalling in glial cells. Trends Neurosci *19*, 346-52.

Vernadakis, A. (1996). Glia-neuron intercommunications and synaptic plasticity. Prog Neurobiol *49*, 185-214.

von Blankenfeld, G., and Kettenmann, H. (1991). Glutamate and GABA receptors in vertebrate glial cells. Mol Neurobiol *5*, 31-43.

Vornov, J. J. (1998). Ion channels and exchangers that mediate ischemic neuronal injury. Curr Opin Neurol *11*, 39-43.

Wahl, M. I., Jones, G. A., Nishibe, S., Rhee, S. G., and Carpenter, G. (1992). Growth factor stimulation of phospholipase C-gamma 1 activity. Comparative properties of control and activated enzymes. J Biol Chem *267*, 10447-56.

Walker, J. W., Somlyo, A. V., Goldman, Y. E., Somlyo, A. P., and Trentham, D. R. (1987). Kinetics of smooth and skeletal muscle activation by laser pulse photolysis of caged inositol 1,4,5-trisphosphate. Nature *327*, 249-52.

Wang, Z., Tymianski, M., Jones, O. T., and Nedergaard, M. (1997). Impact of cytoplasmic calcium buffering on the spatial and temporal characteristics of intercellular calcium signals in astrocytes. J Neurosci *17*, 7359-71.

White, T. W., Bruzzone, R., and Paul, D. L. (1995). The connexin family of intercellular channel forming proteins. Kidney Int *48*, 1148-57.

Willems, P. H., Van de Put, F. H., Engbersen, R., Bosch, R. R., Van Hoof, H. J., and de Pont, J. J. (1994). Induction of Ca2+ oscillations by selective, U73122-mediated, depletion of inositol-trisphosphate-sensitive Ca2+ stores in rabbit pancreatic acinar cells. Pflugers Arch *427*, 233-43.

Wolburg, H., and Rohlmann, A. (1995). Structure--function relationships in gap junctions. Int Rev Cytol *157*, 315-73.

Wood, A., Wing, M. G., Benham, C. D., and Compston, D. A. (1993). Specific induction of intracellular calcium oscillations by complement membrane attack on

oligodendroglia. J Neurosci *13*, 3319-32.

Woods, R. P., Iacoboni, M., and Mazziotta, J. C. (1994). Brief report: bilateral spreading cerebral hypoperfusion during spontaneous migraine headache. N Engl J Med *331*, 1689-92.

Wouterlood, F. G., Mugnaini, E., Osen, K. K., and Dahl, A. L. (1984). Stellate neurons in rat dorsal cochlear nucleus studies with combined Golgi impregnation and electron microscopy: synaptic connections and mutual coupling by gap junctions. J Neurocytol *13*, 639-64.

Yagodin, S., Holtzclaw, L. A., and Russell, J. T. (1995). Subcellular calcium oscillators and calcium influx support agonist- induced calcium waves in cultured astrocytes. Mol Cell Biochem *149-150*, 137-44.

Yagodin, S. V., Holtzclaw, L., Sheppard, C. A., and Russell, J. T. (1994). Nonlinear propagation of agonist-induced cytoplasmic calcium waves in single astrocytes. J Neurobiol *25*, 265-80.

Yamamoto-Hino, M., Miyawaki, A., Kawano, H., Sugiyama, T., Furuichi, T., Hasegawa, M., and Mikoshiba, K. (1995). Immunohistochemical study of inositol 1,4,5-trisphosphate receptor type 3 in rat central nervous system. Neuroreport *6*, 273-6.

Yamasaki, T., Enomoto, K., Moritake, K., and Maeno, T. (1994). Analysis of intra- and intercellular calcium signaling in a mouse malignant glioma cell line. J Neurosurg *81*, 420-6.

Yeager, M., and Nicholson, B. J. (1996). Structure of gap junction intercellular channels. Curr Opin Struct Biol *6*, 183-92.

Yu, A. C., Schousboe, A., and Hertz, L. (1982). Metabolic fate of 14C-labeled glutamate in astrocytes in primary cultures. J Neurochem *39*, 954-60.

Yule, D. I., Stuenkel, E., and Williams, J. A. (1996). Intercellular calcium waves in rat pancreatic acini: mechanism of transmission. Am J Physiol *271*, C1285-94.

Zanotti, S., and Charles, A. (1997). Extracellular calcium sensing by glial cells: low extracellular calcium induces intracellular calcium release and intercellular signaling. J Neurochem *69*, 594-602.

Zimmermann, B., and Walz, B. (1997). Serotonin-induced intercellular calcium waves in salivary glands of the blowfly Calliphora erythrocephala. J Physiol (Lond) *500*, 17-28.

APPENDIX

PUBLICATIONS

Strahonja A. and Sanderson M.J. Intercellular Ca^{2+} waves in glia induce temporo-spatially specific intracellular Ca^{2+} oscillations. Glia (in press).

Leybaert L., Paemeleire K., **Strahonja A.**, Sanderson, M.J. (1998) Inositol-trisphosphate-dependent intercellular calcium signaling in and between astrocytes and endothelial cells. Glia 24:398-407.

Sneyd J., Wilkins M., **Strahonja A.**, Sanderson M.J. (1998) Calcium waves and oscillations driven by an intercellular gradient of inositol (1,4,5)-trisphosphate. Biophysical Chemistry 72:101-109.

Sanderson, M.J., Paemeleire, K., **Strahonja A.**, Leybaert L. (1998) Intercellular Ca2+ signaling between glial and endothelial cells. Gap Junctions , R.Werner (Ed.), IOS Press. 261-266.

Reprinted from

Biophysical Chemistry

Biophysical Chemistry 72 (1998) 101–109

Calcium waves and oscillations driven by an intercellular gradient of inositol (1,4,5)-trisphosphate

James Sneyd[a,*], Matthew Wilkins[b,1], Andreja Strahonja[c], Michael J. Sanderson[c]

[a]*Department of Mathematics, University of Michigan, 2072 East Hall, 525 East University Avenue, Ann Arbor, MI, 48109–1109, USA*
[b]*Department of Mathematics and Statistics, University of Canterbury, Christchurch, New Zealand*
[c]*Department of Physiology, University of Massachusetts Medical Center, Worcester, Massachusetts, USA*

Revision received 26 January 1998; accepted 13 February 1998

ELSEVIER

ELSEVIER

Biophysical Chemistry 72 (1998) 101–109

Biophysical Chemistry

Calcium waves and oscillations driven by an intercellular gradient of inositol (1,4,5)-trisphosphate

James Sneyd[a,*], Matthew Wilkins[b,1], Andreja Strahonja[c], Michael J. Sanderson[c]

[a]*Department of Mathematics, University of Michigan, 2072 East Hall, 525 East University Avenue, Ann Arbor, MI, 48109–1109, USA*
[b]*Department of Mathematics and Statistics, University of Canterbury, Christchurch, New Zealand*
[c]*Department of Physiology, University of Massachusetts Medical Center, Worcester, Massachusetts, USA*

Revision received 26 January 1998; accepted 13 February 1998

Abstract

In response to a local mechanical stimulus, mixed glial cells initially exhibit a propagating intercellular Ca^{2+} wave. Subsequently, cells within a zone, at a specific distance from the stimulated cell, display asynchronous intracellular Ca^{2+} oscillations. The experimental hypothesis that the initial Ca^{2+} wave could be mediated by the passive diffusion of inositol (1,4,5)-trisphosphate (IP_3) from the stimulated cell has been verified by model simulations. Further simulations with the same model also show that Ca^{2+} oscillations can only occur within model cells when the IP_3 concentration is within a specific range. Thus, this passive diffusion model predicts (a) that the IP_3 concentration gradient established in the cells following mechanical stimulation will initiate Ca^{2+} oscillations in cells in a specific zone along this gradient and (b) that different Ca^{2+} oscillatory patterns will occur within a specified oscillatory zone. Both of these predictions have been confirmed by experimental data. The failure of experimentally observed Ca^{2+} oscillations to approach synchrony or entrain indicates a low intercellular calcium permeability of about 0.1 μm/s, and further suggests that Ca^{2+} does not appear to act as a significant messenger in the initiation of these intercellular Ca^{2+} waves or oscillations. In conclusion a passive diffusion of IP_3, but not Ca^{2+}, through gap junctions remains the preferred hypothesis for the mechanism underlying mechanically-stimulated intercellular calcium waves and Ca^{2+} oscillations.

Keywords: Calcium waves; Oscillations; Intercellular gradient

1. Introduction

A wide diversity of cell types can communicate with their neighbors by means of an intercellular calcium (Ca^{2+}) wave, i.e. the propagation of an increase in intracellular Ca^{2+} concentration from cell to cell [1,2]. Intercellular Ca^{2+} waves can be initiated by a focal mechanical, electrical, or hormonal stimulus, and by propagating to numerous adjacent cells, may serve to coordinate a global cellular response. For instance, mechanical stimulation of a single ciliated tracheal epithelial cell causes an intercellular Ca^{2+} wave that propagates to surrounding cells, inducing

* Corresponding author. Fax: +1 734 7630937; e-mail: jsneyd@math.lsa.umich.edu
[1] Present address: Courant Institute, New York University, New York, NY, USA.

0301-4622/98/$19.00
PII S0301-4622(98)00126-4

an increase in ciliate beat frequency over an area much larger than that of a single cell.

Intercellular Ca^{2+} waves also propagate between different cell types. Ca^{2+} waves between airway epithelial and smooth muscle cells [3] may regulate airway caliber whereas Ca^{2+} waves propagating between glial and endothelial cells may influence the function of the blood-brain barrier [4]. Intercellular Ca^{2+} waves between glial and neurons suggest a role in information processing by neuronal networks [5–7].

In mixed glial cultures, a mechanically stimulated intercellular wave is followed by asynchronous intracellular Ca^{2+} oscillations, that are not transmitted between cells. Further, cells displaying such oscillations can still transmit an intercellular wave.

1.1. The IP_3 passive diffusion hypothesis

Over the past few years, a great deal of experimental evidence has accumulated supporting the hypothesis that mechanically-stimulated intercellular Ca^{2+} waves can result from the diffusion of inositol 1,4,5-trisphosphate (IP_3) through gap junctions [2]. According to this hypothesis (illustrated in Fig. 1), IP_3 is initially produced in a single cell in response to mechanical stimulation. This IP_3 binds to IP_3 receptors (IPR) on the endoplasmic reticulum (ER) to stimulate the release of Ca^{2+} into the cytoplasm. Although Ca^{2+} can move through gap junctions, a cellular Ca^{2+} wave is the cellular response to a diffusing bolus of IP_3, passing between cells via gap junctions [1,4].

It is important to emphasize that this diffusional hypothesis of wave propagation cannot fully account for the observed behavior of all Ca^{2+} waves. For example, the intercellular Ca^{2+} waves observed in liver lobules [8,9] in hippocampal slices [7], or the intracellular Ca^{2+} waves observed in *Xenopus* oocytes [10], propagate over large distances and cannot simply rely on the diffusion of a messenger from a single point or cell. In these cases, it is likely that a process of regeneration is required to actively propagate the wave. However, the identity of the messenger passing between cells may still be IP_3. Alternatively, Ca^{2+} waves may result from the diffusion or release of an extracellular messenger [11–13]. An analysis of these actively propagated intercellular waves is considered in a separate paper [14].

To evaluate quantitatively our experimental data describing mechanically-stimulated intercellular Ca^{2+} waves in epithelial or glial cultures, we constructed a mathematical model that simulates wave propagation [15]. As this model assumed that IP_3 moved between cells by passive diffusion through gap junctions but that Ca^{2+} did not move between cells, we have called this model the IP_3 *passive diffusion hypothesis*. Although the model is in excellent agreement with a wide range of experimental data, we have subjected it to a further series of tests. Firstly, we estimate an approximate value for the intercellular Ca^{2+} permeability and conclude that inter cellular diffusion of Ca^{2+} makes no qualitative difference to Ca^{2+} wave propagation. Secondly, we verify that a diffusive gradient of IP_3 is established between cells by examining the spatial distribution and temporal properties of Ca^{2+} oscillations induced by the propagation of a Ca^{2+} wave. A detailed description of the experimental results upon which this paper is based is presented by Strahonja and Sanderson (unpublished data).

2. The model

As the model has been presented in detail [15], we give only a brief description here. There are only minor changes from the previous presentation, mostly for the purposes of improvement and clarity. We assume that:

1. Mechanical stimulation initiates the production of IP_3 only in the stimulated cell, and that this IP_3 diffuses from cell to cell through gap junctions. As the IP_3 diffuses through the cytoplasm, it binds to IP_3 receptors on the ER to release Ca^{2+} from the ER.
2. The Ca^{2+} flux through the IPR is dependent on the cytoplasmic free Ca^{2+} concentration. In combination with IP_3, Ca^{2+} initially enhances Ca^{2+} release, but subsequently, slowly inactivates Ca^{2+} release. Thus Ca^{2+} release occurs in an autocatalytic fashion through the IPR, a process called Ca^{2+}-induced Ca^{2+} release, or CICR.
3. The flux of IP_3 through gap junctions is proportional to its concentration difference across the gap junction; similarly for Ca^{2+}.

4. IP_3 is degraded with saturable kinetics, and the Ca^{2+} released from the ER is pumped either back into the ER or out of the cell.

Let p and c denote the cytoplasmic concentrations of IP_3 and Ca^{2+}, respectively. Then, within each cell the equation for p is

$$\frac{\partial p}{\partial t}=D_p\nabla^2 p-\frac{V_p p}{k_p+p} \tag{1}$$

where D_p is the diffusion coefficient of IP_3, $\nabla^2 p$ represents the diffusion of IP_3, V_p is the maximal rate of IP_3 degradation, and k_p is the concentration at which IP_3 degradation is half-maximal.

At each cell boundary,

$$D_p\nabla p\cdot \mathbf{n}=F_p(p_+-p_-) \tag{2}$$

where p_+ and p_- denote the IP_3 concentrations on either side of the boundary, and $\mathbf{n}$ is the unit normal vector to the boundary. F_p is the permeability coefficient, with units of distance/time. Note that, although ∇p is continuous across the boundary, p is not. In our simulations we avoid any problems caused by the orientation of the boundary by solving on a regular grid aligned with the coordinate axes, and defining the cells such that all the cell boundaries are also aligned with the coordinate axes (cf. Fig. 2).

The equations for the Ca^{2+} dynamics are slightly more complicated, due to the nature of Ca^{2+} release and uptake. As Ca^{2+} is released into the cytoplasm through the IP_3 receptor (J_{flux}) or unspecified channels (J_{leak}) and is removed from the cytoplasm by the action of Ca^{2+} ATPase pumps (J_{pump}), we have the conservation equation

$$\frac{\partial c}{\partial t}=D_c\nabla^2 c+J_{flux}=J_{pump}+J_{leak} \tag{3}$$

J_{leak} is assumed to be a constant,

$$J_{leak}=\beta \tag{4}$$

J_{pump} is determined from the data of Lytton et al. [16] to be

$$J_{pump}=\frac{\gamma c^2}{k_\gamma^2+c^2} \tag{5}$$

To model J_{flux} we assume that the IP_3 receptor has four binding sites, one for IP_3 and three for Ca^{2+} (one activating, and two inactivating). Binding of IP_3 opens the receptor, and Ca^{2+} binding to the activating site further activates the receptor. Receptor inactivation occurs when Ca^{2+} is bound to either of the inactivating binding sites.

The binding of IP_3 and Ca^{2+} to the activating site is fast. The binding of Ca^{2+} to the inactivating sites is slow. It is assumed that all three different types of binding sites act independently. Thus, if we let h denote the probability that both of the inactivating sites are unoccupied, we have

$$J_{flux}=k_f\left(\frac{p}{k_\mu+p}\right)\left(\frac{c}{k_1+c}\right)h \tag{6}$$

where

$$\tau_h(c+K_4)\frac{dh}{dt}=K_4K_3-h(c^2+K_4c+K_3K_4) \tag{7}$$

This equation for h is derived in Appendix A; it is a generalized form of the original expression of Atri et al. [17].

Due to independence, the open probability of the receptor is the product of the occupation probability of each type of binding site: $p/(k_\mu + p)$ is the probability IP_3 is bound to the receptor, $c/(k_1 + c)$ is the probability Ca^{2+} is bound to the activating site. Both of these expressions assume simple Michaelis–Menten binding kinetics. The overall form of J_{flux} was chosen so as to agree with experimental data from a variety of cell types, including *Xenopus* oocytes, and rat brain synaptosomes. However, to obtain better agreement with the observed responses in glial cells, the steady state open probability curve was shifted slightly to lower Ca^{2+} concentrations. Little data is available on the IP_3 receptors of rat brain glial cells, or tracheal epithelium, the two cell types to which the model has been applied. It should be noted that this model cannot reproduce all features of the open probability curve of type I IP_3 receptors observed in lipid bilayers. For instance, recent results of Kaftan et al. [18] show that, as the background IP_3 concentration increases, the peak of the open probability curve of the type I IP_3 receptor shifts to higher calcium concentrations, a feature which is not present in our model. However, a simple theoretical analysis, not given here, shows that the opposite behavior is predicted for type III IP_3 receptors. Since the exact distribution of IP_3 receptor subtypes is not known for our cell types, it is not clear

Table 1
Glossary of model parameters

$k_1 = 0.35\ \mu M$	$k_f = 6\ \mu M/s$
$K_3 = 2.0\ \mu M$	$K_4 = 0.05\ \mu M$
$k\gamma = 0.135\ \mu M$	$k_\mu = 0.1\ \mu M$
$k_p = 1\ \mu M$	$V_p = 0.04\ \mu M/s$
$\gamma = 0.75\ \mu M/s$	$\beta = 0.00375\ \mu M/s$
$\tau_h = 1$ S	$D_p = 300\ \mu m^2/s$
$D_c = 20\ \mu m^2/s$	$F_p = 1\ \mu m/s$

k_1, K_3 and K_4 were chosen so as to obtain the correct steady state open probability of the IP_3 receptor, as measured in *Xenopus* oocytes (Parys et al. [21]; Atri et al. [17]. γ and β were chosen to give physiologically reasonable resting Ca^{2+} concentrations, and V_p, k_p and k_μ, were taken from Sneyd et al. [15]. D_p and D_c were taken from Allbritton et al. [22]. k_f is just a scaling factor. The value for τ_h was chosen between the values used by Atri et al. [17] and Sneyd et al. [15], while the value for F_p is based on the previous modeling work of Sneyd et al. [15].

what changes should be made to the model to incorporate this shift of the open probability curve. Preliminary computations with other models indicate that this shifting of the open probability curve has no effect on the model predictions presented here.

At each cell boundary,

$$D_c \nabla c \cdot \mathbf{n} = F_c(c_+ - c_-) \tag{8}$$

where, as before, c_+ and c_- denote the Ca^{2+} concentrations on either side of the boundary, and $\mathbf{n}$ is the unit normal vector to the boundary. F_c is the permeability coefficient for Ca^{2+}.

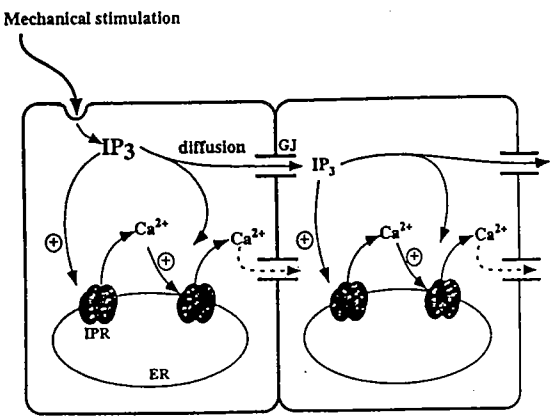

Fig. 1. Schematic diagram of the passive diffusion hypothesis for the propagation of intercellular Ca^{2+} waves. IPR, IP_3 receptor/Ca^{2+} channel; ER, endoplasmic reticulum; GJ, gap junction. The + sign denotes Ca^{2+}-induced Ca^{2+} release.

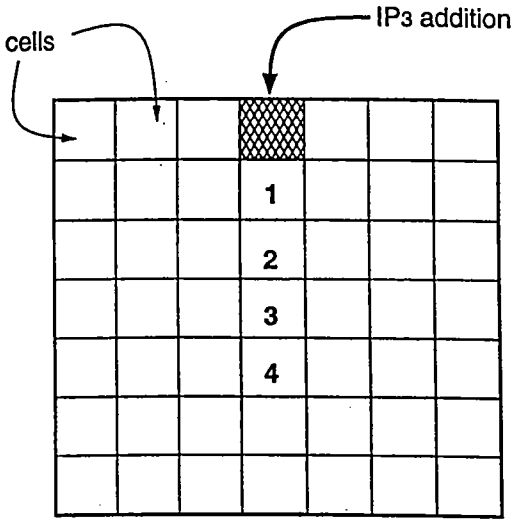

Fig. 2. Diagram of the grid upon which the numerical simulations were performed. Each cell was 24 μm × 24 μm. The boundary conditions around the edge of the grid were no-flux. Numbers represent cells analyzed in subsequent figures.

Values for the model parameters are given in Table 1.

2.1. Numerical methods

The model equations were solved by the Douglas–Rachford ADI algorithm on a grid of 7 × 7 cells, each containing 16 × 16 gridpoints. Since each cell is approximately 15–25 μm in diameter, this discretization corresponds to about two grid points for every 3 μm.

Simulations with more grid points in each cell showed no significant differences from the results given here (computations not shown). Initially, c and h were set to their steady state values corresponding to $p = 0$. To simulate a mechanical stimulation IP_3 was added at a rate of 1 μM/s for the first 15 s, to the shaded cell in Fig. 2.

3. Results

3.1. Spatially-independent oscillations

If the IP_3 concentration is steadily increased in all cells, a situation that precludes the diffusion of IP_3 or Ca^{2+} between cells, each model cell will exhibit Ca^{2+} oscillations but only within a specific physiological

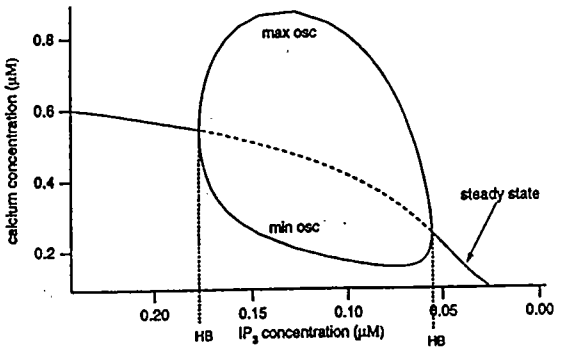

Fig. 3. Bifurcation diagram of a model cell (in the absence of diffusion of p or c). Stable steady states are denoted by solid lines, and unstable ones by dashed lines. At the points labeled HB, the steady state changes stability in a Hopf bifurcation, leading to the existence of a branch of stable limit cycles. Note that Ca^{2+} oscillations occur only for an intermediate range of IP_3 concentrations.

range of IP_3 concentrations (Fig. 3). Treating p as a bifurcation parameter, a branch of stable limit cycles appears via a supercritical Hopf bifurcation at $P = 0.06$ μM and disappears at a supercritical Hopf bifurcation at $P = 0.18$ μM. In other words, intracellular Ca^{2+} oscillations exist only when $[IP_3]$ is between 0.06 and 0.18 μM. The importance of this fact will be apparent later.

3.2. The intercellular diffusion of calcium

To evaluate the role of intercellular Ca^{2+} diffusion on the Ca^{2+} waves and subsequent Ca^{2+} oscillations, we performed four simulations with different values of F_c, the intercellular calcium permeability (Fig. 4). The $[Ca^{2+}]$, measured at the middle grid point of the indicated cell (cf. Fig. 2), is plotted as a function of time from three cells. The mechanical stimulation was initiated at time 0. When $F_c = 0$ μm/s the Ca^{2+} oscillations induced by the Ca^{2+} wave remain asynchronous, and show no phase locking. These features are preserved when $F_c = 0.1$ μm/s. However, when $F_c = 1$ μm/s, the Ca^{2+} oscillations begin to become synchronized just prior to the time at which the Ca^{2+} oscillations start to subside. When $F_c = 10$, the Ca^{2+} oscillations of each cell become synchronized quick-

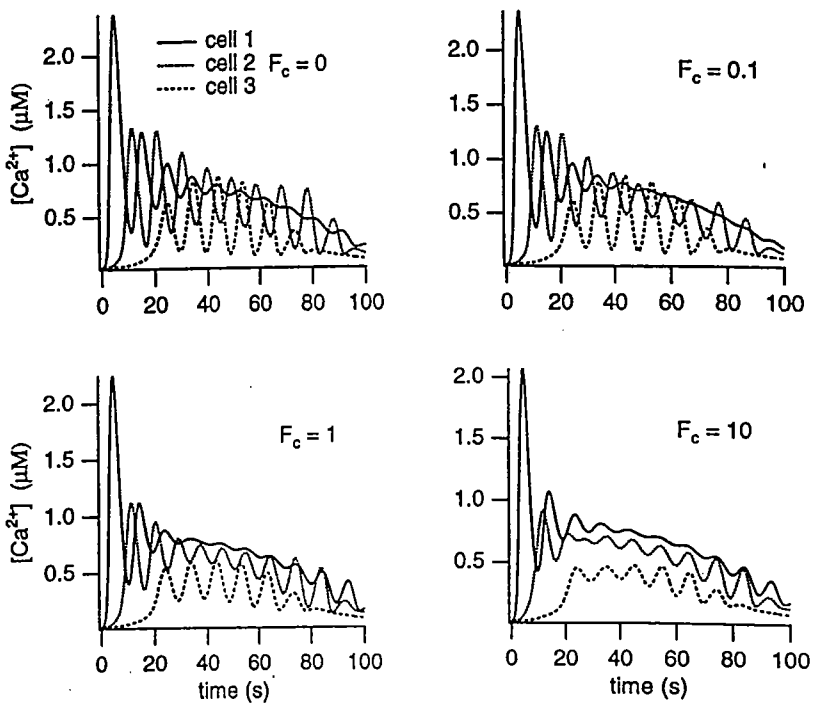

Fig. 4. Synchronization of intracellular Ca^{2+} oscillations by intercellular Ca^{2+} diffusion. In each panel, the first peak of each trace corresponds to the intercellular wave. When F_c *is* high, the intracellular oscillations after the wave quickly synchronize. Since this is not observed experimentally, we conclude that F_c must be between 0.1 and 1 μm/s.

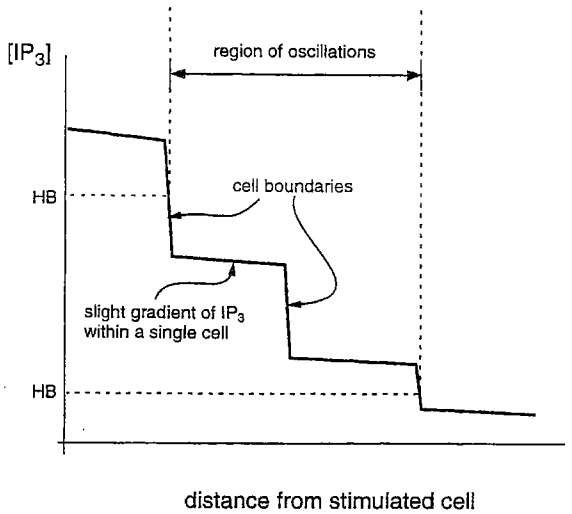

Fig. 5. Schematic diagram (not to scale) of the spatial gradient of IP_3 set up by the mechanical stimulation. Since oscillations occur only when $[IP_3]$ is in an intermediate range, it follows that oscillations will be seen only in a band a certain distance from the stimulated cell. HB denotes the position of the Hopf bifurcations shown in Fig. 3.

ly. However, experimental data does not show signs of synchrony between neighboring cells [19, Strahonja and Sanderson, unpublished data]. Consequently, it follows that F_c must be less than 1 μm/s, and probably closer to 0.1 μm/s. This estimate agrees well with a previous estimate of 0.1 μm/s obtained by measuring Ca^{2+} wave speeds in the intact liver [14].

When $F_c = 0.1$ μm/s, diffusion of Ca^{2+} also has almost no effect on the properties of the intercellular wave (computations not shown). Therefore, we conclude that intercellular Ca^{2+} diffusion is not likely to be a significant modulator of intercellular Ca^{2+} waves. This prediction is unaffected by the intercellular permeability to IP_3, as the model assumes that the intracellular oscillations are coupled by the diffusion of Ca^{2+}, not IP_3, between cells. This is because Ca^{2+} oscillations occur at a constant level of IP_3; for instance, when $F_p = \infty$ and $F_c = 0$ the intracellular oscillations are uncoupled. It follows that the coupling of intracellular Ca^{2+} oscillations occurs by a different mechanism than that causing the intercellular wave.

3.3. The spatial gradient of IP_3

The passive diffusion hypothesis predicts that a mechanical stimulation sets up a spatial gradient o IP_3 across the culture. Since Ca^{2+} oscillations occu only when $[IP_3]$ is between the two Hopf bifurcatio points (labeled HB in Fig. 3), the gradient of IP_3 established by the mechanical stimulation, predict that intracellular Ca^{2+} oscillations will occur in zone of cells at a specific distance from the stimulate cell, as illustrated schematically in Fig. 5. This pre diction was confirmed by the experimental data (Fig 6). Furthermore, the IP_3 gradient predicts that cell closer to the stimulated cell will show a differen oscillatory pattern than cells further from the stimulated cell.

According to the model (Fig. 7), the cell closest t the stimulated cell (cell 1) will show some initia

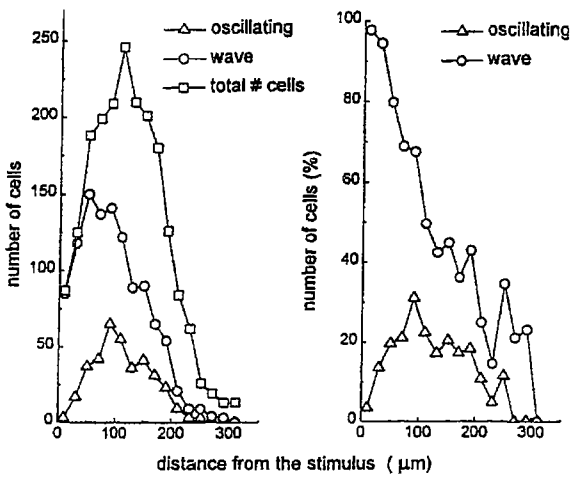

Fig. 6. Experimental data, showing how Ca^{2+} oscillations induced by a Ca^{2+} wave occur mostly in a zone around the stimulated cell. The data was collected from mixed glial cell cultures; full details are given in Strahonja and Sanderson (unpublished data). Primary cultures of mixed glial cells were prepared from the brains of 1–2-day-old rat pups, and immunofluorescence staining for cell specific markers was performed to quantify the different cell types in the culture. Mechanical stimulation of a single cell was performed by distorting the cell surface with a micropipette attached to a piezoelectric element, as described in Charles et al. [19]. Cultured cells were loaded with the Ca^{2+}-sensitive dye fura-2, and the calcium fluorescence was recorded on an optical memory disc recorder for later analysis. The left panel shows the number of cells that exhibit an intercellular wave, that oscillate after the wave, and the total number of cells, all as a function of distance from the stimulated cell. The right panel shows the same data, but this time the numbers of cells that exhibit a wave or that oscillate are expressed as percentages of the total number of cells. The data was taken from 35 experiments, in which a total of 1988 cells were analyzed.

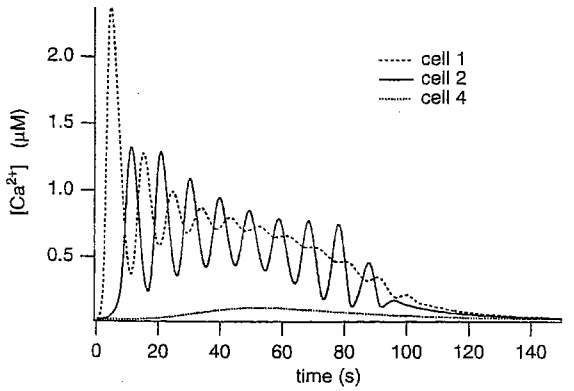

Fig. 7. Response of the model to the addition of IP_3 to the shaded cell in Fig, 2. IP_3 was added at 1 μM/s for 15 s, starting at time 0, and the Ca^{2+} responses were measured from cells 1, 2 and 4, as indicated by the labels in Fig. 2.

oscillations in $[Ca^{2+}]$, but these oscillations die away leaving $[Ca^{2+}]$ at a high level that slowly declines. Cells further away from the stimulated cell (cell 2) will show continuous oscillations, while farther away (cell 4) very little rise in $[Ca^{2+}]$ is seen in response to the stimulation. Again, these prediction were confirmed by experimental data (Strahonja and Sanderson, unpublished data). In experiments, a number of oscillatory patterns emerge, one of which is an initial smaller oscillation, followed by a plateau which gradually decreases (Fig. 8); we call this a fast type or F pattern. A second commonly seen oscillatory pattern is one in which the cell exhibits regular oscillations; we call this a continuous type or C pattern. Examination of a number of mechanically-stimulated intercellular waves shows that type F oscillations tend to occur closer to the stimulated cells than do type C oscillations, as is predicted by the model (Strahonja and Sanderson, unpublished data).

Modulation of the spatial gradient of IP_3 would be predicted to change the oscillatory pattern. This can be achieved by the addition of acetylcholine (ACh) to the culture to produce an approximately uniform rise in $[IP_3]$ across the culture. This change in IP_3 concentration will shift the band of oscillating cells. The model predicts that addition of 0.3 μM IP_3 uniformly across the culture at 40 s after mechanical stimulation changes cell 4 from a non-responsive cell to a C-type oscillator, and changes cell 2 from a C-type oscillator to an F-type (Fig. 9). The change in cell 4 results from the fact that the $[IP_3]$ in cell 4 is now large enough to cause oscillations. Similarly, the $[IP_3]$ in cell 2 has become too large to support oscillations (the upper Hopf bifurcation point is crossed.) Again, these predictions are confirmed by experimentation (Fig. 10).

Another example of how modulation of the IP_3 gradient can change the oscillatory properties can be seen when a background concentration of 0.05 μM IP_3 is added to the model before mechanical stimulation. In this case, the band of C-type oscillations moves further away from the stimulated cell. As can be seen from Fig. 11, addition of background IP_3 turns cell 4 into a C-type oscillator, while cell 2 behaves in a manner intermediate between an F-type and a C-type oscillator. In addition, the oscillations occur later in the presence of a background IP_3 concentration.

3.4. F-type oscillations

An intuitive prediction of the passive diffusion hypothesis is that if F-type oscillations occur when the $[IP_3]$ gets too high, C-type oscillations should occur as the $[IP_3]$ decreases to lower values. Surprisingly, F-type oscillations followed by C-type oscillations were not observed in either experiments or model simulations. One explanation for this apparent contradiction is that the dynamic nature of the decrease in $[IP_3]$ prevents the establishment of Ca^{2+} oscillations (i.e. $[IP_3]$ is changing too fast).

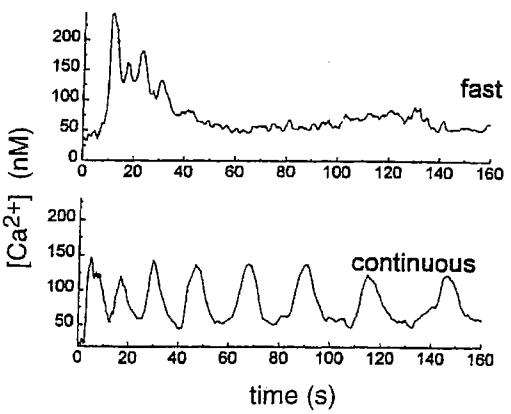

Fig. 8. Experimental data from mixed glial cell cultures, showing two typical responses. Closer to the stimulated cell, the response tends to show an initial oscillatory period, followed by a long plateau which slowly declines (upper panel). A similar response is seen in cell 1 in the numerical simulations (cf. Fig. 7). Further from the stimulated cell, the response is more like a continuous oscillation, as is seen in cell 2 in the model (lower panel). Data taken from Strahonja and Sanderson, unpublished data.

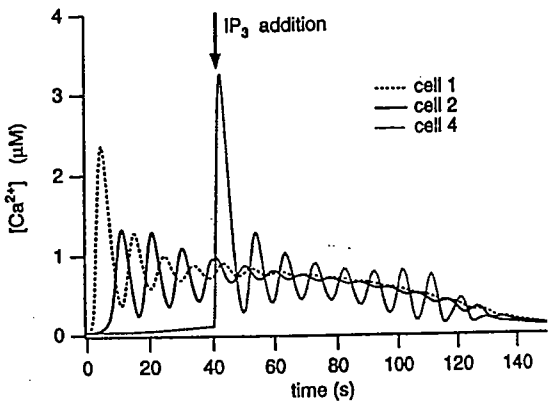

Fig. 9. Model simulations, showing the response to an addition of IP_3, 40 s after a mechanical stimulation. Cell 4 becomes oscillatory, while the oscillations in cell 2 disappear.

Since this feature is insensitive to noise (as it occurs in experiment also) it is unlikely that it can be explained by the work of Baer et al. [20], who studied the delayed onset of oscillations after passage through a Hopf bifurcation. However, further investigation is needed to confirm this aspect of the hypothesis.

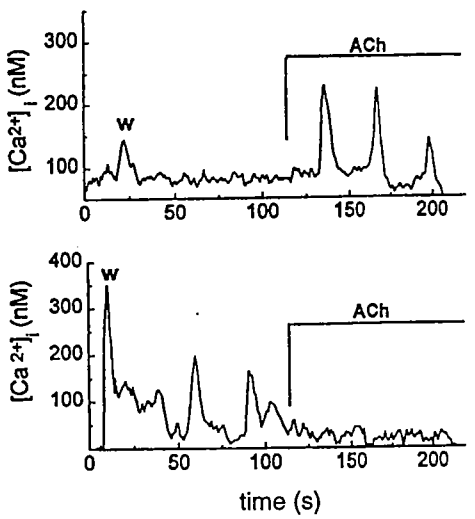

Fig. 10. Experimental data from mixed glial cell cultures, showing the responses to addition of ACh after a mechanical stimulation. Further from the stimulated cell, the ACh tends to initiate oscillations (upper panel), while, closer to the stimulated cell, the ACh tends to eliminate oscillations (lower panel), as predicted by the model results presented in Fig. 9. Data taken from Strallonja and Sanderson, unpublished data.

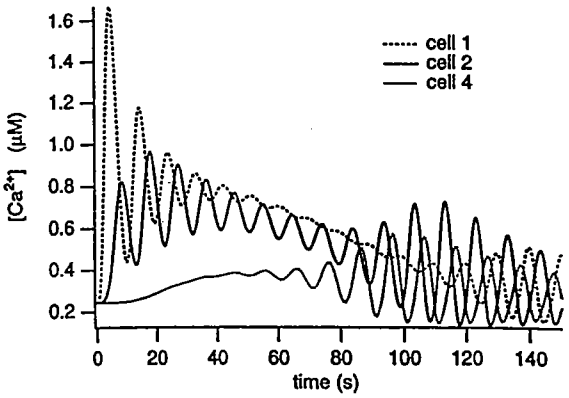

Fig. 11. Model simulations of a mechanical stimulation in the presence of a background IP_3 concentration of 0.05 μM. Oscillations occur in cell 4, but at a later time, while the behavior of cell 2 is intermediate between F-type and C-type oscillations.

4. Conclusions

A mathematical model, describing the passive diffusive hypothesis for intercellular Ca^{2+} signaling is presented. Previous work demonstrated that this model accurately predicted the experimental Ca^{2+} wave parameters of arrival time and intercellular delay as well as the peak Ca^{2+} concentrations achieved [15]. Here we demonstrate, by comparison with experimental data, that this same model accurately predicts (a) that Ca^{2+} oscillations induced by a Ca^{2+} wave occur in a cellular zone at a specific distance from the stimulated cell, and (b) that the position of this zone is dependent on the background IP_3. In addition, the model predicts that with an intercellular Ca^{2+} permeability in the order of 0.1 μm/s the intercellular diffusion of Ca^{2+} is not a major modulator of the intercellular wave.

Acknowledgements

This work was supported by NIH grant HL49288 to

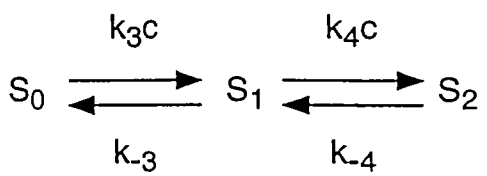

Fig. 12. Binding diagram of the inactivation binding site of the IP_3 receptor.

MJS and NSF grant DMS-9706565 and NIH grant R01 GM56126 to JS. MW was supported by the Marsden Fund of the Royal Society of New Zealand, and by the University of Canterbury, New Zealand.

Appendix A Derivation of the equation for h

We assume that the IP_3 receptor must bind two Ca^{2+} ions to be inactivated; the binding diagram of the inactivation site is given in Fig. 12. Assuming mass action kinetics, we get

$$\frac{dS_1}{dt} = k_3 c S_0 - k_3 S_1 + k_{-4} S_2 - k_4 c S_1 \tag{9}$$

$$\frac{dS_2}{dt} = -k_{-4} S_2 + k_4 c S_1 \tag{10}$$

Due to the law of conservation, $S_0 + S_1 + S_2 = 1$ the equation for S_0 is not needed. Assuming that binding of the second inactivating Ca^{2+} is much faster than binding of the first (and thus the receptor shows extreme positive cooperativity), we get the quasi-steady state relation $cS_1 = K_4 S_2$, where $K_4 = k_{-4}/k_4$. Hence, letting $h = S_0$, we get

$$\tau_h (c + K_4) \frac{dh}{dt} = k_3 k_4 - h\,(c^2 + K_4 c + K_3 K_4) \tag{11}$$

where $K_3 = k_{-3}/k_3$ and $\tau_h = 1/k_3$.

References

[1] M.J. Sanderson, A.C. Charles, S. Boitano, E.R. Dirksen, Mol. Cell. Endocrinol. 98 (1994) 173.
[2] M.J. Sanderson, News Physiol. Sci. 11 (1996) 262.
[3] L. Moore, M.J. Sanderson, J. Cell Sci., (1997) in press.
[4] L. Leybaert, K. Paemeleire, A. Strahonja, M.J. Sanderson (1997) in press.
[5] A.C. Charles, Dev. Neurosci. 16 (1994) 196.
[6] M. Nedergaard, Science 263 (1994) 1768.
[7] J.W. Dani, S.J. Smith, Ciba Found. Symp. 188 (1995) 195.
[8] M.H. Nathanson, A.D. Burgstahler, A. Mennone, M.B. Fallon, C.B. Gonzalez, J.C. Saez, Am. J. Physiol. 269 (1995) G167.
[9] L.D. Robb-Gaspers, A.P. Thomas, J. Biol. Chem. 270 (1995) 8102.
[10] D.E. Clapham, J. Sneyd, Adv. Second Messenger Phosphoprotein Res. 30 (1995) 1.
[11] Y. Osipchuk, M. Cahalan, Nature 359 (1992) 241.
[12] T.D. Hassinger, P.B. Guthrie, P.B. Atkinson, M.V. Bennett, S.B. Kater, Proc. Natl. Acad. Sci. USA 93 (1996) 13268.
[13] M.K. Frame, A.W. de Feijter, Exp. Cell Res. 230 (1997) 197.
[14] M. Wilkins, J. Sneyd, J. Theor. Biol. (1998) in press.
[15] J. Sneyd, B. Wetton, A.C. Charles, M.J. Sanderson, Am. J. Physiol. (Cell Physiol.) 268 (1995) C1537.
[16] J. Lytton, M. Westlin, S.E. Burk, G.E. Shull, D.H. MacLennan, J. Biol. Chem. 267 (1992) 14483.
[17] A. Atri, J. Amundson, D. Clapham, J. Sneyd, Biophys. J. 65 (1993) 1727.
[18] E.J. Kaftan, B.E. Ehrlich, J. Watras, J. Gen. Physiol. 110 (1997) 529.
[19] A.C. Charles, J.E. Merrill, E.R. Dirksen, M.J. Sanderson, Neuron 6 (1991) 983.
[20] S. Baer, T. Erneux, J. Rirlzel, SIAM J. Appl. Math. 49 (1989) 55.
[21] J.B. Parys, S.W. Semett, S. DeLisle, P.M. Snyder, M.J. Welsh, K.P. Campbell, J. Biol. Chem. 267 (1992) 18776.
[22] N.L. Allbritton, T. Meyer, L. Stryer, Science 258 (1992) 1812.

Intercellular Ca^{2+} Signaling Between Glial and Endothelial Cells

Michael J. Sanderson, Koen Paemeleire*, Andreja Strahonja and Luc Leybaert*
*Department of Physiology, University of Massachusetts Medical Center, Worcester, MA, USA and *Laboratory of Physiology, University of Gent, Gent, Belgium*

Abstract. To explore the hypothesis that intercellular Ca^{2+} waves are a mechanism of heterotypic cell communication and convey information across biological interfaces, such as the blood-brain barrier, intercellular Ca^{2+} signaling was investigated in co-cultures of glial and endothelial cells. Mechanically-initiated, intercellular Ca^{2+} waves were found to propagate from glial to endothelial cells or vice versa. To determine if glial-endothelial Ca^{2+} waves propagate by the intercellular diffusion of inositol trisphosphate (IP_3) through gap junctions, the multicellular Ca^{2+} responses to increases in intracellular concentrations of IP_3 and Ca^{2+}, generated by the photolysis of caged compounds, were examined. Caged-IP_3 was microinjected into a single cell but was free to diffuse to adjacent cells. Photolytic release of IP_3 in the injected cell or in a distal, non-injected cell, initiated an intercellular Ca^{2+} wave. By contrast, photolysis of caged-Ca^{2+} induced an increase in $[Ca^{2+}]_i$ in the illuminated cell but did not initiate an intercellular Ca^{2+} wave. These results indicate that 1) intercellular Ca^{2+} waves propagate over short distances by the intercellular diffusion of IP_3 via gap junctions, 2) Ca^{2+} itself does not serve as an intercellular messenger in these cells and 3) Ca^{2+} waves may contribute to the regulation of blood-brain barrier function.

1. Introduction: Intercellular Ca^{2+} Waves

Intercellular Ca^{2+} waves occur in a diversity of tissues and consist of increases in intracellular Ca^{2+} concentration ($[Ca^{2+}]_i$) that propagate between adjacent cells[1, 2]. Ca^{2+} waves also propagate between different cell types, e.g. between glia and neurons [3-5] or between airway epithelial and smooth muscle cells [6]. Thus, intercellular Ca^{2+} waves appear to be an important mechanism of heterotypic cell communication and may carry information across biological interfaces that are composed of different cell types such as the blood-brain barrier. To explore this hypothesis, intercellular Ca^{2+} signaling was investigated in co-cultures of glial and endothelial cells. In co-culture, endothelial cells often were surrounded by glial cells and together formed an easily recognized cell interface or boundary. Mechanical stimulation of a single glial cell near the cell boundary induced an intercellular Ca^{2+} wave that propagated from the glial cells, across the boundary, and through neighboring endothelial cells (Fig. 1). A prolonged delay in wave propagation was observed at the cell boundary. Mechanical stimulation of an endothelial cell induced the reverse response.

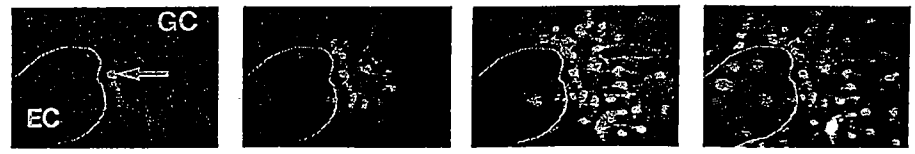

Figure 1: An intercellular Ca^{2+} wave evoked by mechanical stimulation (arrow) of a single glial cell (GC) propagates to adjacent glial cells, crosses the cellular interface (white line) and propagates through neighboring endothelial cells (EC). Images presented represent the changes in $[Ca^{2+}]_i$ as measured with fluo-3.

a) The passive diffusion hypothesis of intercellular Ca^{2+} wave propagation

The mechanism of mechanically-induced intercellular Ca^{2+} waves has been investigated extensively in epithelial and glial cells [7, 8] and these studies have led to the "passive diffusion" hypothesis [2]. In brief, this hypothesis states that Ca^{2+} waves propagate from cell to cell by the diffusion of inositol trisphosphate (IP_3) through gap junctions. As IP_3 enters each cell it releases Ca^{2+} from intracellular stores in the endoplasmic reticulum via the IP_3 receptor. Because this process is amplified by Ca^{2+}-induced Ca^{2+} release (CICR), an IP_3 concentration gradient can stimulate a near maximal Ca^{2+} response in each cell as long as the $[IP_3]_i$ exceeds the activation threshold of the IP_3 receptor (Fig. 2).

The reliance of wave propagation on a diffusive rather than a regenerative process was predicted by the limited propagation distances (5-15 cells in any direction) of mechanically-stimulated Ca^{2+} waves. A role for gap junctions was implicated by the circuitous path and propagation delays at cell borders of the Ca^{2+} wave [7, 9] and was confirmed by the inability of C6 glioma cells that lack connexin 43 gap junctions to propagate Ca^{2+} waves. C6 glioma cells transfected to express connexin 43 displayed dye-coupling and propagated Ca^{2+} waves [10]. Gap junction blockers inhibited wave propagation [6, 7, 11] while agonists that influenced gap junction conductivity altered the extent of wave propagation [12].

The idea that IP_3 was the diffusing messenger was indicated by the facts that Ca^{2+} waves a) are propagated by the release of intracellular Ca^{2+} stores, b) are initiated by iontophoresis of IP_3 into a cell [7, 8] and c) are inhibited by heparin, an antagonist of the IP_3 receptor [13]. The diffusion hypothesis requires that IP_3 is produced only in the stimulated cell and the inhibition of Ca^{2+} waves by U73122, a phospholipase C (PLC) antagonist [14], suggests that mechanical stimulation may activate PLC [7, 15]. Although Ca^{2+} is a potential intercellular messenger and can pass though gap junctions [16], Ca^{2+} does not appear to play a major role as an intercellular messenger. Ca^{2+} waves can be initiated without an increase in $[Ca^{2+}]_i$ in the stimulated cell [7] and can propagate similar distances when the elevation of $[Ca^{2+}]_i$ is reduced by dantrolene, an inhibitor of CICR [17]. Furthermore, Ca^{2+} waves themselves can initiate asynchronous Ca^{2+} oscillations but the Ca^{2+} elevation associated with the oscillations does not initiate Ca^{2+} waves even though gap junction communication is present [8, 13, 18]. In comparison to IP_3, Ca^{2+} is a poor candidate for a long range intercellular messenger because its diffusion rate is greatly impaired by cytoplasmic Ca^{2+} buffering proteins [19].

The diffusion hypothesis also explains variations in experimentally observed Ca^{2+} waves. Because the characteristics of Ca^{2+} waves are based on the Ca^{2+} signaling machinery of the each cell, variations in PLC activity, Ca^{2+} stores, IP_3 receptor sensitivity and distribution, and the extent of gap junction coupling will all influence Ca^{2+} wave initiation and propagation. However, in certain preparations of glial cells, brain slices and liver lobules, Ca^{2+} waves can travel over hundreds [20, 21] or thousands of cells [22, 23]. The propagation of long-distance Ca^{2+} waves cannot be explained by diffusion alone and probably requires some form of regenerative process that acts in combination with a diffusive process.

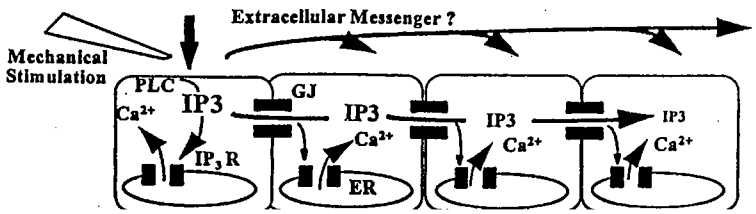

b) Ca^{2+} wave propagation by the diffusion of an extracellular messenger

In certain cases, intercellular Ca^{2+} waves associated with mast, glial, liver and insulinoma cells [3, 21, 24-26] involve the release and diffusion of an extracellular messenger (Fig. 2). The messenger (e.g. ATP in mast cells) stimulates adjacent cells via membrane receptors to release internal Ca^{2+} stores and to propagate Ca^{2+} waves without cell contact. Although an extracellular fluid flow biases the Ca^{2+} wave propagation in one direction in a variety of cell types, a limited amount of upstream propagation remains indicating that intercellular diffusion may also occur simultaneously [11]. In mast cells, the ATP is released by each cell but it is not clear if a regenerative process also occurs in other cell types or if a messenger is released just from the initiating cell. An involvement of extracellular ATP in Ca^{2+} waves of epithelial cells was ruled out because Ca^{2+} wave propagation was not influenced by an external fluid flow or by suramin, an antagonist of purinergic receptors [27]. A combination of intercellular and extracellular messenger diffusion may help explain why some waves propagate very large distances.

2. Results: The intercellular messenger

To test the hypothesis that IP_3 acts as an intercellular messenger between glial and endothelial cells, the effect of increasing $[IP_3]_i$ in a single cell by the photolysis of caged-IP_3 was examined. Based on the premise that caged-IP_3 (MW 635 Daltons) diffuses through gap junctions (permeability <1000 Daltons) in a manner similar to IP_3 (MW 437 Daltons) [28], caged-IP_3 should diffuse through a cell culture from a single injected cell (Fig. 3). Caged-IP_3 can be indirectly detected when exposed to UV light; caged-IP_3 liberates active IP_3 which in turn releases intracellular Ca^{2+} and this can be detected with the Ca^{2+}-specific fluorescent dye fluo-3.

a) Photolysis of Caged-IP_3

Following the pressure microinjection of a glial cell with caged-IP_3, a focused beam of UV light was used to illuminate briefly *(flash)* the injected cell. A one to two second UV flash increased $[Ca^{2+}]_i$ in the flashed cell and initiated an intercellular Ca^{2+} wave that propagated to adjacent glial cells up to 80 μm away. The propagation distance of the Ca^{2+} wave was dependent on the duration of the UV flash. This indicates that only a limited amount of IP_3 is released in the exposed cell and that a Ca^{2+}-dependent regeneration of IP_3 does not occur. Similar Ca^{2+} waves were induced by photolysis in endothelial cells but the distance travelled was generally smaller, perhaps due to differences in gap junctional coupling or sensitivity to IP_3.

Approximately 10 minutes, but up to two hours, after microinjection of caged-IP_3, a UV flash focused on a non-injected glial cell up to 100 μm away from the injected cell again evoked an increase in $[Ca^{2+}]_i$ and initiated an intercellular Ca^{2+} wave (Fig. 4). These results indicate that caged-IP_3 had reached the distal cells by diffusion through the inter-

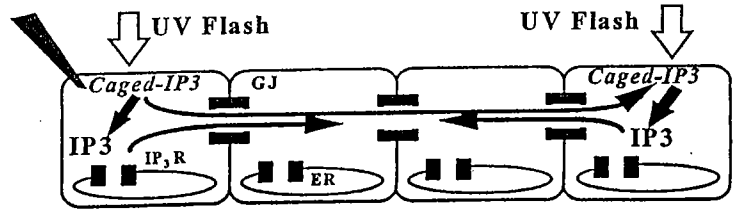

Figure 4: An intercellular calcium wave initiated by the photolytic release of IP_3 (long arrow) from caged-IP_3 in a distal, non-injected cell. Position of injected cell is indicated by the short arrow.

vening cells. The charged phosphate groups of caged-IP_3 and the retention of caged-IP_3 in the cells after two hours makes it unlikely that caged-IP_3 reached the distal cells by leakage across cell membranes. Furthermore, the ability to initiate multiple waves from the same cell by successive flashes indicates that the cell is replenished with caged-IP_3 from surrounding cells. A UV flash applied to cells that did not contain caged-IP_3 did not initiate any changes in $[Ca^{2+}]_i$.

Ca^{2+} waves, initiated by the photolysis of caged-IP_3, also propagated from endothelial cells to glial cells. In this case, caged-IP_3 was injected into a glial cell and allowed to diffuse to a distal endothelial cell. Interestingly, a Ca^{2+} wave initiated by photolysis in a glial cell did not propagate into adjacent endothelial cells. This uni-directional communication of a Ca^{2+} wave can be explained by either retification of gap junction permeability for IP_3, a faster rate of IP_3 metabolism or a different sensitivity of the Ca^{2+} signaling structures of the cell.

b) Photolysis of Caged-Ca^{2+}

Because the photolysis of caged-IP_3 increases the $[Ca^{2+}]_i$, the possibility that Ca^{2+} is initiating the Ca^{2+} waves remains. To test this hypothesis, experiments were performed with caged-Ca^{2+}, a photosensitive Ca^{2+} buffer (NP-EGTA) that releases Ca^{2+} upon exposure to UV light [29]. All cells were loaded with an ester form of caged-Ca^{2+} and when a UV flash was applied to a single cell, an increase in $[Ca^{2+}]_i$ was observed only in the flashed cell. By contrast, mechanical stimulation of the same cell evoked an intercellular Ca^{2+} wave indicating that the cells were capable of cell communication and that the caged-Ca^{2+} present in adjacent cells did not prevent Ca^{2+} wave propagation. The increases in $[Ca^{2+}]_i$ in the flashed cell were comparable, as judged by relative changes in dye fluorescence, with those induced by the photolytic release of IP_3. The increase in Ca^{2+} in only the flashed cell also confirmed, because all cells contained caged-Ca^{2+}, that the UV light flash was restricted to one cell.

3. Conclusions

We conclude 1) that intercellular diffusion of IP_3 through gap junctions can mediate the limited propagation of intercellular Ca^{2+} waves, 2) that Ca^{2+} does not act as an intercellular messenger in these Ca^{2+} waves and 3) that gap junction-mediated intercellular Ca^{2+} signaling occurs between endothelial and glial cells. We speculate that intercellular Ca^{2+} waves may serve as a regulatory signal in the blood-brain barrier.

This work was supported by NIH grant HL 49288 to MJS and the Belgium NFWO

References

[1] M.J. Sanderson *et al.*, Mechanisms and function of intercellular calcium signaling, *Mol Cell Endocrinol*, 98 (1994) 173-187.

[2] M.J. Sanderson, Intercellular waves of communication, *News Physiol Sci*, 11 (1996) 262-269.

[3] A.C. Charles, Glia-neuron intercellular calcium signaling, *Dev Neurosci*, 16 (1994) 196-206.

[4] M. Nedergaard, Direct signaling from astrocytes to neurons in cultures of mammalian brain cells, *Science*, 263 (1994) 1768-1771.

[5] E.A. Newman and K.R. Zahs, Calcium waves in retinal glial cells, *Science*, 275 (1997) 844-847.

[6] L. Moore and M.J. Sanderson, Intercellular Ca^{2+} signaling between airway epithelial and smooth muscle cells, *J Cell Sci*, Submitted (1997).

[7] M.J. Sanderson *et al.*, Mechanical stimulation and intercellular communication increases intracellular Ca^{2+} in epithelial cells, *Cell Regul*, 1 (1990) 585-596.

[8] A.C. Charles *et al.*, Intercellular signaling in glial cells: calcium waves and oscillations in response to mechanical stimulation and glutamate, *Neuron*, 6 (1991) 983-992.

[9] M.J. Sanderson *et al.*, Intercellular communication between ciliated cells in culture, *Am J Physiol*, 254 (1988) C63-74.

[10] A.C. Charles *et al.*, Intercellular calcium signaling via gap junctions in glioma cells, *J Cell Biol*, 118 (1992) 195-201.

[11] L. Venance *et al.*, Mechanism involved in initiation and propagation of receptor-induced intercellular calcium signaling in cultured rat astrocytes, *J Neurosci*, 17 (1997) 1981-1992.

[12] M.O. Enkvist and K.D. McCarthy, Astroglial gap junction communication is increased by treatment with either glutamate or high K^+ concentration, *J Neurochem*, 62 (1994) 489-495.

[13] S. Boitano *et al.*, Intercellular propagation of calcium waves mediated by inositol trisphosphate, *Science*, 258 (1992) 292-295.

[14] M. Hansen *et al.*, A role for phospholipase C activity but not ryanodine receptors in the initiation and propagation of intercellular calcium waves, *J Cell Sci*, 108 (1995) 2583-2590.

[15] J.A. Felix *et al.*, Stretch increases inositol 1,4,5-trisphosphate concentration in airway epithelial cells, *Am J Respir Cell Mol Biol*, 14 (1996) 296-301.

[16] J.C. Saez *et al.*, Hepatocyte gap junctions are permeable to the second messenger, inositol 1,4,5-trisphosphate, and to calcium ions, *Proc Natl Acad Sci U S A*, 86 (1989) 2708-2712.

[17] A.C. Charles *et al.*, Mechanisms of intercellular calcium signaling in glial cells studied with dantrolene and thapsigargin, *Glia*, 7 (1993) 134-145.

[18] A. Strahonja and M.J. Sanderson, Intracellular Ca^{2+} oscillations induced in glial by intercellular Ca^{2+} waves, Submitted (1997).

[19] N.L. Allbritton and T. Meyer, Localized calcium spikes and propagating calcium waves, *Cell Calcium*, 14 (1993) 691-697.

[20] A.H. Cornell-Bell and S.M. Finkbeiner, Ca^{2+} waves in astrocytes, *Cell Calcium*, 12 (1991) 185-204.

[21] T.D. Hassinger *et al.*, An extracellular signaling component in propagation of astrocytic calcium waves, *Proc Natl Acad Sci U S A*, 93 (1996) 13268-13273.

[22] M.H. Nathanson *et al.*, Ca^{2+} waves are organized among hepatocytes in the intact organ, *Am J Physiol*, 269 (1995) G167-171.

[23] L.D. Robb-Gaspers and A.P. Thomas, Coordination of Ca^{2+} signaling by intercellular propagation of Ca^{2+} waves in the intact liver, *J Biol Chem*, 270 (1995) 8102-8107.

[24] Y. Osipchuk and M. Cahalan, Cell-to-cell spread of calcium signals mediated by ATP receptors in mast cells, *Nature*, 359 (1992) 241-244.

[25] D. Cao *et al.*, Mechanisms for the coordination of intercellular calcium signaling in insulin-secreting cells, *J Cell Sci*, 110 (1997) 497-504.

[26] M.K. Frame and A.W. de Feijter, Propagation of mechanically induced intercellular calcium waves via gap junctions and ATP receptors in rat liver epithelial cells, *Exp Cell Res*, 230 (1997) 197-207.

[27] M. Hansen *et al.*, Intercellular calcium signaling induced by extracellular adenosine 5'- triphosphate and mechanical stimulation in airway epithelial cells, *J Cell Sci*, 106 (1993) 995-1004.

[28] T.D. Carter *et al.*, Porcine aortic endothelial gap junctions: identification and permeation by caged InsP3, *J Cell Sci*, 109 (1996) 1765-1773.

[29] G.C. Ellis-Davies and J.H. Kaplan, Nitrophenyl-EGTA, a photolabile chelator that selectively binds Ca^{2+} with high affinity and releases it rapidly upon photolysis, *Proc Natl Acad Sci U S A*, 91 (1994) 187-191.

GLIA 24:398–407 (1998)

Inositol-Trisphosphate-Dependent Intercellular Calcium Signaling in and Between Astrocytes and Endothelial Cells

LUC LEYBAERT,[1]* KOEN PAEMELEIRE,[1] ANDREJA STRAHONJA,[2] AND MICHAEL J. SANDERSON[2]
[1]*Department of Physiology and Pathophysiology, University Ghent, Ghent, Belgium*
[2]*Department of Physiology, University of Massachusetts Medical Center, Worcester, Massachusetts*

KEY WORDS calcium waves; astrocytes; endothelial cells; co-cultures; blood-brain barrier; flash photolysis; caged inositol trisphosphate; caged calcium; neurovascular coupling

ABSTRACT Interactions between astrocytes and endothelial cells are believed to play an important role in the control of blood-brain barrier permeability and transport. Astrocytes and endothelial cells respond to a variety of stimuli with an increase of intracellular free calcium ($[Ca^{2+}]_i$) that is propagated to adjacent cells as an intercellular Ca^{2+} wave. We hypothesized that intercellular Ca^{2+} signaling also occurs between astrocytes and endothelial cells, and we investigated this possibility in co-cultures of primary astrocytes and an endothelial cell line using caged messengers. Intercellular Ca^{2+} waves, induced by mechanical stimulation of a single cell, propagated from astrocytes to endothelial cells and vice versa. Intercellular Ca^{2+} waves could also be induced by flash photolysis of pressure-injected caged inositol trisphosphate (IP_3) and also by applying the flash to remote noninjected cells. Ca^{2+} waves induced by flash photolysis propagated from endothelial cells to astrocytes but not from astrocytes to endothelial cells even though caged IP_3 diffused between the two cell types. Flash photolysis of caged Ca^{2+} (NP-EGTA) resulted in an increase of $[Ca^{2+}]_i$ but did not initiate an intercellular Ca^{2+} wave. We conclude that an increase of IP_3 in a single cell is sufficient to initiate an intercellular Ca^{2+} wave that is propagated by the diffusion of IP_3 to neighboring cells and that can be communicated between astrocytes and endothelial cells in co-culture. By contrast, Ca^{2+} diffusion via gap junctions does not appear to be sufficient to propagate an intercellular Ca^{2+} wave. We suggest that intercellular Ca^{2+} waves may play a role in astrocyte-endothelial interactions at the blood-brain barrier. *GLIA 24:398–407, 1998.*

INTRODUCTION

In the brain, astrocytes and endothelial cells constitute the blood-brain barrier, which is characterized by its low permeability and the selective transport of substrates. The end-feet of perivascular astrocytes make close contact with capillary endothelial cells to provide an anatomical configuration that is ideally suited for interactions and communication between these two cell types. Astrocyte-endothelial interactions lead, for example, to the formation of tight junctions and the expression of transporter molecules and enzymes in endothelial cells (Janzer and Raff, 1987; Abbott and Revest, 1991; Tontsch and Bauer, 1991; Hayashi et al., 1997). The messenger molecules involved in astrocyte-

Contract grant sponsor: NIH; Contract grant number: HL492888; Contract grant sponsor: Belgian FWO; Contract grant numbers: 31508696, 3G002696, 31552098.

*Correspondence to: Luc Leybaert, M.D., Ph.D., Department of Physiology and Pathophysiology, University Ghent, De Pintelaan 185 (Blok B), B-9000 Ghent, Belgium. E-mail: luc.leybaert@rug.ac.be

Received 2 January 1998; Accepted 24 March 1998

endothelial signaling are largely unknown; the only information available is that interleukin-6 derived from astrocytes can induce alkaline phosphatases in endothelial cells (Takemoto et al., 1994) and that both astrocytes and endothelial cells are biochemically equipped to produce and respond to nitric oxide (Murphy et al., 1993).

One important mechanism of cell-to-cell signaling consists in the propagation of intercellular Ca^{2+} waves. Intercellular Ca^{2+} waves can be initiated both in astrocytes and endothelial cells by chemical, mechanical, or electrical stimuli and consist of an increase in $[Ca^{2+}]_i$ that is propagated from cell to cell (Cornell-Bell et al., 1990; Charles et al., 1991; Demer et al., 1993). Intercellular Ca^{2+} waves can also propagate between different cell types, e.g., between astrocytes and neurons (Nedergaard, 1994; Charles, 1994; Parpura et al., 1994). Consequently, we hypothesized that intercellular Ca^{2+} waves also propagate between astrocytes and endothelial cells at the blood-brain barrier to establish astrocyte-endothelial Ca^{2+} signaling.

The propagation of a Ca^{2+} wave between cells can occur by the diffusion of an intracellular or extracellular messenger or both, but the exact mechanism involved is dependent on the cell type (Osipchuk and Cahalan, 1992; Sanderson et al., 1994; Hassinger et al., 1996; Cao et al., 1997; Frame and Defeijter, 1997 Venance et al., 1997). Experimental evidence from a variety of cell types, including astrocytes and airway epithelial cells, strongly supports the hypothesis that intercellular Ca^{2+} waves can propagate by the diffusion of the intracellular messenger inositol trisphosphate (IP_3) between cells via gap junctions (Boitano et al., 1992; Sanderson et al., 1994; Sanderson, 1996). Intercellular Ca^{2+} waves require functional gap junctions (Charles et al., 1992) and are mediated by the release of Ca^{2+} from intracellular stores without a need for extracellular Ca^{2+} (Sanderson et al., 1990). Furthermore, Ca^{2+} waves are initiated by the microinjection of IP_3 (Sanderson et al., 1990) and inhibited by heparin (Boitano et al., 1992; Newman and Zahs, 1997), an antagonist of the IP_3 receptor, and U-73122 (Hansen et al., 1993), a phospholipase-C inhibitor. This hypothesis is also supported by the experimental evidence for IP_3 permeation through gap junctions (Saez et al., 1989; Carter et al., 1996). As a result, we investigated astrocyte-endothelial Ca^{2+} signaling and its underlying mechanisms by the photolytic release of IP_3 and Ca^{2+} from their caged forms in co-cultures of astrocytes and endothelial cells.

MATERIALS AND METHODS

Co-Cultures

Astrocyte-endothelial co-cultures were prepared from rat brain glial cells enriched for astrocytes (Levison and McCarthy, 1991), and a spontaneously transformed endothelial cell line derived from human umbilical vein (ECV304, European Collection of Animal Cell Cultures, Salisbury, UK). Neonatal rat brains (postnatal day 1 or 2) were isolated, and pieces of frontoparietal cortex were pinched off. After careful removal of the meninges, pieces of cortex were incubated in trypsin 1× solution (prepared from trypsin 10× (1:250; Gibco, Merelbehe, Belgium) for 20 min. The tissue was mechanically dissociated by repeated trituration, and the resulting cell suspension was passed through a 120 μm nylon mesh screen (Scrynel, Vel, Belgium), centrifuged, and further triturated. After passing the suspension onto a 20-μm nylon mesh screen, the remaining cells were seeded in 50 ml Falcon flasks in astrocyte Eagle's basal medium supplemented with 10% fetal calf serum (FCS), 2 mM glutamine (all from Gibco), and 0.6 % (w/v) glucose. The cells were grown to confluency over 7–10 days, and the culture flasks were then shaken overnight (18 h, 250 rpm) to remove the overlaying process-bearing cells and to obtain a culture enriched in astrocytes. ECV304 cells were grown in 50-ml culture flasks in Medium-199 with 2 mM glutamine and 10% FCS (Medium-199-FCS; all culture medium products were from Gibco). Co-cultures were prepared by trypsinizing astrocyte and endothelial cell cultures and plating them simultaneously onto glass bottom microwell dishes (Mattek, Ashwood, MA, USA) at a ratio of five astrocytes to one endothelial cell and cultured in Medium-199-FCS. After 3–4 days, some cultures had formed distinguishable zones of endothelial cells interspersed among the astrocytes. Single endothelial cells were sometimes observed within zones consisting of mainly astrocytes. The plating densities and astrocyte-endothelial ratio were, however, chosen so as to minimize single dispersed endothelial cells and to maximize occurrence of endothelial cell islands. Astrocyte identity was confirmed by immunostaining with Cy-3-conjugated antibodies to glial fibrillary acidic protein (GFAP; Sigma Chemical Co., Bornem, Belgium). Endothelial cell identification was based on the typical phase-contrast appearance of these cells and on their GFAP negativity. On phase-contrast, the ECV304 endothelial cells could easily be distinguished from astrocytes based on their larger size, clearly visible cell linings, clearly distinguishable nucleoli, and the typical cobblestone appearance of endothelial cells. Endothelial cells were, furthermore, the only GFAP-negative cell type present in the co-cultures. Co-cultures kept for longer than 4 days could not be used for experiments, because at that time astrocytes started to grow into the endothelial cell islands. For the experiments we used only cultures with endothelial cell islands that had a clear interface line with the astrocytes and with a minimum of dispersed single endothelial cells within the astrocyte region surrounding the island.

Calcium Imaging

Ca^{2+} waves were monitored with digital video microscopy and the Ca^{2+}-sensitive fluorescent dyes fura-2 or fluo-3 (fluo-3 was used in the flash photolysis experiments). Co-cultures were loaded with Ca^{2+} dyes by

incubation in Hanks' balanced salt solution buffered with 25 mM HEPES (HBSS-HEPES) containing either 10 μM fura-2-AM or fluo-3-AM (Molecular Probes, Eugene, OR) and 0.05% pluronic for 1 hour at 37°C, followed by 1 hour of de-esterification in HBSS-HEPES at room temperature. Cells were viewed with an inverted Nikon Diaphot epifluorescence microscope using a ×40 oil-immersion lens. Fura-2 images were obtained by alternate excitation with 340/380 nm and an emission bandpass at 510 nm; for fluo-3, a single excitation of 480 nm and an emission bandpass at 535 nm was used. Images were captured with a silicon-intensified target camera (Cohu San Diego, CA, USA) or an intensified CCD (Photonic Science, East Sussex, UK) and were stored on an optical memory disk recorder (Panasonic TQ-2026F). Fura-2 fluorescence images were converted to $[Ca^{2+}]_i$ images using a method described by Leybaert et al. (1998). The fluo-3 fluorescence images given in the figures are expressed as the change of fluorescence relative to the resting fluorescence level:

$$\text{i.e. } \frac{\Delta F}{F} = \frac{F_t - F_0}{F_0}.$$

Mechanical Cell Stimulation

Single cells were mechanically stimulated with a glass micropipette (tip size, ±1 μm) attached to a piezoelectric device that was deflected over approximately 4 μm by a rectangular voltage pulse of 150 ms duration.

Caged IP_3 Loading and Photolysis

Single cells were pressure injected with caged IP_3 using glass micropipettes (tip size, <1 μm) filled with a 50 mM K-HEPES solution at pH 7.2 containing 1–2.5 mM D-myo-inositol 1,4,5-trisphosphate, P4(5)-(1-(2-nitrophenyl)ethyl)ester trisodium salt (Molecular Probes, Calbiochem, La Jolla, CA) and applying several pressure pulses of 50–100 kPa lasting 100 ms. The injected volume was estimated to be on the order of 1 pl. Cell impalement and pressure injection of caged IP_3 initiated an intercellular Ca^{2+} wave; therefore, flash photolysis was performed only after recovery of the $[Ca^{2+}]_i$ signal, i.e., minimally 3 min after injection. The ultraviolet (UV) flash was delivered by a Hg-arc lamp coupled to the epifluorescence input via a dichroic mirror with cut-off at 400 nm and focused to the field diaphragm with a biconvex lens (focal distance, 250 mm). The UV beam was bandpass filtered at 330 nm (80 nm half-energy bandwidth), and the exposure time, ranging from 0.5 to 2 s, was controlled by a mechanical shutter (Uniblitz, Vincent Associates, Rochester, NY, USA). The UV spot had a half-energy diameter of 7.1 μm, as determined by flashing a dried layer of caged fluorescein dextran (molecular weight 3000; Molecular Probes) sandwiched between two coverslips. $[Ca^{2+}]_i$ was continuously monitored during exposure to the UV light.

Caged Ca^{2+} Loading

Cells were loaded with caged Ca^{2+} after fluo-3 loading by incubating the cells in 2.5 μM nitrophenyl-EGTA-AM (NP-EGTA-AM; Molecular Probes) in HBSS-HEPES for 10 min at room temperature. This loading protocol had no effect on CA^{2+} waves induced by mechanical stimulation. Longer incubations or higher concentrations had, however, significant Ca^{2+}-buffering effects.

Determination of the Photolytic Efficiency of Caged IP_3

The photolytic efficiency of caged IP_3, i.e., the fraction of IP_3 released upon UV exposure in our system, was calculated by multiplying the measured photolytic efficiency of caged fluorescein-dextran by the ratio of the quantum efficiencies of caged IP_3 (0.65) and caged fluorescein-dextran (approx. 0.25). The photolytic efficiency of caged fluorescein-dextran was determined by exposure of a dried layer of the substance to UV flashes of increasing duration. The half-maximal efficiency occurred at 3.4 s exposure time; at 2 s (exposure time used in most experiments), the photolytic efficiency was 34%. The photolytic efficiency of caged IP_3 was then calculated to be on the order of 85%.

Statistical Analysis

Data are expressed as means ± SEM; n denotes the number of experiments on different cultures.

RESULTS

Mechanical Stimulation Causes Astrocyte-Endothelial Ca^{2+} Waves

The experiments were performed on astrocyte-endothelial co-cultures prepared from primary rat brain astrocytes and a spontaneously transformed endothelial cell line. Three to four days after co-plating these cells, the co-cultures typically appeared with islands of endothelial cells surrounded by a majority of astrocytes, with a distinct interface line where the two cell types were in close contact (Fig. 1A,B). These astrocyte-endothelial co-cultures thus constitute a preparation well suited to study calcium signaling between the two cell types.

Mechanical stimulation of a single astrocyte, by gently poking the cell with a glass micropipette, initiated an intercellular Ca^{2+} wave that propagated through

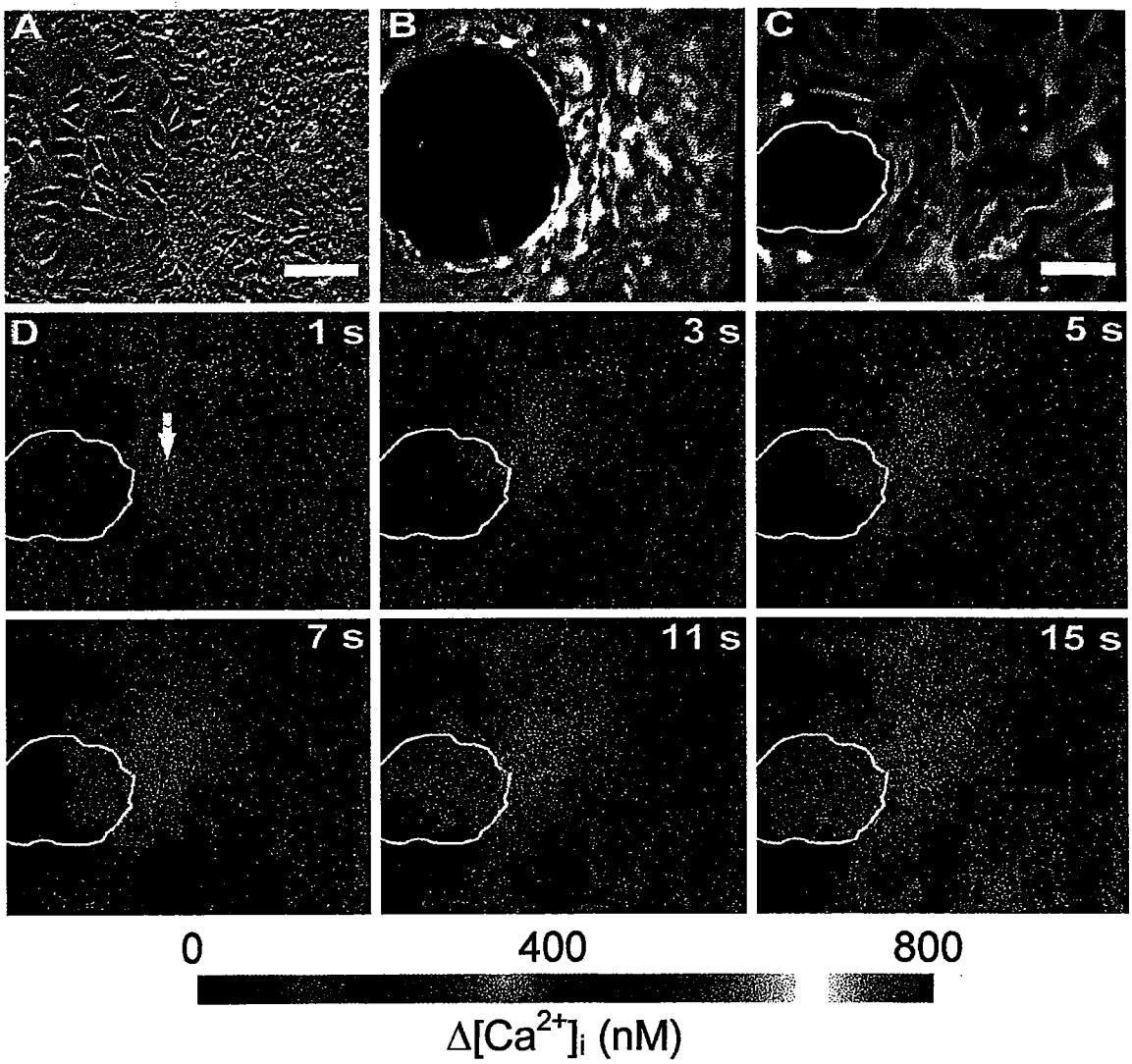

Fig. 1. Propagation of an intercellular Ca^{2+} wave from astrocytes to endothelial cells. **A:** Phase-contrast image of a typical astrocyte-endothelial co-culture. The circular region contains the endothelial cells and is surrounded by astrocytes; both cell types could be easily distinguished on phase-contrast. **B:** GFAP immunostaining of the same culture region shown in A, demonstrating GFAP-positive astrocytes surrounding GFAP-negative endothelial cells. **C:** GFAP immunostaining of a different region of an astrocyte-endothelial co-culture from which $[Ca^{2+}]_i$ images are presented in D. The white line indicates the astrocyte-endothelial interface. **D:** Time series of $[Ca^{2+}]_i$ images calculated from fura-2 fluorescence (time is indicated in the upper right corner). The images represent changes of $[Ca^{2+}]_i$ and are pseudocolored as defined in the calibration bar; each image is the average of eight video frames. The image series shows an intercellular Ca^{2+} wave initiated by mechanical stimulation (at time zero) of the astrocyte marked with an arrow. The Ca^{2+} wave propagated through the astrocytes, crossed the astrocyte-endothelial interface, and propagated further through the endothelial cells. Scale bars: A: 160 μm; C: 40 μm.

the astrocytes, crossed the astrocyte-endothelial interface, and propagated further through the endothelial cells (n = 25; Fig. 1C,D). Astrocyte-endothelial Ca^{2+} waves were observed even with the stimulated astrocyte located as far as 100 μm away from the interface line with the endothelial cells. Conversely, mechanical stimulation of an endothelial cell initiated an intercellular Ca^{2+} wave that propagated from the endothelial cells to the astrocytes (n = 8; not shown). These Ca^{2+} waves propagated through astrocytes and endothelial cells with a velocity of 10 to 20 μm/s and were delayed, for up to 1 s, at the astrocyte-endothelial interface.

Flash Photolysis of Caged IP_3 Induces Intercellular Ca^{2+} Waves in Astrocytes and Endothelial Cells

Microinjection of an astrocyte with caged IP_3 and exposure of the same cell to a focused beam of UV light (duration, 0.5–2 s, applied 3–5 min after injection, hereafter called UV flash) induced an increase of $[Ca^{2+}]_i$ in the exposed cell and initiated an intercellular Ca^{2+} wave that propagated in all directions through the surrounding astrocytes (n = 14; Fig. 2A). Ca^{2+} waves induced by flash photolysis of caged IP_3 traveled radi-

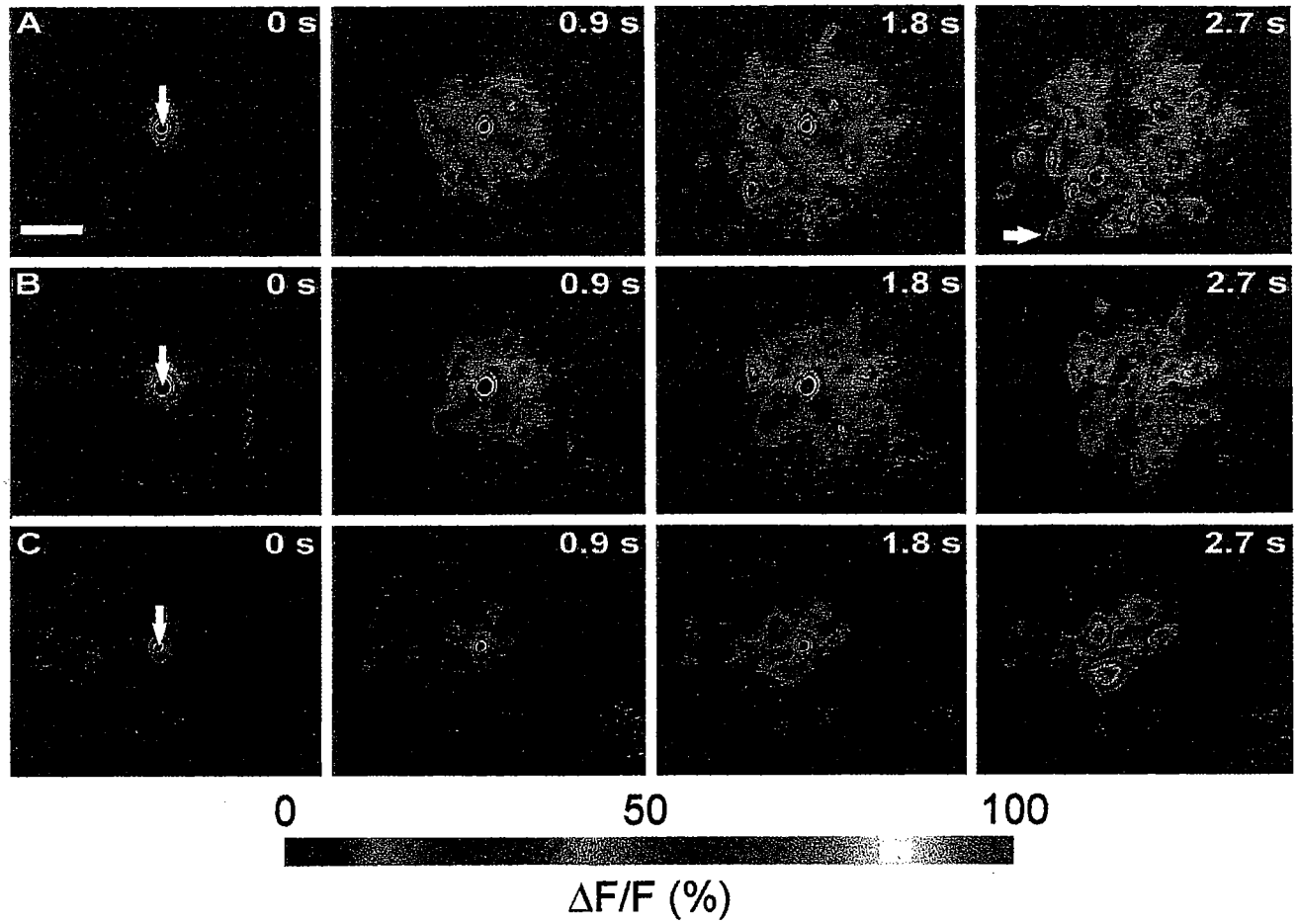

Fig. 2. Time series of fluo-3 fluorescence images illustrating responses induced by photolysis of caged IP_3. The images represent changes in fluorescence relative to the resting level and an increase in the relative fluorescence corresponds to a $[Ca^{2+}]_i$ increase. **A:** Injection of an astrocyte (vertical arrow in the first image) with caged IP_3 and subsequent exposure of this cell to a UV flash for 2 s (first three images) initiated a Ca^{2+} wave that propagated over the surrounding astrocytes in a radial manner. At the end of this experiment, the culture was moved so that the astrocyte marked with a horizontal arrow in the last image was located in the center of the images shown in series B. **B:** Applying the UV flash to the noninjected astrocyte in the center (arrow; this cell was located approx. 100 μm away from the injected astrocyte) also initiated an extensive astrocytic intercellular Ca^{2+} wave. **C:** Flashing an endothelial cell (arrow) injected with caged IP_3 initiated an intercellular Ca^{2+} wave, but wave propagation was limited to immediate neighboring cells. In some experiments (e.g., A), the UV flash appeared to partially bleach the dye in the exposed cell. Scale bar: 40 μm.

ally over distances ranging from 30 to 80 μm, averaging 46 ± 4 μm (n = 14). By contrast, mechanically induced intercellular Ca^{2+} waves often propagated further than 80 μm, indicating that the mechanical stimulus is a stronger stimulus and either results in the production of more IP_3 or additionally releases an extracellularly diffusing Ca^{2+}-mobilizing messenger such as ATP (Osipchuk and Cahalan, 1992; Hassinger et al., 1996; Cao et al., 1997). Injection of caged IP_3 into an endothelial cell followed by a UV flash induced an endothelial intercellular Ca^{2+} wave (n = 4). Ca^{2+} wave propagation in endothelial cells was restricted to a few (one to four) adjacent cells (Fig. 2C), probably because gap junctional coupling is less extensive in endothelial cells as compared with astrocytes. In control experiments in which the cultures were not injected with caged IP_3, the application of a UV flash (0.5–2 s) to individual cells did not induce any change of $[Ca^{2+}]_i$ in the flashed or surrounding cells.

Interestingly, intercellular Ca^{2+} waves could also be initiated by applying a UV flash to astrocytes located up to 100 μm away from the caged IP_3 injection point (n = 30; Fig. 2B). This indicates that caged IP_3 can diffuse between cells, most likely via gap junctions. The propagation distance of Ca^{2+} waves induced by flashing cells 100 μm away from the injection point was approx. 75% of the propagation distance of waves evoked by directly flashing the injected cell (n = 3). Multiple exposures of the injected astrocyte, or a distant astrocyte, to a UV flash, with several minutes in between each exposure, repeatedly initiated intercellular Ca^{2+} waves with a comparable $[Ca^{2+}]_i$ increase and a comparable travel distance. This indicates that a single UV flash does not deplete all of the available caged IP_3 or that caged IP_3 is replenished by diffusion from surrounding cells. Application of a UV flash 2 h after injection was still able to initiate an intercellular Ca^{2+} wave, illustrating that the breakdown of caged IP_3 by phosphatases is very

slow (Walker et al., 1987). Making use of the ability to initiate multiple Ca^{2+} waves by repeated stimulation of the same cell, it was found that the propagation distance of intercellular Ca^{2+} waves increased with the duration of the UV flash (n = 2). This demonstrates that there is a dose-response relationship between the amount of photolytically released IP_3 and the distance traveled by the wave (Fig. 3).

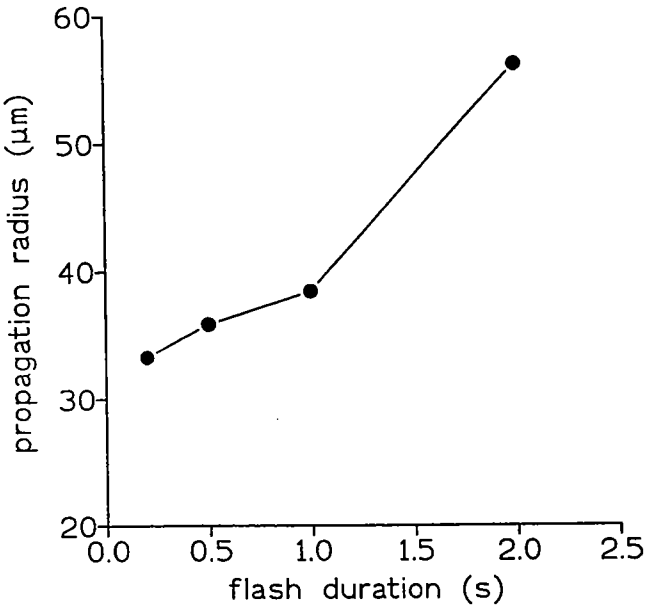

Fig. 3. Graph showing the relation between the duration of the UV flash and the propagation radius of the Ca^{2+} wave in one experiment. In these experiments, an astrocyte injected with caged IP_3 was repeatedly exposed to UV flashes of progressively longer duration, with several minutes between each flash.

Flash Photolysis of Caged Ca^{2+} Induces Only a $[Ca^{2+}]_i$ Increase

The increase in $[Ca^{2+}]_i$ induced in the stimulated cell by flash photolysis of caged IP_3 raises the possibility that the intercellular Ca^{2+} wave was propagated by the diffusion of Ca^{2+} ions to adjacent cells via gap junctions. To test this hypothesis, we performed experiments with caged Ca^{2+} (NP-EGTA). Application of a UV flash, up to 2 s duration, to individual astrocytes in cultures that had been ester loaded with NP-EGTA caused an increase of $[Ca^{2+}]_i$ in the stimulated cell but did not initiate a propagating Ca^{2+} wave (n = 8; Fig. 4A). The $[Ca^{2+}]_i$ increase induced by the photolytic release of Ca^{2+} was of the same order (sometimes even larger), as judged from the increase in fluo-3 fluorescence immediately after the UV flash, of the $[Ca^{2+}]_i$ increase induced by photolytic release of IP_3. Ca^{2+} measurements with fluo-3 cannot be reliably expressed as Ca^{2+} concentrations, but comparison of the fluo-3 fluorescence increase brought about by agonists such as ATP (0.1–1 μM) with the $[Ca^{2+}]_i$ increase induced by the same agonist and ratiometrically measured with fura-2 indicate that the $[Ca^{2+}]_i$ increase after photolytic Ca^{2+} release attained a peak value in the order of 500–750 nM. With the loading conditions used, NP-EGTA by itself had no damping effect on Ca^{2+} waves induced by mechanical cell stimulation (n = 8; Fig. 4B).

Flash Photolysis of Caged IP_3 Induces Ca^{2+} Waves From Endothelial Cells to Astrocytes

Experiments with caged IP_3 were also performed in the neighborhood of the interface between astrocytes and endothelial cells. An astrocyte located two cells away from the interface line was injected with caged IP_3, and after a delay of several minutes to allow for diffusion, UV flashes were applied to either an astrocyte or an endothelial cell close to the interface. Flashing an astrocyte close to the interface induced an astrocytic Ca^{2+}, wave but this wave was never (n = 14) observed to cross the interface line and propagate through the endothelial cells. In contrast, when the UV flash was applied to an endothelial cell close to the interface, this often (n = 7) resulted in an increase of $[Ca^{2+}]_i$ in the flashed endothelial cell that propagated further to a limited number (1–5) of closely situated astrocytes (n = 7; Fig. 5A,B). These observations indicate, first, that caged IP_3 can diffuse from astrocytes to endothelial cells via gap junctions and, second, that the photolytically released IP_3 is able to diffuse, also via gap junctions, from endothelial cells to astrocytes.

DISCUSSION

The present work was performed to study IP_3-dependent Ca^{2+} signaling in and between astrocytes and endothelial cells in co-culture. The experiments show that intercellular Ca^{2+} waves, induced by mechanical cell stimulation, can propagate between astrocytes and endothelial cells in the two directions. Furthermore, the experiments demonstrate that IP_3 released from the caged parent component is sufficient to induce intercellular Ca^{2+} waves in astrocytes and in endothelial cells and can also mediate Ca^{2+} wave propagation at the astrocyte-endothelial interface. These results will be discussed in the next paragraphs.

Mechanical stimulation of a single astrocyte induced a Ca^{2+} wave that propagated from astrocytes to endothelial cells. A direct effect of the mechanical stimulus on the endothelial cells is very unlikely in these experiments because there was always a clear delay (seconds) between the application of the stimulus and the arrival of the Ca^{2+} wave in the endothelial cells. Compatible with this conclusion is the fact that astrocyte-endothelial Ca^{2+} waves were also observed after mechanical stimulation of astrocytes located at a considerable distance (up to 100 μm) from the interface with the endothelial cells.

Flash photolysis of caged IP_3 initiated intercellularly propagating Ca^{2+} waves, both in astrocytes and endothe-

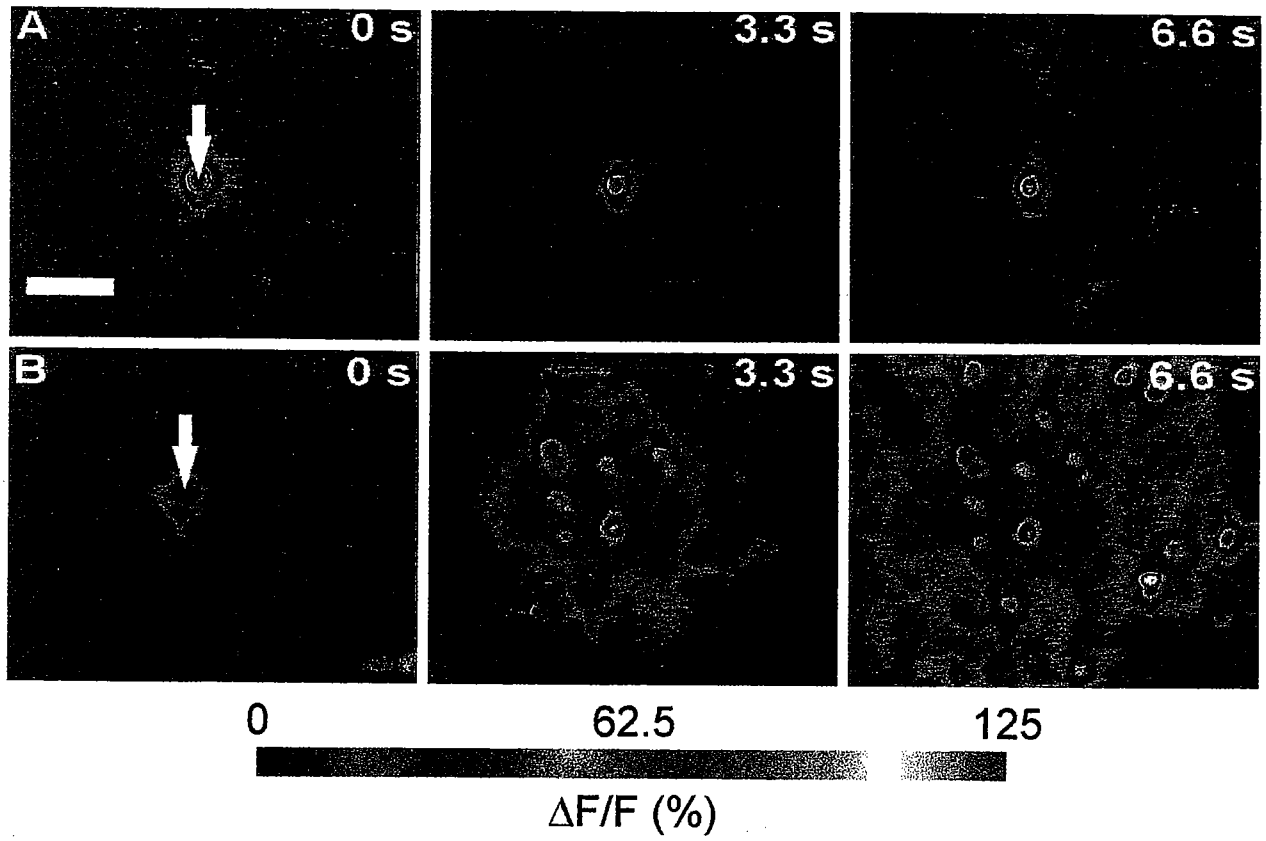

Fig. 4. Time series of fluo-3 images (relative fluorescence changes) illustrating responses induced by photolysis of caged Ca^{2+} (NP-EGTA). **A:** Flashing an astrocyte (arrow) for 1.5 s increased $[Ca^{2+}]_i$ only in the stimulated cell. **B:** Mechanical stimulation (arrow) of the same cell initiated an intercellular Ca^{2+} wave, demonstrating that NP-EGTA loading was without effect on Ca^{2+} wave propagation. Similar results were obtained when the mechanical stimulation was done before the UV flash. Scale bar: 40 μm.

lial cells. Such Ca^{2+} waves can be propagated by the intercellular diffusion of either the IP_3 liberated upon flash photolysis, of intracellular Ca^{2+} ions released by IP_3 receptor activation, or of an extracellular messenger released by the $[Ca^{2+}]_i$ increase and capable of increasing $[Ca^{2+}]_i$ in adjacent cells. The experiments with caged Ca^{2+} showed that a $[Ca^{2+}]_i$ increase with a magnitude similar to the $[Ca^{2+}]_i$ increase induced by flash photolysis of caged IP_3 was not enough by itself to induce an intercellular Ca^{2+} wave. These experiments, furthermore, indicate that a $[Ca^{2+}]_i$ increase does not result in the release of an extracellular Ca^{2+}-mobilizing messenger and, thus, that the $[Ca^{2+}]_i$ increase in cells that take part in the Ca^{2+} wave will not produce such an extracellular Ca^{2+} messenger. Thus, it follows that intercellular Ca^{2+} waves, initiated by flash photolysis of caged IP_3, are based on the liberation and intercellular diffusion of IP_3 and not of Ca^{2+}. The graded relation observed between wave travel distance and amount of photolytically released IP_3 (Fig. 3) corroborates the primary role of IP_3 in Ca^{2+} wave propagation and further suggests that a regenerative mechanism is probably not involved.

In addition to IP_3 diffusion, the experiments also gave evidence for the diffusion of caged IP_3 between the cells. The most likely pathway for intercellular diffusion of the two inositol phosphate compounds is formed by the gap junctions. The molecular weights of both substances (437 and 635, respectively) are below the maximum for gap junctional permeation (approx. 1000). In addition, both substances carry charged phosphate groups rendering them hydrophilic and making them unlikely to directly traverse the plasma membrane. Similarly, experimental work on other cell types has suggested that IP_3 (Saez et al., 1989) and also caged IP_3 (Carter et al., 1996) can permeate through gap junctions.

The idea that it is IP_3 and not Ca^{2+} that mediates cell-to-cell propagation of Ca^{2+} waves induced by flash photolysis of caged IP_3 is compatible with the fact that the cytoplasmic diffusion of Ca^{2+} is much slower as compared with IP_3 (Allbritton et al., 1992). Consequently, IP_3 diffusing through gap junctions will arrive and exert its effect on IP_3 receptors in advance of Ca^{2+}. Furthermore, Ca^{2+} waves can be initiated without an increase of $[Ca^{2+}]_i$ in the stimulated cell (Sanderson, 1996), Ca^{2+} wave propagation is independent of the magnitude of the $[Ca^{2+}]_i$ increase (Charles et al., 1993), and Ca^{2+} oscillations in individual cells do not initiate intercellular Ca^{2+} waves (Charles et al., 1992). This

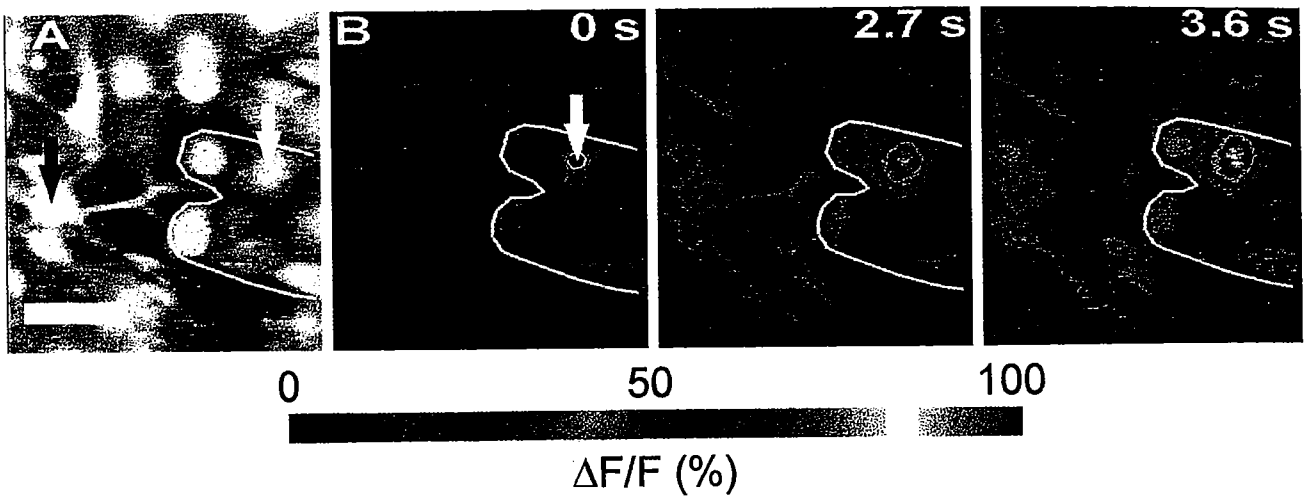

Fig. 5. Time series of fluo-3 images, illustrating an endothelial-astrocyte Ca^{2+} wave initiated by flash photolysis of caged IP_3. **A:** Raw fluo-3 fluorescence image. An astrocyte (black arrow) located approximately 45 μm left of the astrocyte-endothelial interface (white line) was injected with caged IP_3 and an endothelial cell (white arrow) was exposed to a UV flash. **B:** Flashing the endothelial cell (white arrow) induced a $[Ca^{2+}]_i$ increase that propagated to an adjacent endothelial cell and crossed the interface to continue propagation through several astrocytes. Scale bar: 40 μm.

does, however, not exclude the possibility that the cell-to-cell diffusion of Ca^{2+} may contribute to Ca^{2+} wave propagation under certain conditions, such as, for example, after IP_3 receptor sensitization by a low background concentration of IP_3, as described by Yule et al. (1996). Such IP_3 receptor sensitization could transform the cytoplasm to an excited medium that could possibly mediate intercellular Ca^{2+} waves that are initiated by an increase in $[Ca^{2+}]_i$ and that are propagated by Ca^{2+} diffusion and Ca^{2+}-induced Ca^{2+} release (M.J. Berridge, personal communication).

We performed an approximate calculation to obtain an estimate of the IP_3 concentration reached upon flash photolysis in our experiments. Assuming a simple model, whereby the injected amount of caged IP_3 (1 pl at 1 mM concentration) becomes homogeneously distributed over a circular region of 100 μm radius (distance from injection point where a UV flash still caused a Ca^{2+} wave) and 5 μm thickness (cell depth), the intracellular concentration of caged IP_3 was calculated to be approximately 6 μM. Taking into account a photolytic efficiency of approx. 85% (for calculation, see Materials and Methods) and an illumination area of 50% of the cell area, an initial intracellular IP_3 concentration in the order of 2.5 μM appears to be sufficient to initiate an intercellular Ca^{2+} wave. This value is very similar to the IP_3 concentration necessary to produce an intercellular Ca^{2+} wave estimated from modeling studies (3 μM) (Sneyd et al., 1995).

Experiments with caged IP_3 injection in an astrocyte and subsequent application of a UV flash to individual cells at either side of the astrocyte-endothelial interface showed that the Ca^{2+} waves induced in this way propagated from endothelial cells to astrocytes but not vice versa. The reason for this apparent rectification is not clear but may be related to a lower gap junctional conductance in the astrocyte-endothelial direction or to a lower affinity of IP_3 receptors in endothelial cells as compared with astrocytes. Both astrocytes and endothelial cells express connexin-43 (Dermietzel and Spray, 1993), suggesting that rectifying gap junctions are unlikely. Taking into consideration that mechanically induced waves were able to propagate from astrocytes to endothelial cells and that caged IP_3 was able to diffuse from astrocytes to endothelial cells, the most likely interpretation is that the energy of the UV flash was not sufficient to liberate enough IP_3 to initiate waves from astrocytes to endothelial cells.

Currently, the extent of gap junctional coupling between astrocytes and endothelial cells at the blood-brain barrier is not clearly established. Junctional specializations between the two cell types have not been observed with histological techniques, but it is possible that a low density of gap junctions would escape detection by morphological criteria. By contrast, gap junctions are especially abundant during brain development, suggesting that both cell types may be well coupled during embryogenesis. Alternatively, expression of gap junctions might be transiently stimulated under pathological conditions where the barrier is disrupted and is being remodeled, e.g., after brain injury, brain edema, or brain tumors. We suggest that astrocyte-endothelial Ca^{2+} signaling might be to influence certain blood-brain barrier functions. For example, an increase of $[Ca^{2+}]_i$ in endothelial cells can induce cell contraction and thereby increase the permeability of the barrier by opening the paracellular pathway (Bradbury, 1993; Hariri, 1994). An increase of $[Ca^{2+}]_i$ in endothelial cells can also stimulate fluid-phase endocytosis (Stanimirovic et al., 1996). Thus, astrocytic intercellular Ca^{2+} waves, perhaps induced during the acute phase of traumatic brain injury, could contribute to the initiation of brain edema. Another possibility is that astrocyte-endothelial Ca^{2+} waves are

involved in neurovascular coupling, i.e., the matching of the uptake of energy substrates from the microcirculation to the local neuronal metabolic needs. Neuronal metabolic needs depend on the electric activity of the neurons, and glutamate released by neuronal electric activity is known to induce astrocytic Ca^{2+} waves (Dani et al., 1992). Furthermore, the GLUT-1 glucose transporter present in endothelial cells, and also in astrocytes (Vannucci et al., 1997), has been reported to increase its expression in response to an increase in $[Ca^{2+}]_i$ (Mitani et al., 1995, 1996; Dominguez et al., 1996). Astrocyte-endothelial Ca^{2+} signals triggered by neuronal activity could thus act by stimulating glucose uptake from the microcirculation.

In summary, we conclude that an elevation of IP_3 in a single cell is sufficient to initiate an intercellular Ca^{2+} wave that is propagated by the diffusion of IP_3 through gap junctions. Intercellular diffusion of Ca^{2+} via gap junctions does not play a major role in this mode of Ca^{2+} wave initiation. In addition, intercellular Ca^{2+} waves can propagate between astrocytes and endothelial cells in co-culture, and Ca^{2+} wave propagation can, in part, be explained by the diffusion of IP_3 between the two cell types.

ACKNOWLEDGMENTS

This research was supported by NIH Grant HL49288, a Small Grant Program at UMMC to M.J. Sanderson, and the Belgian FWO grants 31508696, 3G002696, and 31552098 to L. Leybaert. We also thank Profs. M.J. Berridge, A.C. Charles, A. Thomas, J. Sneyd, and R. Tsien for their suggestions and comments. MPEG sequences of the experimental results shown in Figs. 1, 2, 4, and 5 can be found on the internet at http://www.ummed.edu/dept/sanderson.lab

REFERENCES

Abbott, N.J. and Revest, P.A. (1991) Control of brain endothelial permeability. Cerebrovasc. *Brain Metab. Rev.,* 3:39–72.

Allbritton, N.L., Meyer, T., and Stryer, L. (1992) Range of messenger action of calcium ions and inositol 1,4,5-trisphosphate. *Science,* 258:1812–1815.

Boitano, S., Dirksen, E.R., and Sanderson, M.J. (1992) Intercellular propagation of calcium waves mediated by inositol trisphosphate. *Science,* 258:292–295.

Bradbury, M.W.W.B. (1993) The blood-brain barrier. *Exp. Physiol.,* 78:453–472.

Cao, D., Lin, G., Westphale, E.M., Beyer, E.C., and Steinberg, T.H. (1997) Mechanisms for the coordination of intercellular calcium signaling in insulin-secreting cells. *J. Cell Sci.,* 110:497–504.

Carter, T.D., Chen, X.Y., Carlile, G., Kalapothakis, E., Ogden, D., and Evans, W.H. (1996) Porcine aortic endothelial gap junctions: identification and permeation by caged $InsP_3$. *J. Cell Sci.,* 109:1765–1773.

Charles, A.C. (1994) Glia-neuron intercellular calcium signaling. *Dev. Neurosci.,* 16:196–206.

Charles, A.C., Dirksen, E.R., Merrill, J.E., and Sanderson, M.J. (1993) Mechanisms of intercellular calcium signaling in glial cells studied with dantrolene and thapsigargin. *Glia,* 7:134–145.

Charles, A.C., Merrill, J.E., Dirksen, E.R., and Sanderson, M.J. (1991) Intercellular signaling in glial cells: calcium waves and oscillations in response to mechanical stimulation and glutamate. *Neuron,* 6:983–992.

Charles, A.C., Naus, C.C., Zhu, D., Kidder, G.M., Dirksen, E.R., and Sanderson, M.J. (1992) Intercellular calcium signaling via gap junctions in glioma cells. *J. Cell Biol.,* 118:195–201.

Cornell-Bell, A.H., Finkbeiner, S.M., Cooper, M.S., and Smith, S.J. (1990) Glutamate induces calcium waves in cultured astrocytes: long range glial signaling. *Science,* 247:470–473.

Dani, J.W., Chernjavsky, A., and Smith, S.J. (1992) Neuronal activity triggers calcium waves in hippocampal astrocyte networks. *Neuron,* 8:429–440.

Demer, L.L., Wortham, C.M., Dirksen, E.R., and Sanderson, M.J. (1993) Mechanical stimulation induces intercellular calcium signaling in bovine aortic endothelial cells. *Am. J. Physiol.,* 264:H2094–H2102.

Dermietzel, R. and Spray, D.C. (1993) Gap junctions in the brain: where, what type, how many and why? *Trends Neurosci.,* 16:186–192.

Dominguez, J.H., Song, B., Liu-Chen, S., Qulali, M., Howard, R., Lee, C.H., and McAteer, J. (1996) Studies of renal injury. II. Activation of the glucose transporter 1 (GLUT1) gene and glycolysis in LLC-PK1 cells under Ca^{2+} stress. *J. Clin. Invest.,* 98:395–404.

Frame, M.K. and Defeijter, A.W. (1997) Propagation of mechanically induced intercellular calcium waves via gap junctions and ATP receptors in rat liver epithelial cells. *Exp. Cell Res.,* 230:197–207.

Hansen, M., Boitano, S., Dirksen, E.R., and Sanderson, M.J. (1993) Intercellular calcium signaling induced by extracellular ATP and mechanical stimulation in airway epithelial cells. *J. Cell Sci.,* 106:995–1004.

Hariri, R.J. (1994) Cerebral edema. *Neurosurg. Clin. North Am.,* 5:687–706.

Hassinger, T.D., Guthrie, T.D., Atkinson, P.B., Bennett, M.V.L., and Kater, S.B. (1996) An extracellular signaling component in propagation of astrocytic calcium waves. *Proc. Natl. Acad. Sci. U.S.A.,* 93:13268–13273.

Hayashi, Y., Nomura, M., Yamagishi, S.I., Harada, S.I., Yamashita, J., and Yamamoto, H. (1997) Induction of various blood-brain barrier properties in non-neuronal endothelial cells by close apposition to co-cultured astrocytes. *Glia,* 19:13–26.

Janzer, R.C. and Raff, M.C. (1987) Astrocytes induce blood-brain barrier properties in endothelial cells. *Nature (Lond.),* 325:253–257.

Levison, S.W. and McCarthy, K.D. (1991) Astroglia in culture. In: *Culturing Nerve Cells.* G. Banker and K. Goslin, eds. MIT Press, Cambridge, MA, pp. 309–336.

Leybaert, L., Sneyd, J., and Sanderson, M.J. (1998) A simple method for high temporal resolution calcium imaging with dual excitation dyes. Biophys J., in press.

Mitani, Y., Behrooz, A., Dubyak, G.R., and Ismail-Beigi, F. (1995) Stimulation of GLUT-1 glucose transporter expression in response to exposure to calcium ionophore A-23187. *Am. J. Physiol.,* 269: C1228–C1234.

Mitani, Y., Dubyak, G.R., and Ismail-Beigi, F. (1996) Induction of GLUT-1 mRNA in response to inhibition of oxidative phosphorylation: role of increased $[Ca^{2+}]_i$. *Am. J. Physiol.,* 270:C235–C242.

Murphy, S., Simmons, M.L., Agullo, L., Garcia, A., Feinstein, D.L., Galea, E., Reis, D.J., Minc-Golomb, D., Schwartz, J.P., and Murphy, S. (1993) Synthesis of nitric oxide in CNS glial cells. *Trends Neurosci.,* 16:323–328.

Nedergaard, M. (1994) Direct signaling from astrocytes to neurons in cultures of mammalian brain cells. *Science,* 263:1768–1771.

Newman, E.A. and Zahs, K.R. (1997) Calcium waves in retinal glial cells. *Science,* 275:844–847.

Osipchuk, Y. and Cahalan, M. (1992) Cell-to-cell spread of calcium signals mediated by ATP receptors in mast cells. *Nature,* 359:241–244.

Parpura, V., Basarsky, T.A., Liu, F., Jeftinija, K., Jeftinija, S., and Haydon, P.G. (1994) Glutamate-mediated astrocytes-neuron signalling. *Nature,* 369:744–747.

Saez, J.C., Connor, J.A., Spray, D.C., and Bennett, M.V. (1989) Hepatocyte gap junctions are permeable to the second messenger, inositol 1,4,5-trisphosphate, and to calcium ions. *Proc. Natl. Acad. Sci. U.S.A.,* 86:2708–2712.

Sanderson, M.J. (1996) Intercellular waves of communication. *News Physiol. Sci.,* 11:262–269.

Sanderson, M.J., Charles, A.C., Boitano, S., and Dirksen, E.R. (1994) Mechanisms and function of intercellular calcium signaling. *Mol. Cell. Endocrinol.,* 98:173–187.

Sanderson, M.J., Charles, A.C., and Dirksen, E.R. (1990) Mechanical stimulation and intercellular communication increases intracellular Ca^{2+} in epithelial cells. *Cell Regul.,* 1:585–596.

Sneyd, J., Wetton, B.T.R., Charles, A.C., and Sanderson, M.J. (1995) Intercellular calcium waves mediated by the diffusion of inositol trisphosphate: a two-dimensional model. *Am. J. Physiol.,* 268:C1537–C1545.

Stanimirovic, D., Morley, P., Ball, R., Hamel, E., Mealing, G., and Durkin, J.P. (1996) Angiotensin II-induced fluid phase endocytosis in human cerebromicrovascular endothelial cells is regulated by the inositol-phosphate signaling pathway. *J. Cell Physiol.,* 169:455–467.

Takemoto, H., Kaneda, K., Hosokawa, M., Ide, M., and Fukushima, H. (1994) Conditioned media of glial cell lines induce alkaline phosphatase activity in cultured artery endothelial cells: identification of interleukin-6 as an induction factor. *FEBS Lett.,* 350:99–103.

Tontsch, U. and Bauer, H.C. (1991) Glial cells and neurons induce blood-brain barrier related enzymes in cultured cerebral endothelial cells. *Brain Res.,* 539:247–253.

Vannucci, S.J., Maher, F., and Simpson, I.A. (1997) Glucose transporter proteins in the brain: delivery of glucose to neurons and glia. *Glia,* 21:2–21.

Venance, L., Stella, N., Glowinsky, J., and Giaume, C. (1997) Mechanisms involved in initiation and propagation of receptor-induced intercellular calcium signaling in cultured rat astrocytes. *J. Neurosci.,* 17:1981–1992.

Walker, J.W., Somlyo, A.V., Goldman, Y.E., Somlyo, A.P., and Trentham, D.R. (1987) Kinetics of smooth and skeletal muscle activation by laser pulse photolysis of caged inositol 1,4,5-trisphosphate. *Nature,* 327:249–252.

Yule, D.I., Stuenkel, E., and Williams, J.A. (1996) Intercellular calcium waves in rat pancreatic acini: mechanisms of transmission. *Am. J. Physiol.,* 271:C1285–C1294.